

CHAPTER 1

1.0 INTRODUCTION

Cancer is an ailment in which cells escape from the normal regulatory mechanisms and behave ectopically, characterized by uncontrollable proliferation, unregulated differentiation, and invasion to surrounding tissues and organs (Laundry de Mesquita *et al.*, 2009). Cancer can be treated successfully by surgical removal of the tumours if the malignant cells are localized. However, most malignant tumours are capable of detaching from the primary tumour mass, entering the blood stream or lymphatic channels, followed by localization and growth of secondary tumours at new sites (Hayot *et al.*, 2006). The dispersion of tumour within the body is known as metastasis which significantly results in mortality making cancer a devastating disease.

Conventional approaches for combating cancers, namely surgery, chemotherapy and radiation therapy are not effective in curing a patient with metastatic cancer. These therapies kill a large number of normal cells along with the cancer cells due to their low specificity. It is also a painfully evident that chemotherapy and radiation cause severe adverse effects, such as bone marrow suppression resulting in cytopoenia, and subsequent devastation of the immune responses (Devasagayam & Sainis, 2002), in addition to exhibiting limited curative value for most advance cancers. Based on these scenarios, agents that can inhibit the metastatic activity of the cancer cells are considered as a promising cancer treatment.

One approach to control metastasis cancer is through growth inhibition by which the disease can be prevented, slowed-down, or reversed substantially. As with any drug development, an empirical screening for examining the biochemical influences of the

agents are essential in order to understand the cytotoxic effects (Vani, Vanisree, & Shyamaladevi, 2006).

Many experimental studies and clinical trials indicated that natural immunity possesses the ability to control the growth of primary tumours and block metastasis (Schantz, Brown, Lira, Taylor, & Beddingfield, 1987). Macrophages and natural killer (NK) cells are the most relevant effectors among the immune-related cells that act against tumour cells (Andreesen *et al.*, 1990; Barlozzari, Leonhardt, Wiltrout, Heberman, & Reynolds, 1985). In addition, the activation of macrophages and NK cells are able to elicit functions which suppress tumour growth and inhibit metastasis activity (Yoon *et al.*, 2004). Based on this scenario, the enhancement of host immune responses have been recognized as a potential avenue of inhibiting tumour growth without harming the host (Tu, Sun, & Ye, 2008). Therefore, the search of novel therapeutic substances with immunomodulatory property is an important approach in the field of cancer treatment and prevention.

Numerous epidemiological, biological and clinical studies have indicated a strong correlation between dietary factors and cancer prevention (Rogers, Zeisel, & Groopman, 1993; Surh, 2003). Herbs possess various pharmacological activities including antioxidant and anti-inflammatory effects which are associated with anti-mutagenic and anti-carcinogenic properties (Bode, Ma, Surh, & Dong, 2001). Oxidative and inflammatory tissue damages occur mostly during the promotion stage. A compound with strong antioxidant and anti-inflammatory properties are believed to function as an anti-tumour promoter (Ippoushi, Takeuchi, Ito, Horie, & Azuma, 2007). In this study, the Zingiberaceae plants, which have proved to exhibit various biological properties, were opted for investigation. Investigations of nutraceuticals and phytochemicals as an alternative for cancer chemoprevention have become a flourishing field of research over the past decades

(Manson, 2003; Surh & Ferguson, 2003; Gosslau & Chen, 2004; Wei, Ma, Cai, Yang, & Liu, 2005).

This main objective of this study is to evaluate the immunomodulatory and anti-metastatic activities of ten selected local *Zingiberaceae* species, namely *Alpinia galanga*, *Boesenbergia rotunda*, *Curcuma aeruginosa*, *C. domestica*, *C. mangga*, *C. xanthorrhiza*, *Kaempferia galanga*, *Zingiber officinale*, *Z. montanum*, and *Z. zerumbet*. Each species were extracted with petroleum ether, chloroform and methanol using Soxhlet extractor system. A total of 30 crude *Zingiberaceae* extracts were obtained for the screening tests. Literally, the objectives include:

- (i) evaluation of the extracts for their immunomodulatory activities by screening on their nitric oxide (NO) inhibitory potentials in murine macrophages cells (RAW 264.7) using NO assay,
- (ii) evaluation of the extracts for their anti-metastatic activities by screening their anti-proliferative potentials against human breast cancer cells (MDA-MB-231) using MTT assay, cell migration inhibition potentials on MDA-MB-231 cells using the scratch wound assay,
- (iii) examination of the most active extracts based on (ii) for their toxicity against human lung fibroblast cells (MRC-5) using MTT assay, and
- (iv) examination of the chemical groups for the most active extract screened using thin-layer Chromatography (TLC).

CHAPTER 2

2.0 LITERATURE REVIEW

2.1 Cancer

Cancer is a genetic disease as it occurs when specific genes in an organism have undergone alterations. In most of the cases, it is not an inherited disease. The genetic alterations that lead to cancer ailments usually originate in the DNA of a somatic cell during the lifetime of the cancer patients, rather than inherited from the chromosomes of their parents. In contrast to other diseases that require modifications of a large number of cells, cancer is said to be monoclonal as it results from uncontrolled proliferation of a single wayward cells (Karp, 2008).

Development of a malignant tumour or carcinogenesis is characterized by progression of permanent alterations in a single line of cells, which are able to attain many successive cell divisions and take years to complete. Each genetic change is responsible for a particular character of the malignant state, such as protection from apoptosis in order escape the host defence mechanism (Karp, 2008). These genetic changes result in lack of control of the cancer cells proliferation and consequently, forming malignant tumours which become increasingly less responsive to the body's normal regulatory machinery and better able to invade the surrounding healthy tissues and organs (Laundry de Mesquita *et al.*, 2009).

Based on this concept, cells responsible for initiating cancer must be capable of acquiring large number of cell divisions in tumorigenesis. The most common solid tumours, such as those derived from breast, colon, prostate, and lung are arise in the epithelial tissues that are involved in a relatively high level of cell divisions. Since extensive cell divisions are critically important for tumour formation, two general scenarios have been considered

for the origin of tumours. The first scenario indicated that cancer arises from within a small population of stem cells in a tissue. Stem cells, which possess unlimited proliferation potential, undergo massive cell divisions to accumulate mutations required for malignant formation. In a different scenario, progenitor cells can form malignant tumours by acquiring certain properties, such as capacity of uncontrollably proliferation or tumour progression (Karp, 2008). However, these two scenarios are not mutually exclusive as whether the tumours arise from stem cells or progenitor cells depend on the types of cancer.

In vitro system is a fundamental avenue to study the behavior of cancer cells. Different cell lines have their unique characteristics, while at the same time possessing similar basic properties of cancer cells. Normal cells and cancer cells have similar capacity to grow and divide when being cultured under the same condition with substantial growing media. However, the growth ceases when the proliferated normal cells cover the bottom layer of the culture dish, remaining as a monolayer. Grow rates decreases as normal cells respond to the inhibitory factors from the environment, such as depletion of growth factors in the culture medium or due to the contact between cells in the culture dish. In contrast, cancer cells grow indefinitely regardless of the growth signals. As a result, cancer cells grow continuously, pilling on top of one another and form clumps in the culture dish (Karp, 2008).

Cancer cells can grow in the absence of growth signals which are mandatory for growing normal cells. Therefore, cancer cells have the potential to grow without serum which provide the nutrition for cells, because the cell cycle for cancer cells are independent of the interaction between the growth factors and their receptors located on the cell surfaces. The ability of uncontrollable proliferation of cancer cells is due to the presence of telomerase in the chromosomes of the cancer cells. Telomerase is an enzyme that remains

telomeres at the tips of chromosomes, which keep promoting the cells for divisions. It is said that normal cells are protected against tumour growth by the absence of telomerase (Karp, 2008).

Massive research effort on cancer treatments has been carried out for decades. Although the understanding of the cellular and molecular basis of cancer has increased through the years, there is still not much impact on reducing the incidence of cancer deaths. In addition, current cancer treatments, such as chemotherapy and radiation therapy not only lack the specificity in killing cancer cells, but also results in serious side effects to the patients (Karp, 2008).

2.1.1 Carcinogenesis

Carcinogenesis is a multi-step process which consists of three main stages such as initiation, promotion and progression. In the initiation stage, the genetic changes that occur during tumorigenesis are accompanied by histological changes. Cells with initial changes are identified as “precancerous”, indicating that the cells exhibit some cancerous properties, such as lack of growth control, but lack the capability to invade normal tissues or metastasize to distant sites. Alterations of the types and numbers of cell-adhesion molecules or interference of the cell-adhesion ability to other cells or to extracellular matrices are implicated in the promotion stage towards metastasis. The cancer progression involves the detachment of tumour cells from the primary tumour mass and dispersion to a new location far from the original points, which leads to the process of metastasis (Hayot *et al.*, 2006).

The genes that are implicated in carcinogenesis can be grouped under two broad categories: tumour-suppressor genes and oncogenes. Tumour-suppressor genes encode proteins that restrain proliferation of the mutated cells and prevent the cells from becoming

malignant. Loss of functions of one or more tumour-suppressor genes lead to the transformation of a normal cell to a cancer cell. This is to say that, tumour-suppressor genes encode proteins that help maintain genetic stability. Most of the products encoded by tumour-suppressor genes act as negative regulators of cell proliferation. Thus, dysfunctional or elimination of the genes commonly results in lack of growth control (Karp, 2008).

Oncogenes, on the other hand, encode proteins that promote uncontrolled cell growth and the conversion of a cell to malignant state. Most oncogenes facilitate cell proliferations, but they are also implicated in other roles. Oncogenes interfere with the cell's normal activities, which lead to genetic instability, and may even promote metastatic activity. Genetic alterations such as gene mutation, gene duplication, or chromosome rearrangement can cause a cell to function abnormally to normal growth controls, leading it to behave as a malignant cell. Oncogenes are the dominant genes, which mean that a single copy of an oncogene can alter the phenotype of the cell, regardless of whether or not there is a normal gene on the homologous chromosome (Karp, 2008).

Oncogenes were discovered through the investigation of RNA tumour viruses. The existence of oncogene in RNA viruses encode protein that interfere with the cell's normal regulatory system and thus transform the normal cell to malignant state. Mutation in one of the two copies (alleles) of an oncogene may be sufficient to cause a cell to lose growth control. In contrast, both copies of a tumour-suppressor gene must be knocked out in order to induce the same effects. Oncogenes arise from proto-oncogenes due to the result of gain-of-function mutations, i.e., mutations that cause gene product to exhibit new functions that lead to malignancy. On the other hand, tumour-suppressor genes suffer loss-of-function

mutations and/or epigenetic inactivation that render them unable to restrain cell growth (Figure 2.1) (Karp, 2008).

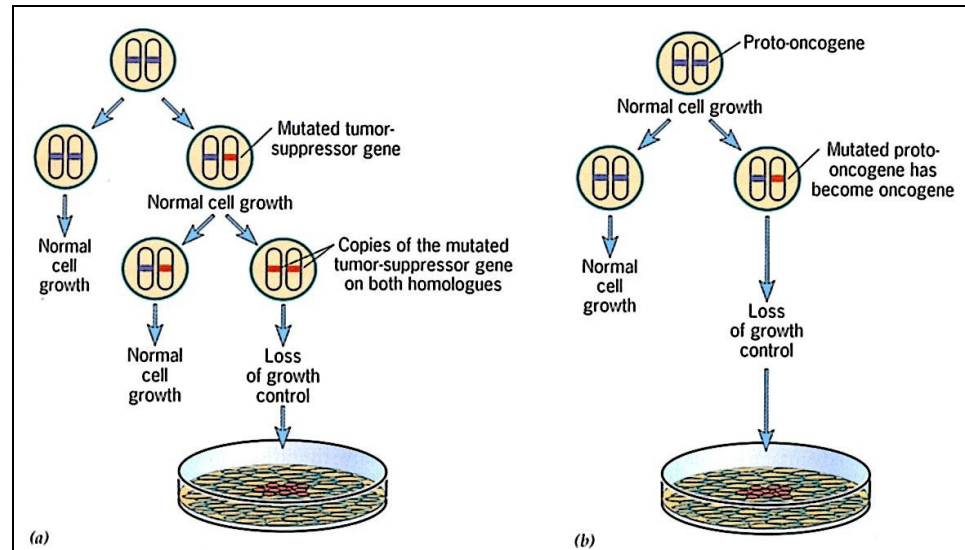


Figure 2.1: Contrasting effects of mutations in (a) tumour suppressor genes and (b) oncogenes (Karp, 2008).

2.1.2 Cancer Metastasis

Malignant tumours are ranked as the second largest deadly disease after heart disease (Tu, Sun, & Ye, 2008). Neoplastic disease detected early can be cured successfully through the removal of the primary tumours as solid cancer in the early stage is often localized. However, more than 90% of the mortality for cancer patients is not due to primary tumour but the dissemination of the primary tumours to secondary sites by a series of events known as the metastatic cascade (Entschladen, Drell IV, Lang, Joseph, & Zaenker, 2004; Fidler, 1991; Liotta, Steeg, & Stetler-Stevenson, 1991; Sporn, 1996).

Cancer metastasis consists of a complex cascade of events that ultimately allow tumour cells to escape and grow (Yoon, Kim, & Chung, 2001). Metastasis is characterized by a series of sequential events involving loss of intercellular cohesion, cell migration,

angiogenesis, accession to the systemic blood circulation (intra-vasation), survival in circulation, arrest and subsequent extra-vasation, evasion of local immune responses, as well as growth at distant organs (Chambers *et al.*, 2001; Fidler, 1999). An estimation of $3 - 4 \times 10^6$ cells/g of tumour can reach the blood stream per day in animal models. However, only a minority of those cancer cells will survive and grow at distant sites (Fidler, 1970; Weiss, 1990).

Metastatic cells are cancer cells that are able to initiate the formation of secondary tumours. They are thought to exhibit unique properties that are distinct from other cells in the tumours. Metastatic cells must be less adhesive than other cells in order to detach from the tumour mass. Besides that, metastatic cells must be capable of penetrating numerous barriers, such as the extracellular matrices of surrounding connective tissue as well as the basement membranes that line the blood vessels that carry them to distant sites. In addition, the cells must be able to invade normal tissues to form secondary colonies (Karp, 2008).

Bone is one of the most frequent sites of metastasis. Breast cancer is one of the leading causes for the majority of the skeletal metastases (Cecchini, Watterwald, van der Pluijm, & Thalmann, 2005). Many researches on the molecular mechanism of breast cancer development have been carried out, however, pathway for initiating the development of breast malignancy still remain elusive (Choi *et al.*, 2009).

Based on Figure 2.2, invasive phenotypes, such as loss of cell-cell adhesion, increased motility, and matrix degradation are conferred by epithelial mesenchymal transition (EMT). At the same time, primary tumour promotes angiogenesis, which aid in access of the cancer cells to the systemic circulation, through a process known as intravasation. This event is followed by aggregation between cancer cells, platelets and leukocytes to form cell emboli. The aggregation protects the tumour cells from immune

responses and facilitates arrest in the bone capillaries by a mechanical mechanism and by adhesion to bone marrow endothelium-specific cell adhesion molecules. Chemokines and bone matrix molecules mediate their bone marrow or bone microenvironment. Cancer cells are exposed to the survival and growth support normally exerted on haemopoietic cells by marrow stromal cells, known as stromal fibroblasts and tissue macrophages, as well as endothelial cells. Furthermore, osteoblasts and osteoclasts, or matrix-integrated secrete bone cytokines, which are released and activated during bone reabsorption, and contribute critically to survival and proliferation of the metastatic cancer cells (Cecchini *et al.*, 2005).

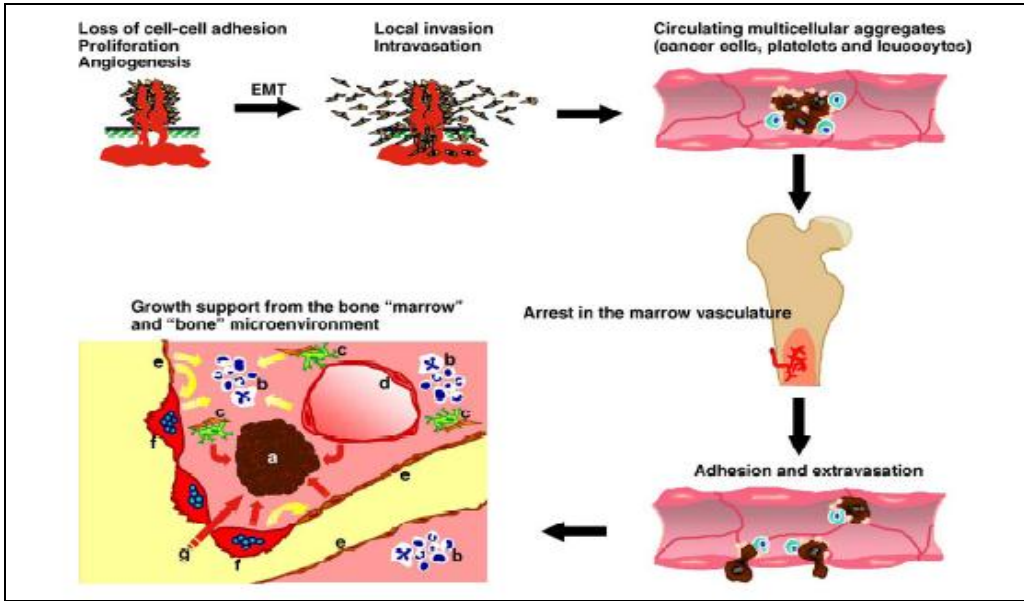


Figure 2.2: Series of events involve in cancer cell metastasis from primary tumour sites to the skeleton (Cecchini *et al.*, 2005).

Breast carcinoma cells lack tight junctions (TJs) (Hoover, Liao, & Bryant, 1998), resulting in loss of cell-cell adhesion essential for tumour invasion (Glukhova, Kotliansky, Sastre, & Thiery, 1995). TJs are the association areas of two cells whose membranes adhere together to form a primary barrier for paracellular transportation of solutes across the cells (Figure 2.3). TJs play crucial roles in holding adjacent cells together. Besides that, it helps to maintain epithelial cell polarity by acting as diffusion barrier for protein and lipid transportation within the plasma membrane (Choi *et al.*, 2009). TJs also prevent the passage of molecules or ions through the spaces between cells, which is to control over substances that are allowed to pass through. In precancerous lesions of the epithelial and cancerous epithelial, TJs' functions are interfered and destructed as TJs strands become disorganized or lost altogether (Soler *et al.*, 1999).

Tight junctions consist of a variety of claudins, which form homodimers or heterodimers to produce paired strands between adjacent cells, are the major integral membrane proteins that structure the backbone of TJs. Several studies have reported that aberrant claudins are found in various cancers that function distinctly as in the TJs complexes. For example, claudin-3 and claudin-4 are overexpressed in breast carcinoma cells and in metastatic cells in particular, that the cells possess great tendency to spread to other sites (Kominsky, 2006). However, the roles of claudin overexpression in metastasis cancer development are still remained unclear (Choi *et al.*, 2009).

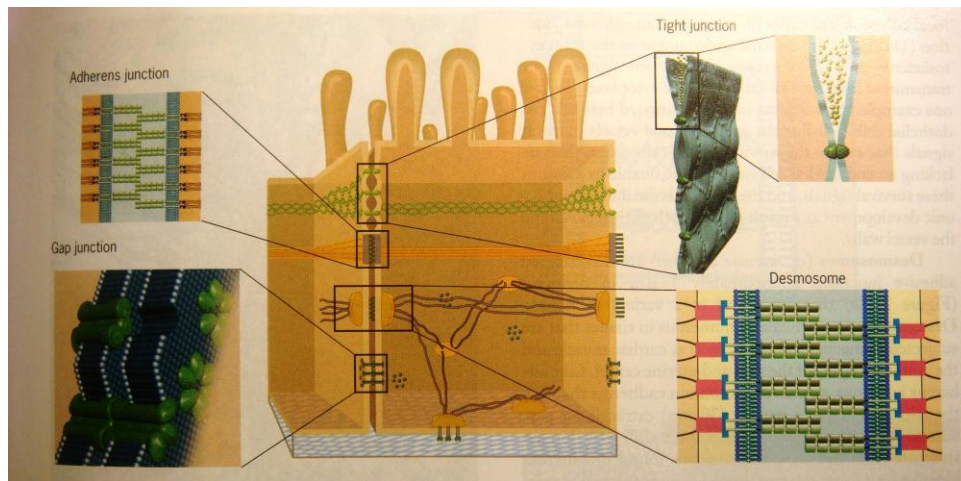


Figure 2.3: Schematic diagram showing an intercellular junctional complex. The complex consists of a tight junction (zonula occludens), adherens junction (zonula), and desmosome (macula adherens). Adherens junction and tight junction encircle the cells. Desmosomes and gap junctions are restricted to particular site between adjacent cells. Other gap junctions and desmosomes are located deeper along the lateral surfaces of the cells (Karp, 2008).

A family of Zn-dependent endopeptidases, known as matrix metalloproteinase (MMPs) is also implicated as possible mediators for invasion and penetration of extracellular matrices (ECM) components including collagen, fibronectin, and lamina in metastasis of breast cancers. MMPs are ECM-digesting enzymes which play important roles in several biological processes, but are also collectively capable of cleaving virtually all extracellular matrix substrates that implicated in various physiological and pathological processes in metastasis (Zucker, Cao, & Chen, 2000; Mook, Frederiks, & Van Noorden, 2004). In cancer metastasis, these enzymes degrade the proteins and proteoglycans resulting in cancer cell migration. In addition, MMPs that cleave certain proteins of ECM produces active protein fragments that act back on the cancer cells to stimulate their growth and invasive characters.

Studies have found that mRNA transcripts of MMP-2 and MMP-9 are overexpressed in breast cancer cells (Canning, Postovit, Clarke, & Graham, 2001; Bartsch,

Staren, & Appert, 2003). Both MMP-2 and MMP-9 are implicated with the invasive metastatic potential of tumour cells (Choi *et al.*, 2009; Rose, Huang, Ong, & Whiteman, 2005). MMPs have become a prominent target of the pharmaceutical industry due to their apparent roles in the development of malignant tumours. Since synthetic MMP inhibitors were demonstrated to be able to reduce metastasis *in vivo*, several clinical trials were conducted. Unfortunately, the inhibitors only hold a little promise in treating late-stage tumour progression. In some cases, the inhibitors show adverse effect such as joint damage. To date, Periostat is the only MMP inhibitor approved by Food and Drug Administration (FDA) for treating periodontal disease.

2.1.3 Angiogenesis

Angiogenesis is the process of new blood vessel development from the pre-existing vascular network, which is regulated by the balance of various stimulators and inhibitors (Folkman, 2006). Development of new blood vessels occurs mostly during embryogenesis and pathogenic periods. New blood vessels are developed via two distinct processes, namely vasculogenesis and angiogenesis. Vasculogenesis involves the formation of vascular cells that originate from undifferentiated precursors. On the other hand, angiogenesis is responsible for the vascularization in embryos, growing and repairing tissues, as well as in the uterine and ovarian cycles (Goodwin, 2007; Ribatti, Vacca, Nico, Roncali, & Dammacco, 2001).

Physiological angiogenesis is under strict regulation, which activated only when development or tissue repair are required. However, disruption of the balance between stimulating and inhibiting factors, leads to excessive blood vessels formation and consequently, results in pathological angiogenesis (Kim, Lee, Kim, Yu, & Kim, 2009).

Either insufficient or excessive blood vessel formations results in diseases pathogenesis which are critically fatal. Excessive blood vessel formations through angiogenesis have been found in disorders, such as cancer, rheumatoid arthritis, and retinopathies (Goodwin, 2007). As tumour grows in size, it stimulates the formation of new blood vessels. Blood vessels function to deliver nutrients and oxygen to the tumour and remove waste products from the tumour. Besides that, new blood vessels formed provide the conduits for cancer cells and facilitate them to disperse and spread to other sites in the body (Karp, 2008).

Sequence of Events during Angiogenesis

Angiogenesis involves a sequences of events, such as degradation of the extracellular matrix surrounding the parent vessel, migration and proliferation of the endothelial cells and mural cells to adduct the new vessel, as well as morphogenesis by forming lumen and smooth muscle cells associated with the mural cells (Goodwin, 2007; Carmeliet, 2000) (Figure 2.4). Endothelial cells are the major constituent for developing new blood vessels.

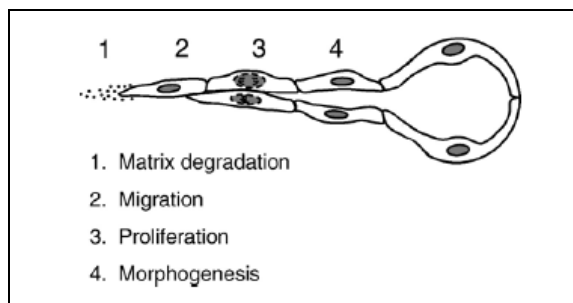


Figure 2.4: Stages of endothelial cell functions involve in angiogenesis (Goodwin, 2007)

Matrix degradation is the primary event for vessel sprouting, which involves degradation of the laminin-rich basement membrane surrounding the endothelial cells, and

proteolysis of the collagen-rich extracellular matrix of the surrounding connective tissues. This process is followed by activation of angiogenic proteins or secreting matrix- or membrane-bound growth factors that facilitate angiogenesis by the tumour cells (Davis & Senger, 2005; Pepper, 2001, Rundhaug, 2005; van Hinsbergh, Engelse, & Quax, 2006).

Matrix degradation is carried out proteases, typically MMPs, as well as other metalloproteinases, cysteine cathepsins, serine proteases, and aminopeptidases. Activated MMPs digest matrix components, such as collagen, fibrin, laminin and fibronectin in order to separate the endothelial cells for sprouting (Rundhaug, 2005; van Hinsbergh *et al.*, 2006). Based on the functions of MMPs and other proteases that facilitate tumour invasion and angiogenesis, agents that inhibit their activities have been tested as anti-cancer agents (Egeblad & Werb, 2002; Liekens, De Clercq, & Neyts, 2001; Mannello, Tonti, & Papa, 2005; Overall & Lopez-Otin, 2002).

Matrix degradation of endothelial cells is followed by the migration process. Endothelial cells migrate to surrounding tissues in response to angiogenic chemokines. Growth factors facilitate endothelial cell motility by causing random cell movement (chemokinesis) or directed migration toward a stimulatory factor (chemotaxis) (Goodwin, 2007). Since cell migration is significant in tumour invasion and tumour angiogenesis, anti-cancer agents that can prevent or halt the migration activity can be an effective cancer therapeutic avenue.

Once the endothelial cells are migrated, tumour cells secrete growth factors, such as VEGF, that act on the endothelial cells of the surrounding blood vessels, and stimulate them to proliferate and develop into new blood vessels (Karp, 2008) (Figure 2.5). Finally, endothelial cells must assemble in an appropriate order to acquire the morphology of vessel tubes (Goodwin, 2007).

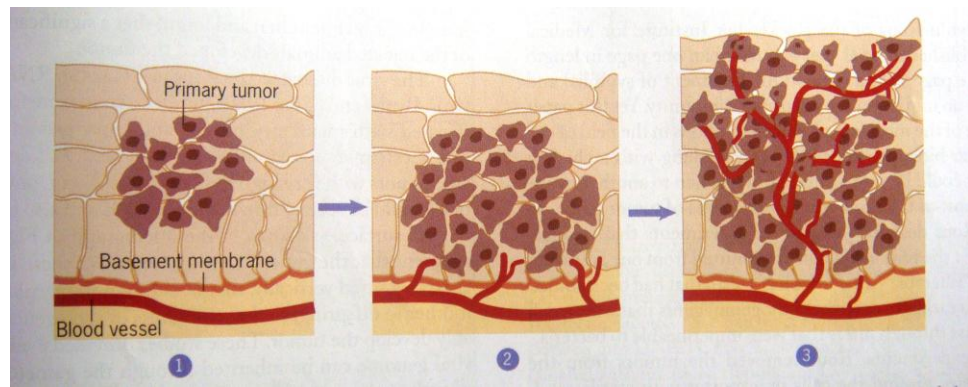


Figure 2.5: Angiogenesis and growth of primary tumour. In step 1, primary tumour proliferates to form a small mass of cells. The tumour remains very small (1–2 mm) as long as it is avascular (without blood vessel). In step 2, the tumour mass has produced angiogenic factors that stimulate the endothelial cells to grow toward the tumour cells. In step 3, the tumour has vascularized and capable of unlimited grow (Karp, 2008).

Naturally occurring inhibitors of angiogenesis are endostatin and thrombospondin. Biotechnology companies have developed various angiogenic inhibitors for cancer treatment studies. Development of angiogenic inhibitors are a promising cancer therapy because they do not interfere with normal physiological activities as angiogenesis is not a required activity in a mature adult. Besides that, angiogenic inhibitors act on cell lining of the bloodstream, which can directly accessible to blood-borne drugs, and should be effective against various types of tumours. Although angiogenic inhibitors were effectively inhibit tumour growths in preclinical studies on mice and rats, inhibiting angiogenesis in human tumours are far more complicated and difficult to achieve (Karp, 2008). To date, the best anticancer strategy is still prevention and early detection.

2.2 Innate Immune Responses

Innate immune responses are non-specific, quickly recognizing and responding to a broad range of microbes regardless of their actual identity. The most prominent defense mechanism is phagocytosis, the ingestion of invading microorganisms by phagocytes

(Campbell & Reece, 2005). Phagocytes, such as macrophages and dendritic cells mount the initial contact with any invading pathogens. These phagocytes possess a great variety of receptor proteins on their surface that can identify certain highly conserved macromolecules belonging to foreign viruses and bacteria. Several pathogen receptors have been identified, the most prominent of which are the Toll-like receptors (TLRs) (Karp, 2008).

Humans can express at least ten functional TLRs which are made up of transmembrane protein, and located on the surfaces or within certain cytoplasmic membranes of many distinct cell types. These receptors possess the ability to recognize the lipopolysaccharide or peptidoglycan components on the bacterial cell wall, the protein flagellin on the bacterial flagella, double-stranded RNA in replicating viruses, and unmethylated CpG dinucleotides on bacterial DNA. Activation of TLRs by pathogen-derived molecules leads to a series of signal transduction within the cell and eventually resulting in the activation of a variety immune defence response including the adaptive immunity. Therefore, agents or drugs that can stimulate the activity of TLRs are believed to be able to enhance the body's immune responses (Karp, 2008).

Innate immune responses to invading pathogens are always accompanied by the process of inflammation at the infected area, where fluid, cells, and dissolved substances leak out of the blood into the affected tissues. During inflammation, the body defense agents concentrate at the affected site, causing local redness, swelling, and fever (Campbell & Reece, 2005; Karp, 2008). Phagocytic cells will move to the affected area in response to the chemoattractants released at the site, recognize, engulf, and then destroy the pathogen. However, the process of inflammation must terminate in a timely manner as prolonged

inflammation results in damages to the body normal tissues and eventually lead to chronic diseases (Campbell & Reece, 2005).

Phagocytosis is not the sole mechanism in the innate immune response against extracellular pathogens. Epithelial cells and lymphocytes secrete a variety of antimicrobial peptides or defensins, which are able to bind to viruses, bacteria or fungi and destroy them. Besides that, blood contains soluble protein, called the complement which is able to bind and trigger destruction to the pathogen (Campbell & Reece, 2005).

On the other hand, innate immune response to intracellular pathogen is basically protected by a non-specific lymphocyte, called natural killer (NK) cell. NK cells are not phagocytic, but they attach to the infected cells, and induce apoptosis to the cells (Campbell & Reece, 2005). Normal cells possess surface molecules that protect them from being attacked by the NK cells. There is another type of innate antiviral response, which is initiated by the infected cell itself. The virus-infected cells secrete a substance, called type-1 interferons (interferon α and interferon β) into the extracellular space, where they bind to the surface of non-infected cells, rendering them resistant to infection (Karp, 2008).

Innate immune responses work closely with the adaptive immune response to accomplish the whole immune defence with the adaptive immunity, organisms are able to effectively destroy specific microorganisms, cancer cells and viruses (Campbell & Reece, 2005). Phagocytic cells and NK cells are two important elements for stimulating the much slower, more specific adaptive immune responses.

2.2.1 Macrophage

Phagocytes (macrophages, monocytes, dendritic cells, and neutrophils) are the key participants in the innate immune responses as they form the first line defense against

invading pathogens after the physical barriers provided by epithelial layers. Macrophages are ancient and phylogenetically-conserved, long-lived cells, which constitute about 5% of the circulating white blood cells. Macrophages originated from the blood monocyte in all multicellular organisms (Schepetkin & Quinn, 2006).

Based on Figure 2.6, a hematopoietic stem cell can give rise to myeloid progenitor cell and lymphoid progenitor cell. A myeloid progenitor cells can differentiate into various blood cells (e.g., erythrocytes, basophils, and neutrophils), macrophages, or dendritic cells. A lymphoid progenitor cells can differentiate into various types of lymphocytes, such as NK cells, T cells, or B cells. T-cell precursors migrate to the thymus where they differentiated into T cells; whereas B cells undergo differentiation in the bone marrow (Karp, 2008).

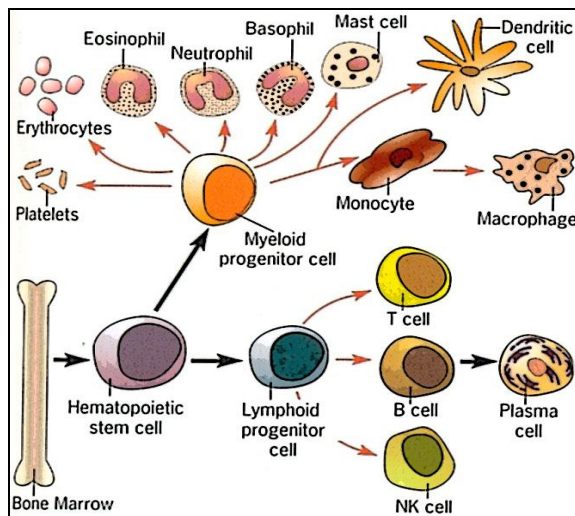


Figure 2.6: Differentiation pathway of a bone marrow hematopoietic stem cell (Karp, 2008)

Macrophages play an important role in the innate immune responses against foreign agents. Some macrophages patrol throughout the body, while others reside permanently in certain organs or tissues. (Campbell & Reece, 2005). The functions of macrophages include surveillance, chemotaxis, phagocytosis resulting in destruction to the targeted organisms,

such as fungi, bacteria, and virus-infected cells (Beutler, 2004). Besides that, macrophages are also involved in tissue remodeling during embryogenesis, wound repair, removal of cell debris or apoptotic cells and hematopoiesis (Klimp, de Vries, Scherphof, & Daemen, 2002; Lingen, 2001). In addition, macrophages act as antigen-presenting cells to T lymphocytes in order to activate the adaptive immune responses (Kinne, Brauer, Stuhlmüller, Palombino-Kinne, & Burmester, 2000). Therefore, macrophage is the key event for initiating adaptive immunity.

Activation of macrophages occurs when the host is stimulated by foreign pathogens or injury. Macrophages possess TLRs on the surface, which can recognize lipopolysaccharides and peptidoglycan present on the surface of foreign pathogens, such as bacterial cell wall. The overall activation is a complex system that requires a series of intracellular signaling events controlled by a variety of signaling enzymes, such as protein tyrosine kinases, phosphatidylinositol 3-kinase/Akt, mitogen-activated protein kinases (MAPKs), as well as various transcriptional factors, such as nuclear factor [NF]- κ B (Sekine *et al.*, 2006).

Activated macrophages function prominently in the host defense against neoplastic growth in experimental tumour systems (Kimoto *et al.*, 1998; Oršolić & Bašić, 2003). Upon activation, macrophages release numerous pro-inflammatory cytokines (e.g., tumour necrosis factor [TNF]- α and interleukin [IL]-1), chemokines and chemoattractants (e.g. IL-8 and monocyte chemoattractant protein [MCP]-1), as well as cytotoxic and inflammatory molecules (e.g., nitric oxide [NO], reactive oxygen species [ROS], and prostaglandin [PG] E₂). These secretory products are involved in the destruction of susceptible tumour cells and inhibition of DNA synthesis in target cells (Stuehr & Nathan, 1989). The production of cytokines, nitric oxide, and prostaglandin are mediated by the activation of the transcription

factor, NF- κ B. In addition, up-regulation of the surface levels of glycoprotein (e.g., costimulatory molecules [CD80 and CD86]) and adhesion molecules (e.g., selectins and integrins) of macrophages occurs simultaneously (Bresnihan, 1999; Burmester, Stuhlmuller, Keyszer, & Kinne, 1997; Gracie *et al.*, 1999).

Activation of macrophages are important in the field of imunomodulation as its secretory products involve in regulating activities of B- and T-cells (Oršolić, Knežević, Šver, Terzić, & Bašić, 2004). However, the overall event must be controlled and regulated delicately as excessive secretions of macrophages-derived inflammatory molecules are toxic to normal tissues and causes chronic inflammatory diseases, such as septic shocks, rheumatic arthritis, and arteriosclerosis (Gracie *et al.*, 1999; Michaelsson *et al.*, 1995; Stuhlmuller *et al.*, 2000). Therefore, effective regulations of macrophages are the key element for enhancing the body defense mechanisms.

2.2.2 Inflammatory responses

Inflammation is one of the primary responses to infection. Tissue injury or invading pathogen leads to the production of various chemical signals (e.g., histamine) that results in the initiation of localized inflammatory response. Histamine released by mast cell triggers dilation and increases permeability of nearby capillaries. Activated macrophages discharge additional chemical signals (e.g., prostaglandins) and pro-inflammatory molecules (e.g., NO and ROS) that promote blood flow to the injured site. Increased blood supply to the injured area results in local redness, heat, and swelling (Campbell & Reece, 2005).

Vascular changes during inflammation facilitate transportation of antimicrobial protein and clotting materials to the injured area. Chemokines secreted by blood vessel endothelial cells near the injured site attract the migration of macrophages to the injured

area and trigger phagocytosis. Blood clotting components aid in repairing the wound and blocking the spread of microbe to other parts of the body. Toxins from pathogens and chemical substances released by macrophages set the body's thermostat at a higher temperature, causing fever to the patient. Moderate fever can promote phagocytosis but sustainable high fever can be fatal (Campbell & Reece, 2005).

Local inflammation occurs with minor injury or infection. When severe tissue damages and infectious occur, the body mounts a systemic (widespread) inflammatory response. In this case, injured cells secrete various chemicals that induce the bone marrow to produce more neutrophils (Campbell & Reece, 2005). Neutrophils, a phagocytic leucocyte capable of carrying out a rapid, nonspecific attack on invading pathogens, normally present in the blood stream are stimulated to transverse the endothelial layer that lines the smallest veins (venules) in the region and enter the tissue. Members of leucocytes increase by several folds within several hours of the initial inflammation event (Campbell & Reece, 2005).

More serious bacterial infections can trigger an overwhelming systemic inflammatory response, known as septic shock. This condition is characterized by very high fever and low blood pressure which can lead to death (Campbell & Reece, 2005). Besides that, an overzealous inflammatory response can also leads to asthma, toxic shock syndrome, and respiratory distress syndrome (Karp, 2008). Literally, local inflammation is essential for healing but systemic inflammation is devastating.

2.2.3 Cytokines

Cytokines are regulatory polypeptides and low-molecular proteins produced by virtually all cells in response to the presence of appropriate stimuli (Thompson, 1998; Tu *et*

al., 2008). One of the most common stimuli is lipopolysaccharide (LPS) from gram negative bacteria, which stimulate, increased gene expression for various cytokines including TNF- α and IL-1 β (Evans, Kamdar, & Duffy, 1991) and inducible nitric oxide synthase (iNOS) which catalyzes the conversion of arginine to citrulline and secretes NO (Bogdan, 2001). TNF- α and IL-1 are two main cytokines involved in the initiation of inflammatory responses.

LPS binds to its specific receptor CD14 on the surface of macrophages, through LPS-binding plasma protein (Barbour, Wong, Rabah, Kapur, & Carter, 1998; Kim *et al.*, 2006) in order to elicit the pro-inflammatory signals. Exposure of LPS increases the expression of CD14 (Barbour *et al.*, 1998; Kim *et al.*, 2006) as well as its co-stimulatory molecules including CD40 (Grewal & Flavell, 1996), CD80, and CD86 also present on the surface of macrophage (Hathcock, Laszlo, Pucillo, Linsley, & Hodes, 1994). The gene expression for cytokines production is partly regulated by activated transcription factors, such as NF- κ B and AP-1 (Lantz, Chen, Solyom, Jolad, & Timmermann, 2005).

Cytokines plays a pivotal role in the immune system as many immune-related disease conditions are associated with the alterations in cytokine network, which may interfere with TH1/Th2-type immunity (Xing & Wang, 2000). The subclasses of T helper (CD4⁺) lymphocytes exhibit Th1 and Th2 cells which are responsible in secreting various cytokines. Mature Th1 cells synthesize IL-2, IFN- γ , and TNF- α , whereas Th2 cells generate IL-4, IL-5, IL-6, IL-9, IL-10. However, Th1 and Th2 cells do secrete the same cytokines such as IL-3, and GM-CSF (Mossman & Coffman, 1989; Rosmagnani, 1994).

Th1 and Th2-type cytokines play two distinct roles in the immune system. Th1-type cytokines are effective in eliminating cancer cells, whereas Th2-type cytokines inhibit the Th1-mediated anti-cancer activity (Gorelik, Prokhorova, & Mokyr, 1994; Takeuchi *et al.*,

1997). An imbalance between Th1 and Th2 cytokine productions can result in various infections and autoimmune diseases (Kmoníčková, Melkusová, Farghali, Holý, & Ziděk, 2007). For example, a shift from Th1 to Th2 predominance can promote progression of AIDS and deteriorate the conditions of HIV-infected patients (Clerici & Shearer, 1992; Klein *et al.*, 1997).

Since Th1/Th2 balance is significant in maintaining the homogeneity of the immune system, the manipulation of cytokine network has been the central paradigm for successful immunotherapy (Kmoníčková *et al.*, 2007). Although IL-2, IL-4, and IL-7 possess immunomodulatory properties to cure cancer patients, the research for new drugs that can modulate the cytokine productions has garnered attention in the immunopharmacological area. Table 2.1 shows the action of certain cytokine produced by macrophages.

Table 2.1: Action of certain cytokines produced by macrophages (Campbell & Reece, 2005)

Cytokine	Local Effects¹	Systemic Effects
Interleukin-1 (IL-1)	Tissue destruction; increase access off other leukocytes	Fever
Interleukin-6 (IL-6)	Stimulates adaptive immune response (antibody production)	Fever
Interleukin-8 (IL-8)	Chemotactic factors; attracts leukocytes including neutrophils to infected area	
Interleukin-12 (IL-12)	Activates NK cells; also induces CD4 T cells to differentiate	
Tumour-necrosis factor-alpha (TNF- α)	Increases permeability of blood capillaries in infected area	Fever; shock

¹ Most cytokines exert multiple effects; the cytokines listed here are the most relevant.

2.2.4 Nitric Oxide

Nitric Oxide (NO) has been implicated in various diseases such as cancer, rheumatoid arthritis, diabetes, liver cirrhosis, septic shock and cardiovascular diseases

(Lechner, Lirk, & Rieder, 2005). NO is an inorganic gaseous free radical synthesized by amino acid L-arginine in a reaction that requires oxygen and nicotinamide adenine dinucleotide phosphate-oxidase (NADPH) and catalyzed by the enzyme nitric oxide synthase (NOS) (Konkimalla, Blunder, Bauer, & Efferth, 2010). Two main types of distinguishable NOS are known. They are constitutive isoform (cNOS) and inducible nitric oxide synthase (iNOS).

Constitutive isoform, cNOS is subdivided into neuronal (nNOS) and endothelial (eNOS) NOS which is calcium-dependent and produce only low concentrations of NO for mediating tissue homeostasis (Min *et al.*, 2009). Sustainable NO release by cNOS is to actively vasodilate the vasculature in order to maintain normal blood pressure (Kim, Murakami, Nakamura, & Ohigashi, 1998). On the other hand, iNOS generates a large quantity of NO, plays an important role in various physiological and pathophysiological conditions such as tumoricidal, bactericidal, inflammatory and immunoregulatory activities (Ippoushi, Azuma, Ito, Horie, & Higashio, 2003; Konkimalla *et al.*, 2010).

Nitric oxide generated by iNOS defends against pathogens and regulates immune system, but overproduced NO by up-regulation of iNOS is known to be carcinogenic as high level of NO can result in mutagenesis through NO-mediated DNA damage, deamination of DNA bases or hindrance to DNA repair (Felley-Bosco, 1998). Absence of NO can even stimulate tumour growth and cancer metastasis through the promotion of migratory, invasive, and angiogenic activities of tumour cells (Murakami & Ohigashi, 2007; Perwez Hussain & Harris, 2007; Sawa & Oshima, 2006). Thus, excessive NO generations during chronic infection or inflammation can lead to carcinogenesis (Ippoushi *et al.*, 2003).

Overproduced intracellular NO usually reacts with superoxide anions resulting in the formation potent oxidizing and nitrating molecules such as peroxynitrite (ONOO⁻).

Peroxynitrite is reactive nitrogen species (RNS) which is toxic to mitochondrion as well as macromolecules such as DNA, proteins and lipids (Ippoushi *et al.*, 2003) and eventually, causing cell death to the surrounding tissues, destructing the tissue homeostasis (Coleman, 2001). Moreover, macrophages will further increase the NO and superoxide anion (O_2^-) production during inflammation, reacts spontaneously with each other to generate peroxynitrite (Ischiropoulos, Zhu, & Beckman, 1992; Xia & Zweier, 1997). Peroxynitrite formed activates two types of rate-determining enzymes for prostaglandin biosynthesis, known as the constitutive and inducible forms of cyclooxygenase (COX-1 and COX-2) during the inflammation conditions (Landino, Crews, Timmons, Morrow, & Marnett, 1996; Salvemini *et al.*, 1993). This reaction will lead to the incidence of chronic inflammation and eventually carcinogenesis.

Inducible nitric oxide synthase-stimulated NO production is known to be associated with the conversion of L-arginine to L-citrulline (Kerwin & Heller, 1994; Szabo, Mitchell, Thiemermann, & Vane, 1993). However, some L-arginine analogs have been reported as iNOS inhibitors which inhibit NO production in activated murine macrophages, such as aminoguanidine, N^G-nitro-L-arginine methyl ester (L-NAME), N-iminoethyl-L-ornithine (L-NIO) and N^G-nitro-L-arginine (L-NNA) (Kmoníčková, 2007; Liew *et al.*, 1991; Migliorini, G. Corradin, & S. Corradin, 1991).

Besides that, high-output of NO production due to iNOS activation is also correlated with the action of cytokines. Endotoxin and some cytokines such as interleukin and interferon are responsible for the expression of iNOS in macrophages (Kim *et al.*, 1998). The inhibitory effect of phytochemicals on NO generation and the underlying iNOS activity are associated with the suppression of specific cytokines such as TNF- α , IL-1, IL-6 or IL-10 (Jiang *et al.*, 2003; Radtke, Kiderlen, Kayser, & Kolodziej, 2004).

Nitric oxide is an important signaling molecule that can activate both pro- and anti-proliferative signal transduction pathway which is dependent to its concentration levels. The concentration of NO is critical as low levels of NO stimulate the growth of tumour cells, whereas high levels of NO are toxic to cells (Verma & Goldin, 2003). Phytochemicals NO inhibitors exhibit valuable therapeutic properties for immunomodulatory and anti-inflammatory responses (Konkimalla *et al.*, 2010). Several studies based on phytochemicals NO inhibitors have been shown to suppress the activation and translocation of the transcription factor NFκB from the cytoplasm to the nucleus. This indicates that NFκB is an important mediator for the NO inhibition pathway (Ko, Kuo, Wei, & Chiou, 2005).

Previous studies have indicated that tumours contain higher amounts of NO and iNOS as compared to normal tissues (Jang & Kim, 2002). Therefore, NO and iNOS is not only important for diagnosis and prognosis, but also potent as a target for novel therapeutic options (Hirst & Robson, 2007).

2.3 Adaptive Immune Responses

Adaptive or acquired immune response is highly specific and can differentiate between two very similar molecules. Unlike the innate immune system, adaptive immune system has a “memory” for previous infections. Besides that, adaptive immune responses do not act immediately as the innate immune responses. It requires a lag period to be activated in order to attack the foreign agents (Campbell & Reece, 2005).

Adaptive immunity can be divided into two categories, known as the humoral immunity and cell-mediated immunity. Both types of the immunity are mediated by lymphocytes, that circulate between the blood and lymphoid or organs. Humoral and cell-

mediated immunity are mediated by B and T lymphocytes, respectively (Karp, 2008). B and T cells are derived from the same precursor cells, called hematopoietic stem cell, but they differentiate in distinct pathways and lymphoid organs. B lymphocytes differentiate in fetal liver or adult bone marrow, whereas T lymphocytes differentiate in the thymus gland (Campbell & Reece, 2005; Karp, 2008).

In humoral immunity, B lymphocytes (B cells) differentiate into cells that produce antibodies when activated. Antibodies can effectively protect the body against foreign materials outside the body's cells (Karp, 2008). Antibodies act by binding to protein and polysaccharide components on the bacterial cell walls, bacterial toxins, and viral coat proteins. Antibodies function as "tags" that bind to the invading pathogens and mark them for destructions. Destructions are carried out by phagocytes or by complement molecules present in the blood. Some of the bacterial toxin and viral particle with attached antibodies are prevented from entering the host cell directly. However, antibodies are not effective against intracellular pathogens. Cell-mediated immunity is carried out by T lymphocytes (T cells), can specifically identify and kill an infected cells when activated (Campbell & Reece, 2005; Karp, 2008).

2.4 Cancer and Immunity

Defects and derangements in the innate and adaptive immune response lead to immunodeficiency, allergy, autoimmunity and immune-malignancies (Agarwal & Singh, 1999). Therefore, enhancement of the immunity is an effective preventive measure to resist diseases (Hackett, 2003; Lolis & Bucala, 2003).

Researches on innate immunity as of novel therapeutic strategies hold a great promise for combating various diseases. Since plant-derived immunomodulatory

compounds have been used extensively in traditional medicine, research on them are on the rise. These researches show that some of the plant-derived immunomodulators have been proved to possess the ability to modulate the macrophages activities, leading to various beneficial pharmacological effects (Schepetkin & Quinn, 2006).

An immunomodulator can be defined as biological or synthetic substance which can stimulate, suppress or modulate any component of the immune system, including both innate and adaptive arms of the immune response (Agarwal & Singh, 1999). This means that, immunomodulators exert biphasic effects. Some tend to boost the immune responses, while others tend to control or inhibit the activated immune responses to certain magnitude (Deharo, Baelmans, Gimenez, Quenevo, & Bourdy, 2004).

The search for new cancer treatment strategy has been one of the starting points in the field of immunomodulation. Plant-derived immunomodulatory polysaccharides, proteins, peptides, and lectins have been shown to possess immunomodulatory activities (Schepetkin & Quinn, 2006). Some of the plants with proven immunomodulatory activities are *Astragalus membranaceus* (Cho & Leung, 2007), *Brassica oleraceae* (Thejass & Kuttan, 2007), *Hibiscus cannabinus* (Lee *et al.*, 2007), *Piper longum* (Sunila & Kuttan, 2004), *Tinospora cordifolia* (Sonel & Kuttan, 1999), *Withania somnifera* (Davis & Kuttan, 2000), etc.

2.4.1 Immunomodulators

Immunomodulators can be categorized into three main classes according to the clinical perspective, known as immunoadjuvants, immunostimulants, and immunosuppressant. Immunoadjuvants, also known as specific immune stimulants are prominently used to enhance the efficacy of vaccines. These agents are important in aiding

the development of new vaccines, however, the lack of availability of appropriate immunoadjuvant has been the major stumbling stone for producing effective vaccines (Agarwal & Singh, 1999). One of the popular immunoadjuvant is Freund's adjuvant, but it is not suitable for human use due to the presence of Bacillus Calmette Guiren (BCG) (Claassen, de Leeuw, de Greeve, Hendriksen, & Boersma, 1992).

Immunostimulants are envisaged for augmenting the host immune responses against foreign pathogens. The agents are also known as non-specific immunostimulants, which can enhance both arms of the innate and adaptive immune responses. Immunostimulants are expected to serve as preventive agents that augment the immune responses against infectious agents in a healthy individual. These agents hold a promise as immunotherapeutic agents for immune deficiencies patients (Agarwal & Singh, 1999).

Immunosuppressants are implied for controlling pathological immune response in autoimmune diseases, graft rejection, graft versus host diseases, immediate or hypersensitivity immune reaction, as well as immune pathology associated with infections. It is used extensively in the prevention of graft rejection as well as treatment of autoimmune diseases (Agarwal & Singh, 1999).

The search for a safe and effective compound with immunomodulatory properties for clinical use has become a major goal of many research laboratories since the immune system plays the fundamental roles in host defense against pathogens as well as surveillance against tumours. Different immunomodulators can affect the immune responses at various levels, either to promote or to depress the ability to mount an immune system, or to defend against pathogens or tumours (Cho & Leung, 2007).

2.5 Natural Products and Phytochemicals

Plants contains of a wide variety of biologically active phytochemicals which have been consumed as dietary agents and many have been applied in traditional medicines for thousands of years (Aggarwal & Shishodia, 2006). Several population-based studies indicate that populations with colon, gastrointestinal, prostate and breast cancers in South East Asia countries are lower than the Western counterparts (Dorai & Aggarwal, 2004). Epidemiological studies show that the appearance in cancer incidences between South East Asia and Western countries are strongly believed to cause by environmental factors, particularly the differences of diet intake between both populations (Karp, 2008).

There is a general consensus among epidemiologists, indicating that diet which possesses high amount of animal fats and alcohol increases the risks of cancer development, whereas fruits, vegetables or tea reduce the risks (Karp, 2008). Indeed, many fruits, vegetables and herbs rich in phytochemicals have been proven to possess cancer chemopreventive activities, both *in vitro* and *in vivo* (Kim, Chun, Kundu, & Surh, 2004; Mahmoud *et al.*, 2000; Murakami *et al.*, 2004; Surh, 1999). According to Cragg and Newman (2000), more than 50% of the anti-cancer drugs applied in clinical trials were isolated from natural products. Hence, the search for anti-cancer drugs from natural products is one of the most prominent researches for cancer treatment.

2.6 Zingiberaceae

Zingiberaceae, or the ginger family is a family of flowering plants with perennial herbs, rarely epiphytic, and mostly with creeping horizontal or tuberous rhizomes. The stems of the plants are usually short, replaced by pseudostems derived from leaf sheaths. The leaves are alternate and distichous, those that grow towards the base are bladeless and

reduced to sheath, and the blades are mostly linear to elliptic with penni-parallel, strongly ascending veins. *Zingiberaceae* species grow naturally in damp, shaded parts of low-land or hill slopes, as scattered plants or thickets (Yap *et al.*, 2007).

Zingiberaceae species are among the most prolific plants in the tropical rain forest (Ruslay *et al.*, 2007). The *Zingiberaceae* family comprises of about 50 genera and 1300 species that are distributed throughout the tropics, especially in the Southeast Asia. Some species can be found in America and the tropics of Africa (Wu & Kai, 2000). The Peninsular Malaysia, is estimated to consist of approximately 150 species of the ginger with 23 genera (Holtom, 1950).

The rhizomes of *Zingiberaceae* are usually spicy, and are widely used around the world as an important spice or flavouring agents in culinary. Members of the family which are commonly cultivated for these purposes are *Zingiber officinale*, *Curcuma longa*, and *Zingiber zerumbet*, etc. Some species are widely cultivated as ornamental plants, namely *Alpinia speciosa*, *Alpinia purpurata*, *Hedychium coronarium* Koenig, the ginger lily, etc (Lock, 1985). *Zingiberaceae* plants are also well-known as the medicinal plants in Asia, the Ayurveda, and Chinese medical systems since thousands of years ago (Kala, 2006). The rhizomes of various ginger exhibit health-promoting effects that have been utilized for ailments, such as stomach, diarrhea, digestive disorder, rheumatism, swelling, common cold and cough (Yap *et al.*, 2007).

Zingiberaceae species consist of a great variety of chemical constituents which vary based on the place of origin, weather as well as whether the rhizomes are fresh or dried (Ali, Blunden, Tanira, & Nemmar, 2008). Some phenolic compounds present in most of the *Zingiberaceae* plants, possess strong anti-inflammatory and anti-oxidative properties and are potent in inducing anti-oxidative and anti-mutagenic activities (Surh, 2002; Surh, E.

Lee, & J. Lee, 1998; Surh *et al.*, 1999). These phytochemicals are believe to work potentially in the suppression of transformation, hyperproliferation, and inflammatory activities, all of which are crucial in initiating carcinogenesis, angiogenesis and metastasis (Shukla & Singh, 2007).

2.6.1 *Alpinia galanga*



Figure 2.7: Rhizome of *Alpinia galanga*

The herb *A. galanga* is distributed in South and Southeast Asian countries. It is commonly known as greater galangal, blue ginger or Thai ginger, and lengkuas in Malaysia. The rhizome of this plant (Figure 2.7) is globally used as a spice or ginger substitute for flavouring foods, especially soup and curry. In addition to the culinary uses, the rhizome has been used as in traditional medicine as stomachic, carminative, antifatulent, antifungal and anti-itching agents (Kaur *et al.*, 2010).

Scientists have studied on the rhizome of *A. galanga* and found that it exhibits various biological activities, such as antifungal, antibacterial, antimycobacterial, antiviral, anticancer, antitrypanosomal etc. The main compounds found in the rhizome are phenylpropanoids, and most abundantly of which are 1'S-1'-acetoxychavicol acetate (Chappuis *et al.*, 2007), 1'S-1'-acetoxyeugenol acetate (Laguna, 2003), and p-coumaryl

diacetate (Desjeux, 2001) etc. Most of the biological activities are due to the presence of phenylpropanoids (Kaur *et al.*, 2010).

2.6.2 *Boesenbergia rotunda*



Figure 2.8: Rhizomes of *Boesenbergia rotunda*

The perennial herb *B. rotunda* is the most abundant *Boesenbergia* species found in Malaysia and is locally known as Temu kunci. It is a herbaceous plant with short and slender rhizomes. The rhizomes (Figure 2.8) which have a characteristic aroma and slightly pungent in taste, are usually used as food ingredients in Southeast Asia.

In the olden days, it is a medicinal plant for several disease treatments, such as aphthous ulcer, dry mouth, stomach discomfort, leucorrhea and dysentery. Besides that, the rhizomes are given as tonics to women after childbirths, or applied in lotions for rheumatism and muscular pains, and into pastes for application to the body after confinement (Burkill, 1935). The biological properties of *B. rotunda* includes antimutagenic, antitumor, antibacterial, antifungal, analgesic, antipyretic, antispasmodic, anti-inflammatory and insecticidal activities (Cheenpracha, Karalai, Ponglimanont, Subhadhirasakul, & Tewtrakul, 2005).

2.6.3 *Curcuma aeruginosa*



Figure 2.9: Rhizomes of *Curcuma aeruginosa*

Curcuma aeruginosa is a native tropical plant of the Southeast Asia, especially Myanmar, Cambodia, Vietnam, Malaysia, Indonesia and Thailand (Sirirugsa, 1992). It is commonly known as blue or pink ginger in English, temu hitam in Malaysia, and waan-maa-haa-mek or kajeawdang in Thailand (Thaina, Tungcharoen, Wongnawa, Reanmongkol, & Subhadhirasakul, 2009). Fresh rhizome of the plant (Figure 2.9) emits a mild ginger-like aroma (Srivastava *et al.*, 2006).

In traditional medicines, the rhizome of *C. aeruginosa* has been used for gastrointestinal remedies in the treatment of asthma, cough, scurvy, mental derangement, diarrhea and colic, used in women for postpartum care, uterine involution, treatment of uterine pain and uterine inflammation (Perry, 1980). It is regarded as an active ingredient in many Thai herbal preparations as a tonic to alleviate irregular, painful or excessive menstruation in female and for uterine pain or dysfunction (Pongbunrod, 1979). It is also considered as a depurative which can be used both internally and externally for treating exanthema and act as a poultice for itching (Perry, 1980).

2.6.4 *Curcuma domestica*



Figure 2.10: Rhizomes of *Curcuma domestica*

The dried ground rhizome of *C. domestica* (Figure 2.10) is commonly known as turmeric in English, haldi in Hindi, ukon in Japanese, and kunyit in Malaysia and Indonesia (Sharma, Gescher, & Steward, 2005). Turmeric is used extensively in foods for its aromatic, flavouring and yellow colouring properties.

Turmeric has been used in Asian medicine since the second millennium BC (Brouk, 1975). It has a long history of traditional uses in Chinese and Ayurvedic medical systems for the treatments of flatulence, jaundice, menstrual difficulties, hematuria, hemorrhage, and colic. Dietary consumption of turmeric in certain Southeast Asia communities is as high as 1.5g per person, however, smaller quantities of turmeric tend to be used for medicinal purposes (Eigner & Sholz, 1999).

The active principle identified in turmeric is curcumin which has been shown to exhibit antioxidant, anti-inflammatory, antimicrobial, and anti-carcinogenic activities. Besides that, it also possesses hepatoprotective and nephroprotective activities, thrombosis suppression, protects against myocardial infarction, as well as hypoglycemic and anti-

rheumatic properties (Anand *et al.*, 2008). Chemical structure of curcumin is shown in Figure 2.11.

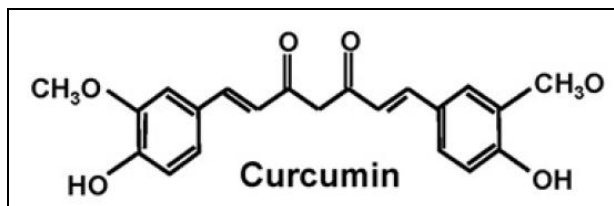


Figure 2.11: Chemical structure of curcumin (Anand *et al.*, 2008)

2.6.5 *Curcuma mangga*



Figure 2.12: Rhizomes of *Curcuma mangga*

Curcuma mangga is widely distributed throughout South India. It has been first reported by Balakrishnan and Bhargaya (1984) from the Andaman Islands. It is a bush perennial and has stalk rhizomes (Figure 2.12). The flesh of the rhizome is yellowish in the outer layer, and light yellow in the center layer.

The rhizome has a unique characteristic of raw mango taste, and because of that the plant is also known as mango ginger. It is also called white turmeric in English and temu pauh in Malaysia. The rhizomes of *C. mangga* are usually used as a spice to pickle foods in South India. In addition to its culinary uses, the rhizomes are utilized in traditional

medicines as a stomachic for the treatments of chest pains, fever, general debility, as well as aid in womb healing (Suhaila, Suzana, Saleh, Ali, & Sepiah, 1996).

2.6.6 *Curcuma xanthorrhiza*



Figure 2.13: Rhizomes of *Curcuma xanthorrhiza*

Curcuma xanthorrhiza is commonly known as false turmeric in English, temu lawak in Malaysia and Javanese turmeric in Indonesia. When the rhizome is cut, the flesh is orange in colour with a characteristic aroma. The rhizome of *C. xanthorrhiza* (Figure 2.13) is popularly used as an ingredient for preparing traditional health supplements, known as ‘jamu’ and ‘maajun’, or used individually as a remedy for certain health problems. The juice made from the rhizome of the plant is used as a remedy for indigestion, constipation, bloody diarrhea, dysentery, rheumatism, or applied to the body after childbirth (Hwang, Shim, & Pyun, 2000; Ruslay *et al.*, 2007), asthma and respiratory disorders in traditional medicines (Ikawati, Wahyuono, & Maeyama, 2001). Moreover, the syrup made from the rhizome is used as appetizer for the children.

2.6.7 *Kaempferia galanga*



Figure 2.14: Rhizomes of *Kaempferia galanga*

Kaempferia galanga is commonly known as sand ginger in English, proh hom in Thai (Kanjapothi *et al.*, 2004), Shan-nai in Chinese (Perry & Metzger, 1980), kencur in Indonesia, and cekur in Malaysia. It is an acaulescent perennial aromatic rhizomous herb (Figure 2.14) that grows in Southern China, Indochina, Malaysia, and India (Kanjapothi *et al.*, 2004). It is globally used as a spice, food favouring agent, and an ingredient for ‘jamu’ preparation, which is a local tonic consumed by the Malays (Othman, Ibrahim, Mohd, Mustafa, & Awang, 2006).

The rhizome of *K. galanga* is well recognized as carminative, diuretic, aromatic stomachic, insecticidal, and incense (Huang, Yagura, & Chen, 2008). The aromatic essential oil from the rhizomes is valuable for perfumery industry (Chithra, Martin, Sunandakumari, & Madhusoodanan, 2005). It possesses a strong characteristic balsamic aroma, has a long history in fragrance use for the alleviation of stressfulness, restlessness, anxiety and depression. In Japan, it has been utilized as one of the main ingredients in scent bag, which is useful in improving sleep, relaxation and minimizing stress (Huang, Yagura, & Chen, 2008).

Besides that, the rhizomes contain essential oils and have been used traditionally in a decoction or powder for indigestion, cold, pectoral and abdominal pains, headache and toothache (Kanjapothi *et al.*, 2004), hypertension, asthma and inflammatory tumours (Huang *et al.*, 2008). The alcoholic maceration of the rhizome has been applied as liniment for rheumatism. In addition, the rhizome extract is also useful for the treatments of skin diseases, wounds, spleen disorders, cough, and pectoral afflictions (Chithra *et al.*, 2005).

The herbs exhibit a broad spectrum of pharmacological and biological activities, such as larvicidal (Kiuchi, Nakamura, Tsuda, Kondo, & Yoshimura, 1988), amebicidal (Chu, Miles, Toney, Ngyuen, & Marciano-Cabral, 1998), antibacterial (George & Pandalai, 1949), antimicrobial (Gupta & Banerjee, 1976), antifungal, antiviral (Vimala, Norhanom, & Yadav, 1999), anticancer (Kosuge *et al.*, 1985), antioxidant (Gupta & Banerjee, 1976), vasorelaxant active, anti-inflammatory and smooth muscle relaxant effects (Othman, Ibrahim, Mohd, Mustafa, & Awang, 2006).

2.6.8 *Zingiber montanum*



Figure 2.15: Rhizomes of *Zingiber montanum*

Zingiber montanum is probably native to India but is now widely cultivated in tropical Asia. It is also a popular home-garden plant in Southeast Asia. It is commonly

known as bonglai in Malaysia. The rhizomes (Figure 2.15) are used as a spice and food flavouring agent in culinary due to its characteristic aroma.

Besides that, it is a medicinal plant that popularly applied in traditional medicines for various common sicknesses. It acts as a carminative and stimulant for stomach, as well as used to treat diarrhea and colic. In Thai traditional medicine, the consumption of the rhizomes can help in relieving asthma as well as muscle and joint pain (Bua-in & Paisooksantivatana, 2009). It was also applied to paralysis in the olden days.

2.6.9 Zingiber officinale



Figure 2.16: Rhizomes of *Zingiber officinale*

Ginger (*Zingiber officinale*) is the most popular species in the family of Zingiberaceae, which has been cultivated for thousands of years as a spice as well as for medicinal purposes in South East Asian countries (Park & Pizzuto, 2002). Ginger rhizome (Figure 2.16) is a very common condiment in culinary for preparing vegetable and meat dishes and as a flavouring agent in beverages, especially in countries such as India and China (Shukla & Singh, 2007). It is also consumed directly as fresh paste, dried powder, slices preserved in syrup or flavouring tea. Nowadays, ginger rhizome is widely

commercialized in food industries as candy, crystallized ginger chips, ginger crackers, ginger tea, ginger beer, ginger soother, ginger oil, pickled ginger etc.

Ginger rhizome has been used extensively in China and India as a traditional medicine since ancient times (Altman & Marcussen, 2001). It has been a popular ingredient among Chinese, Ayurvedic and Tibb-Unani herbal medicines for treating a great range of disease such as colds, flu-like symptoms, nausea, headaches, toothache, constipation, painful menstrual period, catarrh, rheumatism, nervous disease, gingivitis, toothache, asthma, stroke and diabetes (Awang, 1992; Grant & Lutz, 2000; W. Wang & Z. Wang, 2005).

Besides that, ginger rhizome is also applied in herbal medicine practice for the treatment of rheumatoid arthritis and muscular discomfort in Western countries (Bordia, Verma, & Srivastava, 1997; Langner, Greifenberg, & Gruenwald., 1998). Based on its variable health-protective effects, it has been studied greatly as botanical dietary supplement in USA and Europe, particularly in the treatment of inflammatory diseases (Aggarwal & Shishodia, 2004; Park & Pizzuto, 2002; Srivastava & Mustafa, 1992).

Ginger extracts have been scientifically proven to possess anti-inflammation (Mascolo, N. Jain, R. Jain, Capasso, 1989; Penna *et al.*, 2003; Zhou, Deng, & Xie, 2006), anti-emesis (Sharma & Gupta, 1998), analgesic effect (Mascolo *et al.*, 1989; Young *et al.*, 2005), anti-tumour (Katiyar, Aggarwal, & Mukhtar, 1996) and anti-oxidant (Masuda, Kikuzaki, Hisamoto, & Nakatani, 2004) properties. In addition, its major pungent constituent, [6]-gingerol (1-[4' -hydroxy-3' -methoxyphenyl]-5-hydroxy-3-decanone) (Figure 2.17) has been reported to possess interesting biochemical activities in inhibiting of cyclooxygenase pathway and lipoxygenase pathway (Lee & Surh, 1998).

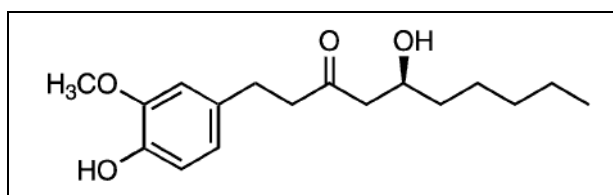


Figure 2.17: Chemical structure of [6]-gingerol (Miyoshi *et al.*, 2003)

2.6.10 *Zingiber zerumbet*



Figure 2.18: Rhizomes of *Zingiber zerumbet*

Zingiber zerumbet, a wild ginger in the Zingiberaceae family is commonly known as lempoyang in Malaysia. It has important economic properties as the plants are widely used in various fields, including culinary, gardening as well as traditional medical systems. The “pine cones” of the plant are popularly used as an ornamental in gardening, and the milky juice from the pine cones is used as a shampoo in Hawaii (Chien, Chen, C. Lee, F. Lee, & Wang, 2008).

In traditional medical systems, fresh rhizomes of the plant (Figure 2.18) are consumed as an appetizer (Ruslay *et al.*, 2007). It is also employed to relieve stomachache, as a diuretic, and becomes depurative when macerated in alcohol (Songsiang, Pitchuancom, Boonyarat, Hahnvajanawong, & Yenjai, 2010). Studies have shown that *Z.*

zerumbet plays a significant role in anti-allergic effects (Tewtrakul & Subhadhirasakul, 2007), and well recognized as antifatulent and anti-inflammatory agents.

The major component in the rhizome of *Z. zerumbet* is a crystalline sesquiterpene, called zerumbone (Figure 2.19), which is also readily available from a widespread of natural sources (Songsiang *et al.*, 2010). Zerumbone has been studied for various biological activities since it possesses promising anti-cancer properties. It acts to suppress tumour promoters (Murakami *et al.*, 2002) and has been slow down to inhibit the proliferation of human leukemia cell lines (Huang, Chien, & Wang, 2005). In addition, it is also an anti-proliferative and anti-platelet activating factor (Jantan, Rafi, & Jalil, 2005), and possesses anti-HIV activities (Dai, Cardellina, McMahon, & Boyd, 1997).

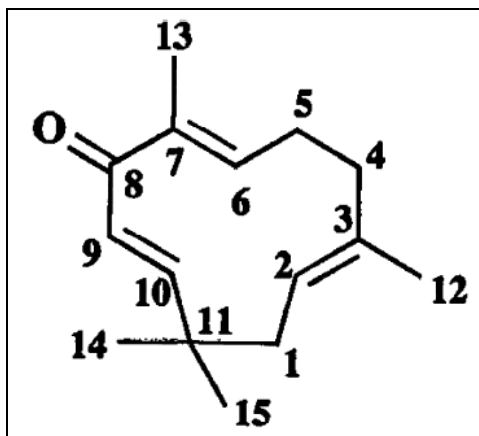


Figure 2.19: Chemical structure of zerumbone (Tanaka *et al.*, 2001)

2.7 *In Vitro* Nitric Oxide Assay for Assessment of Immunomodulatory Agents

Nitric oxide has been implicated with various diseases including cancer (*refer* section 2.2.4). Assessment of NO synthesis is of particular interest because NO level strongly correlates with the status of L -Arginine/NO pathway (Tsikas, 2007).

The NO assay is the most frequently used method for analysis of nitrite and nitrate concentrations based on the Griess reaction. Johann Peter Griess (1822-1888), a German chemist originally reported the Griess reaction as a diazotization reaction in 1879. In the original work, nitrite reacts with sulfanilic acid under acidic conditions, i.e. nitrous acid to form a diazonium ion which couples to form a readily water-soluble, red-violet coloured azo-dye (Tsikas, 2007).

In this study, immunomodulatory effects of *Zingiberaceae* extracts on NO generation in macrophages cells, RAW 264.7 was assessed using *in vitro* NO assay. In the *in vitro* NO assay, the nitrite levels in culture supernatant as an index of NO generation is measured using Griess reaction (Green *et al.*, 1982). In the Griess reaction, nitrate is to reduce to nitrite prior to diazotization. The colorimetric change can be quantified spectrophotometry and correlated with nitrite concentrations.

2.8 *In Vitro* Assays of Angiogenesis for Assessment of Anti-metastatic Agents

Endothelial cells are specialized epithelial cells that form the inner layer of blood vessels. These cells play a key role in angiogenesis which involves matrix degradation, migration, proliferation, and morphogenesis (Figure 2.4) eventually resulting in cancer metastasis. Numerous *in vitro* techniques have been introduced to assess the functions of endothelial cells (Table 2.2).

Continuous cell proliferations with the increasing survivals supply the cells for generating new vessel. Effects of anti-angiogenic factors on proliferation can be determined through direct cell counts, thymidine or BrdU incorporation (quantification of DNA synthesis), or MTT assay (assessment of metabolic activity) (Goodwin, 2007). As cell migration is required for both tumour invasion and tumour angiogenesis, it is of particular

interest in the search of anti-cancer therapeutic agents (Eccles, 2004). Assays that allow measurement of cell migration include scratch wound assay, Transwell or Boyden chamber assay, and under-agarose assay. In this study, effects of *Zingiberaceae* extracts on proliferation and migration of breast cancer cells, MDA-MB-231 were assessed using MTT assay and scratch wound assay, respectively.

Table 2.2: *In vitro* assays of angiogenesis (Goodwin, 2007)

Assay	Angiogenic functions assed
<i>Endothelial cell assays</i>	
Zymogen assay	Matric degradation
Scratch wound assay	Migration
Transwell/Boyden chamber assay	Migration
Under-agarose assay	Migration
Cell counting	Proliferation
Thymidine incorporation	Proliferation
BrdU incorporation	Proliferation
MTT assay	Proliferation
TUNEL assay	Apoptosis
Annexin V assay	Apoptosis
On-Matrigel assay	Morphogenesis
In-collagen/Matrigel assay	Morphogenesis
Collagen sandwich assay	Morphogenesis
Matrix invasion assay	All
Microbead assay	All
<i>Stem cell and organ culture assays</i>	
Embryoid body assay	All
Aortic ring assay	All
Mouse metatarsal assay	All

The MTT colorimetric assay measures the mitochondria activity as a mean of number of viable cells. Active mitochondria in viable cells convert the yellow, soluble tetrazolium salt [3-(4,5-dimethylthiazol-2-yl)-2,5-diphenyltetrazolium bromide] (MTT) into an insoluble, purple formazan precipitate (Denizot & Lang, 1986; Mosmann, 1983). Tetrazolium salts accept electrons from oxidized substrates or enzymes, such as NADH and

NADPH. Particularly, MTT is reduced at the ubiquinone and cytochrome b and c sites of the mitochondrial electron transport system and is due to succinate dehydrogenase activity. This reaction converts the yellow salt to purple formazan which can be dissolved in organic solvent, such as dimethyl sulphoxide (DMSO). The colorimetric change can be quantified using spectrophotometry and correlated with cell viability (S. Ahmad, A. Ahmad, Schneider, & White, 2006; Trevisi, Pighin, Bazzan, & Luciani, 2006).

In the scratch wound assay, a wound is created on the monolayer confluent cells using a pipet tip, needle, or cell scraper. Since cell filling the cleared area may be due to both migration and proliferation, the migration effect can be accentuated by using anti-proliferation agents or using 0-1% serum media (Choi *et al.*, 2009; Goodwin, 2004; Shanmugaraj *et al.*, 2010). This assay can be quantified by measuring the distance of the wound closure in a time-dependent manner. Both MTT assay and scratch wound assay are well-adapted for large-scale screenings.

2.9 Solvent Extraction for Specific Phytochemical Groups

Solvent extraction is the most popular extraction method used in preparing crude extracts from natural products. Decisions have to be made in selecting appropriate solvents for extraction in order to acquire desirable active compounds. However, in most cases, there is no preconception about the chemical nature of the active compounds that are being sought. One approach for solving this problem is to extract the plant samples with a series of solvents with increasing polarity, in order to acquire different classes of chemical compounds for screening assays. This is based on the basic principles of 'like dissolves like', where non-polar solvents will extract out non-polar substances, whereas polar solvents will extract out polar substances. Generally, the main groups of compounds are fixed oils,

fats and waxes, volatile or essential oils, carotenoids, alkaloids, glycosides, aglycones, phenolic compounds, polysaccharides and proteins (Houghton & Raman, 1998). Table 2.3 shows the types of phytochemicals extracted by different solvents used.

Table 2.3: Types of phytochemicals extracted by different solvents (Houghton & Raman, 1998)

Polarity	Solvent	Chemical class extracted			
Low	Light petroleum	Waxes	Fats	Fixed oils	Volatile oils
	Hexane	Waxes	Fats	Fixed oils	Volatile oils
	Cyclohexane	Waxes	Fats	Fixed oils	Volatile oils
	Toluene	Alkaloids	Fats	Fixed oils	Volatile oils
	Chloroform	Alkaloids	Aglycones		Volatile oils
Medium	Dichloromethane	Alkaloids	Aglycones		Volatile oils
	Diethylether	Alkaloids	Aglycones		
	Ethylacetate	Alkaloids	Aglycones	Glycosides	
	Acetone	Alkaloids	Aglycones	Glycosides	
	Ethanol			Glycosides	
High	Methanol	Sugars	Amino acids	Glycosides	
	Water	Sugars	Amino acids	Glycosides	
	Aqueous acid	Sugars	Amino acids		Bases
	Aqueous alkali	Sugars	Amino acids		Acids

2.10 Soxhlet Extractor System

Sample preparation is a time-consuming step but is a necessity for analytical process, particularly when solid samples are involved. Solid samples cannot be analyzed directly with analytical instruments and it is therefore, required to transfer the respective analytes to a liquid phase (Luque de Castro & Priego-Capote, 2009). Solvents used in extractions are selected based on the types of phytochemicals needed to be obtained. The plant samples to be extracted are pre-dried to avoid the presence of water in the extracts.

Solvent extraction of solid samples, which is commonly known as solid-liquid extraction, or more appropriately named as leaching or lixiviation in term of physicochemical, is one of the oldest techniques of solid sample preparation. Leaching

process is commonly done by maceration using appropriate solvents with the aids of heat or agitation to increase its efficiency in solubility and the rate of mass transfer. It plays an important role in extracting targeted compounds from insoluble high-molecular-weight fractions as well as removing compounds that could actually interfere with the analytical process (Luque de Castro & García-Ayuso, 1998). Soxhlet has been the most applied leaching technique.

Soxhlet extractor was developed by von Solvent in 1879 (Soxhlet, 1879), and has been used as a standard leaching technique for over a century. Soxhlet extraction methods remain as the predominant reference for measuring the performance of other leaching techniques. The advantages and limitations of soxhlet extraction has been served as the starting points for the development of more advanced leaching techniques with a variety of modifications in order to minimize the shortcomings but at the same time keeping or even improving the former (Luque de Castro & Priego-Capote, 2009).

Conventional soxhlet extraction was originally used to determine fat in milk (Soxhlet, 1879). The conventional soxhlet extractor is composed of three separate component, namely solvent container, sample compartment and reflux condenser. In this method, the solid sample is placed in a thimble at the sample compartment that is gradually filled with fresh solvent from the solvent container. The liquid collected in the sample compartment will aspirate through the siphon when it reaches the over-flow level, and drips into the solvent container, thus carrying extract analytes into bulk liquid. This process is repeated until the extraction is completed. Soxhlet extraction is said to be a continuous-discrete technique due to its characterized operation. Since the solvent is being recycled to percolate the sample, the extraction system also functions in a continuous manner somehow (Luque de Castro & García-Ayuso, 1998).

Conventional soxhlet extraction (Figure 2.20) has been the best leaching technique used for a long time. However, improvement of the conventional extractor by fixing it with modern technologies allows its adaptation for the present necessities. During the past decades, a variety of modifications were made to the former Soxhlet extractor in order to reduce the leaching times with the use of auxiliary energies and automating the extraction procedures. Varieties of more advanced soxhlet extractor system are now available, such as high-pressure soxhlet extraction, automated soxhlet extraction, ultrasound-assisted soxhlet extraction as well as microwave-assisted soxhlet extraction.



Figure 2.20: Conventional Soxhlet extractor system

CHAPTER 3

3.0 MATERIALS AND METHODS

3.1 Plant Materials

Ten local medicinal plants in the Zingiberaceae family, namely *A. galanga*, *B. rotunda*, *C. aeruginosa*, *C. domestica*, *C. mangga*, *C. xanthorrhiza*, *K. galanga*, *Z. montanum*, *Z. officinale*, and *Z. zerumbet* were selected for *in vitro* screening tests. Fresh rhizomes of the selected Zingiberaceae species were bought from Chow Kit Market, Kuala Lumpur, Malaysia. These plants were identified macroscopically.

3.2 Preparation of Plant Extracts

Ten selected species of fresh Zingiberaceae rhizomes were washed with water, cut into small pieces and dried in an oven (Memmert) at 50°C for three days. Dried rhizomes were ground into fine powder using a commercial blender (Waring). The plant samples were extracted using the conventional Soxhlet extractor system (Houghton & Raman, 1998). 20 g of each sample was weighed (Kern 440-49N) and placed in a porous cellulose thimble (Whatman) in a sample compartment (central compartment) with a siphoning device and side-arm both connected to the distillation flask (lower compartment). The solvent was placed in the distillation flask and a reflux condenser (upper compartment) was attached above the sample compartment. Each plant sample was extracted using petroleum ether (Merck), chloroform (Merck) and methanol (Merck) sequentially at their respective boiling points.

Firstly, the flask containing petroleum ether was heated at 45°C using a heating mantle (Topo). The solvent evaporated when the temperature reached its boiling point. The vapour moved up into the central compartment through the side arm, where it was

subjected to condensation due to the cooling effect from the reflux condenser. Then, the vapour condensed, transferred to the liquid phase and dripped into the sample in the thimble. The solvent percolated through the sample and when the liquid exceeded the overflow level, the siphon aspirated the solute from the sample compartment and unloaded it back to the distillation flask. The process was repeated until a colourless extraction liquid was observed in the central compartment.

At the end of the extraction process, which usually lasted for a few days, the resultant extraction liquid in the distillation flask was subjected to evaporation using a rotary evaporator (Buchi). After the implementation of rotary evaporation, crude extract of petroleum ether were obtained. The crude extract was then kept in a specimen tube wrapped with aluminium foil, and left in the fume cupboard (Labconco) for further evaporation in order to remove all the solvent, until it became solid form. Finally, the crude extract was weighed and the yield was calculated according to the equation (Eq)

$$\text{Yield (\%)} = \frac{\text{Weigh of concentrated extract}}{\text{Weigh of sample in the thimble (20 g)}} \times 100$$

Eq. (1)

The crude extract in the specimen tube was enclosed with a stopper and kept in the refrigerator (Whirlpool) at 4°C.

The thimble together with the sample was dried in the fume cupboard when the extraction using petroleum ether was done. When the thimble and the plant sample were completely dried, the same procedure was carried out using chloroform and eventually, methanol at their boiling temperatures, 62°C and 65°C, respectively. Flow chart of the plant extraction procedure using petroleum ether, chloroform, and methanol is shown in Figure 3.1.

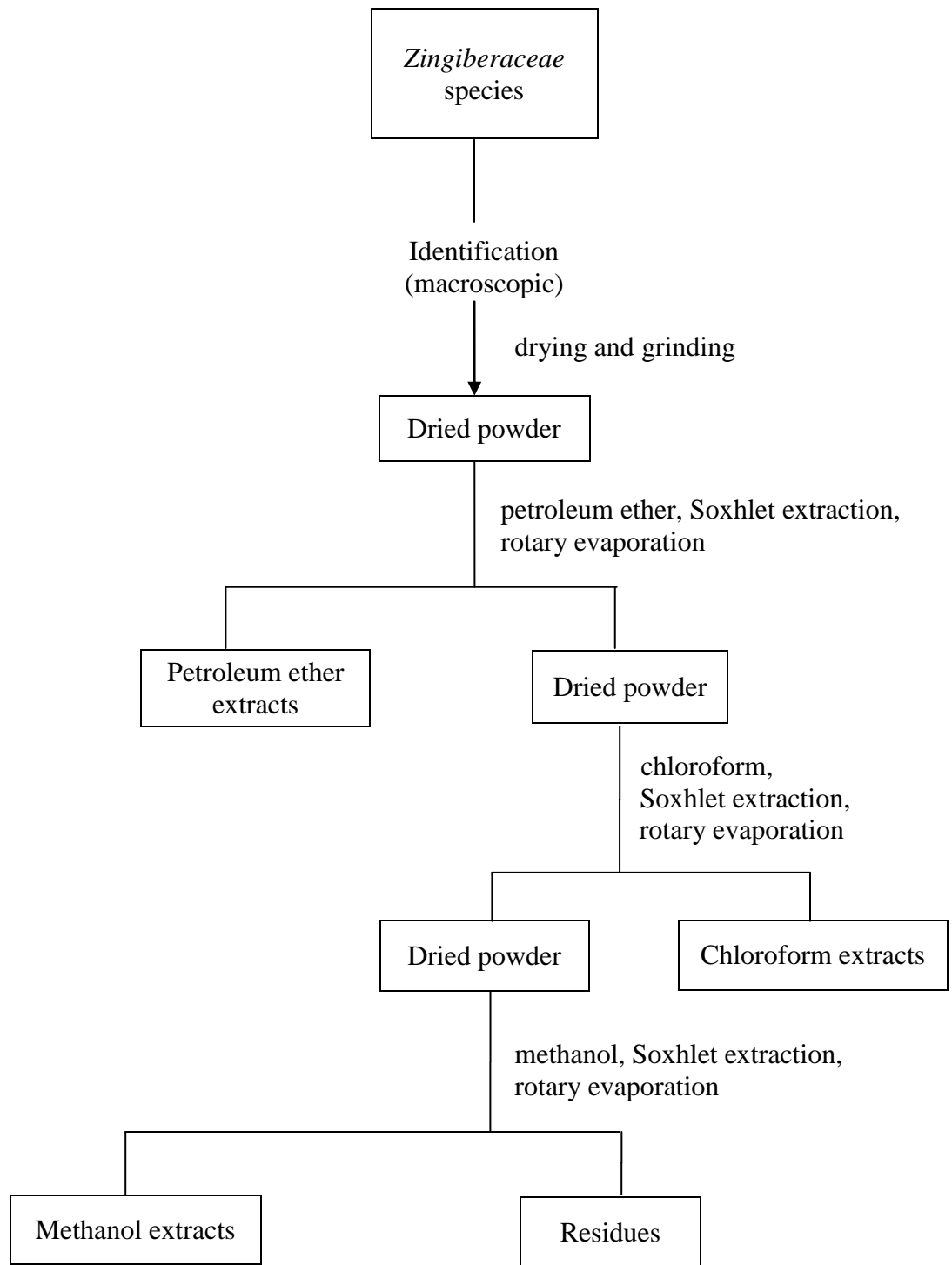


Figure 3.1: Flow chart of the plant extraction procedure using petroleum ether, chloroform, and methanol

3.3 Nitric Oxide Assay

Petroleum ether, chloroform, and methanol extracts from ten selected *Zingiberaceae* species such as *A. galanga*, *B. rotunda*, *C. aeruginosa*, *C. domestica*, *C. mangga*, *C. xanthorrhiza*, *K. galanga*, *Z. montanum*, *Z. officinale*, and *Z. zerumbet* were evaluated for their effects on the nitric oxide production in murine macrophage cells (RAW 264.7) using the nitric oxide assay.

3.3.1 Preparation of diluents and reagents

Preparation of diluents and reagents for NO assay was carried out as showed in Appendix I.

3.3.2 Cell culture for RAW 264.7 cell line

Murine macrophage cell line (RAW 264.7) (Figure 3.2) obtained from the American Type Culture Collection (ATCC, Rockville, MD, USA) was used in this experiment. The cell line was cultured in DMEM media with phenol red, containing high glucose of 4500 mg/mL, L-glutamine, HEPES, and NaHCO₃, supplemented with 10% heat-inactivated FBS, 2% penicillin/streptomycin (PAA Laboratories GmbH, Australia) and 1% amphotericin B (PAA Laboratories GmbH, Australia). The cell culture was maintained in a humidified incubator (Shel Lab, Australia) at 37°C, with 5% carbon dioxide (CO₂) and 95% air. The cells were grown to 90%–100% confluence. Cell culture protocol is showed in Appendix II.

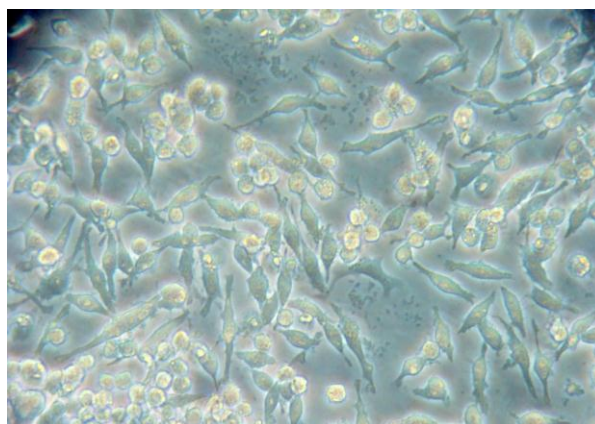


Figure 3.2: Murine macrophage cells (RAW 264.7) observed under phase-contrast microscope with magnification 100×

3.3.3 RAW 264.7 cell preparation and seeding

Murine macrophage cells (RAW 264.7) with confluency of 90%–100% were detached and transferred into a 15 mL centrifuge tube. The cell suspension was centrifuged (Kubota) at 1000 rpm for 5 min at room temperature. The supernatant was removed and 5 mL of fresh diluent B was added to the cell pellet which was then re-suspended gently using a 10 mL disposable serological pipette (Terumo, Japan).

The cell suspension (10 μ L) was taken and mixed gently with 90 μ L of Trypan Blue solution in a microtube (Orange Scientific, Belgium). Subsequently, 10 μ L of the sample was removed and dispensed on glass slide. The number of cells was counted using a haemocytometer (Marienfeld), and the percentage of cell viability was determined. The percentage of cell viability should be at least 95% in order to run the assay.

The cell concentration was adjusted to 2×10^6 cells/mL with diluents B. Then, 100 μ L of cell suspension was dispensed into flat bottom 96-well microplate (Nunc, Denmark). After plating, the plate was incubated for 2 h at 37°C, 5% CO₂ in the humidified incubator.

3.3.4 Sample dilution

Sample stock and substock were prepared before conducting serial dilution. Sample stock was prepared by adding 0.02 g of crude extract with 0.2 mL of 100% DMSO in a microtube and stored at -20°C . Sample stock was thawed at room temperature before use. In this experiment, the required constant percentage of DMSO was 0.1%, and the final concentration for the sample needed was $100\ \mu\text{g/mL}$.

So, for sample stock preparation,

$0.02\ \text{g sample crude extract} = 20\ \text{mg}$

$0.02\ \text{g sample crude extract in } 0.2\ \text{mL } 100\% \text{ DMSO} = 20\ \text{mg}/0.2\text{mL}$

$$= 100\ \text{mg/mL}$$

$$= 100\ 000\ \mu\text{g/mL}$$

Thus, sample stock concentration was $100\ 000\ \mu\text{g/mL}$.

Sample substock was prepared to acquire 0.2% DMSO. To prepare sample substock at $200\ \mu\text{g/mL}$, 0.2% DMSO, calculation were done using the formula below,

$$M_1V_1 = M_2V_2$$

$$(100\ 000\ \mu\text{g/mL})V_1 = (200\ \mu\text{g/mL})(500\ \mu\text{L})$$

$$V_1 = 1\ \mu\text{L}$$

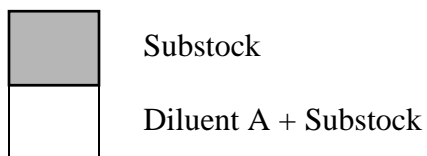
Based on the calculation, $1\ \mu\text{L}$ from sample stock was taken out, and added to $499\ \mu\text{L}$ of diluent B in order obtain $500\ \mu\text{L}$ of sample substock with 0.2% DMSO at $200\ \mu\text{g/mL}$.

After preparing sample substock, serial dilution was conducted. Serial dilution was conducted using a sterile flat bottom 96-well microplate and multi-channel pipettor (HTL, Poland) in a biohazard hood (Essco Class II Biohazard Safety Cabinet). Serial dilution were carried out prior to the NO assay and the plate were sealed and frozen at -20°C .

Firstly, 80 μL of diluent A was dispensed into wells rows B to H (Figure 3.3). Sample substock (160 μL) was added to wells in row A, resulting in the final concentration here to be 200 $\mu\text{g}/\text{mL}$. Subsequently, 80 μL of dilution was transferred from wells in row A to row B, resulting in the final concentration in row B to be 100 $\mu\text{g}/\text{mL}$. The dilution was re-suspended a few times before being transferred to the following row. The steps were repeated until row G, and the last 80 μL of dilution after row G was discarded. Hence, final volume in each well was 80 μL , 0.2% DMSO.

	1	2	3	4	5	6	7	8	9	10	11	12
A												
B												
C												
D												
E												
F												
G												
H												

Figure 3.3: Template of serial dilution for NO assay



After the serial dilution was conducted, the sample concentrations for the wells in each row were 200 µg/mL for row A, 100 µg/mL for row B, 50 µg/mL for row C, 25 µg/mL for row D, 12.5 µg/mL for row E, 6.25 µg/mL for row F, and 3.13 µg/mL for row G.

3.3.5 Treatment of RAW 264.7 cells with plant extracts

After 2 h of incubation time, unattached RAW 264.7 cells were dispersed and the media were discarded using a pipettor (1000 µL) (Eppendorf, Germany). Apart from normal cell controls, all cells were cultured with 50 µL diluent C which contained 10 µg/mL LPS to stimulate the cells seeded in the flat bottom 96-well microplate.

50 µL of serially diluted *Zingiberaceae* extracts in the serial dilution plate were then dispensed into each well except controls and standard. 50 µL of the serially diluted *Zingiberaceae* extracts in media containing DMSO (diluent A) subsequently added each well containing 50 µL of diluent C, yielded a final concentration of DMSO 0.1% per well. Meanwhile, the cells were treated with each *Zingiberaceae* extracts at 1.56 µg/mL, 3.13 µg/mL, 6.25 µg/mL, 12.5 µg/mL, 25 µg/mL, 50 µg/mL, and 100 µg/mL (Figure 3.4).

The same volume of media from the serial dilution plate was added to the same volume of media in the cell plate. Therefore, DMSO and extract concentrations were halved in the wells. Controls for the template in Figure 3.4 were as follows:

Control 1: Supplemented 5% DMEM only

Control 2: Cells in supplemented 5% DMEM with 0.1% DMSO and 10 µg/mL LPS

Control 3: Cells in supplemented 5% DMEM with 10 µg/mL LPS

Control 4: Cells in supplemented 5% DMEM only

Control 5: Cells in supplemented 5% media with 0.1% DMSO, 10 µg/mL LPS and a final concentration of L-NAME (a NOS inhibitor) 250 µM

The absorbance reading for blank control (Control 1) was required for NO calculation. Control 2 and Control 3 represented the negative controls, where the cells were stimulated by the inducer (LPS) to generate NO. Therefore, no inhibition of NO should be detected for the negative control, which was presented as 0% of NO inhibition. Control consisting of cells only (Control 4) should not show any NO generation as there was no inducer. The cells were therefore not stimulated to produce NO. On the other hand, cells treated with inducer and *L*-NAME (iNOS inhibitor) represented the positive control (Control 5). *L*-NAME, an iNOS inhibitor can inhibit about 70% of NO inhibition in the LPS-stimulated RAW 264.7 cells. The cells were incubated for 24 h at 37°C, 5% CO₂, in a fully humidified incubator.

	1	2	3	4	5	6	7	8	9	10	11	12
A	Sample 1			Sample 2			Sample 3			Standard: NaNO ₂		
B	(100 µg/mL)			(100 µg/mL)			(100 µg/mL)			(100 µM)		
C	↓			↓			↓			↓		
D												
E												
F												
G	(1.56 µg/mL)			(1.56 µg/mL)			(1.56 µg/mL)			(1.56 µM)		
H	Control 1		Control 2		Control 3		Control 4		Control 5		NaNO ₂	

Figure 3.4: Template of a 96-well plate for NO assay showing the actual extract concentration (µg in 0.1% DMSO) assayed and NaNO₂ standard concentrations

3.3.6 Measurement of nitrite concentration

Nitrite (NO_2^-) concentrations contained in the culture supernatants as an indicator of NO production were determined by the Griess reaction (Chi, Cheon, & Kim, 2001). After 24 h of incubation time, 50 μL of cell-free supernatants were collected and incubated with 50 μL of Griess reagent (2.5% phosphoric acid, 1% sulphanilamide, and 0.1% N-(1-naphthyl)-ethylene diamine dihydrochloride) to form purple azodye (Green *et al.*, 1982) at room temperature for 10 minutes (Figure 3.5).

Sodium nitrite (NaNO_2) (Sigma, USA) was used to generate a standard curves. A two-fold serial dilution of NaNO_2 was done, starting at 100 μM in columns A11 and A12 (50 μL /well) (Figure 3.4). Last two wells (H11 and H12) were left empty, and only 50 μL of deionized water was added to each well. After that, 50 μL of Griess reagent was added to all wells carefully in order to avoid as much bubbles as possible.

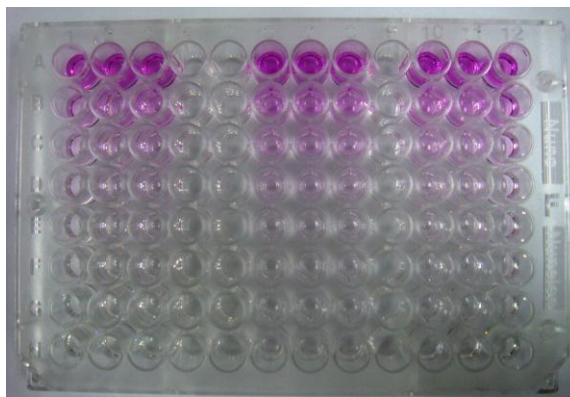


Figure 3.5: Sample plate of purple azodye formed after 50 μL of Griess reagent was added to 50 μL of serially diluted NaNO_2

The optical density at 540 nm (OD_{540}) was measured using the Emax precision microplate reader (Molecular Devices). Nitrite concentrations were determined from a least squares linear regression analysis of NaNO_2 standard curve. Percentage of NO inhibition

was calculated based on the ability of the extracts in inhibiting nitrite production by comparing with the negative control with 0% of nitrite inhibition.

A standard curve was plotted using average value for each standard value versus the concentration of standard (Appendix III). The average absorbance value of the blank wells (Control 1) was subtracted from all other pairs of wells. The absorbance values for each pair of triplicate wells were averaged. The concentration of each unknown was determined by interpolation from standard curve. The percent inhibition of each samples were calculated according to the equation:

$$\text{Percentage of NO inhibition (\%)} = \frac{[\text{Control 2}] - [\text{Sample}]}{[\text{Control 2}]} \times 100$$

Eq. (2)

3.3.7 Measurement of RAW 264.7 cell viability using the MTT assay

Mitochondrial respiration, an indicator of RAW 264.7 cell viability, was assessed by the mitochondria-dependent reduction of 3-[4,5-dimethylthiazol-2-yl]-2,5-diphenyltetrazolium bromide (MTT) to formazan (Szabó, Thiernemann, & Vane, 1993). The cytotoxicity effects of the extracts were evaluated using the conventional MTT assay. RAW 264.7 cells remaining in the flat bottom 96-well microplate following removal of media for NO assay were topped up with 100 μL of fresh DMEM with phenol red supplemented with 5% heat-inactivated FBS for each well. Then, 20 μL of 5 mg/mL MTT (Sigma, USA) in phosphate buffer saline (PBS) pH 7.2 was added to each well, and incubated at 37°C, 5% CO_2 in the humidified incubator for 4 h.

After 4 h of incubation time (Figure 3.6), the media was carefully discarded. The formazan salt which formed at the bottom of each well was dissolved in 100 μL of DMSO

(Figure 3.7), and mixed in a mixer for 15 min. The optical density at 540 nm (OD_{540}) was determined using the Emax precision microplate reader. The absorbance of formazan in control (untreated cell) was taken as 100% viability, and the percentage of cell viability was calculated according to the equation:

$$\text{Percentage of cell viability (\%)} = \frac{\text{OD Sample}}{\text{OD Control 2}} \times 100$$

Eq. (3)



Figure 3.6: After 4 h of RAW 264.7 cells incubated with fresh DMEM and MTT in PBS pH 7.2, viable cells formed brown colour formazan in the 96-well flat bottom plate

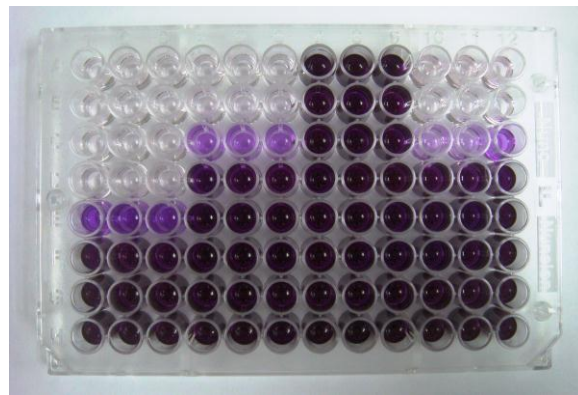


Figure 3.7: After removal of the media, the formazan formed at the bottom of each well were dissolved with 100 μ L of DMSO, forming purple colour solvent

3.3.8 Statistical analysis

Statistical analysis was performed using the Statistical Package for the Social Sciences Version 16.0 (SPSS 16.0). All experiments were performed at least three times (N=3). All quantitative data were presented as mean \pm standard error of mean (S.E.M) and analysed via analysis of variance (ANOVA). Statistically significant differences among the means of the groups were tested at $p < 0.05$ using Duncan's multiple range test. *P* values less than 0.05 were considered statistically significant.

3.4 Cell Proliferation and Viability Assay on MDA-MB-231 Cell Line

Petroleum ether, chloroform, and methanol extracts from ten selected *Zingiberaceae* species such as *A. galanga*, *B. rotunda*, *C. aeruginosa*, *C. domestica*, *C. mangga*, *C. xanthorrhiza*, *K. galanga*, *Z. montanum*, *Z. officinale*, and *Z. zerumbet* were evaluated for their anti-proliferative effects against human breast cancer cells (MDA-MB-231) using cell proliferation and viability assay.

3.4.1 Preparations of diluents and reagents

Two types of diluents, namely diluent A, diluent B were prepared as in Appendix I (Section 1.1.2).

3.4.2 Cell culture for MDA-MB-231 cell line

Human breast cancer cell line, MDA-MB-231 (oestrogen-receptor negative, ER-) (Figure 3.8), obtained from ATCC was used in this experiment. The cell line was cultured in DMEM with phenol red, containing high glucose of 4500 mg/mL, L-glutamine, HEPES, and NaHCO₃, supplemented with 10% heat-inactivated FBS, 2% penicillin/streptomycin

and 1% amphotericin B. Cell culture were maintained in a humidified incubator at 37°C, with 5% CO₂ and 95% air. The cells were grown to 90–100% confluence. Cell culture protocol is showed in Appendix II.

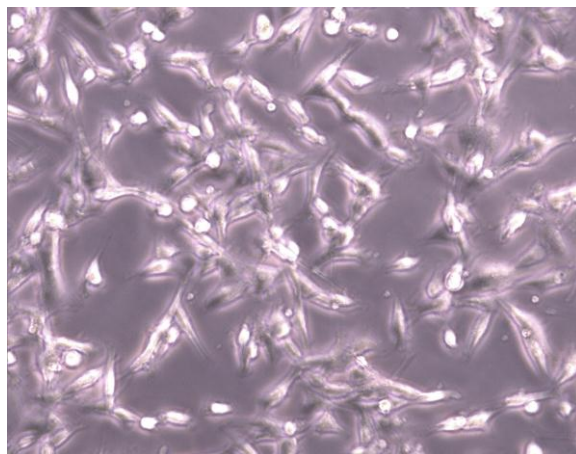


Figure 3.8: Human breast cancer cell line, MDA-MB-231 (oestrogen-receptor negative, ER–) observed under phase-contrast microscope with magnification 100×

3.4.3 MDA-MB-231 cell preparation and seeding

The cytotoxicity of the extracts was tested against MDA-MB-231 tumour cells. MDA-MB-231 cells with confluency of 90%–100% were detached using accutase (Innovative Cell Technologies, San Diego, CA) and transferred into a 15 mL centrifuge tube. The cells were centrifuged for 5 min at 1000 rpm at room temperature. The supernatant was removed and 1 mL of diluent B was added to the cell pellet and resuspended gently using a 1000 mL pipettor.

The well-resuspended cell sample (10 µL) was taken and mixed gently with 90 µL of trypan blue solution in a microtube. 10 µL of the mixture was then removed and dispensed on glass slide. The number of cells was counted using a haemocytometer, and percentage of cell viability was determined. The percentage of cell viability should be at least 95% in order to run the assay.

Cells were seeded in flat bottom 96-well microplate (100 μL /well) at a concentration of 8×10^4 cells/mL culture medium. After plating, the plate was incubated for 24 h at 37°C , 5% CO_2 in the humidified incubator.

3.4.4 Sample dilution

Sample stock and substock were prepared before conducting serial dilution. Sample stock was prepared by adding 0.02 g of crude extract with 0.2 mL of 100% DMSO in microtube and stored at -20°C . Sample stock was thawed at room temperature before used. In this experiment, the required constant percentage of DMSO was 0.1%, and the final concentration for the sample needed was $100 \mu\text{g/mL}$.

So, for sample stock preparation,

$$0.02 \text{ g sample crude extract} = 20 \text{ mg}$$

$$0.02 \text{ g sample crude extract in } 0.2 \text{ mL } 100\% \text{ DMSO} = 20 \text{ mg}/0.2 \text{ mL}$$

$$= 100 \text{ mg/mL}$$

$$= 100\,000 \mu\text{g/mL}$$

Thus, sample stock concentration was $100\,000 \mu\text{g/mL}$.

Sample substock was prepared to acquire 0.2% DMSO. To prepare sample substock at $200 \mu\text{g/mL}$, 0.2% DMSO, calculation were carried out using the formula below,

$$M_1V_1 = M_2V_2$$

$$(100\,000 \mu\text{g/mL})V_1 = (200 \mu\text{g/mL})(500 \mu\text{L})$$

$$V_1 = 1 \mu\text{L}$$

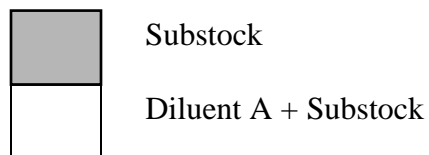
Therefore, $1 \mu\text{L}$ from sample stock was taken out, and added to $499 \mu\text{L}$ of diluent B in order obtain $500 \mu\text{L}$ of sample substock with 0.2% DMSO at $200 \mu\text{g/mL}$.

After preparing sample substocks, serial dilution was conducted. Serial dilution was conducted using a sterile flat bottom 96-well microplate and multi-channel pipettor in a biohazard hood. Serial dilution was done prior to the cell proliferation and viability assay. The plate was sealed and frozen at -20°C .

Firstly, 150 μL of diluent A was dispensed into wells rows B to H (Figure 3.9). Sample substock (300 μL) was added to wells in row A, which the final concentration here was 200 $\mu\text{g}/\text{mL}$. Then, 150 μL of dilution was transferred from wells in row A to row B, resulting in the final concentration in row B to be 100 $\mu\text{g}/\text{mL}$. The mixture was resuspended a few times before transferred to the following row. The steps were repeated until row G, and the last 150 μL of dilution after row G was discarded. Hence, final volume in each well was 150 μL , 0.2% DMSO.

	1	2	3	4	5	6	7	8	9	10	11	12
A												
B												
C												
D												
E												
F												
G												
H												

Figure 3.9: Template of serial dilution for cell proliferation and viability assay



After the serial dilution was conducted, the sample concentrations for the wells in each row were 200 µg/mL for row A, 100 µg/mL for row B, 50 µg/mL for row C, 25 µg/mL for row D, 12.5 µg/mL for row E, 6.25 µg/mL for row F, and 3.13 µg/mL for row G.

3.4.5 Treatment of MDA-MB-231 cells with plant extracts

After 24 h of incubation time, unattached cells were dispersed and the media was discarded using a pipettor. All cells were cultured with 100 µL of fresh DMEM with phenol red, containing high glucose of 4500 mg/mL, L-glutamine, HEPES, and NaHCO₃, supplemented with 10% heat-inactivated FBS, 2% penicillin/streptomycin and 1% amphotericin B.

100 µL of serially diluted *Zingiberaceae* extracts in the serial dilution plate was dispensed into each well except controls. 100 µL of the serially diluted *Zingiberaceae* extracts in media containing DMSO (diluent A) was added to each well containing 100 µL of diluent B, yielded a final concentration of DMSO 0.1% per well. Meanwhile, the MDA-MB-231 cells were treated with each *Zingiberaceae* extracts at 1.56 µg/mL, 3.13 µg/mL, 6.25 µg/mL, 12.5 µg/mL, 25 µg/mL, 50 µg/mL, and 100 µg/mL (Figure 3.10).

Control groups include blank, cells in media containing 0.1% DMSO (negative control), and cells in media containing 0.05–3.13 µg/mL Doxorubicin hydrochloride (Sigma, USA) (positive control). Doxorubicin hydrochloride, a chemotherapy drug that used to treat breast cancers by inhibiting cell proliferation was used as the positive control (Laundry de Mesquita *et al.*, 2009). The cells were incubated for 48 h at 37°C, 5% CO₂, in a fully humidified incubator.

The same volume of media from the serial dilution plate was added to the same volume of media in the cell plate. Therefore, DMSO and extract concentrations were halved in the wells.

	1	2	3	4	5	6	7	8	9	10	11	12
A	Sample 1			Sample 2			Sample 3			Doxorubicin hydrochloride		
B	(100 µg/mL)			(100 µg/mL)			(100 µg/mL)			(12.5 µg/mL)		
C	↓			↓			↓			↓		
D												
E												
F												
G	Sample 1 (1.56 µg/mL)			Sample 2 (1.56 µg/mL)			Sample 3 (1.56 µg/mL)			Doxorubicin hydrochloride (1.20 µg/mL)		
H	Blank			Negative Control								

Figure 3.10: Template of a 96-well plate for Cell proliferation and viability assay showing the actual extract concentration (µg in 0.1% DMSO) and Doxorubicin hydrochloride (µg in 0.1% DMSO) assayed

3.4.6 Measurement of MDA-MB-231 cell proliferation or viability

Growth of tumoral cells was quantified by the ability of living cells to reduce the yellow dye MTT to a blue formazan product (Mosmann, 1983). At the end of 48 h incubation, old media were removed, and treated cells were added with 100 µL of fresh DMEM with phenol red, containing high glucose of 4500 mg/mL, L-glutamine, HEPES,

and NaHCO₃, supplemented with 5% FBS. After that, 20 μL of 5mg/mL MTT was added into each well and incubated for 4 h.

After 4 h of incubation time, the formazan product (Figure 3.11) of MTT reduction was dissolved in 100 μL of DMSO. Then, the plate was mixed in a mixer for 15 min. The optical density at 540nm (OD₅₄₀) was determined using the Emax precision microplate reader. For time-dependent assays, cells were incubated with *Zingiberaceae* extracts for 48 h. The absorbance of formazan in control (untreated cell) was taken as 100% proliferation or viability, and the cytotoxicity index (CI) of cells are expressed as percentage calculated according to the equation:

$$CI = 1 - \frac{OD_{540} \text{ of (treated cells)}}{OD_{540} \text{ of (control cells)}} \times 100$$

Eq. (4)



Figure 3.11: Formazan formed at the bottom of the well were observed under a phase-contrast microscope with magnification 100×

3.4.7 Statistical analysis

All experiments were performed at least three times (N=3). All quantitative data were presented as mean \pm standard error of mean (S.E.M) and analysed using SPSS 16.0 and Graphpad Prism 4.02 programme.

Growth inhibitory effects from exposure of cells to different concentrations of crude *Zingiberaceae* extracts were presented in terms of percentage of cytotoxicity index and IC₅₀ values. Cytostatic concentrations (IC₅₀) were identified as the concentration of crude *Zingiberaceae* extract required to inhibit 50% cell proliferation or viability compared with the control groups. The IC₅₀ values were obtained by nonlinear regression using the GraphPad Prism Version 4.02 programme.

3.5 Cytotoxicity Assay

The most cytotoxic extracts (IC₅₀ \leq 10 μ g/mL) against MDA-MB-231 cells were selected for *in vitro* toxicity study using MTT assay in order to assess their potential toxicity against normal, non-tumoural human lung fibroblast cells, MRC-5. The selected extracts were petroleum ether extracts of *A. galanga*, *B. rotunda*, and *Z. zerumbet*; as well as chloroform extracts of *A. galanga*, *B. rotunda*, and *C. domestica*.

3.5.1 Preparations of diluents and reagents

Two types of diluents, namely diluent A, diluent B were prepared as in Appendix I (Section 1.1.3).

3.5.2 Cell culture for MRC-5 cell line

MRC-5 cell line (Figure 3.12) was cultured in MEM with phenol red, containing L-glutamine, HEPES, NaHCO₃, and sodium pyruvate supplemented with 10% heat-inactivated FBS, 2% penicillin/streptomycin and 1% amphotericin B. Cell culture were maintained in a humidified incubator at 37°C, with 5% CO₂ and 95% air. The cells were grown to 90% to 100% confluence. Cell culture protocol is showed in Appendix II.

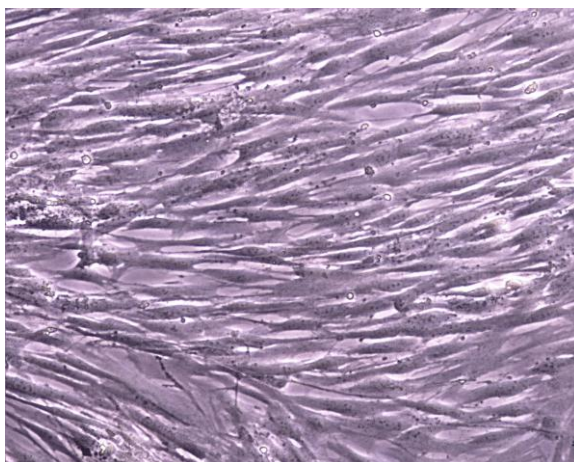


Figure 3.12: Human lung fibroblast cell line (MRC-5) observed under phase-contrast microscope with magnification 100×

3.5.3 MRC-5 cell preparation and seeding

The cytotoxic extracts were tested against MRC-5 cell line. MRC-5 cells with confluency of 90%–100% were detached using accutase and transferred into a 15 mL centrifuge tube. The cells were centrifuged for 5 min at 1000 rpm at room temperature. The supernatant was removed and 1 mL of diluent B was added to the cell pellet and resuspended gently using a 1000 μ L pipettor.

The well-resuspended cell sample (10 μ L) was taken and mixed gently with 90 μ L of trypan blue solution in a microtube. Then, 10 μ L of the sample was removed and

dispensed on glass slide. The number of cells was counted using a haemocytometer, and percentage of cell viability was determined. The percentage of cell viability should be at least 95% in order to run the assay.

Cells were seeded in flat bottom 96-well microplate (100 μ L/well) at a concentration of 8×10^4 cells/mL culture medium. After plating, the plate was incubated for 24 h at 37°C, 5% CO₂ in the humidified incubator.

3.5.4 Sample dilution

Sample dilution was carried out as described in section 3.4.4.

3.5.5 Treatment of MRC-5 cells with selected cytotoxic plant extracts

Treatment of MRC-5 cells with the selected cytotoxic extracts was carried out as described in section 3.4.5.

3.5.6 Measurement of cell viability

Measurement of MRC-5 cell viability using MTT assay was carried out as described in section 3.4.6.

3.5.7 Statistical analysis

Statistical analysis of the experiment was performed as described in section 3.4.7.

3.6 Scratch Wound Assay

Petroleum ether, chloroform, and methanol extracts from ten selected *Zingiberaceae* species such as *A. galanga*, *B. rotunda*, *C. aeruginosa*, *C. domestica*, *C. mangga*, *C.*

xanthorrhiza, *K. galanga*, *Z. montanum*, *Z. officinale*, and *Z. zerumbet* were evaluated for their anti-migration effects against human breast cancer cells (MDA-MB-231) using scratch wound assay.

3.6.1 Preparation of diluents and reagents

Two types of diluents, namely diluent A, diluent B were prepared as in Appendix I (Section 1.1.4).

3.6.2 Cell culture for MDA-MB-231 cell line

Cell culture for MDA-MB-231 cell line was carried out as described in section 3.4.2.

3.6.3 MDA-MB-231 cell preparation and seeding

MDA-MB-231 cells with confluency of 90%–100% were detached using accutase and transferred into a 15 mL centrifuge tube. The cells were centrifuged for 5 min at 1000 rpm at room temperature. The supernatant was removed and 5 mL of diluent B was added to the cell pellet and resuspended gently using a 10 mL disposable serological pipette.

The well-resuspended cell sample (10 μ L) was taken and mixed gently with 90 μ L of Trypan Blue solution in a microtube. Then, 10 μ L of the sample was removed and dispensed on glass slide. The number of cells was counted using a haemocytometer, and percentage of cell viability was determined. The percentage of cell viability should be at least 95% in order to run the assay. Cells were seeded onto six-well plate at a concentration of 1×10^6 cells per well and grown to confluence. The plate was incubated at 37°C, 5% CO₂ in the humidified incubator.

3.6.4 Sample dilution

Sample dilution of stock and substock for use in the scratch wound assay was carried out as described in section 3.4.4.

9980 μL of diluent B was dispensed into a 15 mL centrifuge tube labeled as “Tube 1”, while 5 mL of diluent A was dispensed into another 15 mL centrifuge tube labeled as “Tube 2”. Extract stock (20 μL) was added to “Tube 1”, resulting in a concentration of sample extract to be 200 $\mu\text{g}/\text{mL}$. Subsequently, 5 mL of the well re-suspended dilution was transferred from Tube 1 to Tube 2, resulting in the final concentration of sample extract in Tube 2 to be 100 $\mu\text{g}/\text{mL}$ (Figure 3.13). The dilution was mixed a few times and 3 mL of the dilution in Tube 2 was discarded. The volume in each tube was 5 mL, 0.2% DMSO.

The same procedure of serial dilution was carried out for the subsequent concentrations such as 50 $\mu\text{g}/\text{mL}$, 25 $\mu\text{g}/\text{mL}$, 12.5 $\mu\text{g}/\text{mL}$, etc. Serial dilution was conducted using sterile centrifuge tubes and serological pipette in a biohazard hood. Serial dilution were carried out prior to the scratch wound assay. After the serial dilution was conducted, the sample concentrations for each centrifuge tube were 200 $\mu\text{g}/\text{mL}$ in Tube 1 and 100 $\mu\text{g}/\text{mL}$ in Tube 2.

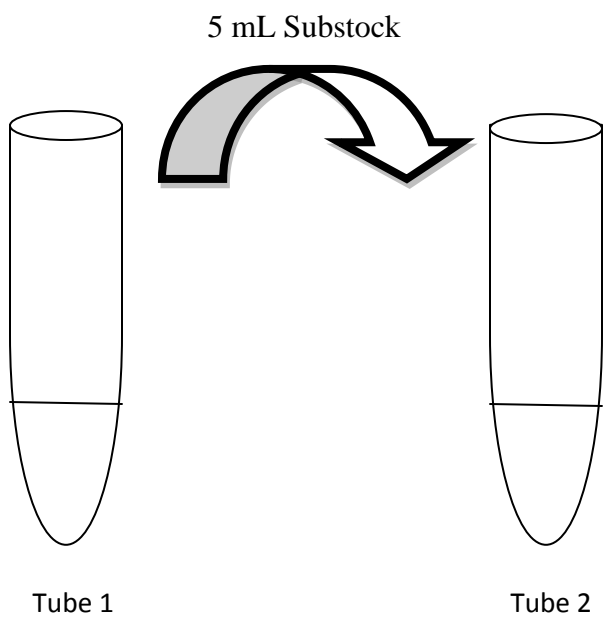
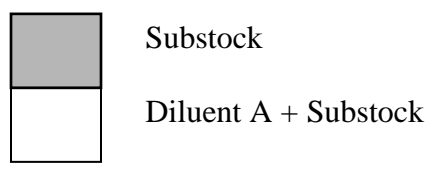


Figure 3.13: Diagram of serial dilution for Scratch wound assay



3.6.5 Treatment of MDA-MB-231 cells with plant extracts

Confluent cell monolayers in the 6-well plate were carefully wounded by scratching with a sterile 200 μ L-pipette tip along the diameter of the well (Figure 3.14). The cells were washed twice with PBS to remove any cell debris before their subsequent incubation with 1%-heated inactivated FBS culture medium in the absence (negative control) or presence of *Zingiberaceae* extracts.

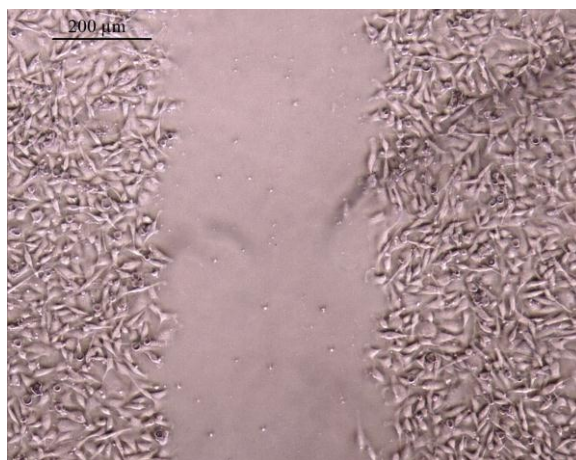


Figure 3.14: Confluent cell monolayers of MDA-MB-231 were wounded using a sterile 200 μ L-pipette tip along the diameter of the well, which was then observed under a phase-contrast microscope with magnification 50 \times

All cells were cultured in 2 mL of fresh DMEM with phenol red, containing high glucose of 4500 mg/mL, L-glutamine, HEPES, and NaHCO₃, supplemented with 1%-heat inactivated FBS (Choi *et al.*, 2009), 2% penicillin/streptomycin and 1% amphotericin B (diluent B).

2 mL of serially diluted *Zingiberaceae* extracts were dispensed into each well except controls. 2 mL of the serially diluted *Zingiberaceae* extracts in media containing DMSO (diluent A) subsequently added to each well containing 2mL of diluent B, yielded a final concentration of DMSO 0.1% per well (Figure 3.15).

The cells were incubated in *Zingiberaceae* extracts at their optimum concentrations or vehicle alone for 48 h at 37°C, 5% CO₂, in a fully humidified incubator and photographed under a phase-contrast microscope. The culture treatments were repeated twice and each sample was assayed in triplicates.

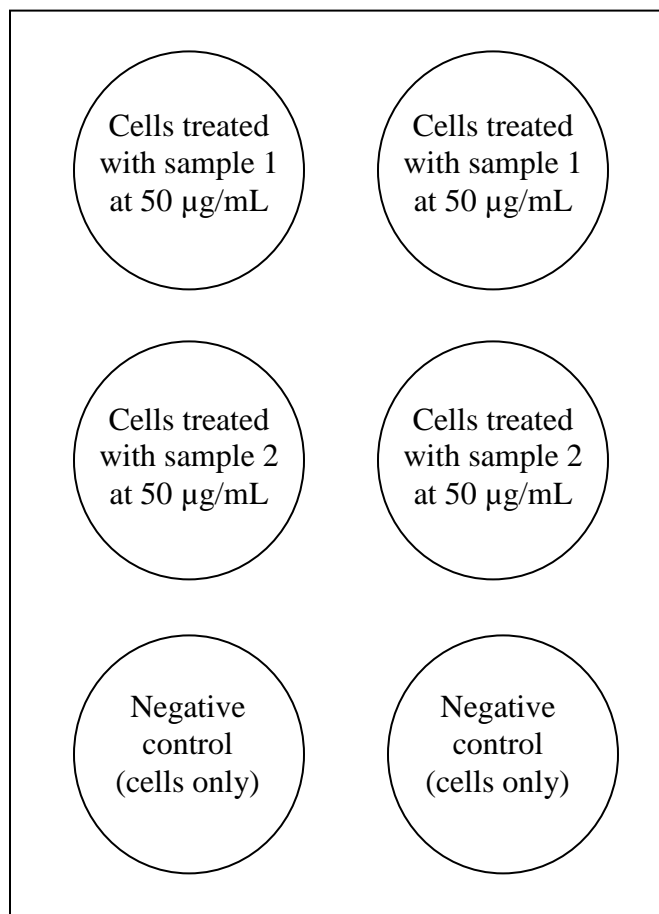


Figure 3.15: Template of a six-well plate for scratch wound assay showing the actual extract concentration (μg in 0.1% DMSO) assayed

The same volume of media from the serial dilution plate was added to the same volume of media in the cell plate. Therefore, DMSO and extract concentrations were halved in the wells.

3.6.6 Measurement of cell migration ability

Cells were serum-starved and stimulated or non-stimulated with *Zingiberaceae* extracts for 24, and 48 h. Wound closure of the cell monolayer was observed under the microscope at 50 \times magnification, and photographs were captured immediately after

treatment (0 h), and after 24 h and 48 h later. Five fields of each of the wounds were captured and mean values for the selected fields per well were analyzed.

The relative cell migration capability has been described by Liu *et al.* (2005) (Peng, Chen, Peng, Su, & Hsieh-Li, 2006), and has been modified by Peng *et al.* (2007) to absolute migration capability (MC_A) as:

$$MC_A (\text{mm/h}) = \frac{G_0 - G_t}{2t} \quad \text{Eq. (5)}$$

where G_0 is the initial gap for the cell line at 0 h (mm),

G_t is the final gap for the cell line treated with *Zingiberaceae* extract at certain concentration or vehicle alone for a time period of t (h) (mm), and t is the overall time period for incubation (h).

3.6.7 Statistical analysis

Statistical analysis was performed using SPSS 16.0. All experiments were performed at least three times (N=3). All quantitative data were presented as mean \pm standard error of mean (S.E.M) and analysed via analysis Paired-Samples *t*-test. *P* values less than 0.05 were considered statistically significant.

3.7 Thin-layer Chromatography

Thin-layer chromatography (TLC) qualitatively analysed components of crude extract. The most potential *Zingiberaceae* extracts based on the screening tests were chloroform extract of *A. galanga*, chloroform extract of *C. domestica*, and petroleum ether extract of *Z. zerumbet*. These extracts showed potent effects in inhibition of nitric

production in activated macrophage cells (RAW 264.7), anti-proliferation and anti-migration activities against human breast cancer cells (MDA-MB-231). More importantly, these extracts possess SX values distinctly greater than 100 which indicated their promising properties for further studies in the development of anti-cancer drugs. Therefore, they were selected for qualitative analysis using TLC to determine the chemical groups contained in the crude extract.

3.7.1 Stationary phase

Commercially available silica gel TLC plate (20 cm × 20 cm) was cut into strips of 2 cm × 10 cm. A straight line was drawn parallel along the width, with 1 cm distance from each end of the thin-layer plate using a pencil (Figure 3.16).

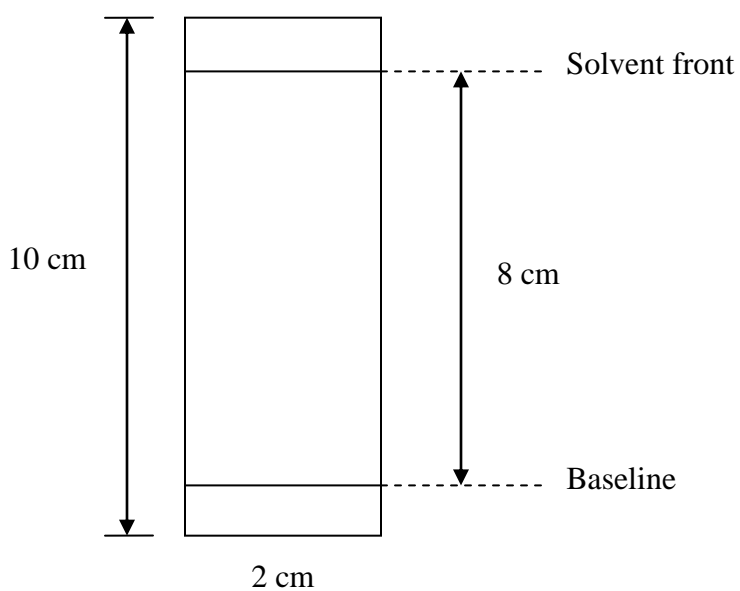


Figure 3.16: A cut of TLC plate (2 cm × 10 cm) with marked baseline and solvent front, which is ready to be used for qualitative analysis

3.7.2 Development of mobile phase

Crude *Zingiberaceae* extract was applied as a short (4 mm), narrow, and horizontal line on the baseline of the TLC plate. Each plate was developed in one of a series of the mobile phases, usually consisting of single solvent and covering a wide range of polarities. Optimization of mobile phase development was conducted according to the concept of PRISMA system (Appendix IV). Nine solvents chosen based on their 'solvent strength' (related to its polarity) (Appendix IV, Table 3.1) for the development of mobile phase were hexane, diethylether, methanol, dimethylformamide, acetic acid, dichloromethane, ethyl acetate, toluene, and chloroform.

A 1:1:1 combination of diethylether, dichloromethane, and ethyl acetate, including the addition of appropriate hexane were used as the mobile phase in the TLC test for crude chloroform extracts of *A. galanga* and *C. domestica*. On the other hand, a 9:1 combination of dichloromethane and chloroform were used as the mobile phase in the TLC test for crude petroleum ether extract of *Z. zerumbet*.

3.7.3 Choice of detection systems

Some of the components of an extract may be coloured, and thus can be visualized on white stationary phase in daylight. However, most of the components have little or no colour, and other methods are used to make them visible. Two most common methods used are examination under Ultraviolet (UV) light and the use of spray reagents to produce fluorescent or colour derivatives. The detection methods used for this experiment are shown in Table 3.1.

Thin-layer chromatography is a highly reproducible method for qualitative chemical analysis of the nature (chemical groups) of the substances contained in a complex mixture. These may already be known as the results of preliminary chemical tests.

Table 3.1: Selection of detection systems for thin-layer chromatography (Houghton & Raman, 1998)

Detection method/ Spray reagent	Treatment	Types of compounds detected
<i>Methods other than chromogenic spray:</i>		
Daylight	-	Coloured substances
UV light 254 nm	Layer which fluoresces at 254 nm was examined in darkened area. Non-fluorescent layer was examined in darkened area.	Compounds containing conjugated double bonds Some fluorescent compounds – usually have extended π electron system
UV light 365 nm	Non-fluorescent layer was examined in darkened area.	Some fluorescent compounds
Exposure to iodine vapour	A sealed iodine chamber was used (iodine crystals in bottle of TLC tank). Layer was left in contact with iodine vapour and then removed. Yellow or brown zone was noted. The zone will quickly disappear but can be revisualized by replacing the layer in the chamber or fixed by spraying with 0.5% w/v starch dextrin solution.	Many types of compounds, particularly if double bonds are present
<i>Chromogenic sprays¹:</i>		
50% Sulphuric acid	Layer sprayed with the reagent was heated at 105°C for 10 min. Then, the layer was observed in daylight.	Most organic compounds give a yellow, brown or black zone
Dragendorff's reagent	Layer sprayed with the reagent was examined in daylight. Layer can be over-sprayed with 5% aqueous iron (III) chloride, 5% aqueous sodium nitrite or 10% sulphuric acid to make zones appear darker.	Alkaloids give orange zones on yellow background
Vanillin/sulphuric acid reagent	Two types of solvents, known as ethanolic sulphuric acid (Solvent A) and ethanolic vanillin (Solvent B) were prepared. Layer was sprayed with Solvent A followed by Solvent B. Then, the layer was heated at 110°C for 10 min.	Terpenoid gives purple spot Phenol gives red zone and other colours

¹ Recipe for solvent preparation for the chromogenic sprays was presented in Appendix IV.

3.7.4 Measurement of retardation factor

Retardation factor or R_f value is a useful parameter to measure a given substance. R_f value is defined as the ratio of the distance from the baseline (point of application) to the centre of the zone divided by the distance from the baseline to the solvent front (Figure 3.17) (Houghton & Raman, 1998).

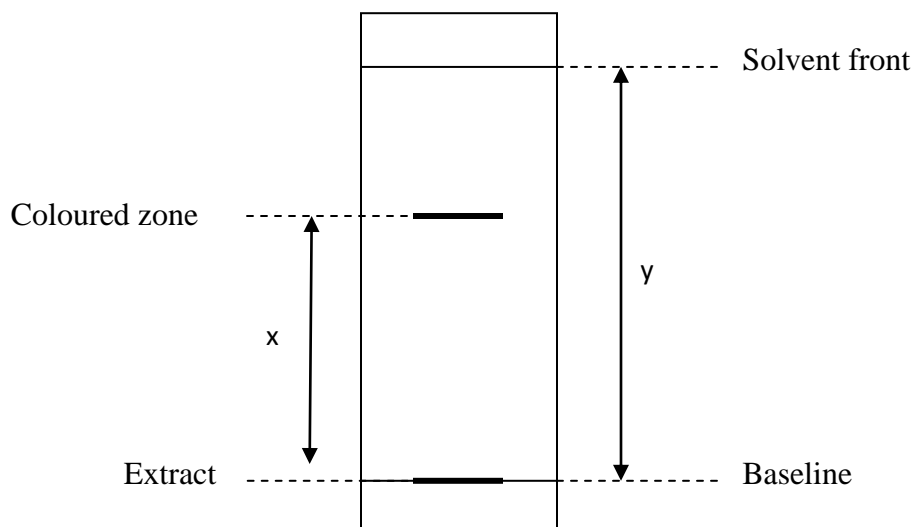


Figure 3.17: Typical TLC chromatogram

R_f can be calculated as

$$R_f = \frac{\text{Distance of the compound moved from the baseline}}{\text{Distance of the solvent from the baseline}} = \frac{x}{y}$$

Eq. (6)

CHAPTER 4

4.0 Results

Ten fresh rhizomes of the selected *Zingiberaceae* species of *A. galanga*, *B. rotunda*, *C. aeruginosa*, *C. domestica*, *C. mangga*, *C. xanthorrhiza*, *K. galanga*, *Z. montanum*, *Z. officinale*, and *Z. zerumbet* were extracted with petroleum ether, chloroform, and methanol using Soxhlet extractor system. The resulting 30 *Zingiberaceae* extracts were then evaluated for NO inhibitory activity in stimulated RAW 264.7 cells, anti-proliferative and anti-migration activities against MDA-MB-231 cells.

4.1 Effects of the *Zingiberaceae* Extracts on Nitric Oxide Inhibitory Activity

A total of 30 *Zingiberaceae* extracts were tested for *in vitro* NO inhibitory activities in LPS (10 µg/mL) stimulated RAW 264.7 cells. The effect at various concentrations was observed after 24 h, and dose-response graphs for the extracts (Figure 4.1–4.10) were generated. The nitrite levels in culture supernatant as an index of NO generation were measured using Griess reaction (Green *et al.*, 1982).

Evaluations were done at seven different concentrations, of 1.56 µg/mL, 3.13 µg/mL, 6.25 µg/mL, 12.5 µg/mL, 25 µg/mL, 50 µg/mL, and 100 µg/mL for each *Zingiberaceae* extracts. Cell viability was determined using the conventional MTT assay to exclude the possibility that the observed effects on NO inhibition were due to their potential cytotoxicity. When samples exhibited marked toxicity (cell viability < 80%) at certain concentrations, the effects of extracts on NO inhibition for that particular concentration were eliminated from being compared. Evaluations were carried out in triplicate and the mean \pm standard error of mean (S.E.M.) were calculated.

Based on Section 3.3.5, control groups used in the experiment included ‘blank or media only’ (Control 1), ‘cells with inducer’ (Control 2 and Control 3), ‘cells only’ (Control 4), and ‘cells with inducer and L-NAME’ (Control 5). The absorbance reading for Control 1 (media only) was required for NO calculation (Appendix III). Cells with inducers (Control 2 and Control 3) represented the negative controls, where cells were stimulated by the inducer (LPS) to generate NO. Therefore, no inhibition of NO could be detected for the negative control, which was presented as 0% of NO inhibition (Figure 4.1–4.10). Control consisting of cells only (Control 4) did not show any NO generation. This was due to the absence of inducer and thus, the cells were therefore not stimulated to produce NO. On the other hand, positive control consisted of cells treated with inducer and L-NAME (iNOS inhibitor). They exhibited about 70% of NO inhibition in the LPS-stimulated RAW 264.7 cells.

(a) *Alpinia galanga*

The results in this study indicated that the extracts could modulate NO production in LPS-activated macrophages. Figure 4.1 showed the effects of crude petroleum ether, chloroform, and methanol extracts of *A. galanga* on nitric oxide production in RAW 264.7 cells. Crude petroleum ether extract inhibited NO production dose-dependently at 78.04% (1.56 µg/mL) and 93.38% (3.13 µg/mL) [Figure 4.1 (A)]. At 6.25–100 µg/mL tested, the extract exerted pronounced cytotoxicity with RAW 264.7 cell viability less than 40% at 6.25 µg/mL and less than 5% at 12.5–100 µg/mL (Table 4.1). The readings from these concentrations were therefore eliminated from being compared. Crude chloroform extract on the other hand inhibited NO production dose-dependently up to 43.97% (1.56 µg/mL), 58.95% (3.13 µg/mL), 81.12% (6.25 µg/mL) and 96.60% (12.5 µg/mL) [Figure 4.1 (B)]. At

higher concentrations tested, the extract exerted marked cytotoxicity with RAW 264.7 cell viability less than 65% at 25 $\mu\text{g}/\text{mL}$ and less than 5% at 50 $\mu\text{g}/\text{mL}$ and 100 $\mu\text{g}/\text{mL}$ (Table 4.1). As before, readings from the concentrations were therefore omitted from being compared. Crude methanol extract dose-dependently inhibited NO production at 16.55% (1.56 $\mu\text{g}/\text{mL}$), 21.17% (3.13 $\mu\text{g}/\text{mL}$), 23.31% (6.25 $\mu\text{g}/\text{mL}$), 27.50% (12.5 $\mu\text{g}/\text{mL}$), 36.23% (25 $\mu\text{g}/\text{mL}$), 46.32% (50 $\mu\text{g}/\text{mL}$) and 57.51% (100 $\mu\text{g}/\text{mL}$) [Figure 4.1 (C)]. The NO inhibitory effects observed were not due to the cytotoxicity effects of the extract as the cell viability was more than 95% at all concentrations evaluated (Table 4.1).

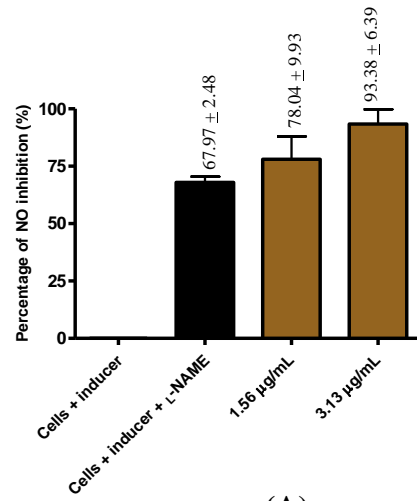
(b) *Boesenbergia rotunda*

Figure 4.2 showed the effects of crude petroleum ether, chloroform, and methanol extracts of *B. rotunda* on nitric oxide production in RAW 264.7 cells. Crude petroleum ether extract dose-dependently inhibited NO production at 21.33% (1.56 $\mu\text{g}/\text{mL}$), 26.11% (3.13 $\mu\text{g}/\text{mL}$), 37.30% (6.25 $\mu\text{g}/\text{mL}$) and 71.45% (12.5 $\mu\text{g}/\text{mL}$) [Figure 4.2 (A)]. At 25–100 $\mu\text{g}/\text{mL}$ tested, the extract exerted pronounced cytotoxicity with RAW 264.7 cell viability about 50% at 25 $\mu\text{g}/\text{mL}$ and less than 5% at 50–100 $\mu\text{g}/\text{mL}$ (Table 4.1). The readings from these concentrations were therefore eliminated from being compared. Crude chloroform extract on the other hand dose-dependently inhibited NO production at 17.32% (1.56 $\mu\text{g}/\text{mL}$), 28.85% (3.13 $\mu\text{g}/\text{mL}$), 44.13% (6.25 $\mu\text{g}/\text{mL}$) and 67.47% (12.5 $\mu\text{g}/\text{mL}$) [Figure 4.2 (B)]. At higher concentrations tested, the extract exerted marked cytotoxicity with RAW 264.7 cell viability less than 50% at 25 $\mu\text{g}/\text{mL}$ and less than 5% at 50 $\mu\text{g}/\text{mL}$ and 100 $\mu\text{g}/\text{mL}$ (Table 4.1). As before, readings from the concentrations were therefore omitted from being compared. Crude methanol extract dose-dependently inhibited NO production up at 6.79% (1.56 $\mu\text{g}/\text{mL}$), 10.06% (3.13 $\mu\text{g}/\text{mL}$), 11.14% (6.25 $\mu\text{g}/\text{mL}$), 16.03% (12.5

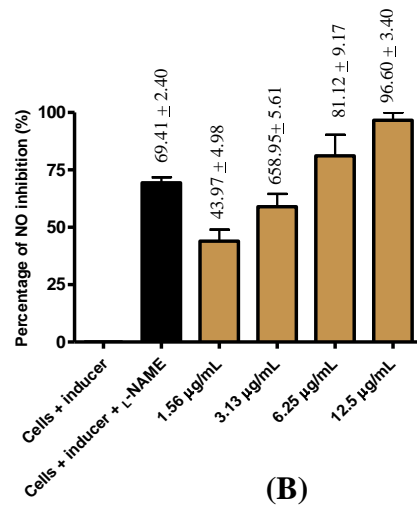
$\mu\text{g/mL}$), 29.13% (25 $\mu\text{g/mL}$) and 54.81% (50 $\mu\text{g/mL}$) [Figure 4.2 (C)]. At 100 $\mu\text{g/mL}$, the extract exerted mild cytotoxicity on RAW 264.7 cells, which the cell viability with 75% (Table 4.1).

(c) *Curcuma aeruginosa*

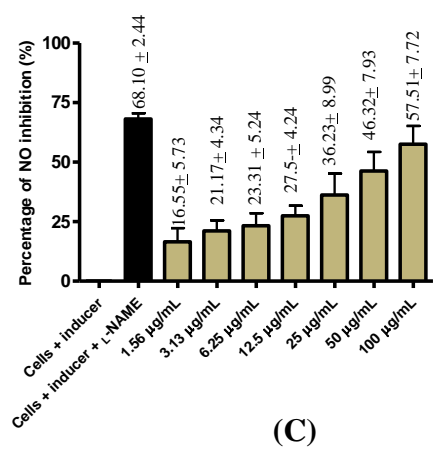
Figure 4.3 showed the effects of crude petroleum ether, chloroform, and methanol extracts of *C. aeruginosa* on nitric oxide production in RAW 264.7 cells. Crude petroleum ether extract dose-dependently inhibited NO production at 11.98% (1.56 $\mu\text{g/mL}$), 15.34% (3.13 $\mu\text{g/mL}$), 26.42% (6.25 $\mu\text{g/mL}$), 38.46% (12.5 $\mu\text{g/mL}$), 64.10% (25 $\mu\text{g/mL}$) [Figure 4.3 (A)]. At 50–100 $\mu\text{g/mL}$ tested, the extract exerted pronounced cytotoxicity with RAW 264.7 cell viability less than 70% at 50 $\mu\text{g/mL}$ and less than 5% at 100 $\mu\text{g/mL}$ (Table 4.1). The readings from these concentrations were therefore eliminated from being compared. Crude chloroform extract on the other hand dose-dependently inhibited NO production at 17.12% (1.56 $\mu\text{g/mL}$), 20.41% (3.13 $\mu\text{g/mL}$), 15.38% (6.25 $\mu\text{g/mL}$) and at 37.81% (12.5 $\mu\text{g/mL}$), 64.30% (25 $\mu\text{g/mL}$) and 89.68% (50 $\mu\text{g/mL}$) [Figure 4.3 (B)]. At 100 $\mu\text{g/mL}$, the extract exerted marked cytotoxicity with RAW 264.7 cell viability less than 15% (Table 4.1). As before, readings from the concentrations were therefore omitted from being compared. Crude methanol extract dose-dependently inhibited NO production up at 10.19% (1.56 $\mu\text{g/mL}$), 12% (3.13 $\mu\text{g/mL}$), 15.01% (6.25 $\mu\text{g/mL}$), 20.36% (12.5 $\mu\text{g/mL}$), 24.17% (25 $\mu\text{g/mL}$), 33.16% (50 $\mu\text{g/mL}$) and 61.07% (100 $\mu\text{g/mL}$) [Figure 4.3 (C)]. The NO inhibitory effects observed were not due to the cytotoxicity effects of the extract as the cell viability was more than 90% at all concentrations evaluated (Table 4.1).



(A)

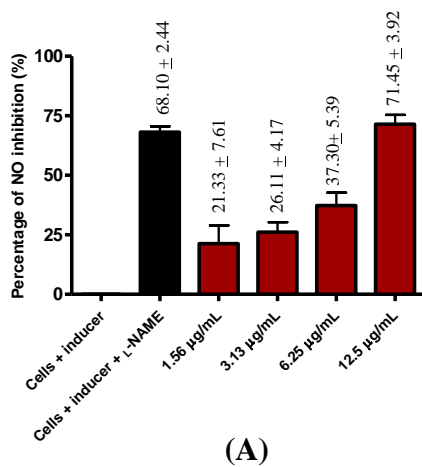


(B)

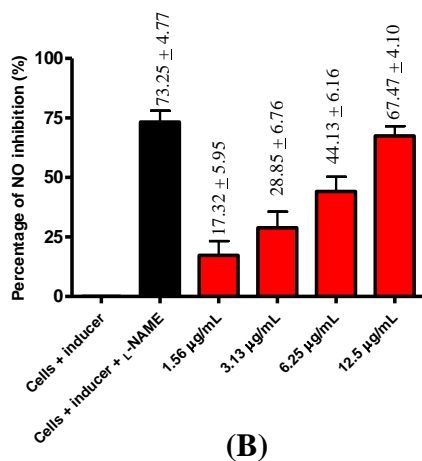


(C)

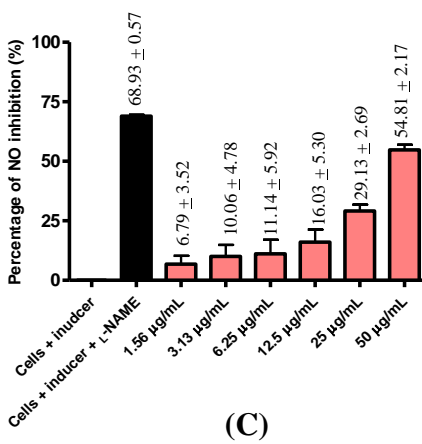
Figure 4.1: Effects of crude (A) petroleum ether, (B) chloroform, and (C) methanol extracts of *Alpinia galanga* on NO production in RAW 264.7 cells. Each bar represents the mean ± S.E. calculated from three independent experiments.



(A)

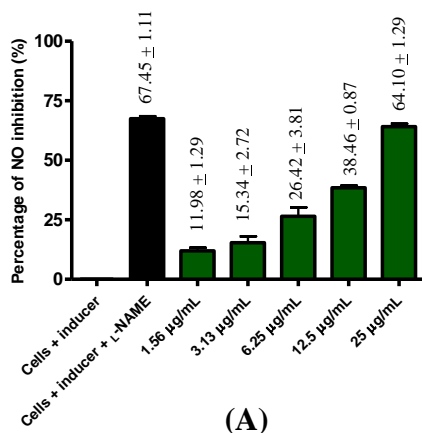


(B)

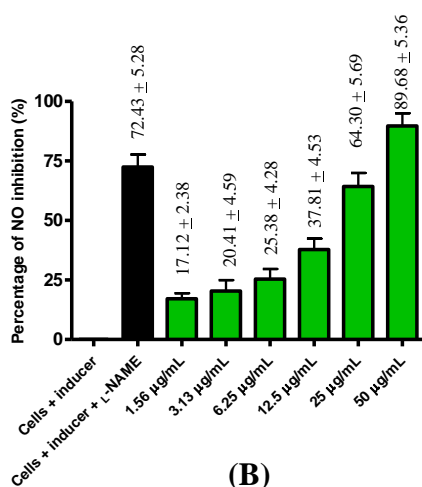


(C)

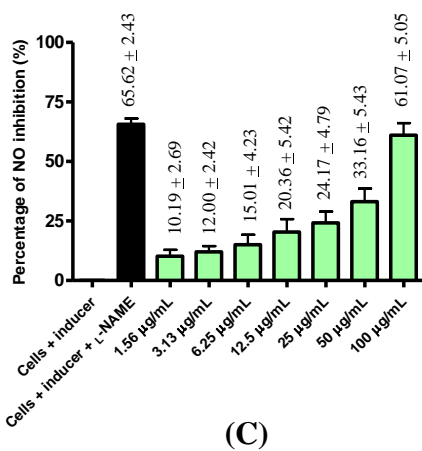
Figure 4.2: Effects of crude (A) petroleum ether, (B) chloroform, and (C) methanol extracts of *Boesenbergia rotunda* on NO production in RAW 264.7 cells. Each bar represents the mean \pm S.E. calculated from three independent experiments.



(A)



(B)

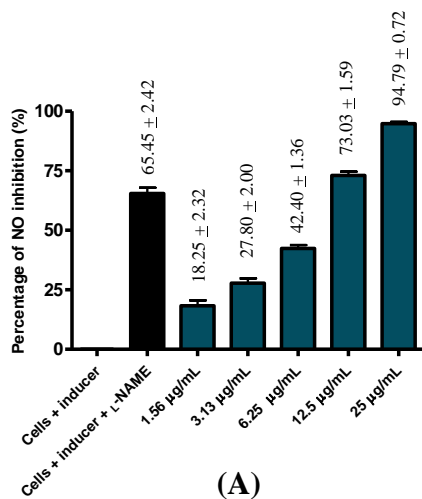


(C)

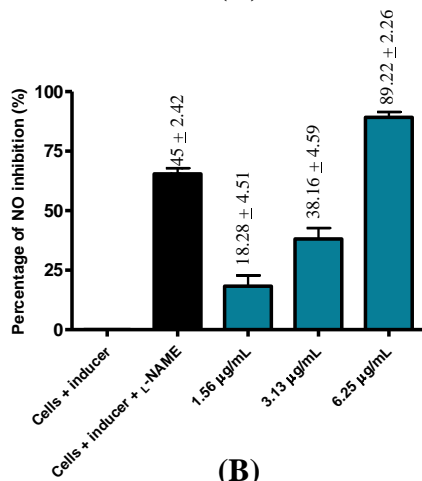
Figure 4.3: Effects of crude (A) petroleum ether, (B) chloroform, and (C) methanol extracts of *Curcuma aeruginosa* on NO production in RAW 264.7 cells. Each bar represents the mean \pm S.E. calculated from three independent experiments.

(d) *Curcuma domestica*

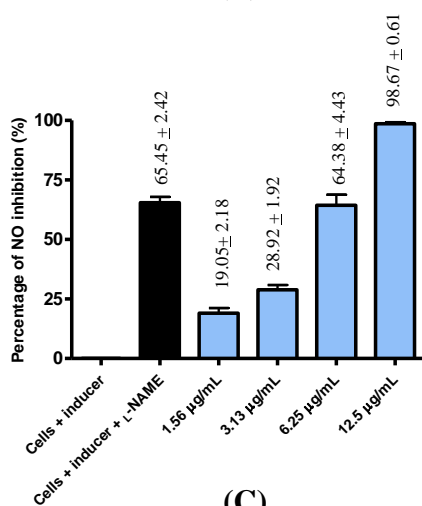
Figure 4.4 showed the effects of crude petroleum ether, chloroform, and methanol extracts of *C. domestica* on nitric oxide production in RAW 264.7 cells. Crude petroleum ether extract dose-dependently inhibited NO production at 18.25% (1.56 µg/mL), 27.80% (3.13 µg/mL), 42.40% (6.25 µg/mL), 70.03% (12.5 µg/mL), 94.79% (25 µg/mL) [Figure 4.4 (A)]. At 50–100 µg/mL tested, the extract exerted pronounced cytotoxicity with RAW 264.7 cell viability less than 75% at 50 µg/mL and less than 5% at 100 µg/mL (Table 4.1). The readings from these concentrations were therefore eliminated from being compared. Crude chloroform extract on the other hand dose-dependently inhibited NO production at 18.28% (1.56 µg/mL), 38.16% (3.13 µg/mL) and 89.22% (6.25 µg/mL) [Figure 4.4 (B)]. At higher concentrations tested, the extract exerted marked cytotoxicity with RAW 264.7 cell viability about 50% at 12.5 µg/mL, less than 15% at 25 µg/mL and less than 10% at 50–100 µg/mL (Table 4.1). As before, readings from the concentrations were therefore omitted from being compared. (Table 4.1). Crude methanol extract dose-dependently inhibited NO production up at 19.05% (1.56 µg/mL), 28.92% (3.13 µg/mL), 64.38% (6.25 µg/mL) and 98.67% (12.5 µg/mL) [Figure 4.4 (C)]. At the higher concentrations tested, the extract exerted cytotoxicity with cell viability less than 60% at 25 µg/mL and less than 10% at 50–100 µg/mL (Table 4.1).



(A)



(B)



(C)

Figure 4.4: Effects of crude (A) petroleum ether, (B) chloroform, and (C) methanol extracts of *Curcuma domestica* on NO production in RAW 264.7 cells. Each bar represents the mean \pm S.E. calculated from three independent experiments.

(e) *Curcuma mangga*

Figure 4.5 showed the effects of crude petroleum ether, chloroform, and methanol extracts of *C. mangga* on nitric oxide production in RAW 264.7 cells. Crude petroleum ether extract dose-dependently inhibited NO production at 9.42% (1.56 µg/mL), 11.85% (3.13 µg/mL), 16.55% (6.25 µg/mL), 20.77% (12.5 µg/mL), 32.46% (25 µg/mL) and 64.49% (50 µg/mL) [Figure 4.5 (A)]. At 100 µg/mL, the extract exerted pronounced cytotoxicity with RAW 264.7 cell viability less than 30% (Table 4.1). The readings from the concentration were therefore eliminated from being compared. Crude chloroform extract on the other hand dose-dependently inhibited NO production at 3% (1.56 µg/mL), 6.64% (3.13 µg/mL), 7.61% (6.25 µg/mL) and at 18.43% (12.5 µg/mL), 33.65% (25 µg/mL) and 73.04% (50 µg/mL) [Figure 4.5 (B)]. At 100 µg/mL, the extract exerted marked cytotoxicity with RAW 264.7 cell viability less than 60% (Table 4.1). As before, readings from the concentrations were therefore omitted from being compared. Crude methanol extract dose-dependently inhibited NO production up at 3.35% (1.56 µg/mL), 4.33% (3.13 µg/mL), 4.65% (6.25 µg/mL), 6.31% (12.5 µg/mL), 8.13% (25 µg/mL), 10.11% (50 µg/mL) and 17.48% (100 µg/mL) [Figure 4.5 (C)]. The NO inhibitory effects observed were not due to the cytotoxicity effects of the extract as the cell viability was more than 95% at all concentrations evaluated (Table 4.1).

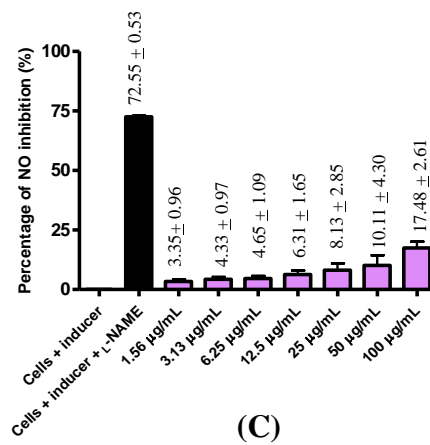
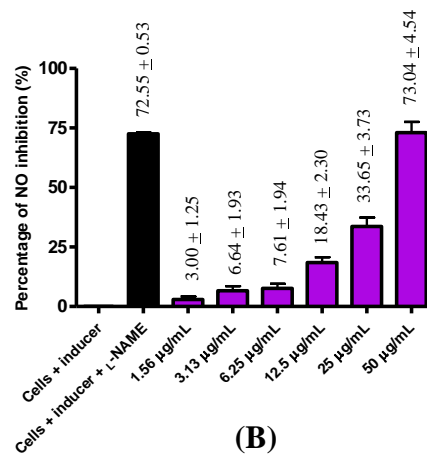
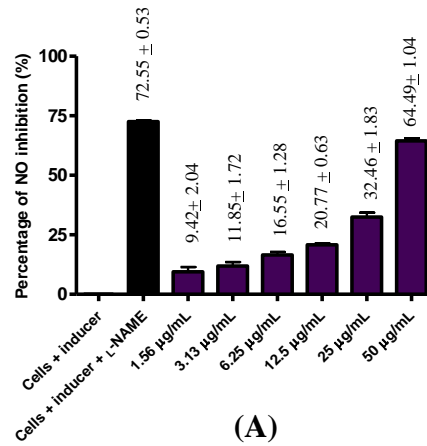


Figure 4.5: Effects of crude (A) petroleum ether, (B) chloroform, and (C) methanol extracts of *Curcuma mangga* on NO production in RAW 264.7 cells. Each bar represents the mean \pm S.E. calculated from three independent experiments.

(f) *Curcuma xanthorrhiza*

Figure 4.6 showed the effects of crude petroleum ether, chloroform, and methanol extracts of *C. xanthorrhiza* on nitric oxide production in RAW 264.7 cells. Crude petroleum ether extract dose-dependently inhibited NO production at 8.79% (1.56 µg/mL), 10.43% (3.13 µg/mL), 20% (6.25 µg/mL), 31.68% (12.5 µg/mL), 60.85% (25 µg/mL) and 90.68% (50 µg/mL) [Figure 4.6 (A)]. At 100 µg/mL, the extract exerted pronounced cytotoxicity with RAW 264.7 cell viability less than 5% (Table 4.1). The readings from the concentration were therefore eliminated from being compared. Crude chloroform extract on the other hand dose-dependently inhibited NO production at 6.49% (1.56 µg/mL), 10.64% (3.13 µg/mL), 29.08% (6.25 µg/mL) and 71.07% (12.5 µg/mL) [Figure 4.6 (B)]. At higher concentrations tested, the extract exerted marked cytotoxicity with RAW 264.7 cell viability less than 60% at 25 µg/mL and less than 10% at 50–100 µg/mL (Table 4.1). As before, readings from the concentrations were therefore omitted from being compared. Crude methanol extract dose-dependently inhibited NO production up at 2.98% (1.56 µg/mL), 4.39% (3.13 µg/mL), 7.14% (6.25 µg/mL), 13.40% (12.5 µg/mL), 36.93% (25 µg/mL), 79.05% (50 µg/mL) and 99.19% (100 µg/mL) [Figure 4.6 (C)]. The NO inhibitory effects observed were not due to the cytotoxicity effects of the extract as the cell viability was more than 95% at all concentrations evaluated (Table 4.1).

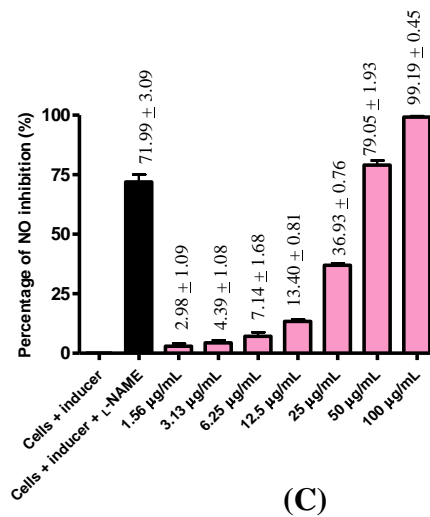
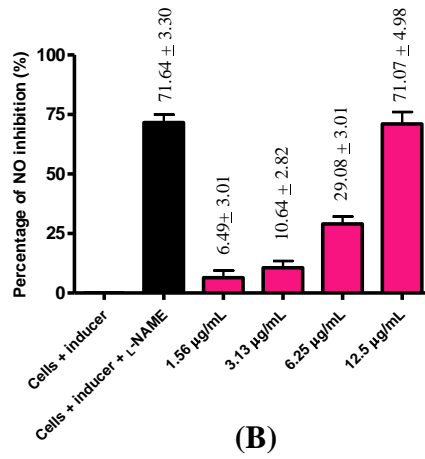
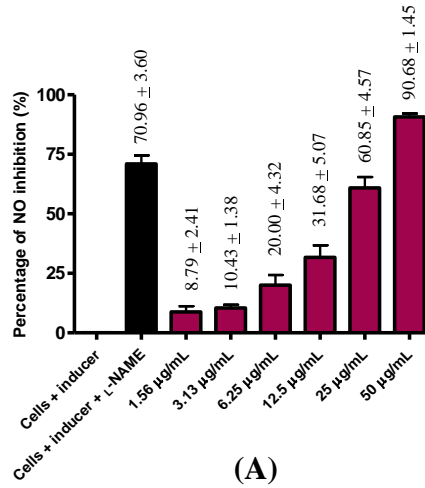


Figure 4.6: Effects of crude (A) petroleum ether, (B) chloroform, and (C) methanol extract of *Curcuma xanthorrhiza* on NO production in RAW 264.7 cells. Each bar represents the mean \pm S.E. calculated from three independent experiments.

(g) *Kaempferia galanga*

Figure 4.7 showed the effects of crude petroleum ether, chloroform, and methanol extracts of *K. galanga* on nitric oxide production in RAW 264.7 cells. Crude petroleum ether extract dose-dependently inhibited NO production at 12.36% (1.56 µg/mL), 17.63% (3.13 µg/mL), 22.11% (6.25 µg/mL), 34.63% (12.5 µg/mL), 55.78% (25 µg/mL), 83.53% (50 µg/mL) and 96.10% (100 µg/mL) [Figure 4.7 (A)]. The NO inhibitory effects observed were not due to the cytotoxicity effects of the extract as the demonstrated RAW 264.7 cell viability were more than 95% at all concentrations tested (Table 4.1). Crude chloroform extract on the other hand dose-dependently inhibited NO production up at 14.62% (1.56 µg/mL), 17.24% (3.13 µg/mL), 22.95% (6.25 µg/mL), 38.53% (12.5 µg/mL), 64.85% (25 µg/mL), 93.05% (50 µg/mL) and 97.90% (100 µg/mL) [Figure 4.7 (B)]. The NO inhibitory effects observed were not due to the cytotoxicity effects of the extract as the demonstrated RAW 264.7 cell viability were more than 95% at all concentrations tested (Table 4.1). Crude methanol extract dose-dependently inhibited NO production up at 8.73% (1.56 µg/mL), 10.33% (3.13 µg/mL), 13.06% (6.25 µg/mL), 17.71% (12.5 µg/mL), 25.26% (25 µg/mL), 42.27% (50 µg/mL) and 69.48% (100 µg/mL) [Figure 4.7 (C)]. The NO inhibitory effects observed were not due to the cytotoxicity effects of the extract as the cell viability was more than 95% at all concentrations evaluated (Table 4.1).

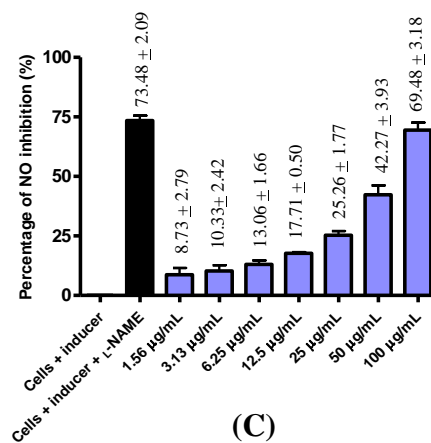
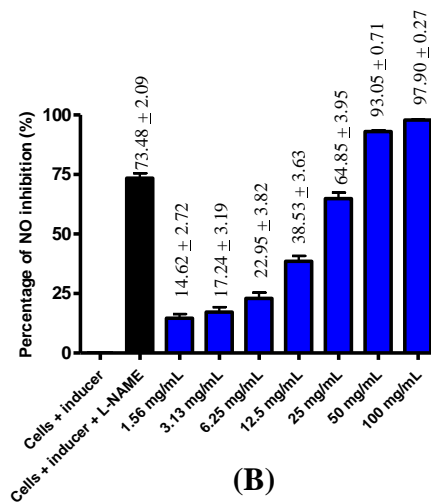
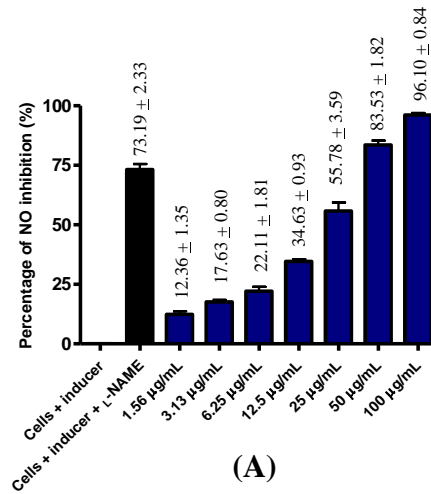


Figure 4.7: Effects of crude (A) petroleum ether, (B) chloroform, and (C) methanol extracts of *Kaempferia galanga* on NO production in RAW 264.7 cells. Each bar represents the mean \pm S.E. calculated from three independent experiments.

(h) *Zingiber montanum*

Figure 4.8 showed the effects of crude petroleum ether, chloroform, and methanol extracts of *Z. montanum* on nitric oxide production in RAW 264.7 cells. Crude petroleum ether extract dose-dependently inhibited NO production at 11.87% (1.56 µg/mL), 22.29% (3.13 µg/mL), 41.17% (6.25 µg/mL), 65.09% (12.5 µg/mL), 77.09% (25 µg/mL) and 93.36% (50 µg/mL) [Figure 4.8 (A)]. At 100 µg/mL, the extract exerted pronounced cytotoxicity with RAW 264.7 cell viability less than 10% (Table 4.1). The readings from the concentration were therefore eliminated from being compared. Crude chloroform extract on the other hand dose-dependently inhibited NO production up at 2.46% (1.56 µg/mL), 7.52% (3.13 µg/mL), 16.17% (6.25 µg/mL), 43.60% (12.5 µg/mL), 87.54% (25 µg/mL), 99.41% (50 µg/mL) and 100% (100 µg/mL) [Figure 4.8 (B)]. The NO inhibitory effects observed were not due to the cytotoxicity effects of the extract as the demonstrated RAW 264.7 cell viability were more than 90% at all concentrations tested (Table 4.1). Crude methanol extract dose-dependently inhibited NO production up at 3.19% (1.56 µg/mL), 4.48% (3.13 µg/mL), 5.90% (6.25 µg/mL), 9.64% (12.5 µg/mL), 12.53% (25 µg/mL), 17.40% (50 µg/mL) and 34.56% (100 µg/mL) [Figure 4.8 (C)]. The NO inhibitory effects observed were not due to the cytotoxicity effects of the extract as the cell viability was more than 95% at all concentrations evaluated (Table 4.1).

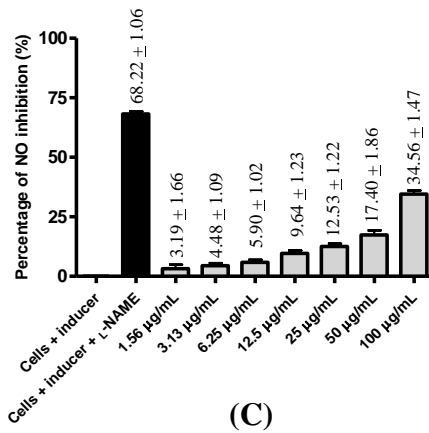
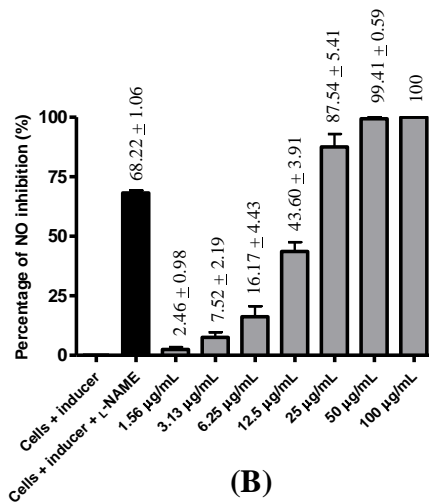
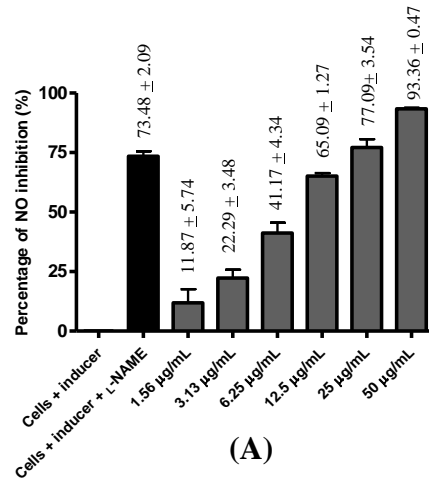


Figure 4.8: Effects of crude (A) petroleum ether, (B) chloroform, and (C) methanol extracts of *Zingiber montanum* on NO production in RAW 264.7 cells. Each bar represents the mean \pm S.E. calculated from three independent experiments.

(i) *Zingiber officinale*

Figure 4.9 showed the effects of crude petroleum ether, chloroform, and methanol extracts of *Z. officinale* on nitric oxide production in RAW 264.7 cells. Crude petroleum ether extract dose-dependently inhibited NO production at 16% (1.56 µg/mL), 21.33% (3.13 µg/mL), 32.41% (6.25 µg/mL), 44.78% (12.5 µg/mL), 72.95% (25 µg/mL) and 98.27% (50 µg/mL) [Figure 4.9 (A)]. At 100 µg/mL, the extract exerted pronounced cytotoxicity with RAW 264.7 cell viability less than 5% (Table 4.1). The readings from the concentration were therefore eliminated from being compared. Crude chloroform extract on the other hand dose-dependently inhibited NO production up at 11.55% (1.56 µg/mL), 16.38% (3.13 µg/mL), 23.90% (6.25 µg/mL), 45.46% (12.5 µg/mL), 83.27% (25 µg/mL) and 95.36% (50 µg/mL) [Figure 4.9 (B)]. At 100 µg/mL, the extract exerted pronounced cytotoxicity with RAW 264.7 cell viability less than 70% (Table 4.1). The readings from the concentration were therefore eliminated from being compared. Crude methanol extract dose-dependently inhibited NO production up at 7.27% (1.56 µg/mL), 7.61% (3.13 µg/mL), 9.07% (6.25 µg/mL), 10.23% (12.5 µg/mL), 15.61% (25 µg/mL), 18.03% (50 µg/mL) and 19.01% (100 µg/mL) [Figure 4.9 (C)]. The NO inhibitory effects observed were not due to the cytotoxicity effects of the extract as the cell viability was more than 95% at all concentrations evaluated (Table 4.1).

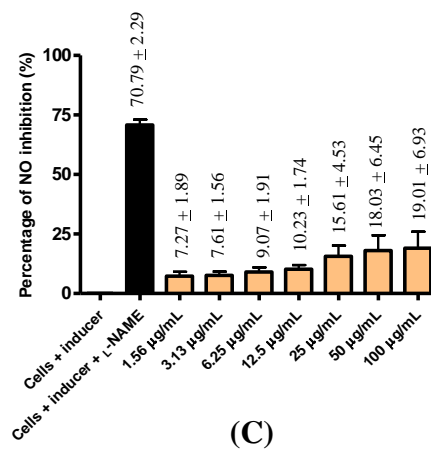
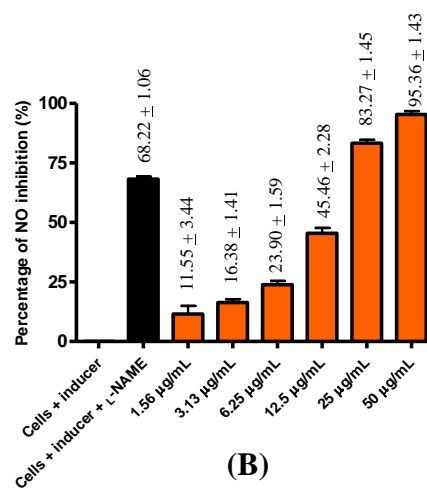
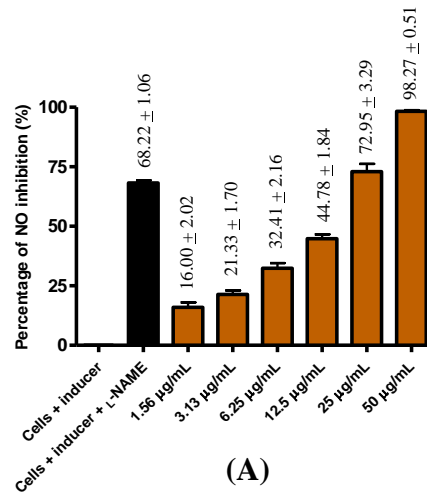


Figure 4.9: Effects of crude (A) petroleum ether, (B) chloroform, and (C) methanol extracts of *Zingiber officinale* on NO production in RAW 264.7 cells. Each bar represents the mean \pm S.E. calculated from three independent experiments.

(j) *Zingiber zerumbet*

Figure 4.10 showed the effects of crude petroleum ether, chloroform, and methanol extracts of *Z. zerumbet* on nitric oxide production in RAW 264.7 cells. Crude petroleum ether extract dose-dependently inhibited NO production at 82.84% (1.56 µg/mL), 95.51% (3.13 µg/mL) and 97.52% (6.25 µg/mL) [Figure 4.10 (A)]. At higher concentrations tested, the extract exerted pronounced cytotoxicity with RAW 264.7 cell viability less than 5% (Table 4.1). The readings from the concentration were therefore eliminated from being compared. Crude chloroform extract on the other hand dose-dependently inhibited NO production up at 40.46% (1.56 µg/mL), 62.31% (3.13 µg/mL), 86.81% (6.25 µg/mL), 91.41% (12.5 µg/mL), 93.38% (25 µg/mL), 94.38% (50 µg/mL) and 94.54% (100 µg/mL) [Figure 4.10 (B)]. The NO inhibitory effects observed were not due to the cytotoxicity effects of the extract as the cell viability was more than 95% at all concentrations evaluated (Table 4.1). The NO inhibitory effects observed were not due to the cytotoxicity effects of the extract as the cell viability was more than 95% at all concentrations evaluated (Table 4.1).

Unlike the other extracts, crude methanol extract of *Z. zerumbet* stimulate NO generation. Percentage of NO generation at each tested concentration was compared with control consisting of cells only (Control 4 as stated in Section 3.3.5) [Figure 4.10 (C)]. In Control 4, NO was not generated (0% of NO) in the absence of inducer. The cells were therefore not stimulated to produce NO. Percentage of NO generation was calculated using Equation (2) as stated in Section 3.36. Crude methanol extract dose-dependently stimulated NO production up at 3.36% (1.56 µg/mL), 13.31% (3.13 µg/mL), 21.74% (6.25 µg/mL), 45.50% (12.5 µg/mL), 56.05% (25 µg/mL), 90.67% (50 µg/mL) and 162.01% (100 µg/mL) [Figure 4.10 (C)].

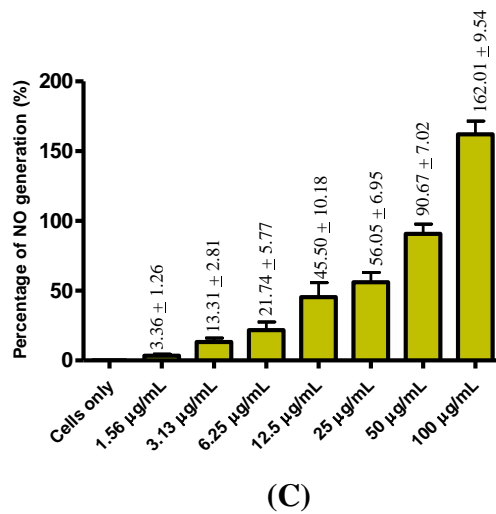
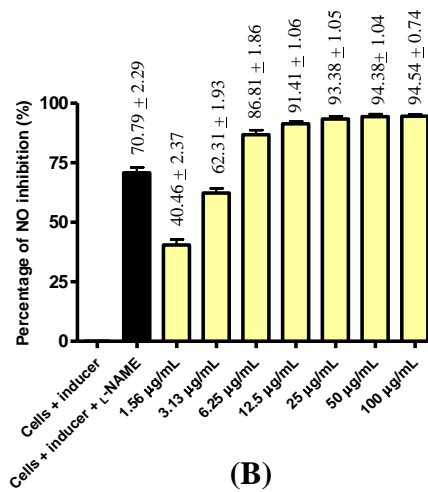
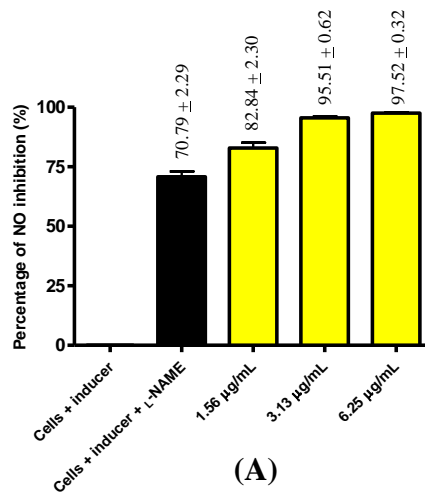


Figure 4.10: Effects of crude (A) petroleum ether, (B) chloroform, and (C) methanol extracts of *Zingiber zerumbet* on NO production in RAW 264.7 cells. Each bar represents the mean \pm S.E. calculated from three independent experiments.

4.1.1 Effects of the Zingiberaceae extracts on viability of RAW 264.7 cells

Effects of the crude *Zingiberaceae* extracts on viability of RAW cells were examined using MTT assay. RAW 264.7 cells viability in the flat bottom 96-well microplate following removal of media for NO assay were immediately tested using MTT assay at 1.56 µg/mL, 3.13 µg/mL, 6.25 µg/mL, 12.5 µg/mL, 25 µg/mL, 50 µg/mL, and 100 µg/mL. The concentrations tested for MTT assay were exactly the same as the concentration tested for NO assay. Effects of the crude *Zingiberaceae* extracts on viability of RAW cells were presented Table 4.1. Most extracts were quite toxic to RAW 264.7 cells except petroleum ether extract of *K. galanga*; chloroform extracts of *K. galanga*, *Z. montanum*, and *Z. zerumbet*; as well as methanol extracts of *A. galanga*, *C. aeruginosa*, *C. mangga*, *K. galanga*, *Z. montanum*, and *Z. officinale*.

Table 4.1: Effects of the *Zingiberaceae* extracts on viability of RAW 264.7 cells

<i>Zingiberaceae</i> sp.	Solvent ¹	Percentage of viability (%)							
		Control	1.56 µg/mL	3.13 µg/mL	6.25µg/mL	12.5 µg/mL	25 µg/mL	50 µg/mL	100 µg/mL
<i>Alpinia galanga</i>	p	100	98.69 ± 0.35	94.35 ± 1.88	39.57 ± 4.56	3.31 ± 0.80	2.34 ± 0.09	2.28 ± 0.17	2.60 ± 0.15
	c	100	99.47 ± 0.46	99.33 ± 0.46	99.16 ± 0.47	95.46 ± 3.46	64.16 ± 6.89	3.87 ± 1.06	2.42 ± 0.72
	m	100	98.56 ± 0.39	99.13 ± 0.24	99.06 ± 0.48	98.78 ± 0.62	99.32 ± 0.45	99.28 ± 0.29	99.62 ± 0.79
<i>Boesenbergia rotunda</i>	p	100	97.39 ± 1.61	94.47 ± 2.56	94.59 ± 2.18	94.07 ± 1.84	51.15 ± 4.11	2.53 ± 0.15	3.18 ± 0.1
	c	100	92.21 ± 1.03	93.66 ± 2.41	93.91 ± 1.33	89.49 ± 2.25	48.17 ± 4.38	2.65 ± 0.13	3.60 ± 0.1
	m	100	96.52 ± 0.78	94.30 ± 1.2	94.22 ± 0.32	94.77 ± 2.14	92.84 ± 0.32	93.86 ± 1.12	75.62 ± 0.55
<i>Curcuma aeruginosa</i>	p	100	96.55 ± 1.16	94.71 ± 0.26	94.81 ± 0.52	96.06 ± 0.46	93.78 ± 0.35	67.24 ± 2.49	3.03 ± 0.25
	c	100	96.61 ± 1.22	95.59 ± 1.31	96.85 ± 1.67	96.69 ± 2.40	95.89 ± 1.6	84.22 ± 2.02	14.57 ± 4.45
	m	100	94.62 ± 2.32	94.66 ± 0.52	92.53 ± 2.37	92.03 ± 3.2	95.16 ± 1.02	97.34 ± 0.24	99.53 ± 0.19
<i>Curcuma domestica</i>	p	100	94.82 ± 0.23	94.95 ± 0.94	94.69 ± 0.71	97.01 ± 1.54	95.03 ± 1.86	73.63 ± 2.83	2.95 ± 0.11
	c	100	98.12 ± 0.93	93.58 ± 1.35	90.72 ± 1.01	51.43 ± 7.55	11.19 ± 1.65	5.76 ± 0.74	9.59 ± 0.97
	m	100	98.33 ± 0.67	98.11 ± 0.26	96.30 ± 0.75	95.48 ± 0.90	58.06 ± 9.42	9.48 ± 3.63	4.15 ± 0.46
<i>Curcuma mangga</i>	p	100	97.13 ± 0.99	97.04 ± 1.32	95.99 ± 0.73	96.86 ± 0.74	96.15 ± 0.46	89.12 ± 1.20	27.92 ± 0.58
	c	100	99.47 ± 0.93	98.04 ± 1.49	98.48 ± 0.15	98.93 ± 0.56	98.54 ± 0.15	92.43 ± 0.48	56.97 ± 1.59
	m	100	98.36 ± 0.23	97.97 ± 0.21	97.79 ± 0.09	97.35 ± 0.01	98.14 ± 0.03	97.31 ± 0.05	98.52 ± 0.55

¹ Solvents used in extraction: p: petroleum ether; c: chloroform, m: methanol.

The cytotoxicity effects of the extracts were evaluated using the conventional MTT assay. Cells remaining in the flat bottom 96-well microplate following removal of media for NO assay were topped up with 100 µL of fresh DMEM with phenol red supplemented with 5% FBS for each well. Then, 20 µL of MTT dye solution was added to each well, and incubated for 4 h. After that, 100 µL of DMSO was added to each well and plate was mixed for 15 min. Absorbance at 540 nm was measured using a microplate reader as a measure of the density of live cells. Results shown are the mean of three-independent experiments with triplicates treatments ± SEM.

Table 4.1 (continued)

<i>Zingiberaceae</i> sp.	Solvent ¹	Percentage of viability (%)							
		Control	1.56 µg/mL	3.13 µg/mL	6.25µg/mL	12.5 µg/mL	25 µg/mL	50 µg/mL	100 µg/mL
<i>Curcuma xanthorrhiza</i>	p	100	99.39 ± 0.15	98.37 ± 0.89	99.12 ± 0.40	99.59 ± 0.38	99.71 ± 0.15	96.02 ± 1.22	3.48 ± 0.29
	c	100	98.96 ± 0.52	98.50 ± 0.58	98.64 ± 0.67	96.09 ± 1.89	57.29 ± 4.28	7.65 ± 1.29	9.97 ± 1.19
	m	100	98.42 ± 0.3	97.97 ± 1.16	99.59 ± 0.3	98.43 ± 0.39	99.36 ± 0.35	99.06 ± 0.25	98.49 ± 0.37
<i>Kaempferia galanga</i>	p	100	96.07 ± 1.06	95.48 ± 1.26	96.38 ± 1.24	94.53 ± 0.89	95.21 ± 1.31	92.97 ± 1.68	89.35 ± 0.37
	c	100	97.79 ± 0.80	95.32 ± 1.62	97.32 ± 0.73	97.40 ± 0.62	97.9 ± 1.08	90.65 ± 2.03	81.00 ± 0.23
	m	100	98.73 ± 0.21	98.62 ± 0.26	98.53 ± 0.79	97.72 ± 1.00	97.67 ± 1.37	98.08 ± 0.85	97.76 ± 0.41
<i>Zingiber montanum</i>	p	100	97.45 ± 2.34	97.06 ± 0.73	96.68 ± 0.88	93.66 ± 2.16	88.35 ± 0.60	82.12 ± 1.06	6.93 ± 2.45
	c	100	97.09 ± 1.36	96.07 ± 1.5	97.41 ± 0.86	97.99 ± 0.96	97.16 ± 0.38	96.99 ± 1.45	85.95 ± 1.92
	m	100	97.59 ± 0.7	96.96 ± 0.73	96.94 ± 0.79	98.23 ± 0.29	98.13 ± 0.92	99.11 ± 0.13	99.17 ± 0.75
<i>Zingiber officinale</i>	p	100	97.11 ± 0.45	97.28 ± 0.42	97.97 ± 0.93	97.51 ± 0.82	97.04 ± 2.17	87.35 ± 1.94	2.31 ± 0.64
	c	100	97.65 ± 0.71	96.68 ± 0.55	95.79 ± 0.27	95.69 ± 0.37	95.77 ± 0.46	86.19 ± 2.56	68.63 ± 2.6
	m	100	97.81 ± 0.36	97.74 ± 0.43	99.19 ± 0.15	99.68 ± 1.00	99.01 ± 0.13	98.68 ± 0.58	96.32 ± 1.25
<i>Zingiber zerumbet</i>	p	100	99.08 ± 0.36	99.17 ± 0.27	95.77 ± 0.25	75.30 ± 1.20	60.16 ± 1.22	45.06 ± 3.41	2.63 ± 0.2
	c	100	99.22 ± 0.71	98.84 ± 0.38	99.21 ± 0.09	99.41 ± 0.17	98.56 ± 0.49	99.21 ± 0.38	98.39 ± 0.71
	m	100	97.21 ± 0.26	97.12 ± 0.46	96.59 ± 0.59	96.67 ± 0.46	96.84 ± 0.36	98.64 ± 0.23	99.05 ± 0.67

¹ Solvents used in extraction: p: petroleum ether, c: chloroform, m: methanol.

The cytotoxicity effects of the extracts were evaluated using the conventional MTT assay. Cells remaining in the flat bottom 96-well microplate following removal of media for NO assay were topped up with 100 µL of fresh DMEM with phenol red supplemented with 5% FBS for each well. Then, 20 µL of MTT dye solution was added to each well, and incubated for 4 h. After that, 100 µL of DMSO was added to each well and plate was mixed for 15 min. Absorbance at 540 nm was measured using a microplate reader as a measure of the density of live cells. Results shown are the mean of three-independent experiments with triplicates treatments ± SEM.

4.1.2 Comparisons on nitric oxide inhibitory activities among *Zingiberaceae* extracts at 1.56–100 µg/mL

The results of screening indicated that 29 (96%) of the extracts exhibit NO inhibitory activity in LPS-stimulated macrophages. The only inactive extract tested was crude methanol extract of *Z. zerumbet*, which surprisingly, showed inverse effect by stimulating NO generation from the lowest concentration (1.56 µg/mL) to the highest concentration (100 µg/mL) tested in a dose-dependent manner [Figure 4.10 (C)]. The active extracts were compared at each concentration (Figure 4.11–4.17).

At the lowest sample concentration tested (**1.56 µg/mL**) (Figure 4.11), crude petroleum ether extracts of *A. galanga* and *Z. zerumbet* exhibited the highest NO inhibitory activity (> 75% inhibition), with no significant difference. Chloroform extracts of *A. galanga* and *Z. zerumbet*, possessed NO inhibitory activity of > 40%, with no significance difference between the two. The rest of the extracts did not showed obvious inhibitory activity at such low concentration. RAW 264.7 cells, treated with the extracts at 1.56 µg/mL showed cell viability \geq 80%.

Based on Figure 4.12, the overall NO inhibitory activities for the extracts tested at **3.13 µg/mL** did not differ significantly when compared with the previous concentration tested (1.56 µg/mL). However, there were increases of NO inhibitory activities for all of the extracts. Crude petroleum ether extracts of *A. galanga* and *Z. zerumbet* represented the most effective extracts at this concentration, with > 90% of NO inhibitory activity. On the other hand, NO inhibitory activities for crude chloroform extracts of *A. galanga* and *Z. zerumbet* increased to > 50%. Even though there were slight increased of NO inhibitory activities for the remaining extracts, the activities were still low (< 40%). RAW 264.7 cells treated with extracts at 3.13 µg/mL showed RAW 264.7 cell viability \geq 80%.

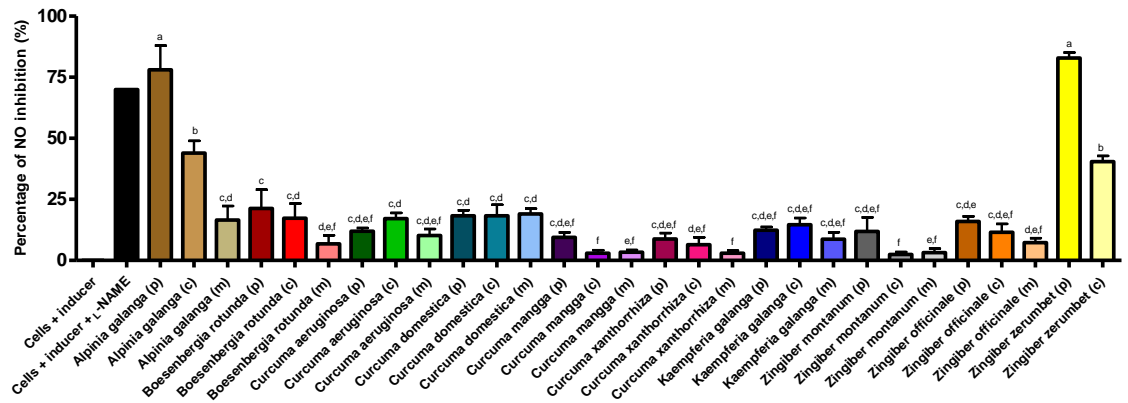


Figure 4.11: Effects of crude *Zingiberaceae* extracts at 1.56 µg/mL on NO production in RAW 264.7 cells. Each bar represents the mean ± S.E. calculated from three independent experiments. Comparisons among different extracts that yielded statistically significant difference ($p < 0.05$) according to ANOVA were indicated by different letters above each bar. Letter 'a' means significantly better than 'b', 'b' means significantly better than 'c', etc.

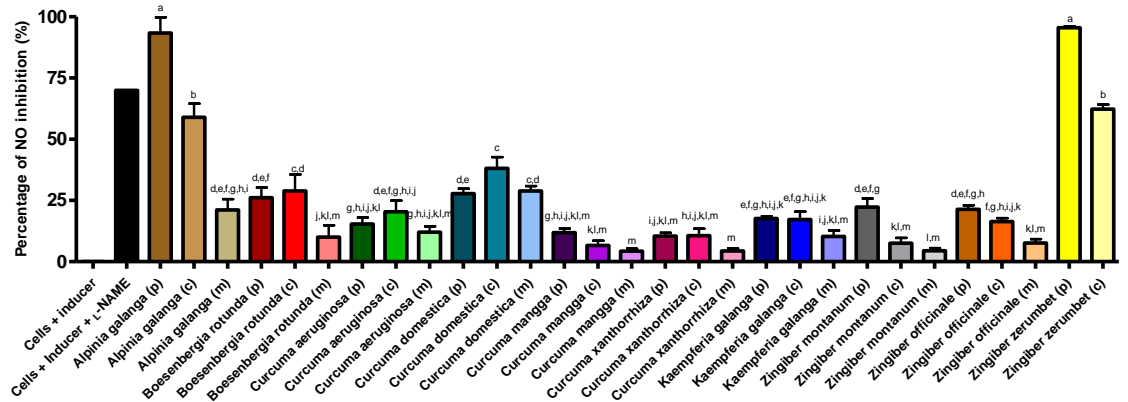


Figure 4.12: Effects of crude *Zingiberaceae* extracts at 3.13 µg/mL on NO production in RAW 264.7 cells. Each bar represents the mean ± S.E. calculated from three independent experiments. Comparisons among different extracts that yielded statistically significant difference ($p < 0.05$) according to ANOVA were indicated by different letters above each bar. Letter 'a' means significantly better than 'b', 'b' means significantly better than 'c', etc.

At the subsequent sample concentration tested, **6.25 µg/mL** (Figure 4.13), the NO inhibitory activities for chloroform extracts of *A. galanga*, *C. domestica*, *Z. zerumbet*; and petroleum ether extract of *Z. zerumbet* were > 75%. The activity for methanol extract of *C. domestica* was increased to > 60%, whereas the activities for the remaining extracts were >

50%. RAW 264.7 cells treated with petroleum ether extract of *A. galanga* showed cell viability < 80% at this concentration. This extract was therefore omitted and not presented in Figure 4.13.

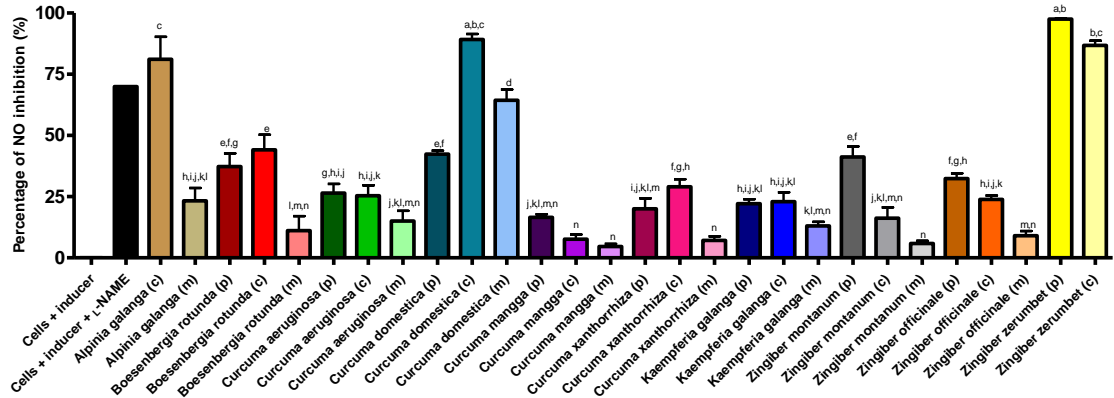


Figure 4.13: Effects of crude *Zingiberaceae* extracts at 6.25 µg/mL on NO production in RAW 264.7 cells. Each bar represents the mean ± S.E. calculated from three independent experiments. Comparisons among different extracts that yielded statistically significant difference ($p < 0.05$) according to ANOVA were indicated by different letters above each bar. Letter ‘a’ means significantly better than ‘b’, ‘b’ means significantly better than ‘c’, etc.

Many extracts exerted obvious boosts of NO inhibitory activity at the subsequent sample concentration tested, **12.5 µg/mL** (Figure 4.14). The most effective extracts were chloroform extracts of *A. galanga*, *Z. zerumbet*; and methanol extract of *C. domestica*, which inhibited > 90% of NO generation in the LPS-stimulated RAW 264.7 cells. Petroleum ether extracts of *B. rotunda*, *C. domestica*, *Z. montanum*; chloroform extracts of *B. rotunda* and *C. xanthorrhiza* exhibited NO inhibitory activity in the range of 60–75%. The activities for the other presented extracts did not exceed 50%. Toxic extracts (resulting in cell viability < 80%) at this concentration tested included petroleum ether extracts of *A. galanga*, *Z. zerumbet*; and chloroform extract of *C. domestica*, which were not presented for comparison.

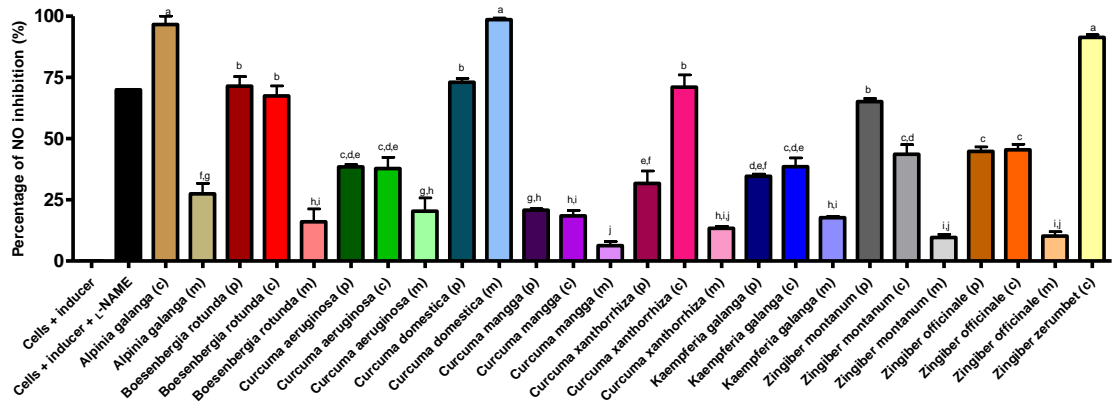


Figure 4.14: Effects of crude *Zingiberaceae* extracts at 12.5 µg/mL on NO production in RAW 264.7 cells. Each bar represents the mean ± S.E. calculated from three independent experiments. Comparisons among different extracts that yielded statistically significant difference ($p < 0.05$) according to ANOVA were indicated by different letters above each bar. Letter ‘a’ means significantly better than ‘b’, ‘b’ means significantly better than ‘c’, etc.

At 25 µg/mL of sample concentration tested (Figure 4.15), petroleum ether extracts of *C. domestica*, *Z. montanum*, *Z. officinale*; chloroform extracts of *Z. montanum*, *Z. officinale*, and *Z. zerumbet* exerted > 70% of NO inhibition. However, petroleum ether extract of *C. domestica*; chloroform extract of *Z. montanum* and *Z. zerumbet* were significantly better than petroleum ether extract of *Z. montanum*, *Z. officinale*; and chloroform extract of *Z. officinale* in NO inhibition. Extracts which were able to inhibit 60–75% of NO generation were petroleum ether extract of *C. aeruginosa*, *C. xanthorrhiza*, *K. galanga*; chloroform extracts of *C. aeruginosa*, and *K. galanga*. RAW 264.7 cells treated with all extracts presented here showed cell viability of $\geq 80\%$.

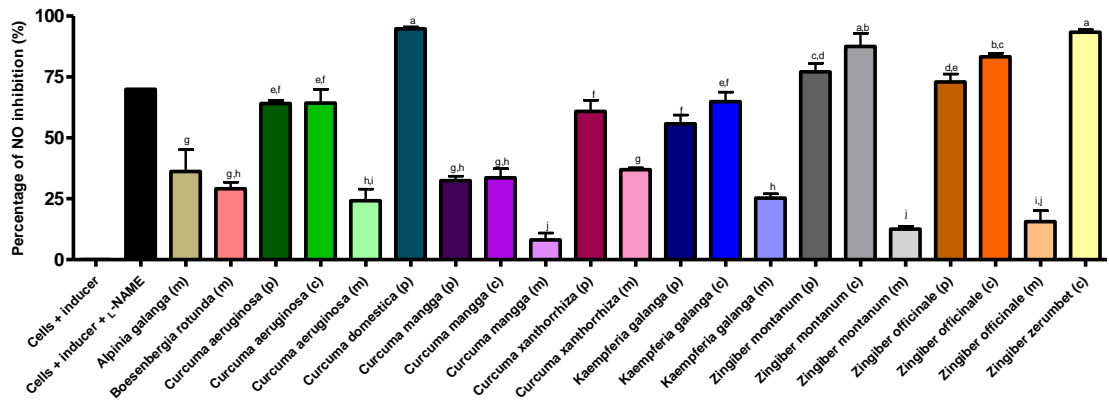


Figure 4.15: Effects of crude *Zingiberaceae* extracts at 25 $\mu\text{g/mL}$ on NO production in RAW 264.7 cells. Each bar represents the mean \pm S.E. calculated from three independent experiments. Comparisons among different extracts that yielded statistically significant difference ($p < 0.05$) according to ANOVA were indicated by different letters above each bar. Letter 'a' means significantly better than 'b', 'b' means significantly better than 'c', etc.

Based on Figure 4.16, most of the extracts were effective in NO inhibition at **50 $\mu\text{g/mL}$** . Chloroform extracts of *C. aeruginosa*, *K. galanga*, *Z. montanum*, *Z. officinale*, *Z. zerumbet*; petroleum ether extracts of *C. xanthorrhiza*, *Z. montanum*, and *Z. officinale* could inhibit almost 90% of NO production in LPS-stimulated RAW 264.7 cells. Methanol extract of *C. xanthorrhiza* and petroleum ether extract of *K. galanga* inhibited NO production in the range of 75–85%, and were significantly better than petroleum ether and chloroform extracts of *C. mangga*, which inhibited NO production at 60% and 70%, respectively. RAW 264.7 cells treated with 19 extracts showed cell viability $\geq 80\%$.

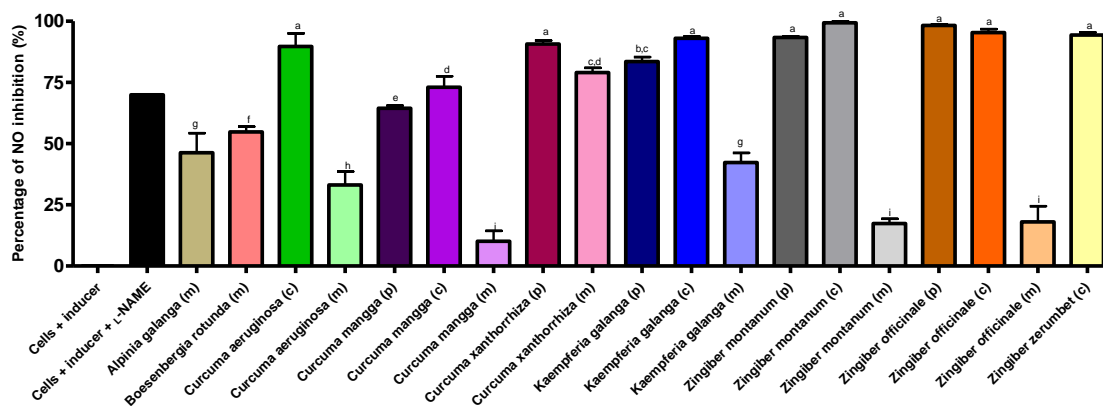


Figure 4.16: Effects of crude *Zingiberaceae* extracts at 50 µg/mL on NO production in RAW 264.7 cells. Each bar represents the mean ± S.E. calculated from three independent experiments. Comparisons among different extracts that yielded statistically significant difference ($p < 0.05$) according to ANOVA were indicated by different letters above each bar. Letter 'a' means significantly better than 'b', 'b' means significantly better than 'c', etc.

The highest concentration tested for each extracts were **100 µg/mL**, only 11 extracts resulted in RAW 264.7 cell viability $\geq 80\%$ and were compared in Figure 4.17. This indicated that most of the crude *Zingiberaceae* extracts were toxic at higher concentrations. Among these extracts, methanol extracts of *C. xanthorrhiza*; petroleum ether extract of *K. galanga*; and chloroform extracts of *K. galanga*, *Z. montanum*, and *Z. zerumbet* inhibited $> 90\%$ of NO generation. The remaining extracts possessed low NO inhibitory activity even at such high concentration.

Crude petroleum ether extracts of *A. galanga* and *Z. zerumbet* elicited the highest percentage of NO inhibition ($> 70\%$) at the lowest concentration (1.56 µg/mL) (Fig. 4.11.). However, their high activity of NO inhibition was correlated with their high toxicity to RAW 264.7 cells, which showed toxicity at 6.25 µg/mL and 12.5 µg/mL, respectively. On the other hand, crude petroleum ether extracts of *K. galanga*; chloroform extracts of *K. galanga*, *Z. montanum*, and *Z. zerumbet*; as well as methanol extracts of *A. galanga*, *C. aeruginosa*, *C. mangga*, *K. galanga*, *Z. montanum*, and *Z. officinale* did not show

cytotoxicity at the pharmacologically doses ($\leq 100 \mu\text{g/mL}$) (Fig. 4.17). Among these extracts, chloroform extract of *Z. zerumbet* were shown to possess high NO inhibition activity to the variable concentrations with no cytotoxicity against RAW 264.7 cells.

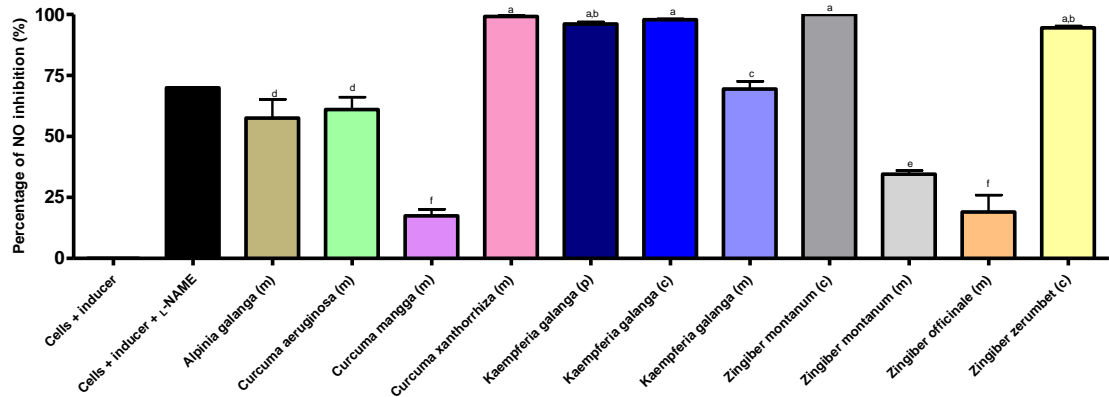


Figure 4.17: Effects of crude *Zingiberaceae* extracts at $100 \mu\text{g/mL}$ on NO production in RAW 264.7 cells. Each bar represents the mean \pm S.E. calculated from three independent experiments. Comparisons among different extracts that yielded statistically significant difference ($p < 0.05$) according to ANOVA were indicated by different letters above each bar. Letter ‘a’ means significantly better than ‘b’, ‘b’ means significantly better than ‘c’, etc.

The effectiveness of NO inhibition activity at each concentration for the extracts was classified into four groups according to its inhibitory rate (IR) as follows: strongly active ($\text{IR} \geq 70\%$), moderately active ($\text{IR}, 50\text{--}60\%$), weakly active ($\text{IR}, 30\text{--}49\%$), and inactive ($\text{IR} \leq 29\%$) (Table 4.2).

Table 4.2: Classifications of the effectiveness of NO inhibition activity of 29 tested crude *Zingiberaceae* extracts¹ at 1.56 µg/mL, 3.13 µg/mL, 6.25 µg/mL, 12.5 µg/mL, 25 µg/mL, 50 µg/mL, and 100 µg/mL in RAW 264.7 cells

Concentration	Strongly active (IR ≥ 70%)	Moderately active (IR, 50 – 60%)	Weakly active (IR, 30 – 49%)	Inactive (IR ≤ 29%)			
1.56 µg/mL	<i>Alpinia galanga</i> (p) <i>Zingiber zerumbet</i> (p)		<i>Alpinia galanga</i> (c)	<i>Alpinia galanga</i> (m) <i>Boesenbergia rotunda</i> (p) <i>Boesenbergia rotunda</i> (c) <i>Boesenbergia rotunda</i> (m) <i>Curcuma aeruginosa</i> (p) <i>Curcuma aeruginosa</i> (c) <i>Curcuma aeruginosa</i> (m) <i>Curcuma domestica</i> (p) <i>Curcuma domestica</i> (c) <i>Curcuma domestica</i> (m) <i>Curcuma mangga</i> (p) <i>Curcuma mangga</i> (c) <i>Curcuma mangga</i> (m) <i>Curcuma xanthorrhiza</i> (p) <i>Curcuma xanthorrhiza</i> (c) <i>Curcuma xanthorrhiza</i> (m) <i>Kaempferia galanga</i> (p) <i>Kaempferia galanga</i> (c) <i>Kaempferia galanga</i> (m) <i>Zingiber montanum</i> (p) <i>Zingiber montanum</i> (c) <i>Zingiber montanum</i> (m) <i>Zingiber officinale</i> (p) <i>Zingiber officinale</i> (c) <i>Zingiber officinale</i> (m)			
			<i>Zingiber zerumbet</i> (c)				
	3.13 µg/mL		<i>Alpinia galanga</i> (p) <i>Zingiber zerumbet</i> (p)			<i>Alpinia galanga</i> (c)	<i>Alpinia galanga</i> (m) <i>Boesenbergia rotunda</i> (p) <i>Boesenbergia rotunda</i> (c) <i>Boesenbergia rotunda</i> (m) <i>Curcuma aeruginosa</i> (p) <i>Curcuma aeruginosa</i> (c) <i>Curcuma aeruginosa</i> (m) <i>Curcuma domestica</i> (p) <i>Curcuma domestica</i> (m) <i>Curcuma mangga</i> (p) <i>Curcuma mangga</i> (c) <i>Curcuma mangga</i> (m) <i>Curcuma xanthorrhiza</i> (p) <i>Curcuma xanthorrhiza</i> (c) <i>Curcuma xanthorrhiza</i> (m) <i>Kaempferia galanga</i> (p) <i>Kaempferia galanga</i> (c) <i>Kaempferia galanga</i> (m) <i>Zingiber montanum</i> (p) <i>Zingiber montanum</i> (c) <i>Zingiber montanum</i> (m) <i>Zingiber officinale</i> (p) <i>Zingiber officinale</i> (c) <i>Zingiber officinale</i> (m)
						<i>Zingiber zerumbet</i> (c)	

¹ Each crude *Zingiberaceae* extract was tested at 1.56 µg/mL, 3.13 µg/mL, 6.25 µg/mL, 12.5 µg/mL, 25 µg/mL, 50 µg/mL, and 100 µg/mL in triplicates (N = 3). RAW 264.7 cells were stimulated with 10µg/ml LPS to generate NO. The effectiveness of the NO inhibition activity was categorized into four groups, namely strongly active, moderately active, weakly active, and inactive according to the IR values. In the Table, p represents petroleum ether extract, c represents chloroform extract, and m represents methanol extract.

Table 4.2 (continued)

Concentration	Strongly active (IR ≥ 70%)	Moderately active (IR, 50 – 60%)	Weakly active (IR, 30 – 49%)	Inactive (IR ≤ 29%)
6.25 µg/mL	<i>Alpinia galanga</i> (c) <i>Curcuma domestica</i> (c) <i>Zingiber zerumbet</i> (p) <i>Zingiber zerumbet</i> (c)	<i>Curcuma domestica</i> (m)	<i>Boesenbergia rotunda</i> (p) <i>Boesenbergia rotunda</i> (c) <i>Curcuma domestica</i> (p) <i>Curcuma mangga</i> (p) <i>Zingiber montanum</i> (p) <i>Zingiber officinale</i> (p)	<i>Alpinia galanga</i> (m) <i>Boesenbergia rotunda</i> (m) <i>Curcuma aeruginosa</i> (p) <i>Curcuma aeruginosa</i> (c) <i>Curcuma aeruginosa</i> (m) <i>Curcuma mangga</i> (p) <i>Curcuma mangga</i> (c) <i>Curcuma mangga</i> (m) <i>Curcuma xanthorrhiza</i> (p) <i>Curcuma xanthorrhiza</i> (c) <i>Curcuma xanthorrhiza</i> (m) <i>Kaempferia galanga</i> (p) <i>Kaempferia galanga</i> (c) <i>Kaempferia galanga</i> (m) <i>Zingiber montanum</i> (c) <i>Zingiber montanum</i> (m) <i>Zingiber officinale</i> (c) <i>Zingiber officinale</i> (m)
12.5 µg/mL	<i>Alpinia galanga</i> (c) <i>Boesenbergia rotunda</i> (p) <i>Curcuma domestica</i> (p) <i>Curcuma xanthorrhiza</i> (c) <i>Zingiber zerumbet</i> (c)	<i>Boesenbergia rotunda</i> (c) <i>Zingiber montanum</i> (p)	<i>Curcuma aeruginosa</i> (p) <i>Curcuma aeruginosa</i> (c) <i>Curcuma xanthorrhiza</i> (p) <i>Kaempferia galanga</i> (p) <i>Kaempferia galanga</i> (c) <i>Zingiber montanum</i> (c) <i>Zingiber officinale</i> (p) <i>Zingiber officinale</i> (c)	<i>Alpinia galanga</i> (m) <i>Boesenbergia rotunda</i> (m) <i>Curcuma aeruginosa</i> (m) <i>Curcuma mangga</i> (p) <i>Curcuma mangga</i> (c) <i>Curcuma mangga</i> (m) <i>Curcuma xanthorrhiza</i> (m) <i>Kaempferia galanga</i> (m) <i>Zingiber montanum</i> (m) <i>Zingiber officinale</i> (m)
25 µg/mL	<i>Curcuma domestica</i> (p) <i>Zingiber montanum</i> (p) <i>Zingiber montanum</i> (c) <i>Zingiber officinale</i> (p) <i>Zingiber officinale</i> (c) <i>Zingiber zerumbet</i> (c)	<i>Curcuma aeruginosa</i> (p) <i>Curcuma aeruginosa</i> (c) <i>Curcuma xanthorrhiza</i> (p) <i>Kaempferia galanga</i> (p) <i>Kaempferia galanga</i> (c)	<i>Alpinia galanga</i> (m) <i>Curcuma mangga</i> (p) <i>Curcuma mangga</i> (c) <i>Curcuma xanthorrhiza</i> (m)	<i>Boesenbergia rotunda</i> (m) <i>Curcuma aeruginosa</i> (m) <i>Curcuma mangga</i> (m) <i>Kaempferia galanga</i> (m) <i>Zingiber montanum</i> (m) <i>Zingiber officinale</i> (m)
50 µg/mL	<i>Curcuma aeruginosa</i> (c) <i>Curcuma mangga</i> (c) <i>Curcuma xanthorrhiza</i> (p) <i>Curcuma xanthorrhiza</i> (m) <i>Kaempferia galanga</i> (p) <i>Kaempferia galanga</i> (c) <i>Zingiber montanum</i> (p) <i>Zingiber montanum</i> (c) <i>Zingiber officinale</i> (p) <i>Zingiber officinale</i> (c) <i>Zingiber zerumbet</i> (c)	<i>Boesenbergia rotunda</i> (m) <i>Curcuma mangga</i> (p) <i>Curcuma mangga</i> (c)	<i>Alpinia galanga</i> (m) <i>Curcuma aeruginosa</i> (m) <i>Kaempferia galanga</i> (m)	<i>Curcuma mangga</i> (m) <i>Zingiber montanum</i> (m) <i>Zingiber officinale</i> (m)
100 µg/mL	<i>Curcuma xanthorrhiza</i> (m) <i>Kaempferia galanga</i> (p) <i>Kaempferia galanga</i> (c) <i>Zingiber montanum</i> (c) <i>Zingiber zerumbet</i> (c)	<i>Alpinia galanga</i> (m) <i>Curcuma aeruginosa</i> (m) <i>Kaempferia galanga</i> (m)	<i>Zingiber montanum</i> (m)	<i>Curcuma mangga</i> (m) <i>Zingiber officinale</i> (m)

¹ Each crude *Zingiberaceae* extract was tested at 1.56 µg/mL, 3.13 µg/mL, 6.25 µg/mL, 12.5 µg/mL, 25 µg/mL, 50 µg/mL, and 100 µg/mL in triplicates (N = 3). RAW 264.7 cells were stimulated with 10µg/ml LPS to generate NO. The effectiveness of the NO inhibition activity was categorized into four groups, namely strongly active, moderately active, weakly active, and inactive according to the IR values. In the Table, p represents petroleum ether extract, c represents chloroform extract, and m represents methanol extract.

Based on Table 4.2, 19 of 30 crude *Zingiberaceae* extracts strongly inhibited (IR \geq 70%) NO generation in RAW 264.7 cells, which were the petroleum ether extracts of *A. galanga*, *B. rotunda*, *C. domestica*, *C. xanthorrhiza*, *K. galanga*, *Z. montanum*, *Z. officinale*, and *Z. zerumbet*; chloroform extracts of *A. galanga*, *C. aeruginosa*, *C. domestica*, *C. xanthorrhiza*, *K. galanga*, *C. mangga*, *Z. montanum*, *Z. officinale*, and *Z. zerumbet*; as well as methanol extracts of *C. domestica* and *C. xanthorrhiza*.

In particular, extracts with markedly high NO inhibitory activities (IR > 90%) were the petroleum ether extracts of *A. galanga* (at 3.13 $\mu\text{g/mL}$), *C. domestica* (at 25 $\mu\text{g/mL}$), *C. xanthorrhiza* (at 50 $\mu\text{g/mL}$), *K. galanga* (at 100 $\mu\text{g/mL}$), *Z. montanum* (at 50 $\mu\text{g/mL}$), *Z. officinale* (at 50 $\mu\text{g/mL}$), and *Z. zerumbet* (at 3.13 $\mu\text{g/mL}$ and 6.25 $\mu\text{g/mL}$); chloroform extracts of *A. galanga* (at 12.5 $\mu\text{g/mL}$), *K. galanga* (at 50 $\mu\text{g/mL}$ and 100 $\mu\text{g/mL}$), *Z. montanum* (at 50 $\mu\text{g/mL}$ and 100 $\mu\text{g/mL}$), *Z. officinale* (at 50 $\mu\text{g/mL}$), and *Z. zerumbet* (at 12.5 $\mu\text{g/mL}$, 25 $\mu\text{g/mL}$, 50 $\mu\text{g/mL}$ and 100 $\mu\text{g/mL}$); as well as methanol extracts of *C. domestica* (at 12.5 $\mu\text{g/mL}$) and *C. xanthorrhiza* (at 100 $\mu\text{g/mL}$).

In this study, petroleum ether extract of *A. galanga* was selected as the most potential extract as it possessed the strongest NO inhibitory activity at the lowest concentration. Overall, nineteen (63%) crude *Zingiberaceae* extracts possess strong NO inhibition activities. Among these active extracts, 14 extracts were effective in reducing NO generation with IR > 90%. These results suggested that the selected *Zingiberaceae* species contain secondary metabolites with immunomodulatory properties that should be further investigated.

4.2 Effects of the Zingiberaceae Extracts on MDA-MB-231 Cell Proliferation or Viability

In the search of natural product with anti-cancer activity, the effects of 30 crude *Zingiberaceae* extracts on proliferation of oestrogen negative human breast cancer cells (MDA-MB-231) were tested. Each extract was tested for cytotoxicity at 1.56 µg/mL, 3.13 µg/mL, 6.25 µg/mL, 12.5 µg/mL, 25 µg/mL, 50 µg/mL, and 100 µg/mL against MDA-MB-231 cells, using the conventional MTT assay. The effect at various concentrations was studied after 48 h, and dose-response graphs for the extracts (Figure 4.18–4.27) were generated. The cells exhibited concentration-dependent growth inhibition by the crude *Zingiberaceae* extracts.

(a) *Alpinia galanga*

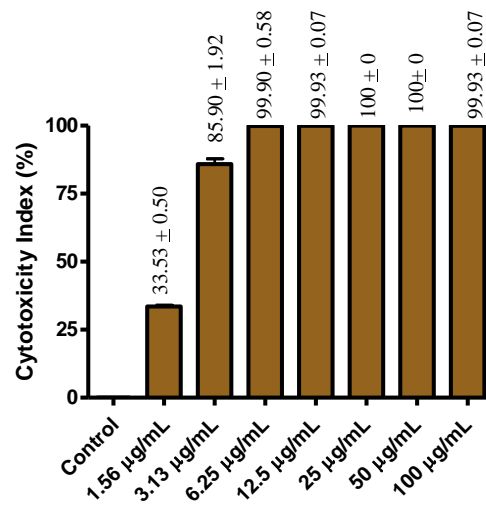
Figure 4.18 showed the cytotoxicity effects of crude petroleum ether, chloroform, and methanol extracts of *A. galanga* on MDA-MB-231 cells. The results indicated that crude petroleum ether extract exerted a pronounced cytotoxic effect against MDA-MB-231 cells, which inhibited at least 80% of cell proliferation at 3.13 µg/mL. At 6.25–100 µg/mL, cell growth inhibition was almost 100% [Figure 4.18 (A)]. Crude chloroform extract inhibited more than 95% of cell proliferation at 12.5–100 µg/mL [Figure 4.18 (B)]. Crude methanol extract was weakly inhibitory against MDA-MB-231 cells even though the cytotoxicity index growth inhibition was showed to be dose-dependently. The highest cytotoxicity index indicated was less than 20% at 100 µg/mL [Figure 4.18 (C)]. Only extracts which inhibit at least 50% of cell growth at < 30 µg/mL are considered as actively cytotoxic (Suffness & Pezzuto, 1990). Those which do not are not considered as cytotoxic. Therefore, based on this, methanol extract of *A. galanga* was not considered as cytotoxic.

(b) *Boesenbergia rotunda*

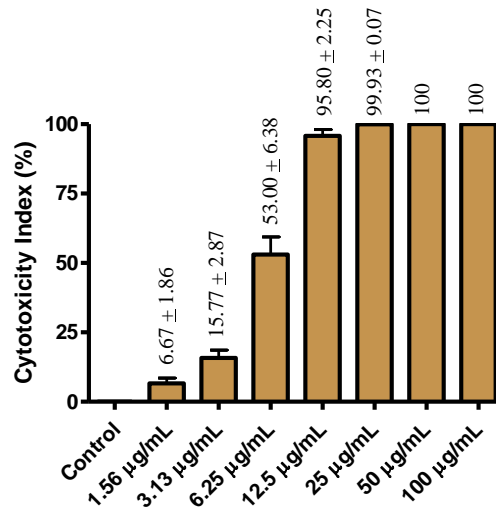
Figure 4.19 showed the cytotoxicity effects of crude petroleum ether, chloroform, and methanol extracts of *B. rotunda* on MDA-MB-231 cells. The results indicated that crude petroleum ether [Figure 4.19 (A)] and chloroform [Figure 4.19 (B)] extracts inhibited almost 100% of cell proliferation at 25–100 $\mu\text{g/mL}$. Crude methanol extract showed a dose-dependent inhibitory effect on cell proliferation against MDA-MB-231 cells [Figure 4.19 (C)]. The highest inhibition was more than 65% at 100 $\mu\text{g/mL}$. However, at concentration 50 $\mu\text{g/mL}$ or lower, the inhibition effects dropped to less than 30%.

(c) *Curcuma aeruginosa*

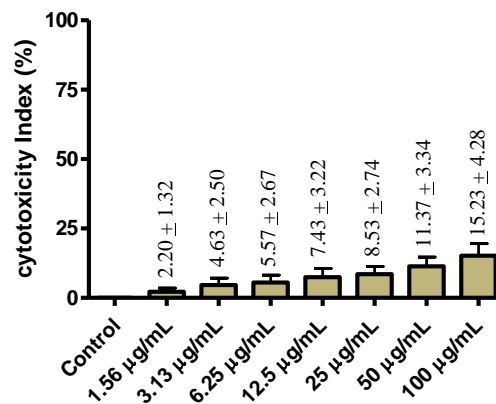
Figure 4.20 showed the cytotoxicity effects of crude petroleum ether, chloroform, and methanol extracts of *C. aeruginosa* on MDA-MB-231 cells. Crude petroleum ether extract showed a dose-dependent inhibitory effect on cell proliferation against MDA-MB-231 cells [Figure 4.20 (A)]. At 50 $\mu\text{g/mL}$ and 100 $\mu\text{g/mL}$, the inhibition of cell proliferation was more than 90%. The inhibition at 25 $\mu\text{g/mL}$ or lower was less than 30%. Crude chloroform extract showed a dose-dependent inhibitory effect on cell proliferation against MDA-MB-231 cells [Figure 4.20 (B)]. The highest cytotoxicity effect was 80% at 100 $\mu\text{g/mL}$. The cytotoxicity effect at 50 $\mu\text{g/mL}$ or lower was less than 30%. Crude methanol extract was weakly inhibitory against MDA-MB-231 cells even though the cytotoxicity index was showed to be dose-dependently [Figure 4.20 (C)]. The overall cytotoxicity effects were less than 15% at 1.56–100 $\mu\text{g/mL}$. Since inhibitory percentage was less than 50% at 30 $\mu\text{g/mL}$, all three extracts of *C. aeruginosa* were deemed as not actively cytotoxic against MDA-MB-231 cells.



(A)

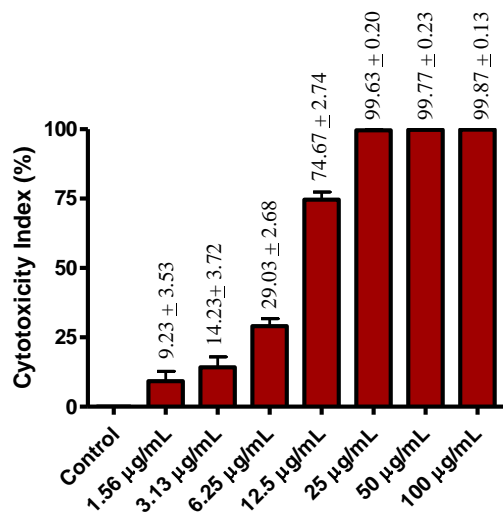


(B)

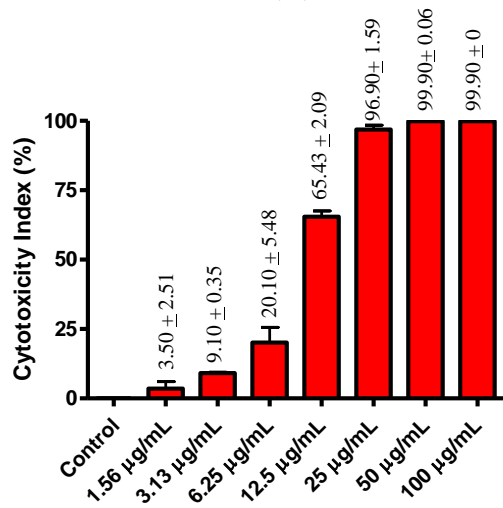


(C)

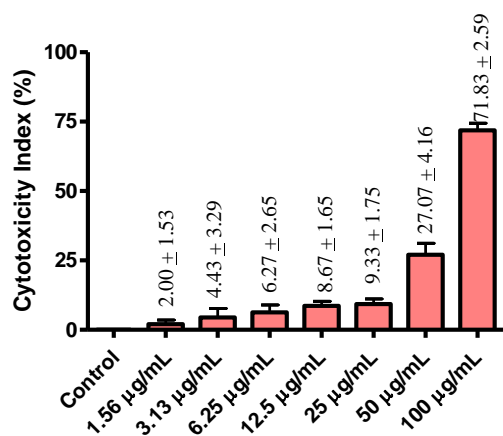
Figure 4.18: Growth inhibition by (A) petroleum ether, (B) chloroform, and (C) methanol extracts of *Alpinia galanga* on MDA-MB-231 cells using the MTT assay. Each bar represents the mean \pm S.E. calculated from three independent experiments.



(A)



(B)



(C)

Figure 4.19: Growth inhibition by (A) petroleum ether, (B) chloroform, and (C) methanol extracts of *Boesenbergia rotunda* on MDA-MB-231 cells using the MTT assay. Each bar represents the mean \pm S.E. calculated from three independent experiments.

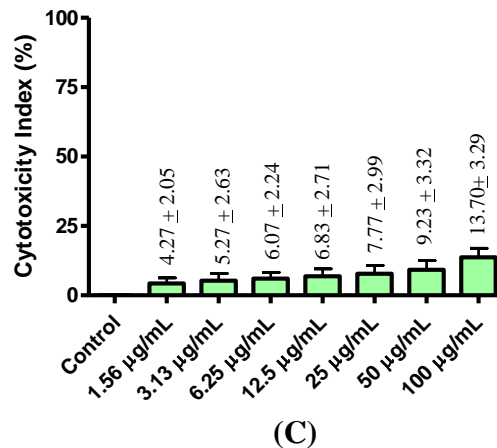
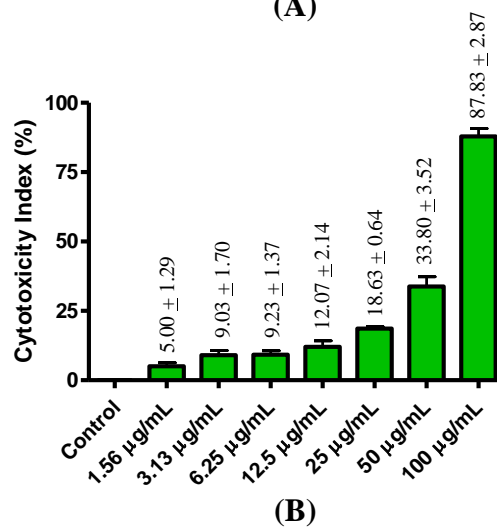
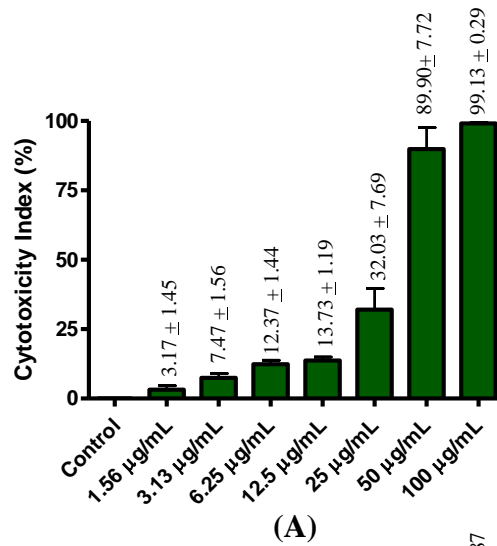


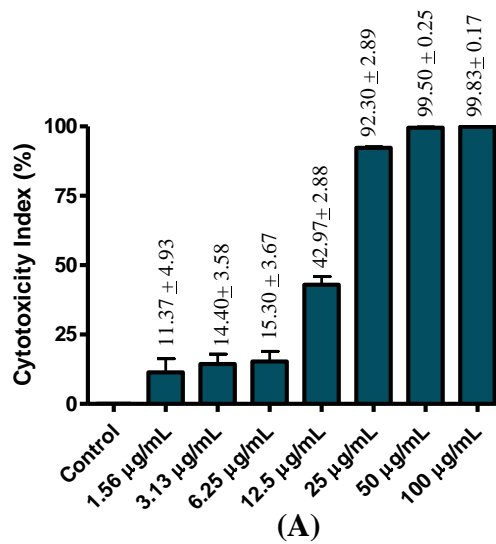
Figure 4.20: Growth inhibition by (A) petroleum ether, (B) chloroform, and (C) methanol extracts of *Curcuma aeruginosa* on MDA-MB-231 cells using the MTT assay. Each bar represents the mean \pm S.E. calculated from three independent experiments.

(d) *Curcuma domestica*

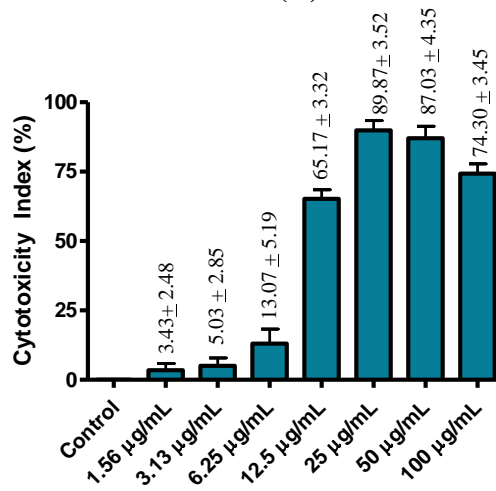
Figure 4.21 showed the cytotoxicity effects of crude petroleum ether, chloroform, and methanol extracts of *C. domestica* on MDA-MB-231 cells. Crude petroleum ether extract inhibited more than 90% of cell proliferation at 25–100 $\mu\text{g/mL}$ [Figure 4.20 (A)]. Based on Figure 4.21 (B), crude chloroform extract inhibited more than 85% of cell proliferation at 25 $\mu\text{g/mL}$. There was a decrease of cytotoxicity index (%) at 50 $\mu\text{g/mL}$ and 100 $\mu\text{g/mL}$. This phenomenon may be due to the heavy pigment of the crude extracts which lead to higher absorbance values obtained using Emax microplate reader. Crude methanol extract showed a dose-dependent inhibitory effect on cell proliferation against MDA-MB-231 cells [Figure 4.21 (C)]. It inhibited more than 80% of cell proliferation at 25–100 $\mu\text{g/mL}$.

(e) *Curcuma mangga*

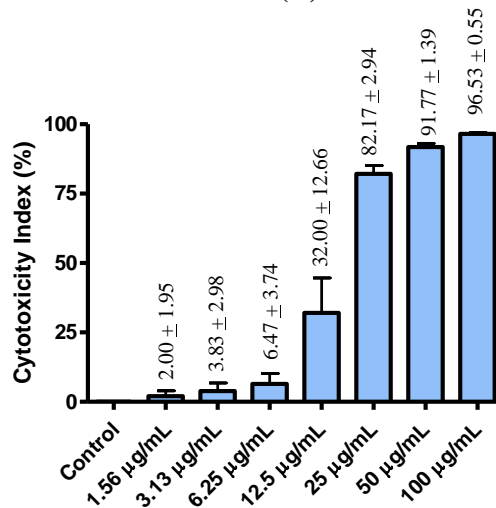
Figure 4.22 showed the cytotoxicity effects of crude petroleum ether, chloroform, and methanol extracts of *C. mangga* on MDA-MB-231 cells. Crude petroleum ether extract showed a dose-dependent inhibitory effect on cell proliferation against MDA-MB-231 cells [Figure 4.22 (A)]. However, the inhibition of cell proliferation was less than 45% at 100 $\mu\text{g/mL}$. Crude chloroform extract showed a dose-dependent inhibitory effect on cell proliferation against MDA-MB-231 cells [Figure 4.22 (B)]. At 6.156 – 25 $\mu\text{g/mL}$, growth inhibition was less than 30%. However, it possessed more than 90% of the cytotoxicity to inhibit cell proliferation at 50–100 $\mu\text{g/mL}$. Crude methanol extract was non-cytotoxic against MDA-MB-231 cells [Figure 4.22 (C)]. The overall inhibitory effects were less than 6%, which could be considered as non-toxic to the cells. Since growth inhibition by all three extracts of *C. mangga* did not even reach 50% at 20 $\mu\text{g/mL}$, these extracts were deemed as not toxic against MDA-MB-231 cells.



(A)

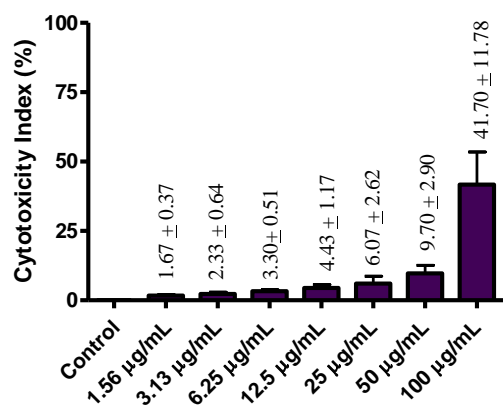


(B)

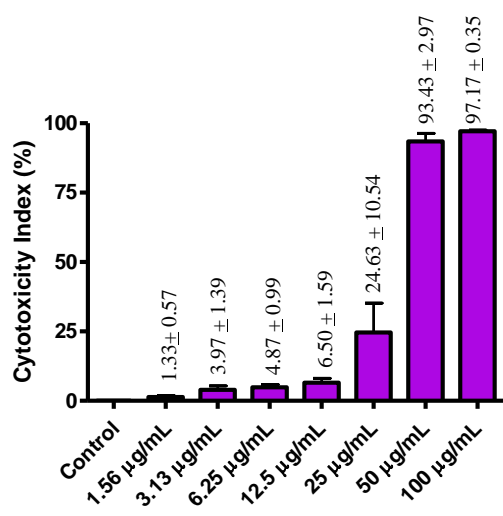


(C)

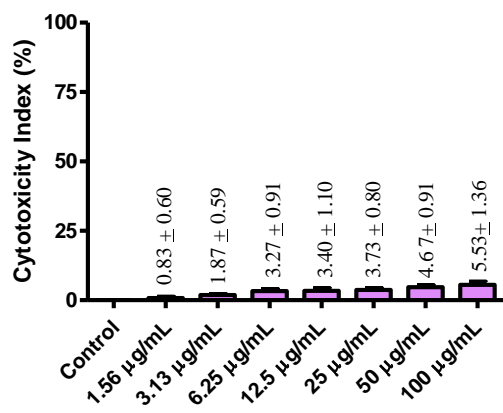
Figure 4.21: Growth inhibition by (A) petroleum ether, (B) chloroform, and (C) methanol extracts of *Curcuma domestica* on MDA-MB-231 cells using the MTT assay. Each bar represents the mean \pm S.E. calculated from three independent experiments.



(A)



(B)

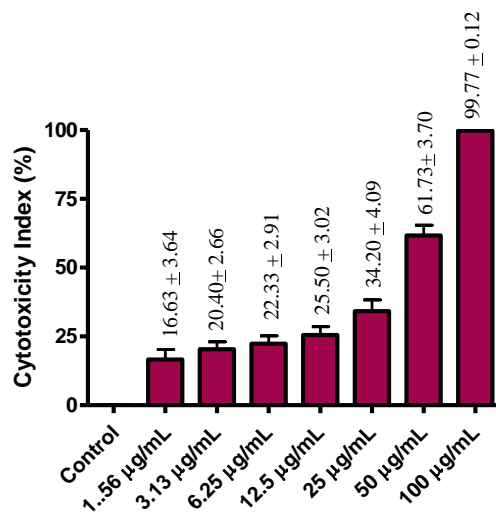


(C)

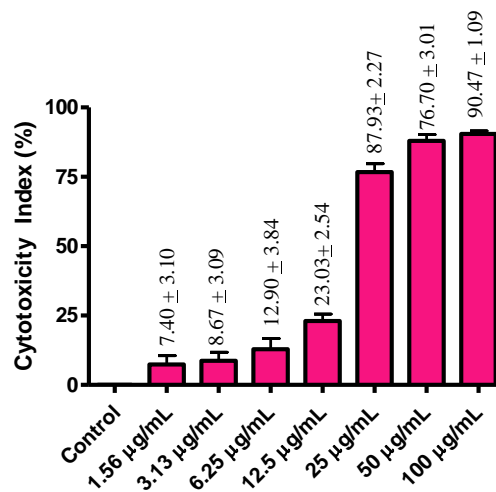
Figure 4.22: Growth inhibition by (A) petroleum ether, (B) chloroform, and (C) methanol extracts of *Curcuma mangga* on MDA-MB-231 cells using the MTT assay. Each bar represents the mean \pm S.E. calculated from three independent experiments.

(f) *Curcuma xanthorrhiza*

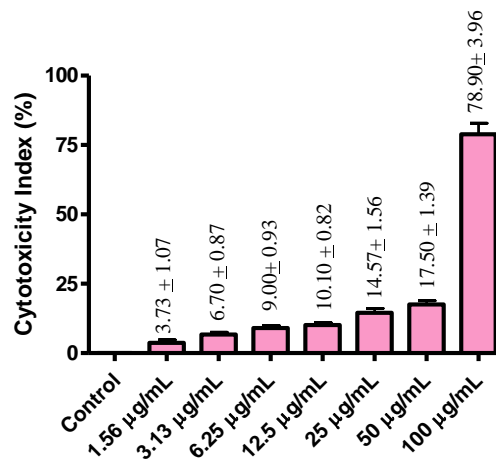
Figure 4.23 showed the cytotoxicity effects of crude petroleum ether, chloroform, and methanol extracts of *C. xanthorrhiza* on MDA-MB-231 cells. Crude petroleum ether extract showed a dose-dependent inhibitory effect on cell proliferation against MDA-MB-231 cells [Figure 4.23 (A)]. At 50 µg/mL, the cytotoxicity was more than 50%, while at 100 µg/mL, it inhibited almost 100% of cell proliferation. Based on Figure 4.23 (B), crude chloroform extract showed a dose-dependent inhibitory effect on cell proliferation against MDA-MB-231 cells. At 25 µg/mL, the cytotoxicity was more than 70%, while at 50–100 µg/mL, it inhibited at least 85% of cell proliferation. Crude methanol extract showed a dose-dependent inhibitory effect on cell proliferation against MDA-MB-231 cells [Figure 4.23 (C)]. The inhibitory effects were less than 20% at 50 µg/mL or lower, but it boosted to more than 75% at 100 µg/mL. Based on the percentages of inhibition at 25 µg/mL (Figure 4.23), chloroform extract of *C. xanthorrhiza* was deemed as actively cytotoxic and those that were not were petroleum ether and methanol extracts of *C. xanthorrhiza*.



(A)



(B)

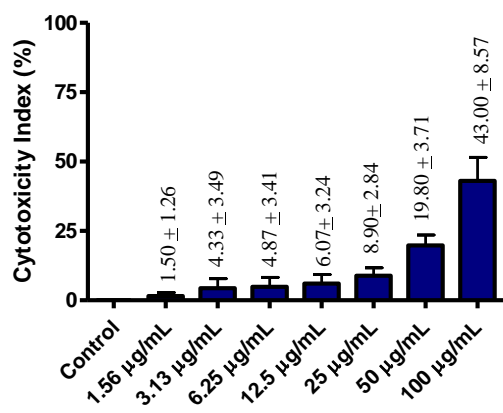


(C)

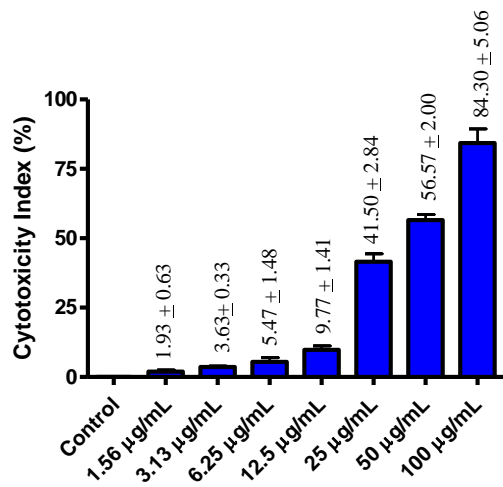
Figure 4.23: Growth inhibition by (A) petroleum ether, (B) chloroform, and (C) methanol extracts of *Curcuma xanthorrhiza* on MDA-MB-231 cells using the MTT assay. Each bar represents the mean \pm S.E. calculated from three independent experiments.

(g) *Kaempferia galanga*

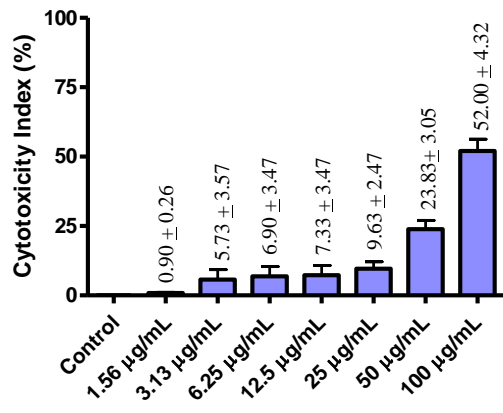
Figure 4.24 showed the cytotoxicity effects of crude petroleum ether, chloroform, and methanol extracts of *K. galanga* on MDA-MB-231 cells. Crude petroleum ether extract was moderately growth inhibitory against MDA-MB-231 cells as showed in the dose-dependently graph [Figure 4.24 (A)]. At 1.56–50 $\mu\text{g/mL}$, growth inhibitory was less than 30%. The highest cytotoxicity to inhibit cell proliferation was less than 45% at 100 $\mu\text{g/mL}$. At the lower concentrations tested, the cytotoxicity were less than 25%. Crude chloroform extract showed a dose-dependent inhibitory effect on cell proliferation against MDA-MB-231 cells [Figure 4.24 (B)]. At 1.56–25 $\mu\text{g/mL}$, growth inhibitory was less than 50%. At higher concentrations, it inhibited more than 50% of cell proliferation at 50 $\mu\text{g/mL}$ and more than 80% at 100 $\mu\text{g/mL}$. Based on Figure 4.24 (C), crude methanol extract showed a dose-dependent inhibitory effect on cell proliferation against MDA-MB-231 cells. It only inhibited more than 50% of cell proliferation at 100 $\mu\text{g/mL}$.



(A)



(B)



(C)

Figure 4.24: Growth inhibition by (A) petroleum ether, (B) chloroform, and (C) methanol extracts of *Kaempferia galanga* MDA-MB-231 cells using the MTT assay. Each bar represents the mean \pm S.E. calculated from three independent experiments.

(h) *Zingiber montanum*

Figure 4.25 showed the cytotoxicity effects of crude petroleum ether, chloroform, and methanol extracts of *Z. montanum* on MDA-MB-231 cells. Crude petroleum ether showed a dose-dependent inhibitory effect on cell proliferation against MDA-MB-231 cells [Figure 4.25 (A)]. It inhibited more than 85% of cell proliferation at 50–100 µg/mL. At the other lower concentrations, the inhibitory effect on cell proliferation was less than 50%. Crude chloroform extract showed a dose-dependent inhibitory effect on cell proliferation against MDA-MB-231 cells [Figure 4.25 (B)]. It inhibited more than 80% of cell proliferation at 50–100 µg/mL. At the other lower concentrations, the inhibition on cell proliferation was less than 50%. Crude methanol extract was not cytotoxic against MDA-MB-231 cells [Figure 2.25 (C)]. The overall inhibitory effects were less than 6%. Therefore, all extracts of *Z. montanum* were considered not cytotoxic against MDA-MB-231 cells.

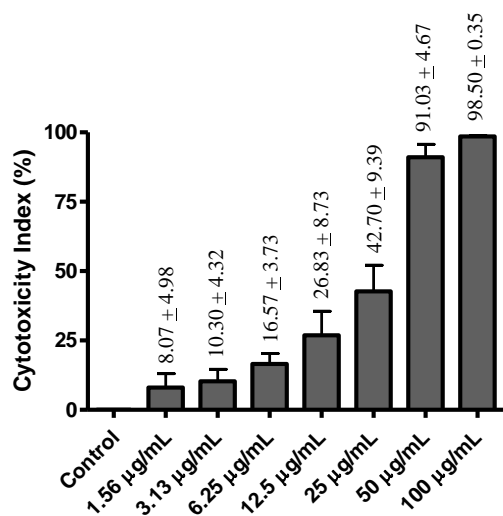
(i) *Zingiber officinale*

Figure 4.26 showed the cytotoxicity effects of crude petroleum ether, chloroform, and methanol extracts of *Z. officinale* on MDA-MB-231 cells. Crude petroleum ether showed a dose-dependent inhibitory effect on cell proliferation against MDA-MB-231 cells [Figure 4.26 (A)]. At 1.56–50 µg/mL, the inhibitory effects were less than 40%, but boosted to more than 75% at 100 µg/mL. Crude chloroform extract showed a dose-dependent inhibitory effect on cell proliferation against MDA-MB-231 cells [Figure 4.26 (B)]. The inhibitory effects were less than 40% at 1.56–25 µg/mL. However, the inhibitory effects were boosted to 60% and 95% at 50 µg/mL and 100 µg/mL, respectively. Crude methanol extract was not cytotoxic against MDA-MB-231 cells [Figure 4.26 (C)]. The

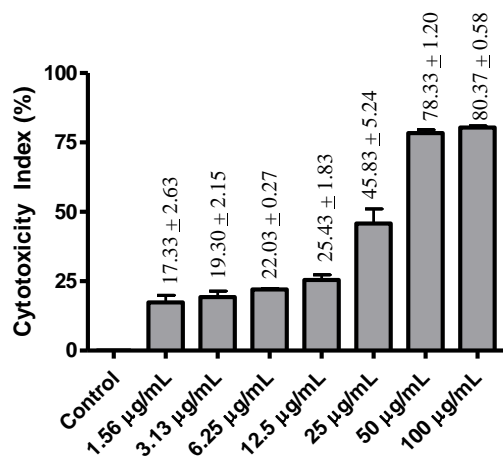
overall inhibitory effects were less than 8%. So all extracts of *Z. officinale* were considered as non-cytotoxic against MDA-MB-231 cells.

(j) *Zingiber zerumbet*

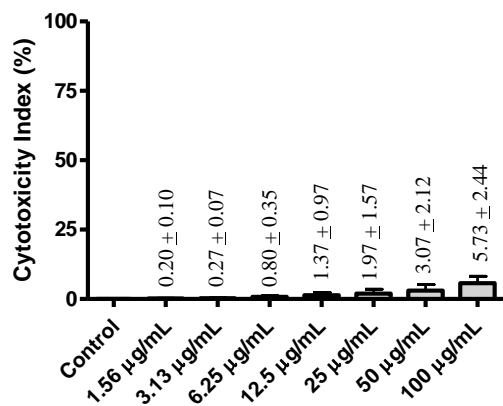
Figure 4.27 showed the cytotoxicity effects of crude petroleum ether, chloroform, and methanol extracts of *Z. zerumbet* on MDA-MB-231 cells. Crude petroleum ether extract showed a dose-dependent inhibitory effect on cell proliferation against MDA-MB-231 cells [Figure 4.27 (A)]. The inhibitory effects on cell proliferation was more than 75% at 12.5 µg/mL and increased to more than 95% at 100 µg/mL. Crude chloroform extract showed a dose-dependent inhibitory effect on cell proliferation against MDA-MB-231 cells [Figure 4.27 (B)]. At 1.56 – 25 µg/mL, the inhibitory effects on MDA-MB-231 cells were less than 40%. The cytotoxicity to inhibit cell proliferation was more than 60% at 50 µg/mL, and 85% at 100 µg/mL. Crude methanol extract was not cytotoxic against MDA-MB-231 cells [Figure 4.27 (C)]. The overall inhibitory effects were less than 8%.



(A)

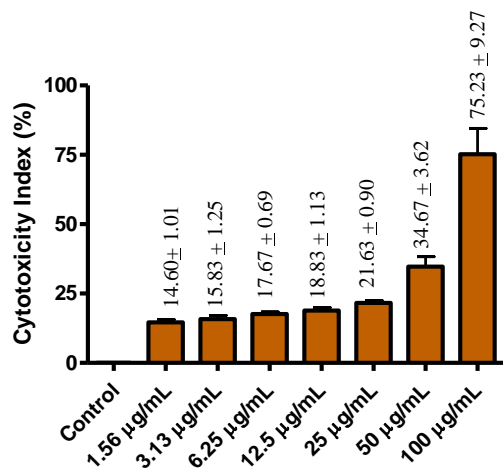


(B)

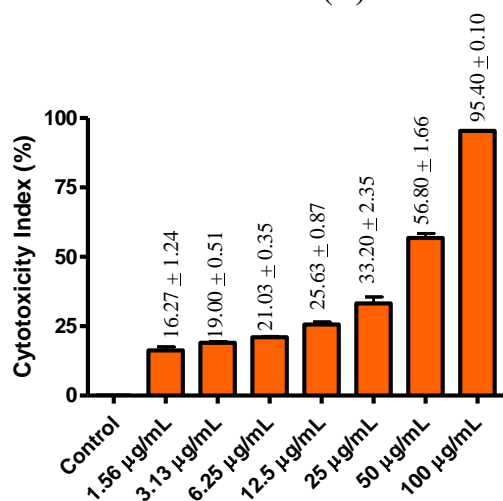


(C)

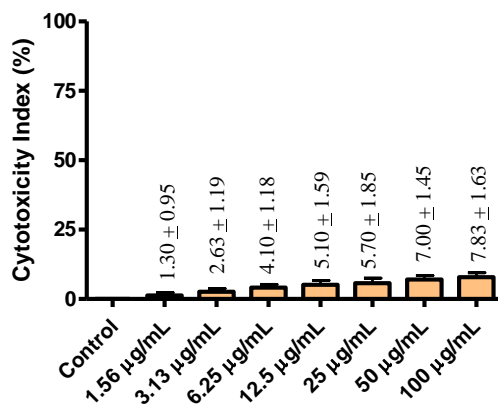
Figure 4.25: Growth inhibition by (A) petroleum ether, (B) chloroform, and (C) methanol extracts of *Zingiber montanum* on MDA-MB-231 cells using the MTT assay. Each bar represents the mean ± S.E. calculated from three independent experiments.



(A)

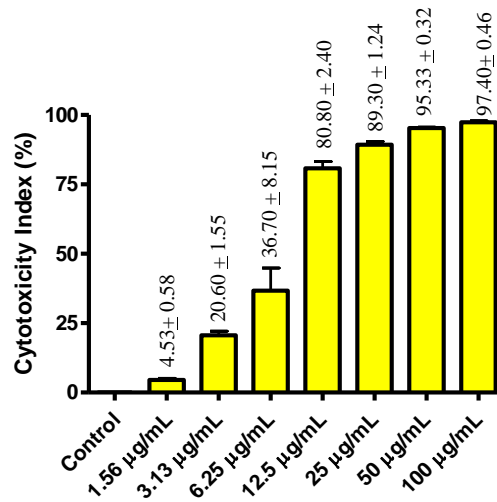


(B)

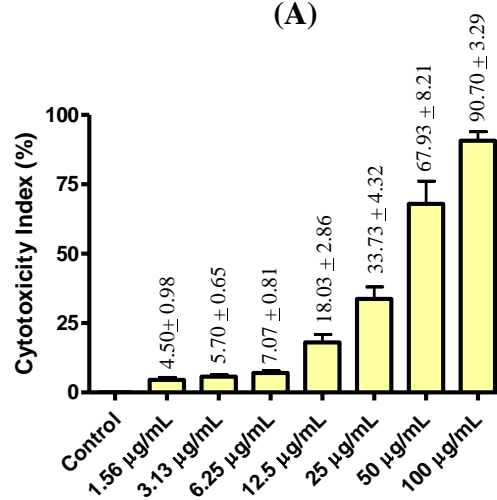


(C)

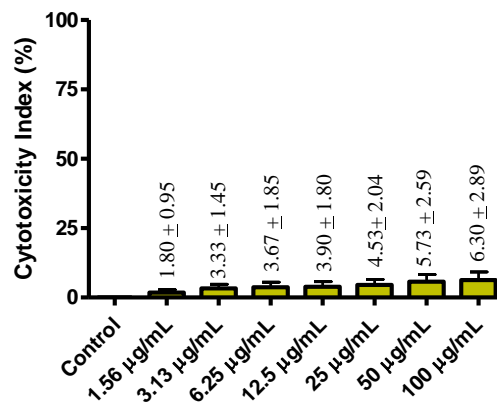
Figure 4.26: Growth inhibition by (A) petroleum ether, (B) chloroform, and (C) methanol extracts of *Zingiber officinale* on MDA-MB-231 cells using the MTT assay. Each bar represents the mean \pm S.E. calculated from three independent experiments.



(A)



(B)



(C)

Figure 4.27: Cytotoxicity of crude (A) petroleum ether, (B) chloroform, and (C) methanol extracts of *Zingiber zerumbet* on MDA-MB-231 cells. Each bar represents the mean \pm S.E. calculated from three independent experiments.

(k) Doxorubicin hydrochloride

Doxorubicin hydrochloride was used as the positive control at 0.05–3.13 $\mu\text{g/mL}$. Based on Figure 4.28 which presented the cytotoxicity effects of doxorubicin hydrochloride on MDA-MB-231 cells, it inhibited more than 50% of the cell proliferation at 1.56 $\mu\text{g/mL}$.

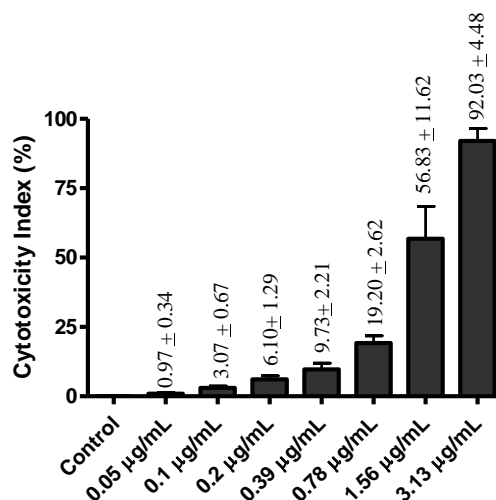


Figure 4.28: Growth inhibition by doxorubicin hydrochloride on MDA-MB-231 cells using the MTT assay. Each bar represents the mean \pm S.E. calculated from three independent experiments.

4.2.1 Comparisons of the Zingiberaceae extracts on inhibitory effects of cell proliferation or viability of MDA-MB-231 cells

Cytostatic concentration (IC_{50}) is defined as the concentration of an inhibitor where the response is reduced by half. In the screening program to the discovery and development of potential anticancer natural compounds, the criteria of the American National Cancer Institute was adopted, that a crude extract with IC_{50} lower than 30 $\mu\text{g/mL}$ was considered to be promising for further purification (Suffness & Pezzuto, 1990). Complete dose-response curves were generated and IC_{50} values were calculated for the *Zingiberaceae* extracts (Table 4.3) against MDA-MB-231 cells line.

Based on the IC₅₀ values indicated in Table 4.3 for the 30 extracts tested, 12 extracts showed IC₅₀ lower than 30 µg/mL, nine showed IC₅₀ lower than 20 µg/mL, and four extracts showed IC₅₀ lower than 10 µg/mL. These extracts with IC₅₀ lower than 30 µg/mL were petroleum ether extracts of *A. galanga*, *B. rotunda*, *C. domestica*, *Z. montanum*, and *Z. zerumbet*; chloroform extracts of *A. galanga*, *B. rotunda*, *C. domestica*, *C. xanthorrhiza*, *K. galanga*, and *Z. montanum*; as well as methanol extract of *C. domestica*. The strongest cytotoxicity activity was detected for the petroleum ether extract of *A. galanga*, which presenting the lowest IC₅₀ value, 2.82 µg/mL.

The results demonstrated that no appreciable loss in cell growth was observed in cells incubated with increased concentrations of methanol extracts of *A. galanga*, *C. aeruginosa*, and *C. mangga*, *Z. montanum*, *Z. officinale* and *Z. zerumbet*; as well as petroleum ether extracts of *C. mangga* and *K. galanga*. These extracts possessed IC₅₀ values which were more than 100 µg/mL.

Table 4.3: *In vitro* cytotoxicity of *Zingiberaceae* extracts on MDA-MB-231 cells measured by the MTT assay

Zingiberaceae species	Solvent ¹	IC ₅₀ (µg/mL)
		MDA-MB-231 cell line
<i>Alpinia galanga</i>	p	2.87
	c	6.19
	m	>100
<i>Boesenbergia rotunda</i>	p	9.21
	c	10.25
	m	55.06
<i>Curcuma aeruginosa</i>	p	30.13
	c	55.68
	m	>100
<i>Curcuma domestica</i>	p	14.34
	c	10.10
	m	15.51
<i>Curcuma mangga</i>	p	>100
	c	30.10
	m	>100
<i>Curcuma xanthorrhiza</i>	p	42.78
	c	17.34
	m	58.78
<i>Kaempferia galanga</i>	p	>100
	c	29.63
	m	48.76
<i>Zingiber montanum</i>	p	26.16
	c	25.38
	m	>100
<i>Zingiber officinale</i>	p	55.93
	c	30.06
	m	>100
<i>Zingiber zerumbet</i>	p	7.46
	c	31.48
	m	>100
Doxorubicin hydrochloride	-	1.27

¹ Solvents used in extraction: p: petroleum ether, c: chloroform, m: methanol

4.3 Cytotoxicity of the Zingiberaceae Extracts on MRC-5 Cells

In the search of new anti-cancer drug, it is desired to find not only the most active, but also the least toxic substances against normal cells. It is very important that such selection could be done at the preliminary stage of *in vitro* studies, which is at the very beginning of drug developmental process (Popiolkiewicz, Polkowski, Skierski, & Mazurek, 2005). Therefore, toxicity of six most active *Zingiberaceae* extracts which exhibited significant inhibitory effect on the proliferation of MDA-MB-231 cells (IC_{50} value ≤ 10 $\mu\text{g/mL}$) (Table 4.3) were further investigated on human normal cells, MRC-5. These extracts were petroleum ether and chloroform extracts of *A. galanga*, petroleum ether and chloroform extracts of *B. rotunda*, chloroform extract of *C. domestica*, and petroleum ether extract of *Z. zerumbet* (Table 4.3). Toxicity of the extracts was measured using conventional MTT assay at 1.56 $\mu\text{g/mL}$, 3.13 $\mu\text{g/mL}$, 6.25 $\mu\text{g/mL}$, 12.5 $\mu\text{g/mL}$, 25 $\mu\text{g/mL}$, 50 $\mu\text{g/mL}$ and 100 $\mu\text{g/mL}$ for 48 h.

(a) Petroleum ether extract of *Alpinia galanga*

Figure 4.29 showed the cytotoxicity effects of crude petroleum ether extract of *A. galanga* against MRC-5 cells. The results indicated that the extract exerted a pronounced cytotoxic effect against MRC-5 cells, which exerted at least 80% of killing effects at 3.13 $\mu\text{g/mL}$. At higher concentrations tested, the killing effects were 100%.

(b) Chloroform extract of *Alpinia galanga*

Figure 4.30 showed the cytotoxicity effects of crude chloroform extract of *A. galanga* against MRC-5 cells. The results indicated that the extract exerted cytotoxic effects against MRC-5 cells in a dose-dependent manner. The cytotoxicity index of the

extract was less than 25% at 1.56–6.25 $\mu\text{g/mL}$, but boost to almost 50% at 12.5 $\mu\text{g/mL}$. At 25–100 $\mu\text{g/mL}$, the cytotoxicity indexes against MRC-5 cells were almost 100%.

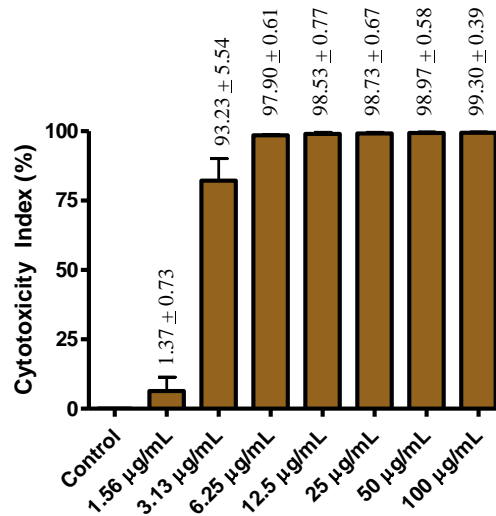


Figure 4.29: Cytotoxic effects of crude petroleum ether extract of *Alpinia galanga* on MRC-5 cells using the MTT assay. Each bar represents the mean \pm S.E. calculated from three independent experiments.

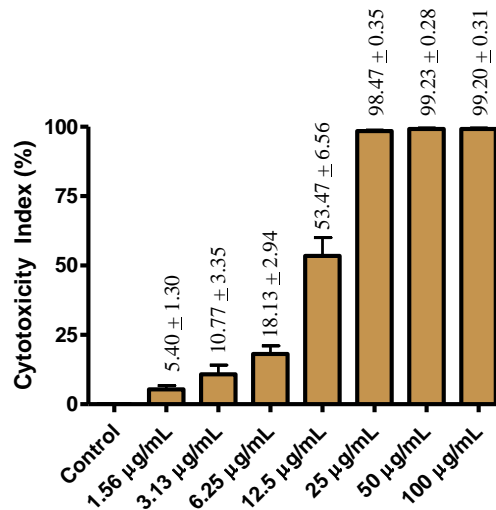


Figure 4.30: Cytotoxic effects of crude chloroform extract of *Alpinia galanga* on MRC-5 cells using the MTT assay. Each bar represents the mean \pm S.E. calculated from three independent experiments.

(c) Petroleum ether extract of *Boesenbergia rotunda*

Figure 4.31 showed the cytotoxicity effects of crude petroleum ether extract of *B. rotunda* against MRC-5 cells. The results indicated that the extract exerted cytotoxic effects against MRC-5 cells in a dose-dependent manner. The cytotoxicity index of the extract was very low at 1.56–6.25 $\mu\text{g/mL}$ (cytotoxicity index < 6%), but boost to almost 50% at 12.5 $\mu\text{g/mL}$. At 25–100 $\mu\text{g/mL}$, the cytotoxicity indexes against MRC-5 cells were almost 100%.

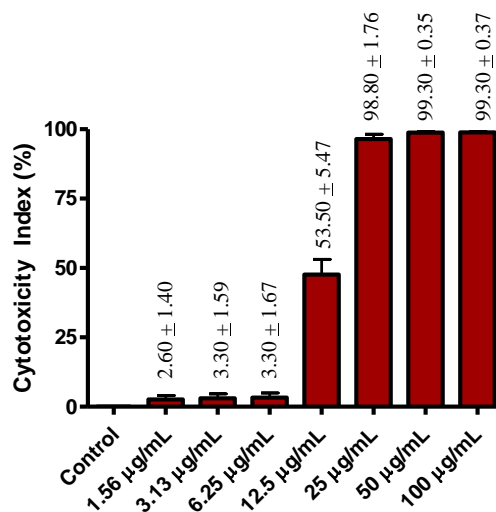


Figure 4.31: Cytotoxic effects of crude petroleum ether extract of *Boesenbergia rotunda* on MRC-5 cells using the MTT assay. Each bar represents the mean \pm S.E. calculated from three independent experiments.

(d) Chloroform extract of *Boesenbergia rotunda*

Figure 4.32 showed the cytotoxicity effects of crude chloroform extract of *B. rotunda* against MRC-5 cells. The results indicated that the extract exerted cytotoxic effects against MRC-5 cells in a dose-dependent manner. The cytotoxicity index of the extract was very low at 1.56–6.25 $\mu\text{g/mL}$ (cytotoxicity index < 6%), increased to about 30% at 12.5 $\mu\text{g/mL}$, and boosted to almost 100% at 25–100 $\mu\text{g/mL}$.

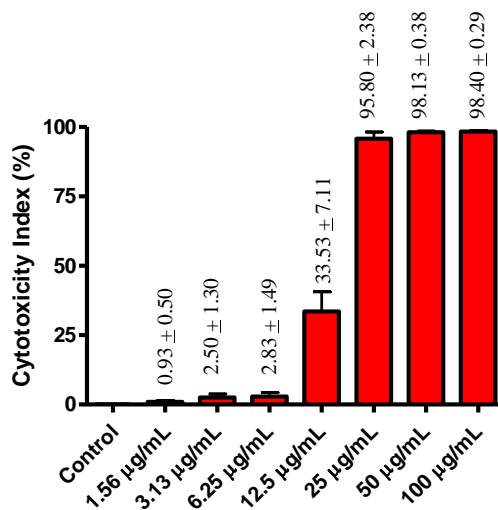


Figure 4.32: Cytotoxic effects of crude chloroform extract of *Boesenbergia rotunda* on MRC-5 cells using the MTT assay. Each bar represents the mean \pm S.E. calculated from three independent experiments.

(e) Chloroform extract of *Curcuma domestica*

Figure 4.33 showed the cytotoxicity effects of crude chloroform extract of *C. domestica* against MRC-5 cells. The results indicated that the extract exerted cytotoxic effects against MRC-5 cells in a dose-dependent manner. The cytotoxicity index of the extract was very low at 1.56–6.25 µg/mL (cytotoxicity index < 10%), increased to about 50% at 12.5 µg/mL, and boosted to more than 90% at 25–100 µg/mL.

(f) Petroleum ether extract of *Zingiber zerumbet*

Figure 4.34 showed the cytotoxicity effects of crude petroleum ether extract of *Z. zerumbet* against MRC-5 cells. The results indicated that the extract exerted cytotoxic effects against MRC-5 cells in a dose-dependent manner. The cytotoxicity index of the extract was very low at 1.56–6.25 µg/mL (cytotoxicity index < 15%), increased to more than 50% at 12.5 µg/mL, and boosted to more than 80% at 25–100 µg/mL.

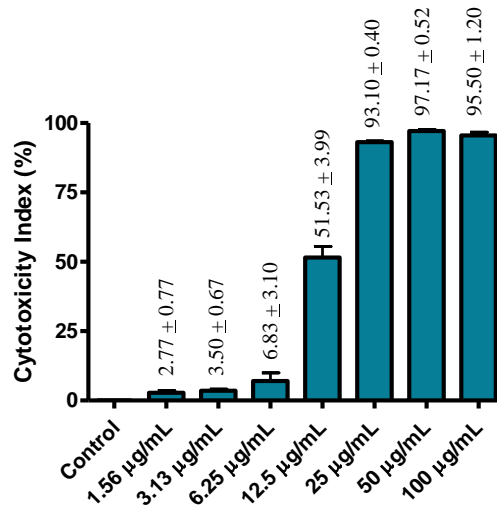


Figure 4.33: Cytotoxic effects of crude chloroform extract of *Curcuma domestica* on MRC-5 cells using the MTT assay. Each bar represents the mean ± S.E. calculated from three independent experiments.

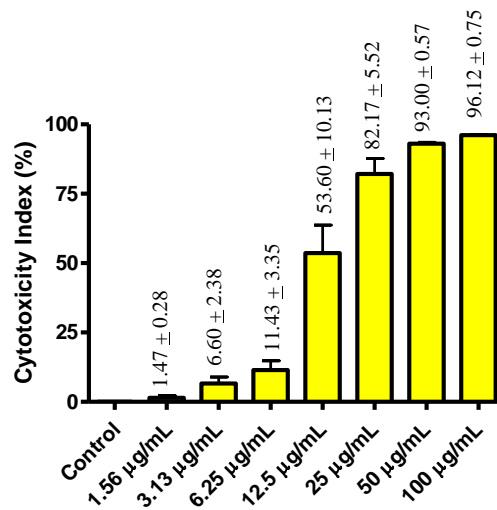


Figure 4.34: Cytotoxic effects of crude petroleum ether extract of *Zingiber zerumbet* on MRC-5 cells using the MTT assay. Each bar represents the mean ± S.E. calculated from three independent experiments.

4.3.1 Comparisons of the Zingiberaceae extracts on viability of MRC-5 cells

Assessment of potential toxicity of the most active *Zingiberaceae* extracts with IC_{50} values $\leq 10 \mu\text{g/mL}$ in the previous screening test (Cell proliferation and viability assay) were selected for cytotoxicity studies against human normal cells, MRC-5 using conventional MTT assay for 48 h. In the selection of the least toxic extracts among the most active ones, a special parameter, known as Selectivity Index (SX) was applied. Selectivity Index is a selectivity indicator of tested substances towards tumour cells (Popiolkiewicz *et al.*, 2005). In this experiment, the SX represents the ratio of IC_{50} obtained in toxicity testing using MRC-5 cells to IC_{50} of the same extract in cytotoxicity test using MDA-MB-231 cells, and then multiplied by 100 ($SX = IC_{50(\text{MRC-5})}/IC_{50(\text{MDA-MB-231})} \times 100$).

The SX value above 100 indicates that the cytotoxic effect of tested substance is greater towards cancer cells. The SX value of 100 or below would suggest that the tested concentration of the substance for achieving therapeutic effect is similar to or lower than the concentration causing toxic effects to normal cells. Therefore, the most promising substances for development of anti-cancer drug would have SX values distinctly higher than 100 (Popiolkiewicz *et al.*, 2005). Table 4.4 demonstrated the SX values for the six selected *Zingiberaceae* extracts tested, which were the crude petroleum ether and chloroform extracts of *A. galanga*, petroleum ether and chloroform extracts of *B. rotunda*, chloroform extract of *C. domestica*, and petroleum ether extract of *Z. zerumbet*.

Table 4.4: *In vitro* cytotoxicity of *Zingiberaceae* extracts on MRC-5 and MDA-MB-231 cells and their selectivity index

Zingiberaceae species	Solvent ¹	Cell line, IC ₅₀ (µg/mL)		Selectivity Index (SX)
		MRC-5	MDA-MB-231	
<i>Alpinia galanga</i>	p	2.86	2.87	100
	c	11.87	6.19	192
<i>Boesenbergia rotunda</i>	p	12.78	9.21	139
	c	13.22	10.25	129
<i>Curcuma domestica</i>	c	12.32	10.10	122
<i>Zingiber zerumbet</i>	p	12.09	7.46	162

¹ Solvents used in extraction: p: petroleum ether, c: chloroform, m: methanol

Based on the result in Table 4.4, only crude petroleum ether extract of *A. galanga* possessed SX value equal to 100. This indicated that the cytotoxicity of this extract to kill cancerous cells (MDA-MB-231 cells) and non-cancerous cell (MRC-5) were similar, and thus it was inappropriate for further studies even though it was the most active extract tested in the NO assay, cell proliferation and viability assay (MTT assay), and scratch wound assay. The other extracts possess SX values distinctly higher than 100, which indicated that their cytotoxicity is more prone to kill cancerous cells (MDA-MB-231) than normal cells (MRC-5), and thus hold potential for further studies in the development of anti-cancer drug.

4.4 Effects of the Zingiberaceae Extracts on the Migration of MDA-MB-231 Cells

Cell migration is an important factor to probe the metastatic potential of cancer cells. The effects of 30 crude *Zingiberaceae* extracts on migration of hormone-independent human breast cancer cells (MDA-MB-231) were tested using the scratch wound assay. In the assay, cells were seeded into six-well plate and cultured to confluence. The confluent monolayer cells were then carefully wounded along the diameter of the well using a sterile 200 μ L-pipette tip and cell debris was removed by washing with PBS. The wounded cell monolayer was incubated in the absence (negative control) or presence of *Zingiberaceae* extract in 1%-serum media for 48 h at 37°C, with 5% CO₂.

This study was conducted at the categorized concentrations of the *Zingiberaceae* extracts based on the IC₅₀ value showed in Table 4.3. Inhibitory effects of the *Zingiberaceae* extracts on the proliferation of MDA-MB-231 cells were classified into four groups (Table 4.5). Anti-migration activity of *Zingiberaceae* extracts in Group 1, Group 2, Group 3 and Group 4 were conducted at 12.5 μ g/mL, 25 μ g/mL, 50 μ g/mL, and 100 μ g/mL, respectively.

Cell migration into the wound area was imaged through phase-contrast microscope (magnification, 50 \times) and photographed at 0 h, 24 h and 48 h [Figure 4.35 (A)–4.65 (A)]. Gap distance for the wound closure was measured at 0 h, 24 h 48 h and the significance difference of the gap distances between control and treated cells were compared at 24 h and 48 h [Figures 4.35 (B)–4.65 (B)]. Extracts resulting in the smallest wound closure (or largest gap measured at post-treatment) are those deemed most effective in inhibiting cell migration. The MDA-MB-231 cells treated with *Zingiberaceae* extracts spread slower along the wound edges than cells with vehicle alone.

Table 4.5: Classifications of the effects of anti-proliferative activity or viability of 30 tested crude *Zingiberaceae* extracts¹ against MDA-MB-231 cells into four groups.

Group 1	Group 2	Group 3	Group 4
<i>Alpinia galanga</i> (p)	<i>Boesenbergia rotunda</i> (m)	<i>Curcuma aeruginosa</i> (c)	<i>Alpinia galanga</i> (m)
<i>Alpinia galanga</i> (c)	<i>Curcuma aeruginosa</i> (p)	<i>Curcuma xanthorrhiza</i> (m)	<i>Curcuma aeruginosa</i> (m)
<i>Boesenbergia rotunda</i> (p)	<i>Curcuma mangga</i> (c)		<i>Curcuma mangga</i> (p)
<i>Boesenbergia rotunda</i> (c)	<i>Curcuma xanthorrhiza</i> (p)		<i>Curcuma mangga</i> (m)
<i>Curcuma domestica</i> (p)	<i>Kaempferia galanga</i> (c)		<i>Kaempferia galanga</i> (p)
<i>Curcuma domestica</i> (c)	<i>Kaempferia galanga</i> (m)		<i>Zingiber montanum</i> (m)
<i>Curcuma domestica</i> (m)	<i>Zingiber montanum</i> (p)		<i>Zingiber officinale</i> (m)
<i>Curcuma xanthorrhiza</i> (c)	<i>Zingiber montanum</i> (c)		<i>Zingiber zerumbet</i> (m)
<i>Zingiber zerumbet</i> (p)	<i>Zingiber officinale</i> (p)		
	<i>Zingiber officinale</i> (c)		
	<i>Zingiber zerumbet</i> (c)		

¹ Each crude *Zingiberaceae* extract was tested at 1.56 µg/mL, 3.13 µg/mL, 6.25 µg/mL, 12.5 µg/mL, 25 µg/mL, 50 µg/mL, and 100 µg/mL in triplicates (N = 3). The extracts were tested against MDA-MB-231 cells using conventional MTT assay. The effects of anti-proliferative activity were categorized into Group 1, Group 2, Group 3 and Group 4 based on their IC₅₀ values. In the Table, p represents petroleum ether extract, c represents chloroform extract, and m represents methanol extract.

(a) *Alpinia galanga*

Effects of crude petroleum ether extract of *A. galanga* (tested at 12.5 µg/mL) on the migration of MDA-MB-231 cells are shown in Figure 4.35. The untreated MDA-MB-231 cells (negative control) spread along the wound edges at 24 h (gap distance, 0.380 mm) and became highly colonised at 48 h (gap distance, 0.146 mm). In contrast, for MDA-MB-231 cells treated with the extracts spread along the wound edges were seen to be slower than that of the untreated cells [Figure 4.35 (A)], with gap distances 0.728 mm and 0.741 mm at 24 h and 48 h, respectively [Figure 4.35 (B)]. Statistical analysis using paired-sample *t*-test ($p < 0.05$) indicate significance differences between the gap distances of control and treated cells (at 24 h and 48 h) [Figure 4.35 (B)]. This showed that petroleum ether extract of *A. galanga* exhibited significant inhibitory effect on migration of MDA-MB-231 cells. There was no cell migration activity observed. Moreover, longer incubation (48 h) with the extract led to greater inhibition of MDA-MB-231 cell migration.

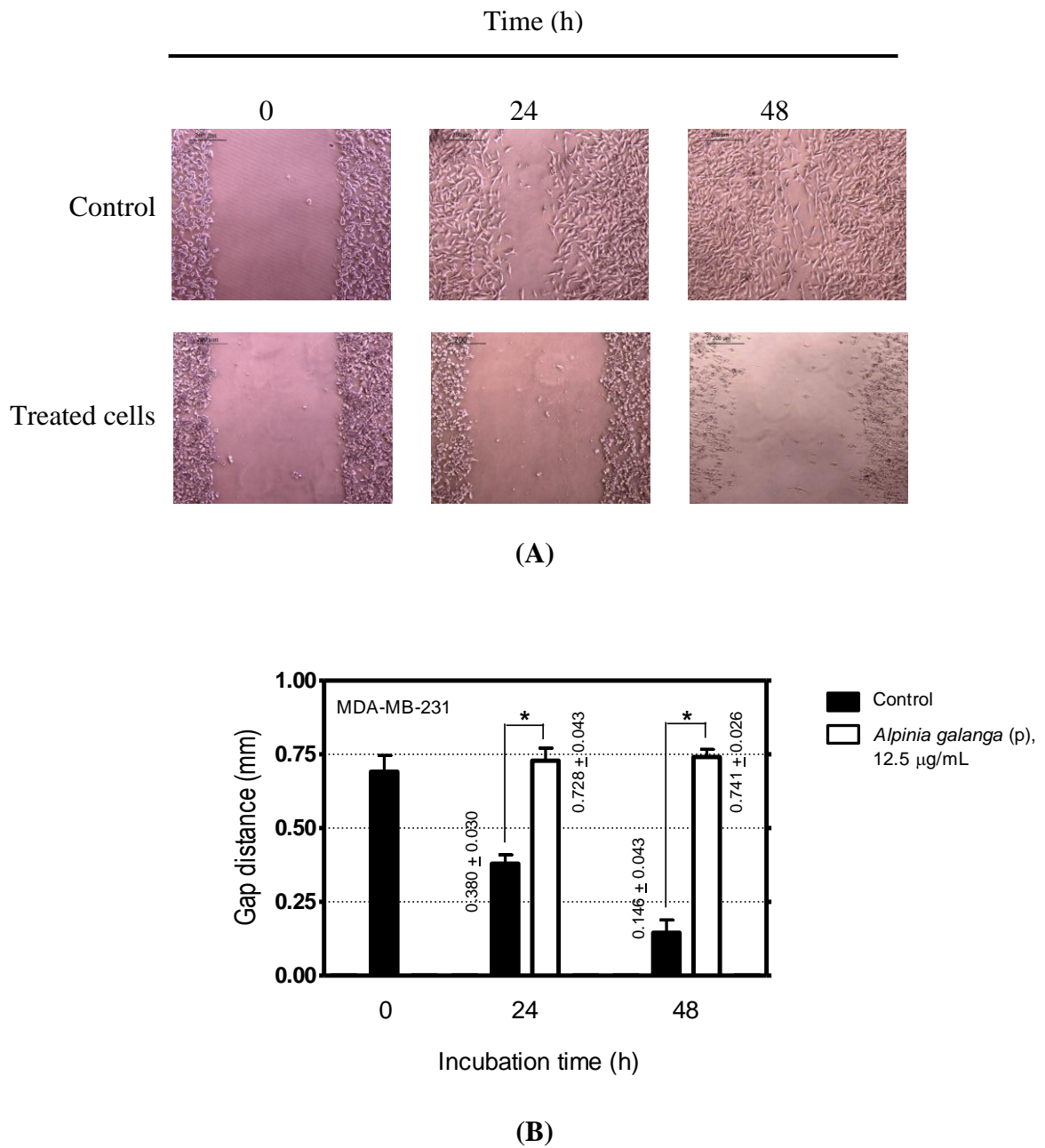
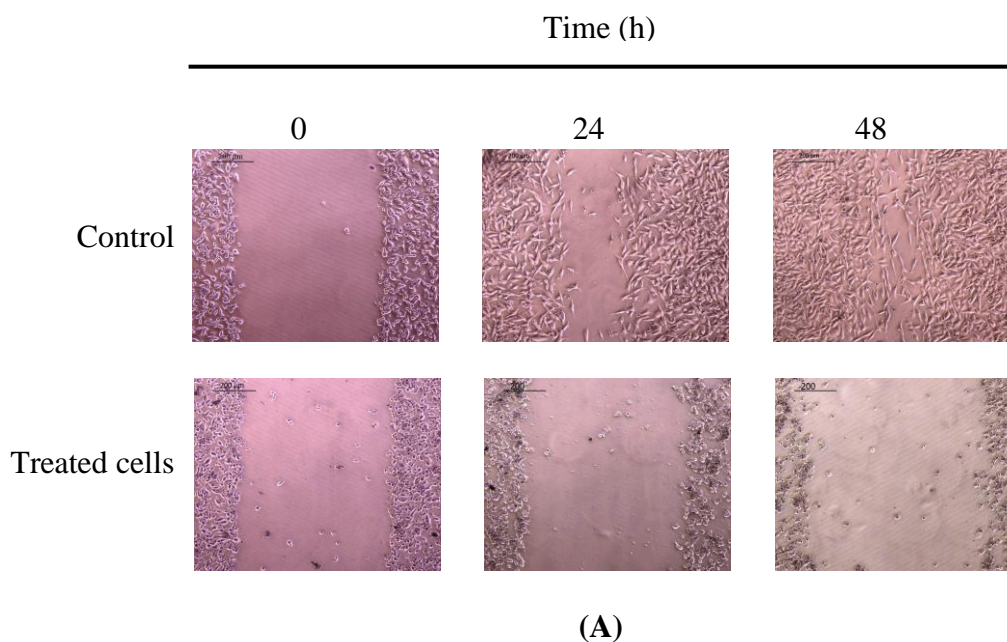
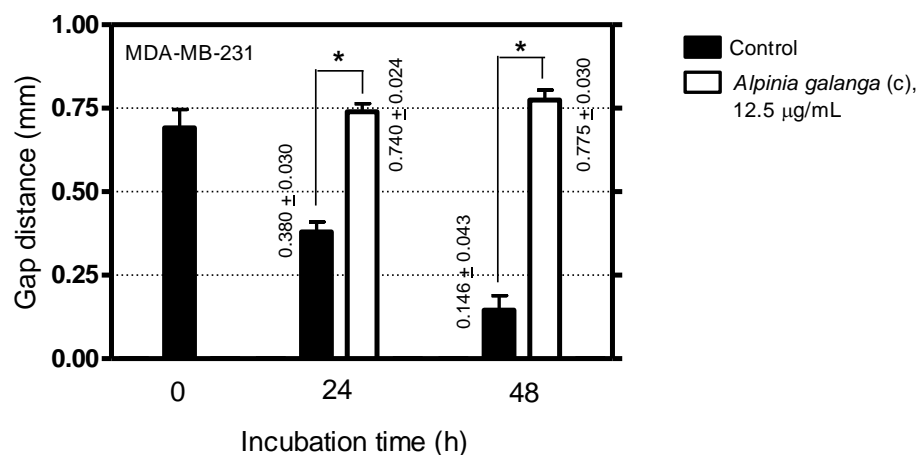


Figure 4.35: Effects of crude petroleum ether extract of *Alpinia galanga* at 12.5 µg/mL on migration in MDA-MB-231 cells. After wounding, the cells treated with vehicle alone (Control) and petroleum ether extract of *Alpinia galanga* at 12.5 µg/mL were (A) photographed under a phase-contrast microscope (magnification, 50×) and (B) the migrating distances were measured and plotted at 0 h, 24 h, and 48 h. The sample was assayed in triplicates (N = 3), and statistically significant difference ($p < 0.05$) according to paired-sample t -test was indicated as * above each bar.

Effects of crude chloroform extract of *A. galanga* (tested at 12.5 $\mu\text{g}/\text{mL}$) on the migration of MDA-MB-231 cells are shown in Figure 4.36. The untreated MDA-MB-231 cells (negative control) spread along the wound edges at 24 h (gap distance, 0.380 mm) and became highly colonised at 48 h (gap distance, 0.146 mm). In contrast, for MDA-MB-231 cells treated with the extracts spread along the wound edges were seen to be slower than that of the untreated cells [Figure 4.36 (A)], with gap distances 0.740 mm and 0.775 mm at 24 h and 48 h, respectively [Figure 4.36 (B)]. Statistical analysis using paired-sample *t*-test ($p < 0.05$) indicate significance differences between the gap distances of control and treated cells (at 24 h and 48 h) [Figure 4.35 (B)]. This showed that chloroform extract of *A. galanga* exhibited significant inhibitory effect on migration of MDA-MB-231 cells. There was no cell migration activity observed. Moreover, longer incubation (48 h) with the extract led to greater inhibition of MDA-MB-231 cell migration.





(B)

Figure 4.36: Effects of crude chloroform extract of *Alpinia galanga* at 12.5 µg/mL on migration in MDA-MB-231 cells. After wounding, the cells treated with vehicle alone (Control) and chloroform extract of *Alpinia galanga* at 12.5 µg/mL were (A) photographed under a phase-contrast microscope (magnification, 50×) and (B) the migrating distances were measured and plotted at 0 h, 24 h, and 48 h. The sample was assayed in triplicates (N = 3), and statistically significant difference ($p < 0.05$) according to paired-sample *t*-test was indicated as * above each bar.

Effects of crude methanol extract of *A. galanga* (tested at 100 µg/mL) on the migration of MDA-MB-231 cells are shown in Figure 4.37. The untreated MDA-MB-231 cells (negative control) spread along the wound edges at 24 h (gap distance, 0.332 mm) and became highly colonised at 48 h (gap distance, 0.116 mm). MDA-MB-231 cells treated with the extracts spread along the wound edges at 24 h (gap distance, 0.348 mm) and become highly colonised at 48 h (gap distance, 0.159 mm). Statistical analysis using paired-sample *t*-test ($p < 0.05$) did not indicate significance differences between the gap distances of control and treated cells (at 24 h and 48 h) [Figure 4.37 (B)]. This showed that methanol extract of *A. galanga* did not exhibit anti-migration activity against MDA-MB-231 cells.

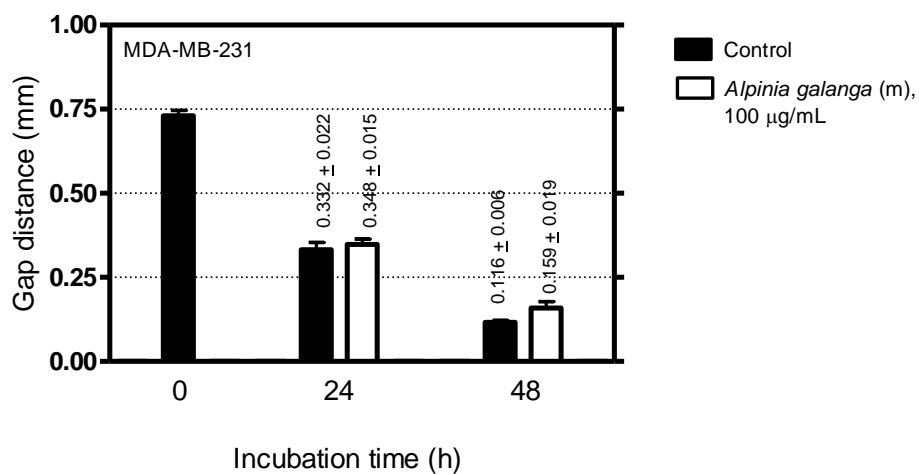
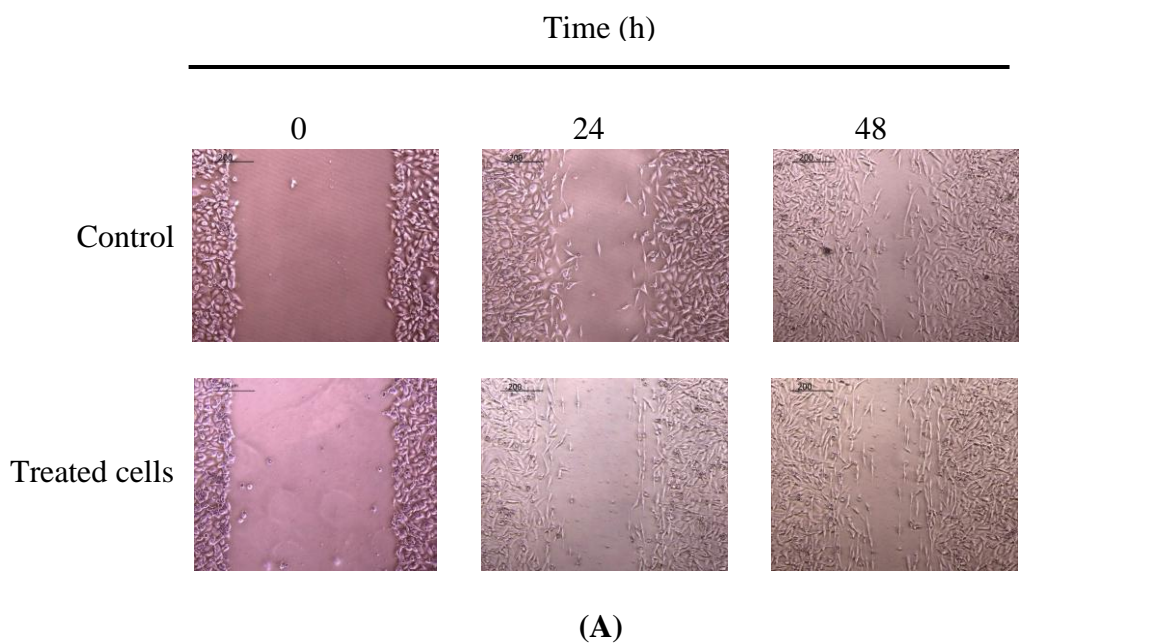
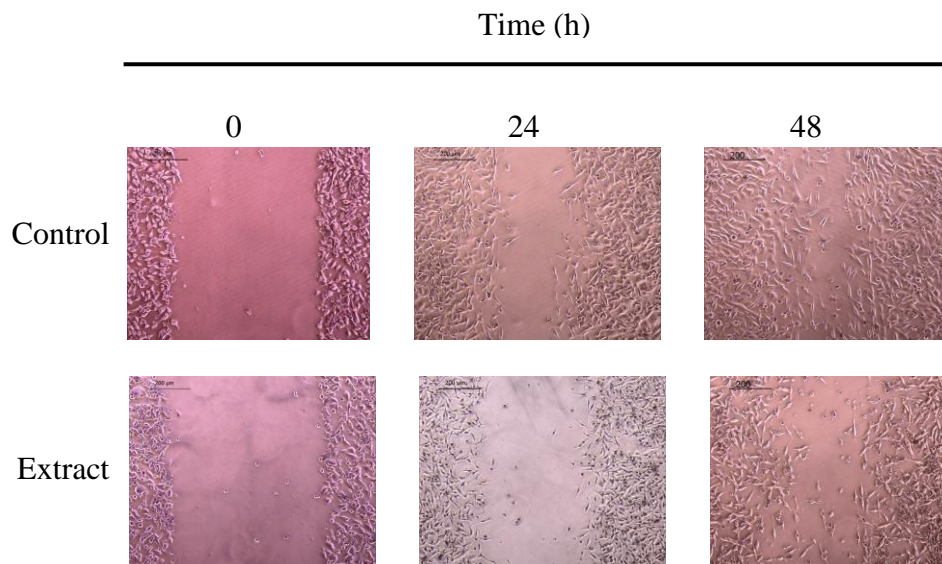


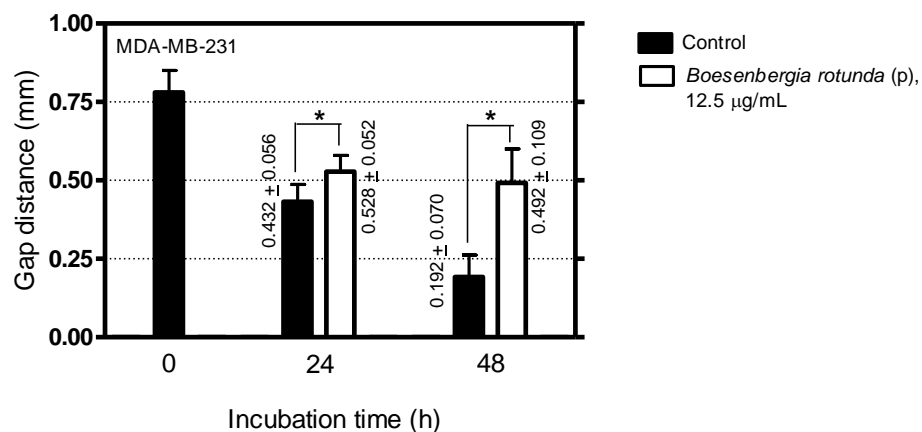
Figure 4.37: Effects of crude methanol extract of *Alpinia galanga* at 100 µg/mL on migration in MDA-MB-231 cells. After wounding, the cells treated with vehicle alone (Control) and methanol extract of *Alpinia galanga* at 100 µg/mL were (A) photographed under a phase-contrast microscope (magnification, 50×) and (B) the migrating distances were measured and plotted at 0 h, 24 h, and 48 h. The sample was assayed in triplicates (N = 3), and statistically significant difference ($p < 0.05$) according to paired-sample *t*-test was indicated as * above each bar.

(b) *Boesenbergia rotunda*

Effects of crude petroleum ether extract of *B. rotunda* (tested at 12.5 µg/mL) on the migration of MDA-MB-231 cells are shown in Figure 4.38. The untreated MDA-MB-231 cells (negative control) spread along the wound edges at 24 h (gap distance, 0.432 mm) and became highly colonised at 48 h (gap distance, 0.192 mm). In contrast, for MDA-MB-231 cells treated with the extracts spread along the wound edges were seen to be slower than that of the untreated cells [Figure 4.38 (A)], with gap distances 0.528 mm and 0.492 mm at 24 h and 48 h, respectively [Figure 4.38 (B)]. Statistical analysis using paired-sample *t*-test ($p < 0.05$) indicate significance differences between the gap distances of control and treated cells (at 24 h and 48 h) [Figure 4.38 (B)]. This showed that petroleum ether extract of *B. rotunda* exhibited significant inhibitory effect on migration of MDA-MB-231 cells. It delayed the cell migration of MDA-MB-231 cells compared to that of the control cells in a time-dependent manner.



(A)



(B)

Figure 4.38: Effects of crude petroleum ether extract of *Boesenbergia rotunda* at 12.5 µg/mL on migration in MDA-MB-231 cells. After wounding, the cells treated with vehicle alone (Control) and petroleum ether extract of *Boesenbergia rotunda* at 12.5 µg/mL were (A) photographed under a phase-contrast microscope (magnification, 50×) and (B) the migrating distances were measured and plotted at 0 h, 24 h, and 48 h. The sample was assayed in triplicates (N = 3), and statistically significant difference ($p < 0.05$) according to paired-sample *t*-test was indicated as * above each bar.

Effects of crude chloroform extract of *B. rotunda* (tested at 12.5 µg/mL) on the migration of MDA-MB-231 cells are shown in Figure 4.39. The untreated MDA-MB-231 cells (negative control) spread along the wound edges at 24 h (gap distance, 0.432 mm) and became highly colonised at 48 h (gap distance, 0.192 mm). In contrast, for MDA-MB-231 cells treated with the extracts spread along the wound edges were seen to be slower than that of the untreated cells [Figure 4.39 (A)], with gap distances 0.592 mm and 0.694 mm at 24 h and 48 h, respectively [Figure 4.39 (B)]. Statistical analysis using paired-sample *t*-test ($p < 0.05$) indicate significance differences between the gap distances of control and treated cells (at 24 h and 48 h) [Figure 4.39 (B)]. This showed that chloroform extract of *B. rotunda* exhibited significant inhibitory effect on migration of MDA-MB-231 cells. It

delayed the cell migration of MDA-MB-231 cells compared to that of the control cells in a time-dependent manner.

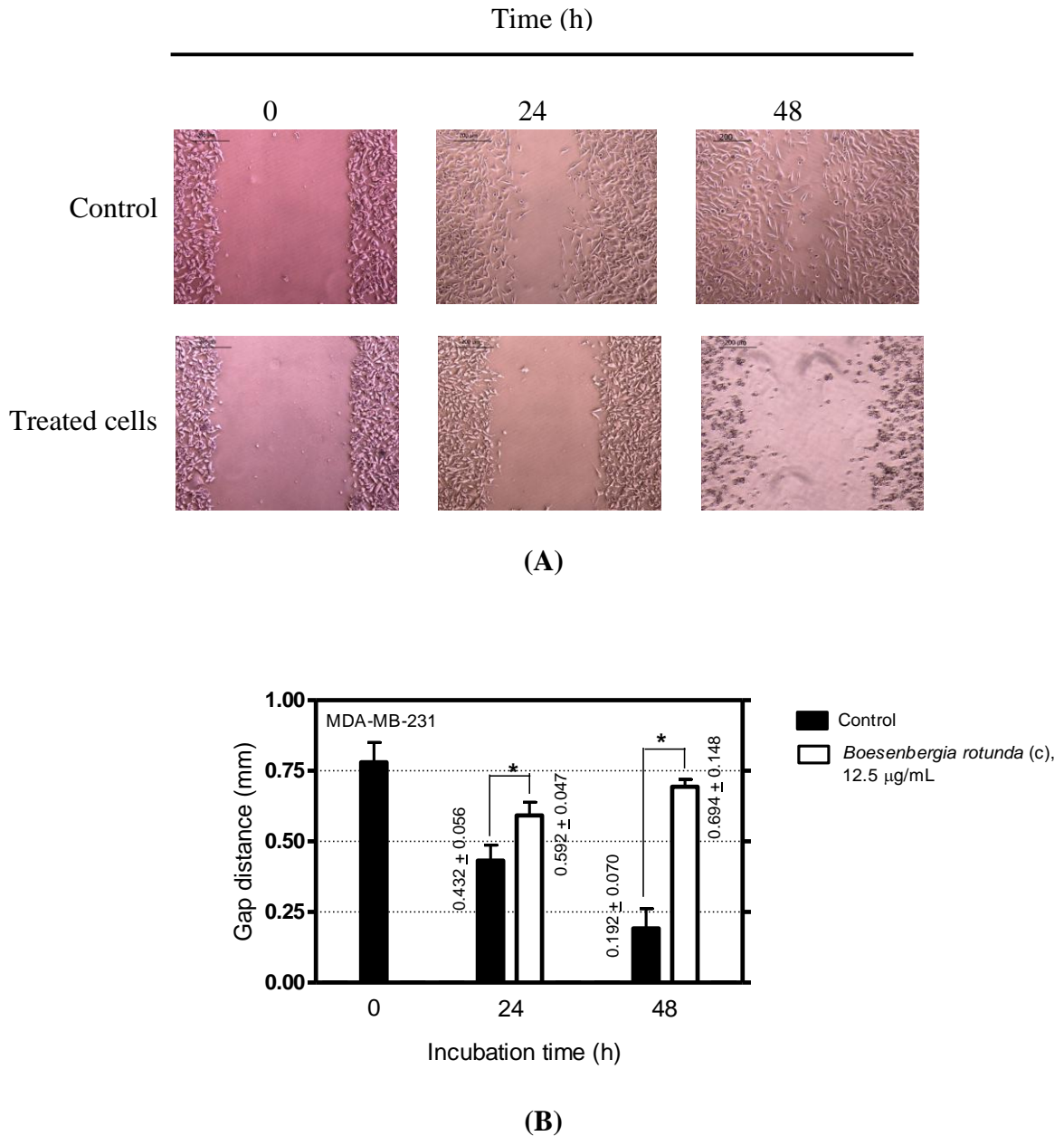
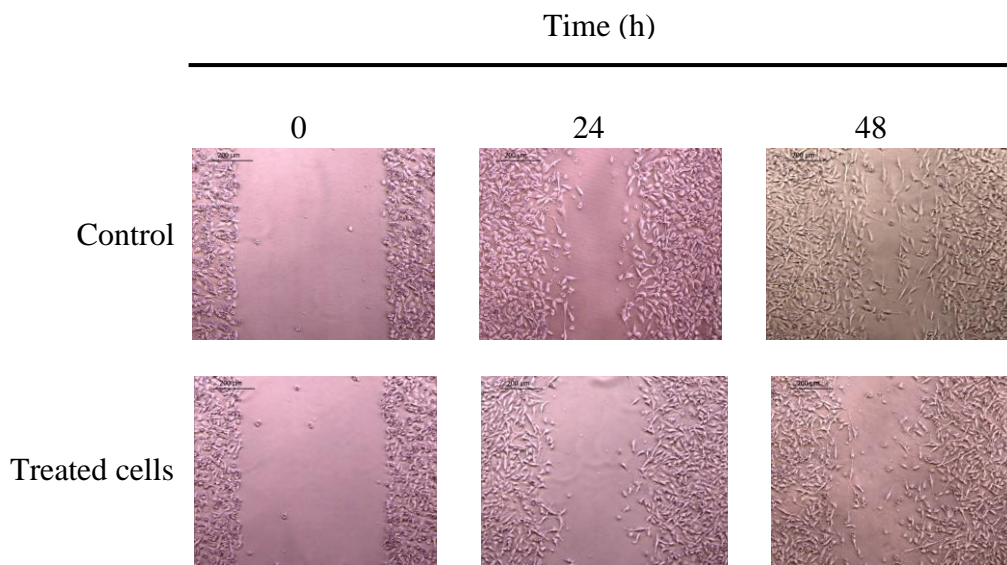
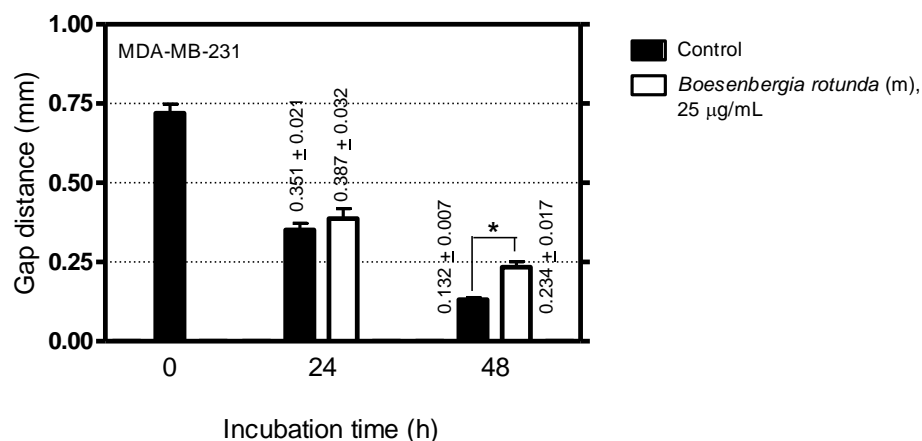


Figure 4.39: Effects of crude chloroform extract of *Boesenbergia rotunda* at 12.5 µg/mL on migration in MDA-MB-231 cells. After wounding, the cells treated with vehicle alone (Control) and chloroform extract of *Boesenbergia rotunda* at 12.5 µg/mL were (A) photographed under a phase-contrast microscope (magnification, 50×) and (B) the migrating distances were measured and plotted at 0 h, 24 h, and 48 h. The sample was assayed in triplicates (N = 3), and statistically significant difference ($p < 0.05$) according to paired-sample t -test was indicated as * above each bar.

Effects of crude methanol extract of *B. rotunda* (tested at 25 µg/mL) on the migration of MDA-MB-231 cells are shown in Figure 4.40. The untreated MDA-MB-231 cells (negative control) spread along the wound edges at 24 h (gap distance, 0.351 mm) and became highly colonised at 48 h (gap distance, 0.132 mm). In contrast, for MDA-MB-231 cells treated with the extracts spread along the wound edges were seen to be slower than that of the untreated cells [Figure 4.40 (A)], with gap distances 0.387 mm and 0.234 mm at 24 h and 48 h, respectively [Figure 4.40 (B)]. Statistical analysis using paired-sample *t*-test ($p < 0.05$) indicate significance differences between the gap distances of control and treated cells at 48 h [Figure 4.40 (B)]. This showed that methanol extract of *B. rotunda* exhibited significant inhibitory effect on migration of MDA-MB-231 cells at 48 h. It delayed the cell migration of MDA-MB-231 cells compared to that of the control cells at 48 h.



(A)



(B)

Figure 4.40: Effects of crude methanol extract of *Boesenbergia rotunda* at 25 µg/mL on migration in MDA-MB-231 cells. After wounding, the cells treated with vehicle alone (Control) and methanol extract of *Boesenbergia rotunda* at 25 µg/mL were (A) photographed under a phase-contrast microscope (magnification, 50×) and (B) the migrating distances were measured and plotted at 0 h, 24 h, and 48 h. The sample was assayed in triplicates (N = 3), and statistically significant difference ($p < 0.05$) according to paired-sample *t*-test was indicated as * above each bar.

(c) *Curcuma aeruginosa*

Effects of crude petroleum ether extract of *C. aeruginosa* (tested at 25 µg/mL) on the migration of MDA-MB-231 cells are shown in Figure 4.41. The untreated MDA-MB-231 cells (negative control) spread along the wound edges at 24 h (gap distance, 0.454 mm) and became highly colonised at 48 h (gap distance, 0.217 mm). In contrast, for MDA-MB-231 cells treated with the extracts spread along the wound edges were seen to be slower than that of the untreated cells [Figure 4.41 (A)], with gap distances 0.560 mm and 0.529 mm at 24 h and 48 h, respectively [Figure 4.41 (B)]. Statistical analysis using paired-sample *t*-test ($p < 0.05$) indicate significance differences between the gap distances of control and treated cells (at 24 h and 48 h) [Figure 4.41 (B)]. This showed that petroleum ether extract of *C. aeruginosa* exhibited significant inhibitory effect on migration of MDA-

MB-231 cells. It delayed the cell migration of MDA-MB-231 cells compared to that of the control cells in a time-dependent manner.

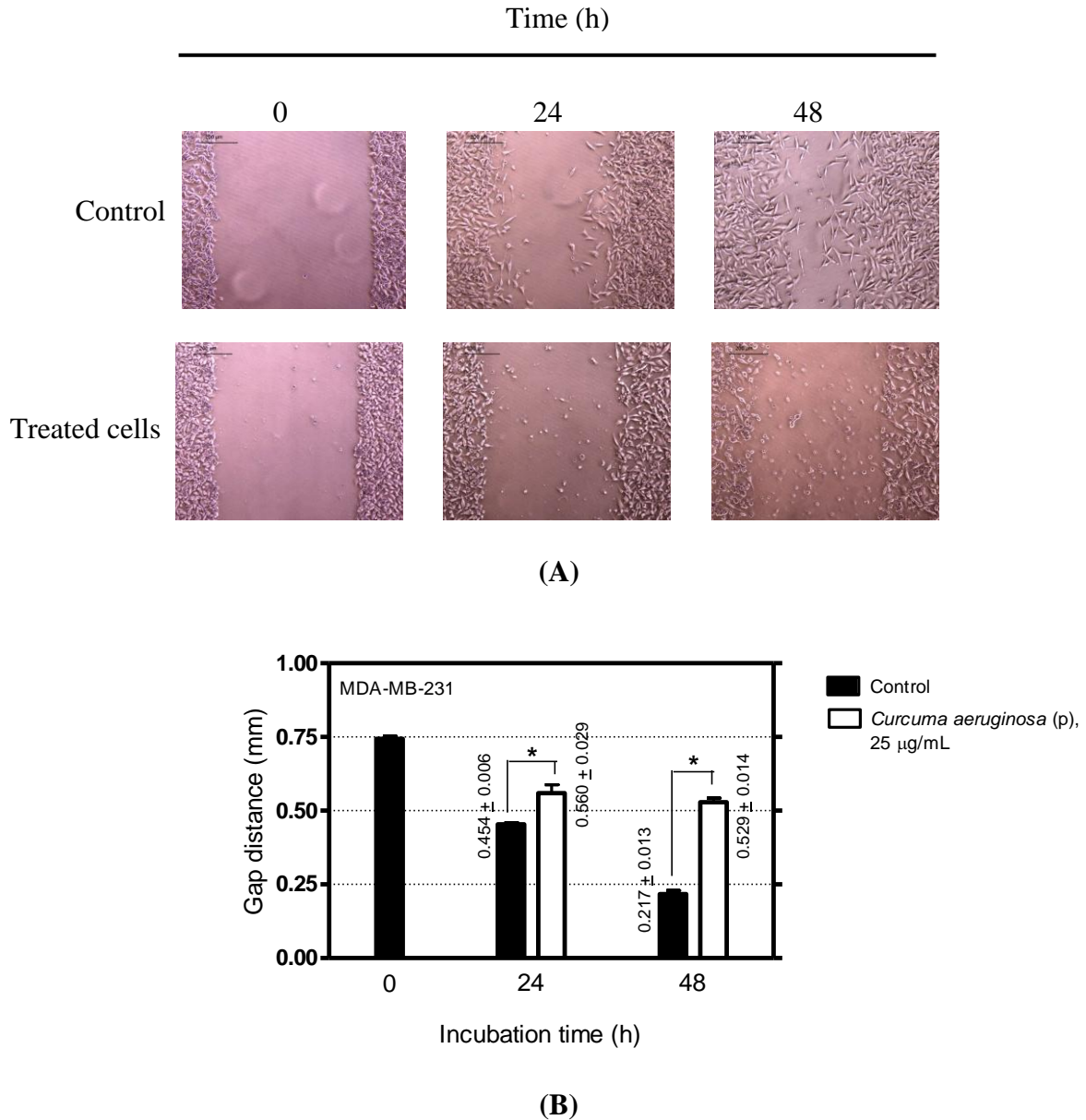
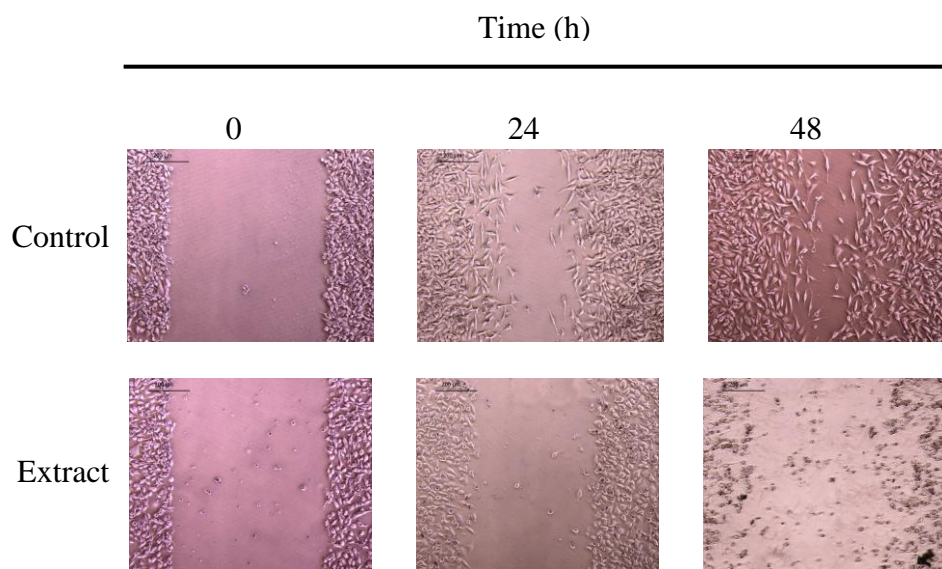
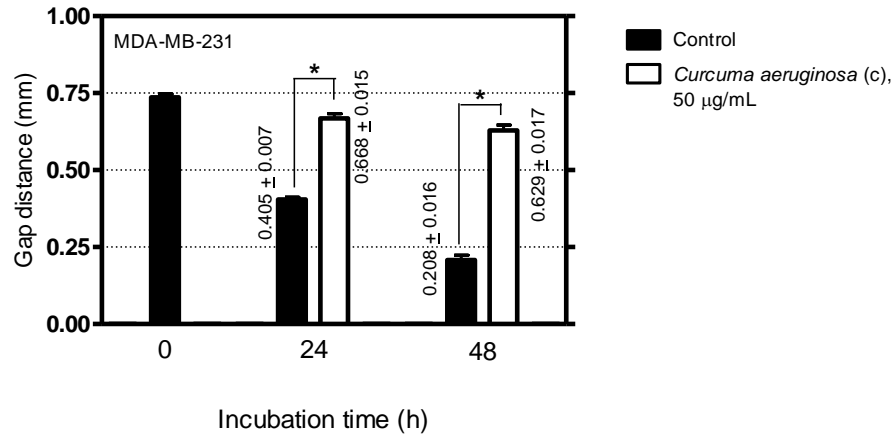


Figure 4.41: Effects of crude petroleum ether extract of *Curcuma aeruginosa* at 25 µg/mL on migration in MDA-MB-231 cells. After wounding, the cells treated with vehicle alone (Control) and petroleum ether extract of *Curcuma aeruginosa* at 25 µg/mL were (A) photographed under a phase-contrast microscope (magnification, 50×) and (B) the migrating distances were measured and plotted at 0 h, 24 h, and 48 h. The sample was assayed in triplicates (N = 3), and statistically significant difference ($p < 0.05$) according to paired-sample t -test was indicated as * above each bar.

Effects of crude chloroform extract of *C. aeruginosa* (tested at 50 $\mu\text{g/mL}$) on the migration of MDA-MB-231 cells are shown in Figure 4.42. The untreated MDA-MB-231 cells (negative control) spread along the wound edges at 24 h (gap distance, 0.405 mm) and became highly colonised at 48 h (gap distance, 0.208 mm). In contrast, for MDA-MB-231 cells treated with the extracts spread along the wound edges were seen to be slower than that of the untreated cells [Figure 4.42 (A)], with gap distances 0.668 mm and 0.629 mm at 24 h and 48 h, respectively [Figure 4.42 (B)]. Statistical analysis using paired-sample *t*-test ($p < 0.05$) indicate significance differences between the gap distances of control and treated cells (at 24 h and 48 h) [Figure 4.42 (B)]. This showed that chloroform extract of *C. aeruginosa* exhibited significant inhibitory effect on migration of MDA-MB-231 cells. It delayed the cell migration of MDA-MB-231 cells compared to that of the control cells in a time-dependent manner.



(A)



(B)

Figure 4.42: Effects of crude chloroform extract of *Curcuma aeruginosa* at 50 µg/mL on migration in MDA-MB-231 cells. After wounding, the cells treated with vehicle alone (Control) and chloroform extract of *Curcuma aeruginosa* at 50 µg/mL were (A) photographed under a phase-contrast microscope (magnification, 50×) and (B) the migrating distances were measured and plotted at 0 h, 24 h, and 48 h. The sample was assayed in triplicates (N = 3), and statistically significant difference ($p < 0.05$) according to paired-sample *t*-test was indicated as * above each bar.

Effects of crude methanol extract of *C. aeruginosa* (tested at 100 µg/mL) on the migration of MDA-MB-231 cells are shown in Figure 4.43. The untreated MDA-MB-231 cells (negative control) spread along the wound edges at 24 h (gap distance, 0.332 mm) and became highly colonised at 48 h (gap distance, 0.116 mm). MDA-MB-231 cells treated with the extracts spread along the wound edges at 24 h (gap distance, 0.327 mm) and become highly colonised at 48 h (gap distance, 0.041 mm). Statistical analysis using paired-sample *t*-test ($p < 0.05$) did not indicate significance differences between the gap distances of control and treated cells (at 24 h and 48 h) [Figure 4.37 (B)]. This showed that methanol extract of *C. aeruginosa* did not exhibit anti-migration activity against MDA-MB-231 cells.

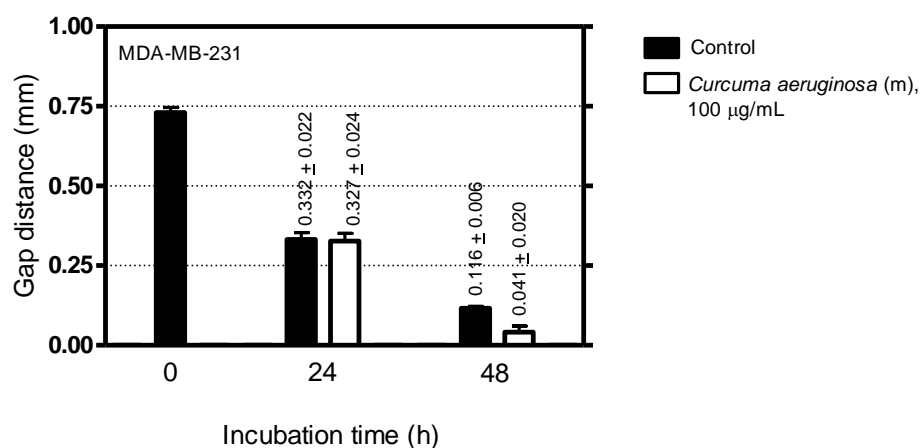
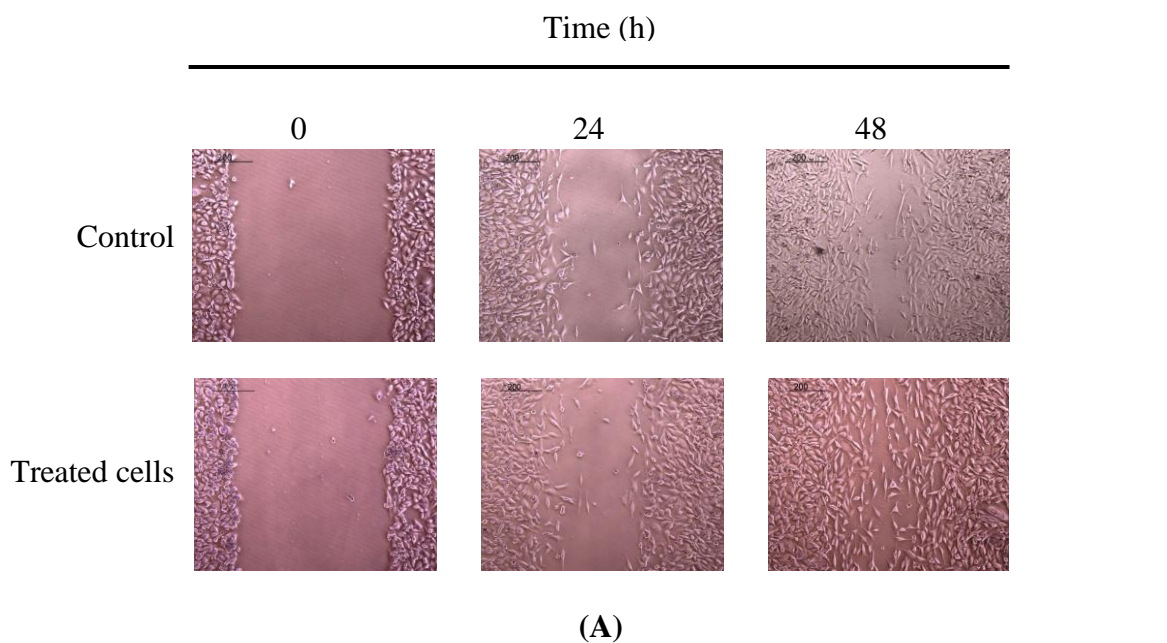
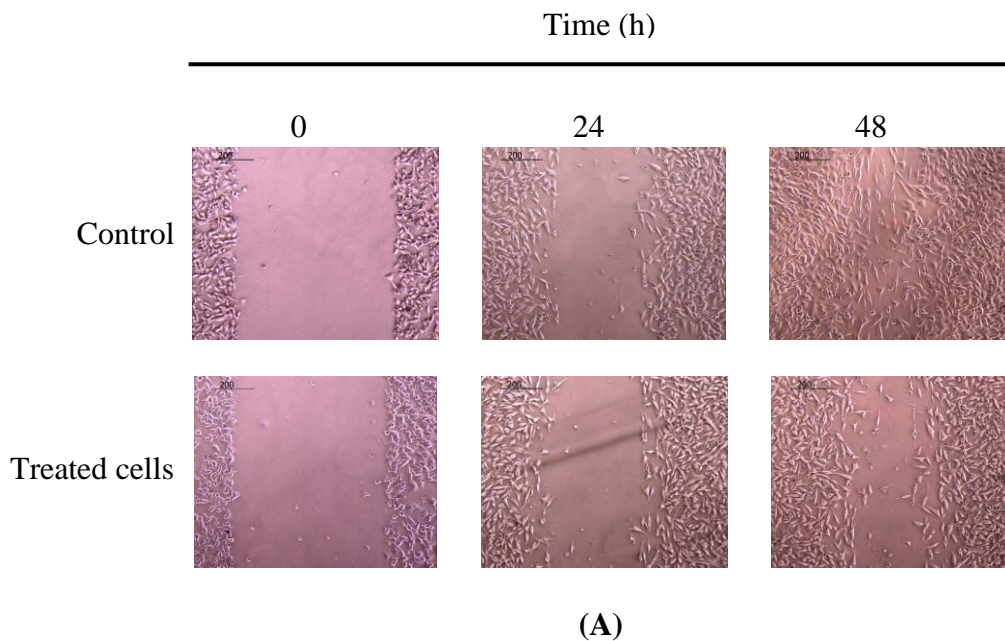
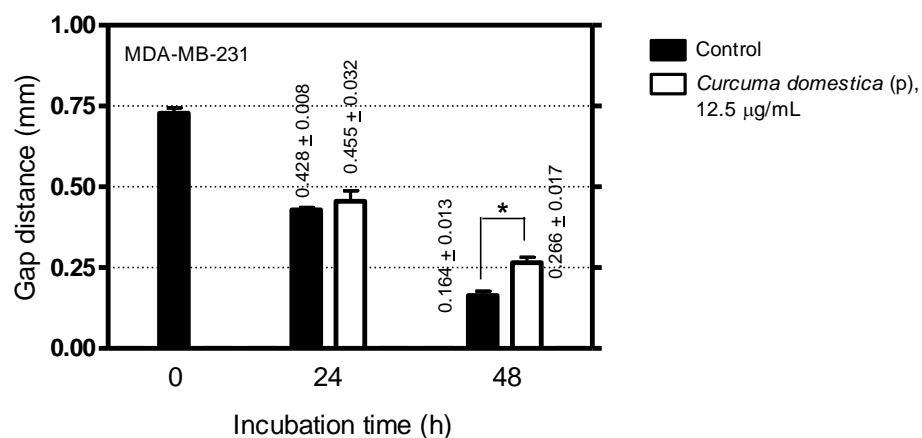


Figure 4.43: Effects of crude methanol extract of *Curcuma aeruginosa* at 100 µg/mL on migration in MDA-MB-231 cells. After wounding, the cells treated with vehicle alone (Control) and methanol extract of *Curcuma aeruginosa* at 100 µg/mL were (A) photographed under a phase-contrast microscope (magnification, 50×) and (B) the migrating distances were measured and plotted at 0 h, 24 h, and 48 h. The sample was assayed in triplicates (N = 3), and statistically significant difference ($p < 0.05$) according to paired-sample t -test was indicated as * above each bar.

(d) *Curcuma domestica*

Effects of crude petroleum ether extract of *C. domestica* (tested at 12.5 $\mu\text{g/mL}$) on the migration of MDA-MB-231 cells are shown in Figure 4.44. The untreated MDA-MB-231 cells (negative control) spread along the wound edges at 24 h (gap distance, 0.428 mm) and became highly colonised at 48 h (gap distance, 0.164 mm). In contrast, for MDA-MB-231 cells treated with the extracts spread along the wound edges were seen to be slower than that of the untreated cells [Figure 4.44 (A)], with gap distances 0.455 mm and 0.266 mm at 24 h and 48 h, respectively [Figure 4.44. (B)]. Statistical analysis using paired-sample *t*-test ($p < 0.05$) indicate significance differences between the gap distances of control and treated cells at 48 h [Figure 4.44 (B)]. This showed that petroleum ether extract of *C. domestica* exhibited significant inhibitory effect on migration of MDA-MB-231 cells at 48 h. It delayed the cell migration of MDA-MB-231 cells compared to that of the control cells at 48 h.





(B)

Figure 4.44: Effects of crude petroleum ether extract of *Curcuma domestica* at 12.5 µg/mL on migration in MDA-MB-231 cells. After wounding, the cells treated with vehicle alone (Control) and petroleum ether extract of *Curcuma domestica* at 12.5 µg/mL were (A) photographed under a phase-contrast microscope (magnification, 50×) and (B) the migrating distances were measured and plotted at 0 h, 24 h, and 48 h. The sample was assayed in triplicates (N = 3), and statistically significant difference ($p < 0.05$) according to paired-sample *t*-test was indicated as * above each bar.

Effects of crude chloroform extract of *C. domestica* (tested at 12.5 µg/mL) on the migration of MDA-MB-231 cells are shown in Figure 4.45. The untreated MDA-MB-231 cells (negative control) spread along the wound edges at 24 h (gap distance, 0.428 mm) and became highly colonised at 48 h (gap distance, 0.164 mm). In contrast, for MDA-MB-231 cells treated with the extracts spread along the wound edges were seen to be slower than that of the untreated cells [Figure 4.45 (A)], with gap distances 0.708 mm and 0.722 mm at 24 h and 48 h, respectively [Figure 4.45 (B)]. Statistical analysis using paired-sample *t*-test ($p < 0.05$) indicate significance differences between the gap distances of control and treated cells (at 24 h and 48 h) [Figure 4.45 (B)]. This showed that chloroform extract of *C. domestica* exhibited significant inhibitory effect on migration of MDA-MB-231 cells. It

delayed the cell migration of MDA-MB-231 cells compared to that of the control cells in a time-dependent manner.

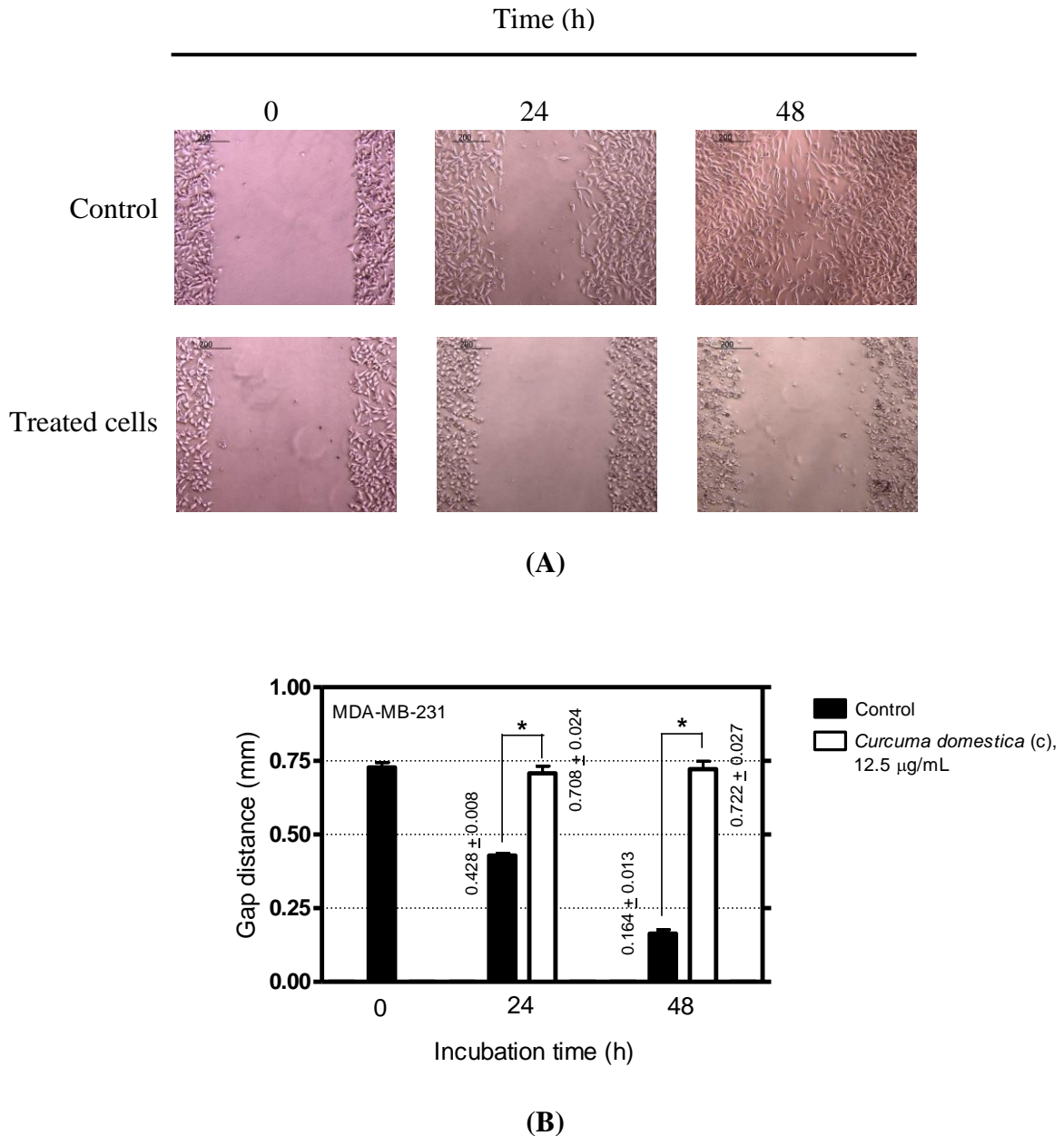
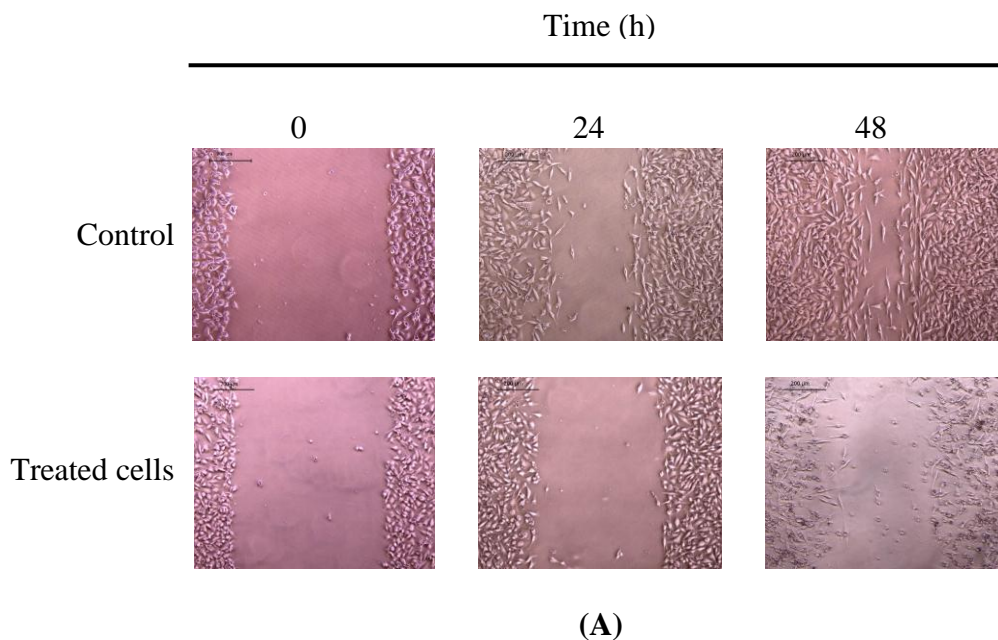
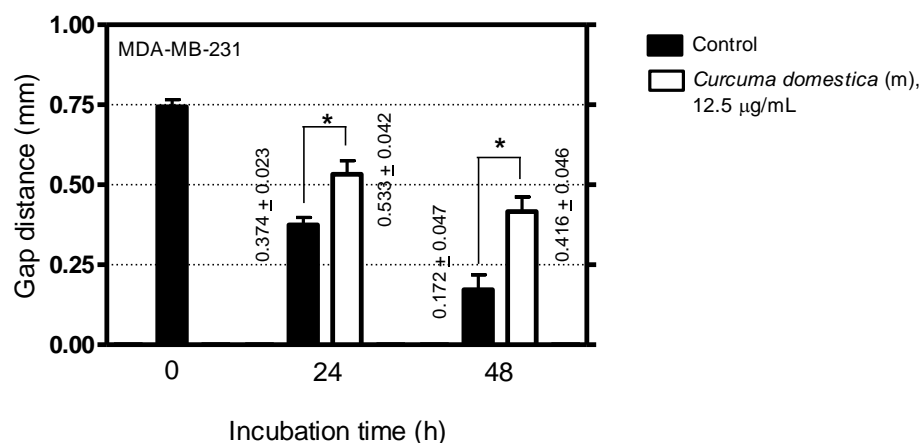


Figure 4.45: Effects of crude chloroform extract of *Curcuma domestica* at 12.5 µg/mL on migration in MDA-MB-231 cells. After wounding, the cells treated with vehicle alone (Control) and chloroform extract of *Curcuma domestica* at 12.5 µg/mL were (A) photographed under a phase-contrast microscope (magnification, 50×) and (B) the migrating distances were measured and plotted at 0 h, 24 h, and 48 h. The sample was assayed in triplicates (N = 3), and statistically significant difference ($p < 0.05$) according to paired-sample t -test was indicated as * above each bar.

Effects of crude methanol extract of *C. domestica* (tested at 12.5 $\mu\text{g/mL}$) on the migration of MDA-MB-231 cells are shown in Figure 4.46. The untreated MDA-MB-231 cells (negative control) spread along the wound edges at 24 h (gap distance, 0.374 mm) and became highly colonised at 48 h (gap distance, 0.172 mm). In contrast, for MDA-MB-231 cells treated with the extracts spread along the wound edges were seen to be slower than that of the untreated cells [Figure 4.46 (A)], with gap distances 0.533 mm and 0.416 mm at 24 h and 48 h, respectively [Figure 4.46 (B)]. Statistical analysis using paired-sample *t*-test ($p < 0.05$) indicate significance differences between the gap distances of control and treated cells (at 24 h and 48 h) [Figure 4.46 (B)]. This showed that methanol extract of *C. domestica* exhibited significant inhibitory effect on migration of MDA-MB-231 cells. It delayed the cell migration of MDA-MB-231 cells compared to that of the control cells in a time-dependent manner.





(B)

Figure 4.46: Effects of crude methanol extract of *Curcuma domestica* at 12.5 µg/mL on migration in MDA-MB-231 cells. After wounding, the cells treated with vehicle alone (Control) and methanol extract of *Curcuma domestica* at 12.5 µg/mL were (A) photographed under a phase-contrast microscope (magnification, 50×) and (B) the migrating distances were measured and plotted at 0 h, 24 h, and 48 h. The sample was assayed in triplicates (N = 3), and statistically significant difference ($p < 0.05$) according to paired-sample *t*-test was indicated as * above each bar.

(e) *Curcuma mangga*

Effects of crude petroleum ether extract of *C. mangga* (tested at 100 µg/mL) on the migration of MDA-MB-231 cells are shown in Figure 4.47. The untreated MDA-MB-231 cells (negative control) spread along the wound edges at 24 h (gap distance, 0.350 mm) and became highly colonised at 48 h (gap distance, 0.120 mm). In contrast, for MDA-MB-231 cells treated with the extracts spread along the wound edges were seen to be slower than that of the untreated cells [Figure 4.47 (A)], with gap distances 0.656 mm and 0.610 mm at 24 h and 48 h, respectively [Figure 4.47 (B)]. Statistical analysis using paired-sample *t*-test ($p < 0.05$) indicate significance differences between the gap distances of control and treated cells (at 24 h and 48 h) [Figure 4.47 (B)]. This showed that petroleum ether extract of *C. mangga* exhibited significant inhibitory effect on migration of MDA-MB-231 cells. It

delayed the cell migration of MDA-MB-231 cells compared to that of the control cells in a time-dependent manner.

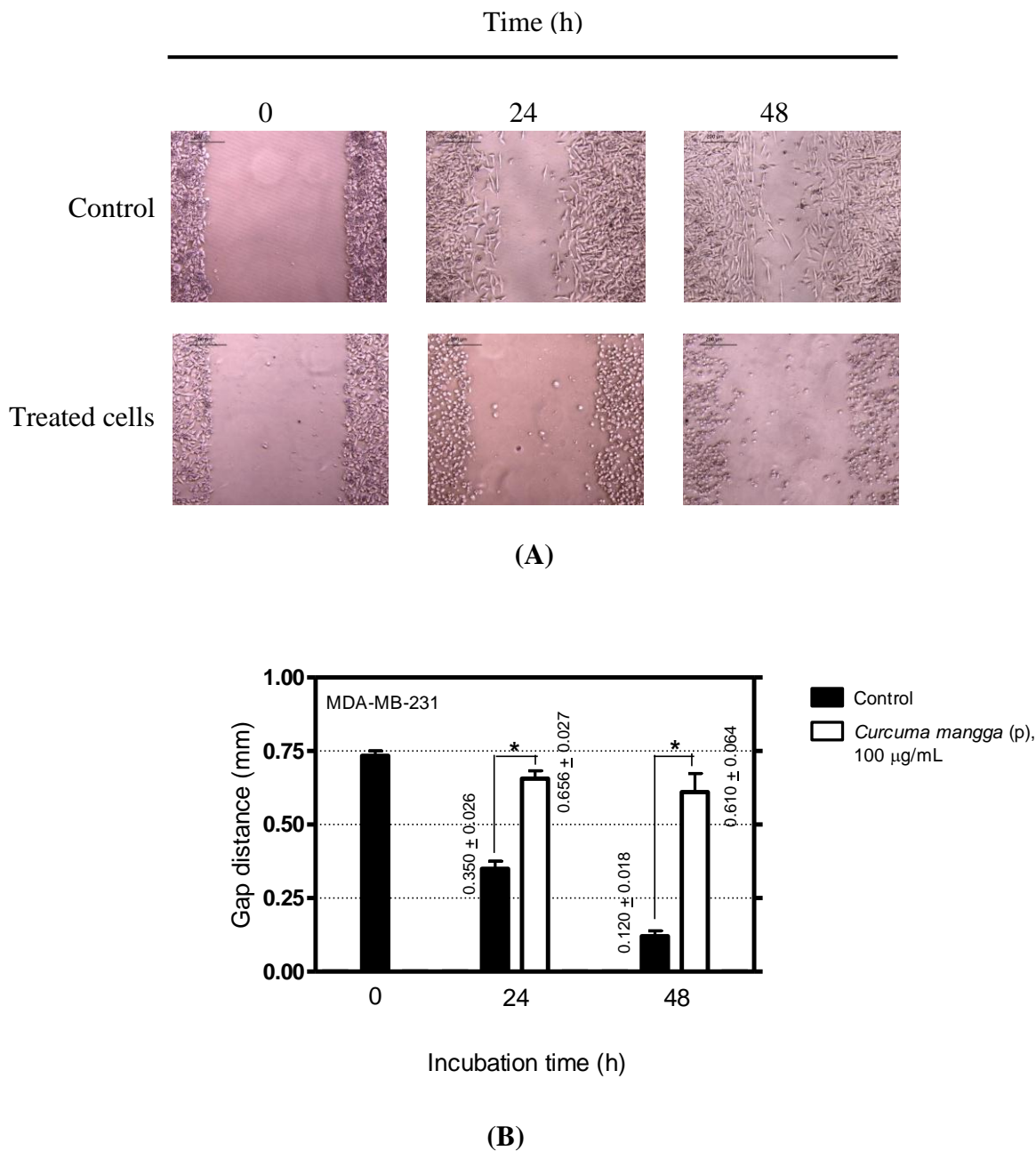
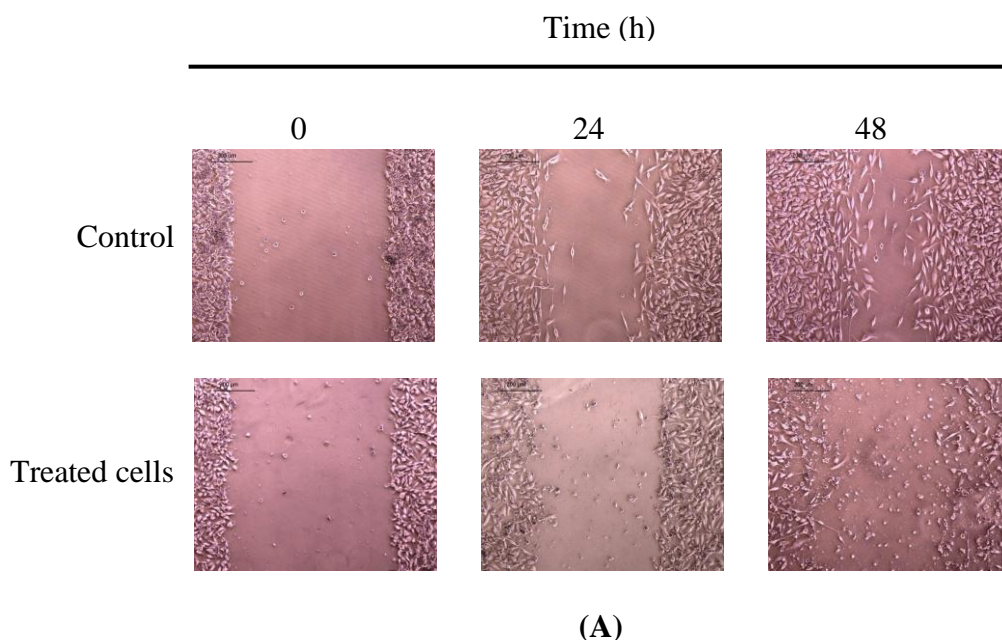
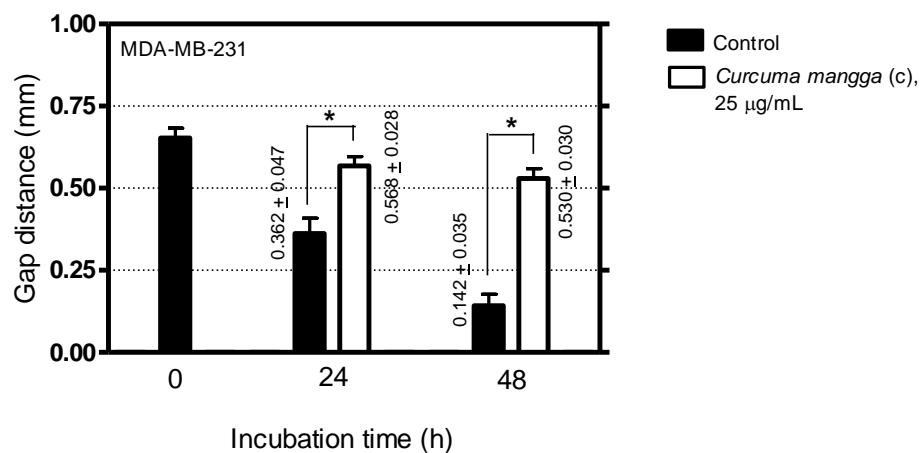


Figure 4.47: Effects of crude petroleum ether extract of *Curcuma mangga* at 100 µg/mL on migration in MDA-MB-231 cells. After wounding, the cells treated with vehicle alone (Control) and petroleum ether extract of *Curcuma mangga* at 100 µg/mL were (A) photographed under a phase-contrast microscope (magnification, 50×) and (B) the migrating distances were measured and plotted at 0 h, 24 h, and 48 h. The sample was assayed in triplicates (N = 3), and statistically significant difference ($p < 0.05$) according to paired-sample t -test was indicated as * above each bar.

Effects of crude chloroform extract of *C. mangga* (tested at 25 $\mu\text{g/mL}$) on the migration of MDA-MB-231 cells are shown in Figure 4.48. The untreated MDA-MB-231 cells (negative control) spread along the wound edges at 24 h (gap distance, 0.362 mm) and became highly colonised at 48 h (gap distance, 0.142 mm). In contrast, for MDA-MB-231 cells treated with the extracts spread along the wound edges were seen to be slower than that of the untreated cells [Figure 4.48 (A)], with gap distances 0.568 mm and 0.530 mm at 24 h and 48 h, respectively [Figure 4.48 (B)]. Statistical analysis using paired-sample *t*-test ($p < 0.05$) indicate significance differences between the gap distances of control and treated cells (at 24 h and 48 h) [Figure 4.48 (B)]. This showed that chloroform extract of *C. mangga* exhibited significant inhibitory effect on migration of MDA-MB-231 cells. It delayed the cell migration of MDA-MB-231 cells compared to that of the control cells in a time-dependent manner.





(B)

Figure 4.48: Effects of crude chloroform extract of *Curcuma mangga* at 25 µg/mL on migration in MDA-MB-231 cells. After wounding, the cells treated with vehicle alone (Control) and chloroform extract of *Curcuma mangga* at 25 µg/mL were (A) photographed under a phase-contrast microscope (magnification, 50×) and (B) the migrating distances were measured and plotted at 0 h, 24 h, and 48 h. The sample was assayed in triplicates (N = 3), and statistically significant difference ($p < 0.05$) according to paired-sample t -test was indicated as * above each bar.

Effects of crude methanol extract of *C. mangga* (tested at 100 µg/mL) on the migration of MDA-MB-231 cells are shown in Figure 4.49. The untreated MDA-MB-231 cells (negative control) spread along the wound edges at 24 h (gap distance, 0.350 mm) and became highly colonised at 48 h (gap distance, 0.120 mm). MDA-MB-231 cells treated with the extracts spread along the wound edges at 24 h (gap distance, 0.380 mm) and become highly colonised at 48 h (gap distance, 0.183 mm). Statistical analysis using paired-sample t -test ($p < 0.05$) did not indicate significance differences between the gap distances of control and treated cells (at 24 h and 48 h) [Figure 4.49 (B)]. This showed that methanol extract of *C. mangga* did not exhibit anti-migration activity against MDA-MB-231 cells.

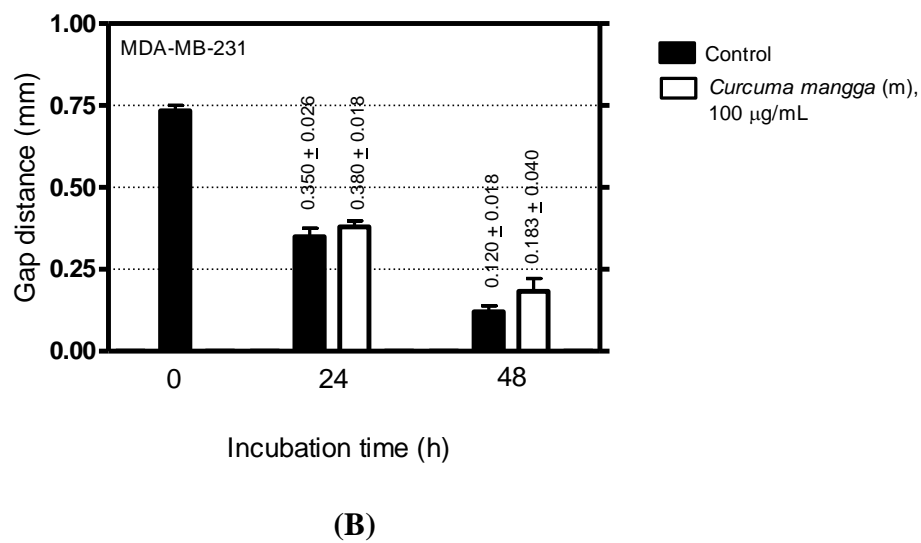
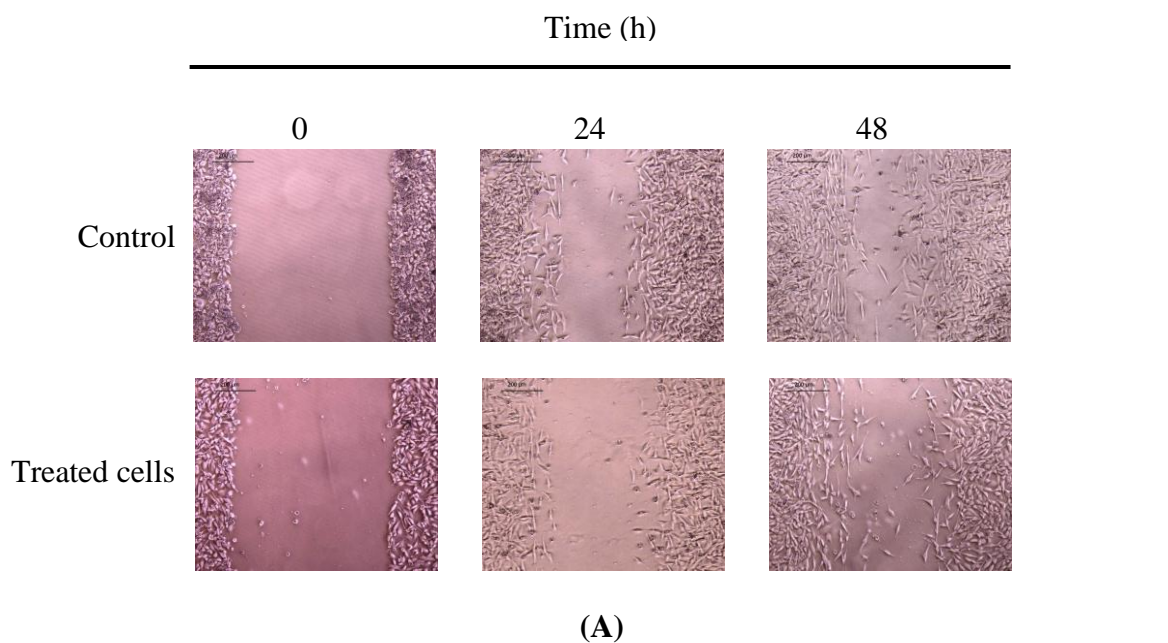
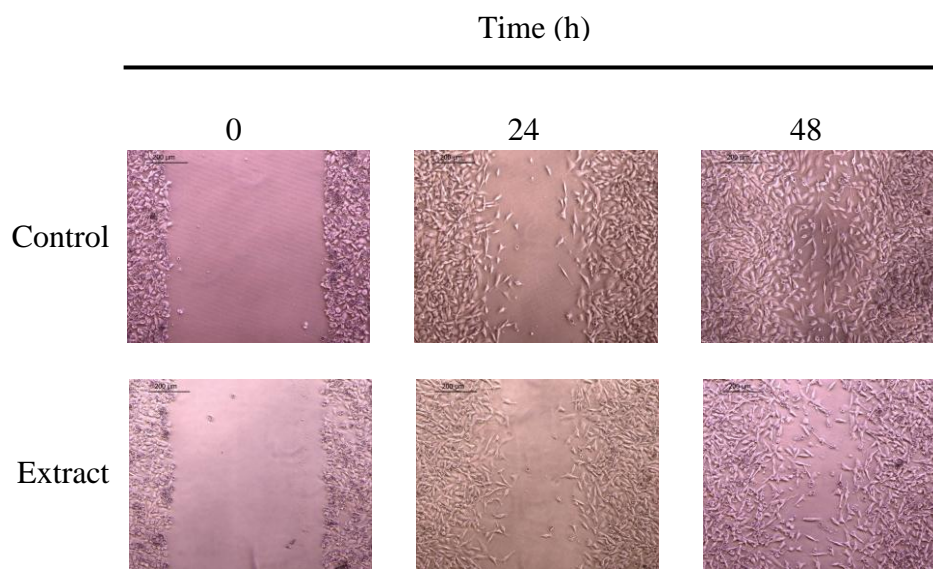
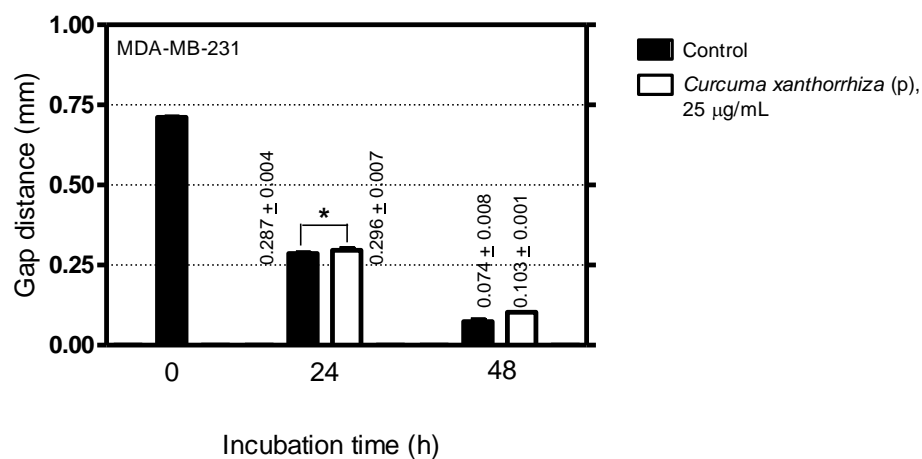


Figure 4.49: Effects of crude methanol extract of *Curcuma mangga* at 100 µg/mL on migration in MDA-MB-23 cells. After wounding, the cells treated with vehicle alone (Control) and methanol extract of *Curcuma mangga* at 100 µg/mL were (A) photographed under a phase-contrast microscope (magnification, 50×) and (B) the migrating distances were measured and plotted at 0 h, 24 h, and 48 h. The sample was assayed in triplicates (N = 3), and statistically significant difference ($p < 0.05$) according to paired-sample t -test was indicated as * above each bar.

Effects of crude petroleum ether extract of *C. xanthorrhiza* (tested at 25 µg/mL) on the migration of MDA-MB-231 cells are shown in Figure 4.50. The untreated MDA-MB-231 cells (negative control) spread along the wound edges at 24 h (gap distance, 0.287 mm) and became highly colonised at 48 h (gap distance, 0.074 mm). MDA-MB-231 cells treated with the extracts spread along the wound edges at 24 h (gap distance, 0.296 mm) and become highly colonised at 48 h (gap distance, 0.103 mm). Statistical analysis using paired-sample *t*-test ($p < 0.05$) did not indicate significance differences between the gap distances of control and treated cells at 48 h [Figure 4.50 (B)]. This showed that petroleum ether extract of *C. xanthorrhiza* did not exhibit anti-migration activity against MDA-MB-231 cells.



(A)



(B)

Figure 4.50: Effects of crude petroleum ether extract of *Curcuma xanthorrhiza* at 25 µg/mL on migration in MDA-MB-23 cells. After wounding, the cells treated with vehicle alone (Control) and petroleum ether extract of *Curcuma xanthorrhiza* at 25 µg/mL were (A) photographed under a phase-contrast microscope (magnification, 50×) and (B) the migrating distances were measured and plotted at 0 h, 24 h, and 48 h. The sample was assayed in triplicates (N = 3), and statistically significant difference ($p < 0.05$) according to paired-sample t -test was indicated as * above each bar.

Effects of crude chloroform extract of *C. xanthorrhiza* (tested at 12.5 µg/mL) on the migration of MDA-MB-231 cells are shown in Figure 4.51. The untreated MDA-MB-231 cells (negative control) spread along the wound edges at 24 h (gap distance, 0.377 mm) and became highly colonised at 48 h (gap distance, 0.172 mm). MDA-MB-231 cells treated with the extracts spread along the wound edges at 24 h (gap distance, 0.498 mm) and become highly colonised at 48 h (gap distance, 0.318 mm). Statistical analysis using paired-sample t -test ($p < 0.05$) did not indicate significance differences between the gap distances of control and treated cells at both 24 h and 48 h [Figure 4.51 (B)]. This showed that chloroform extract of *C. xanthorrhiza* did not exhibit anti-migration activity against MDA-MB-231 cells.

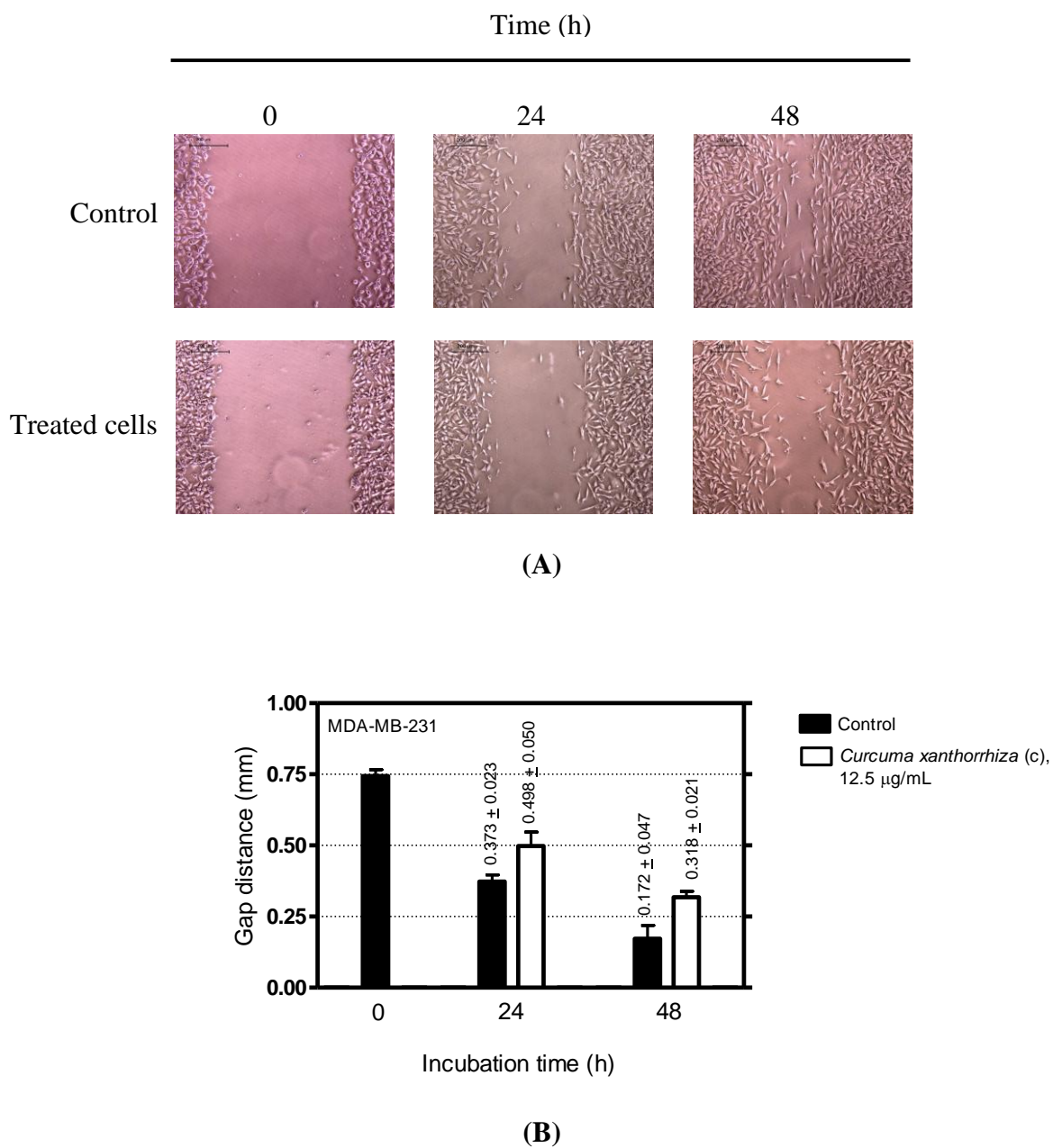
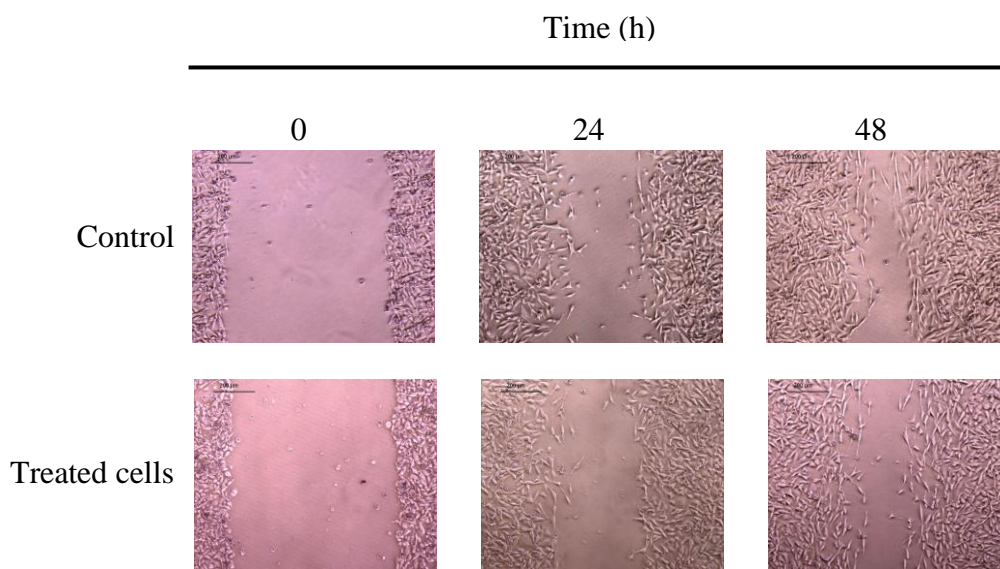
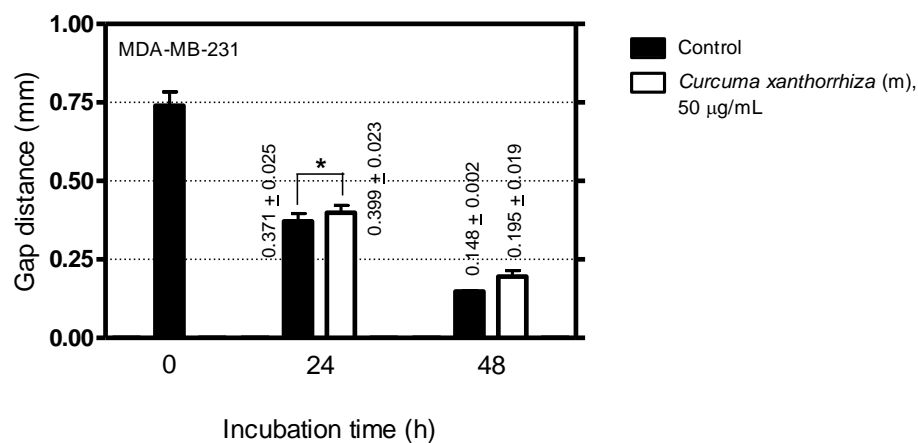


Figure 4.51: Effects of crude chloroform extract of *Curcuma xanthorrhiza* at 12.5 µg/mL on migration in MDA-MB-231 cells. After wounding, the cells treated with vehicle alone (Control) and chloroform extract of *Curcuma xanthorrhiza* at 12.5 µg/mL were (A) photographed under a phase-contrast microscope (magnification, 50×) and (B) the migrating distances were measured and plotted at 0 h, 24 h, and 48 h. The sample was assayed in triplicates (N = 3), and statistically significant difference ($p < 0.05$) according to paired-sample t -test was indicated as * above each bar.

Effects of crude methanol extract of *C. xanthorrhiza* (tested at 50 $\mu\text{g/mL}$) on the migration of MDA-MB-231 cells are shown in Figure 4.52. The untreated MDA-MB-231 cells (negative control) spread along the wound edges at 24 h (gap distance, 0.371 mm) and became highly colonised at 48 h (gap distance, 0.148 mm). MDA-MB-231 cells treated with the extracts spread along the wound edges at 24 h (gap distance, 0.399 mm) and become highly colonised at 48 h (gap distance, 0.195 mm). Statistical analysis using paired-sample *t*-test ($p < 0.05$) did not indicate significance differences between the gap distances of control and treated cells at 48 h [Figure 4.52 (B)]. This showed that methanol extract of *C. xanthorrhiza* did not exhibit anti-migration activity against MDA-MB-231 cells.



(A)



(B)

Figure 4.52: Effects of crude methanol extract of *Curcuma xanthorrhiza* at 50 µg/mL on migration in MDA-MB-231 cells. After wounding, the cells treated with vehicle alone (Control) and methanol extract of *Curcuma xanthorrhiza* at 50 µg/mL were (A) photographed under a phase-contrast microscope (magnification, 50×) and (B) the migrating distances were measured and plotted at 0 h, 24 h, and 48 h. The sample was assayed in triplicates (N = 3), and statistically significant difference ($p < 0.05$) according to paired-sample *t*-test was indicated as * above each bar.

Effects of crude petroleum ether extract of *K. galanga* (tested at 100 µg/mL) on the migration of MDA-MB-231 cells are shown in Figure 4.53. The untreated MDA-MB-231 cells (negative control) spread along the wound edges at 24 h (gap distance, 0.341 mm) and became highly colonised at 48 h (gap distance, 0.104 mm). In contrast, for MDA-MB-231 cells treated with the extracts spread along the wound edges were seen to be slower than that of the untreated cells [Figure 4.53 (A)], with gap distances 0.508 mm and 0.458 mm at 24 h and 48 h, respectively [Figure 4.53 (B)]. Statistical analysis using paired-sample *t*-test ($p < 0.05$) indicate significance differences between the gap distances of control and treated cells (at 24 h and 48 h) [Figure 4.53 (B)]. This showed that petroleum ether extract of *K. galanga* exhibited significant inhibitory effect on migration of MDA-MB-231 cells. It

delayed the cell migration of MDA-MB-231 cells compared to that of the control cells in a time-dependent manner.

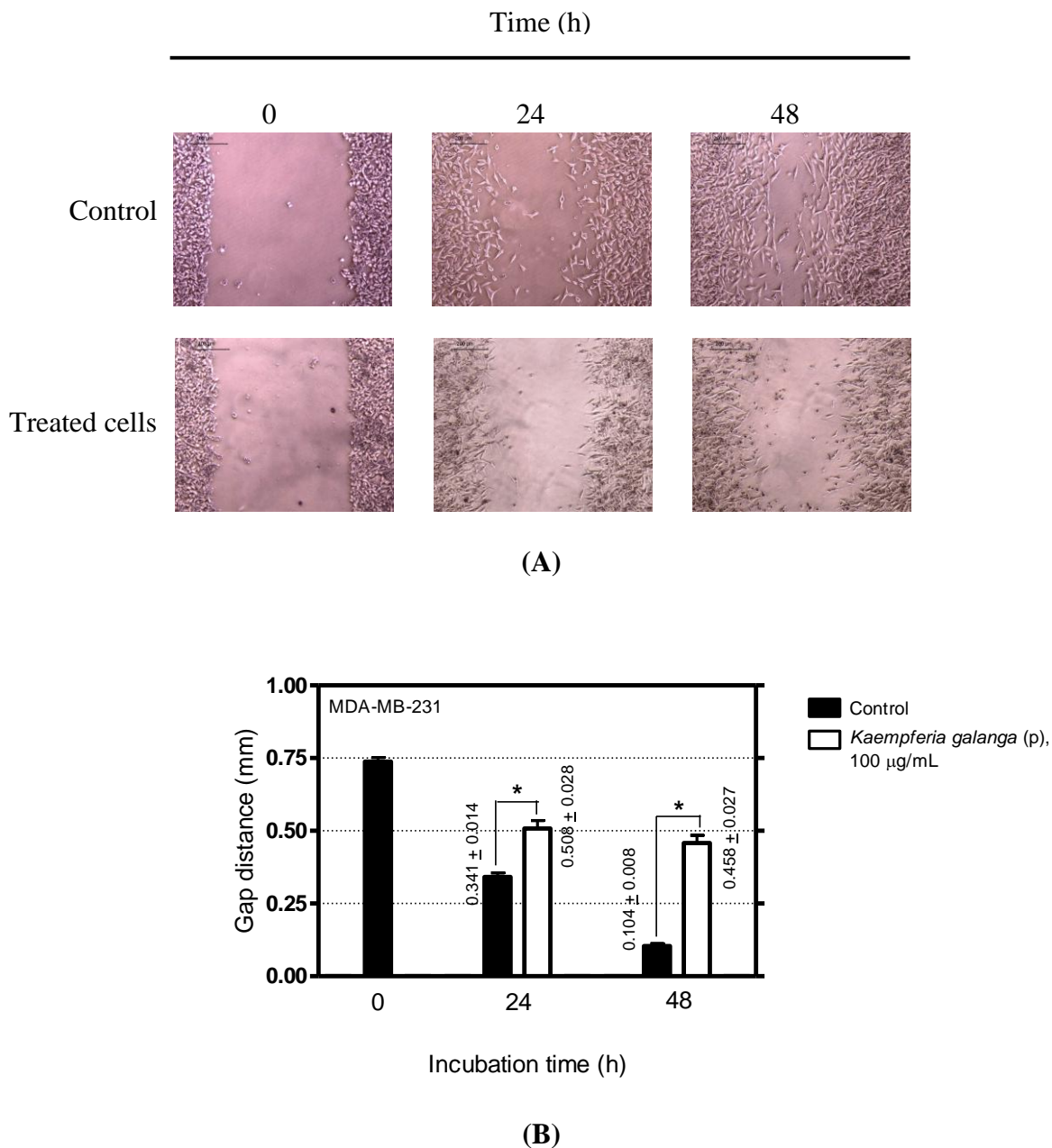
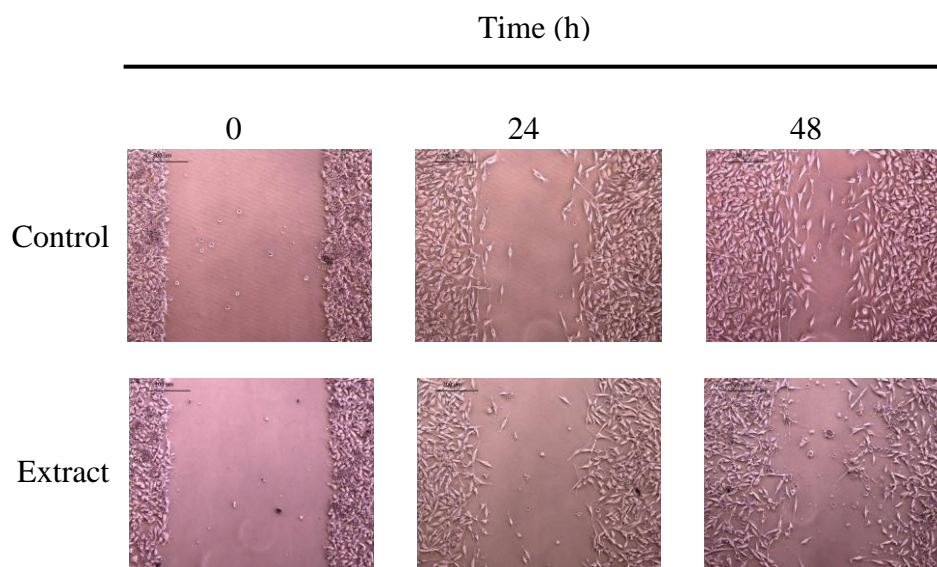
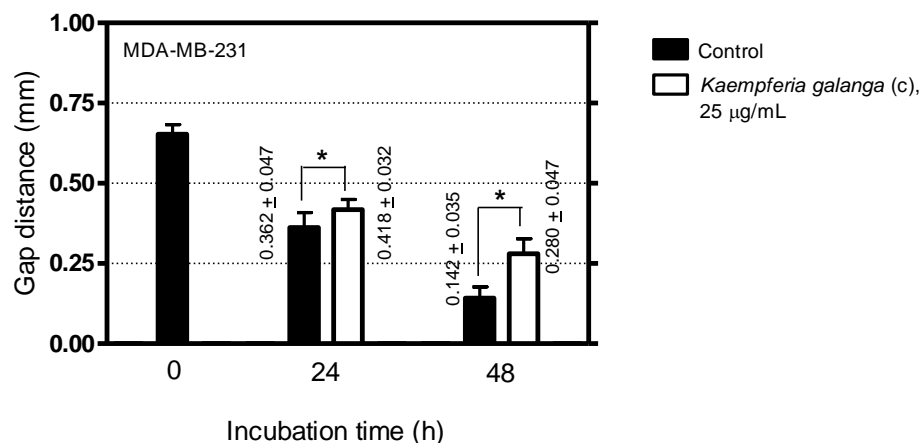


Figure 4.53: Effects of crude petroleum ether extract of *Kaempferia galanga* at 100 µg/mL on migration in MDA-MB-231 cells. After wounding, the cells treated with vehicle alone (Control) and petroleum ether extract of *Kaempferia galanga* at 100 µg/mL were (A) photographed under a phase-contrast microscope (magnification, 50×) and (B) the migrating distances were measured and plotted at 0 h, 24 h, and 48 h. The sample was assayed in triplicates (N = 3), and statistically significant difference ($p < 0.05$) according to paired-sample t -test was indicated as * above each bar.

Effects of crude chloroform extract of *K. galanga* (tested at 25 $\mu\text{g}/\text{mL}$) on the migration of MDA-MB-231 cells are shown in Figure 4.54. The untreated MDA-MB-231 cells (negative control) spread along the wound edges at 24 h (gap distance, 0.362 mm) and became highly colonised at 48 h (gap distance, 0.142 mm). In contrast, for MDA-MB-231 cells treated with the extracts spread along the wound edges were seen to be slower than that of the untreated cells [Figure 4.54 (A)], with gap distances 0.418 mm and 0.280 mm at 24 h and 48 h, respectively [Figure 4.54 (B)]. Statistical analysis using paired-sample *t*-test ($p < 0.05$) indicate significance differences between the gap distances of control and treated cells (at 24 h and 48 h) [Figure 4.54 (B)]. This showed that chloroform extract of *K. galanga* exhibited significant inhibitory effect on migration of MDA-MB-231 cells. It delayed the cell migration of MDA-MB-231 cells compared to that of the control cells in a time-dependent manner.



(A)



(B)

Figure 4.54: Effects of crude chloroform extract of *Kaempferia galanga* at 25 µg/mL on migration in MDA-MB-231 cells. After wounding, the cells treated with vehicle alone (Control) and chloroform extract of *Kaempferia galanga* at 25 µg/mL were (A) photographed under a phase-contrast microscope (magnification, 50×) and (B) the migrating distances were measured and plotted at 0 h, 24 h, and 48 h. The sample was assayed in triplicates (N = 3), and statistically significant difference ($p < 0.05$) according to paired-sample *t*-test was indicated as * above each bar.

Effects of crude methanol extract of *K. galanga* (tested at 25 µg/mL) on the migration of MDA-MB-231 cells are shown in Figure 4.55. The untreated MDA-MB-231 cells (negative control) spread along the wound edges at 24 h (gap distance, 0.287 mm) and became highly colonised at 48 h (gap distance, 0.074 mm). In contrast, for MDA-MB-231 cells treated with the extracts spread along the wound edges were seen to be slower than that of the untreated cells [Figure 4.55 (A)], with gap distances 0.312 mm and 0.132 mm at 24 h and 48 h, respectively [Figure 4.55 (B)]. Statistical analysis using paired-sample *t*-test ($p < 0.05$) indicate significance differences between the gap distances of control and treated cells (at 24 h and 48 h) [Figure 4.55 (B)]. This showed that methanol extract of *K. galanga* exhibited significant inhibitory effect on migration of MDA-MB-231 cells. It delayed the

cell migration of MDA-MB-231 cells compared to that of the control cells in a time-dependent manner.

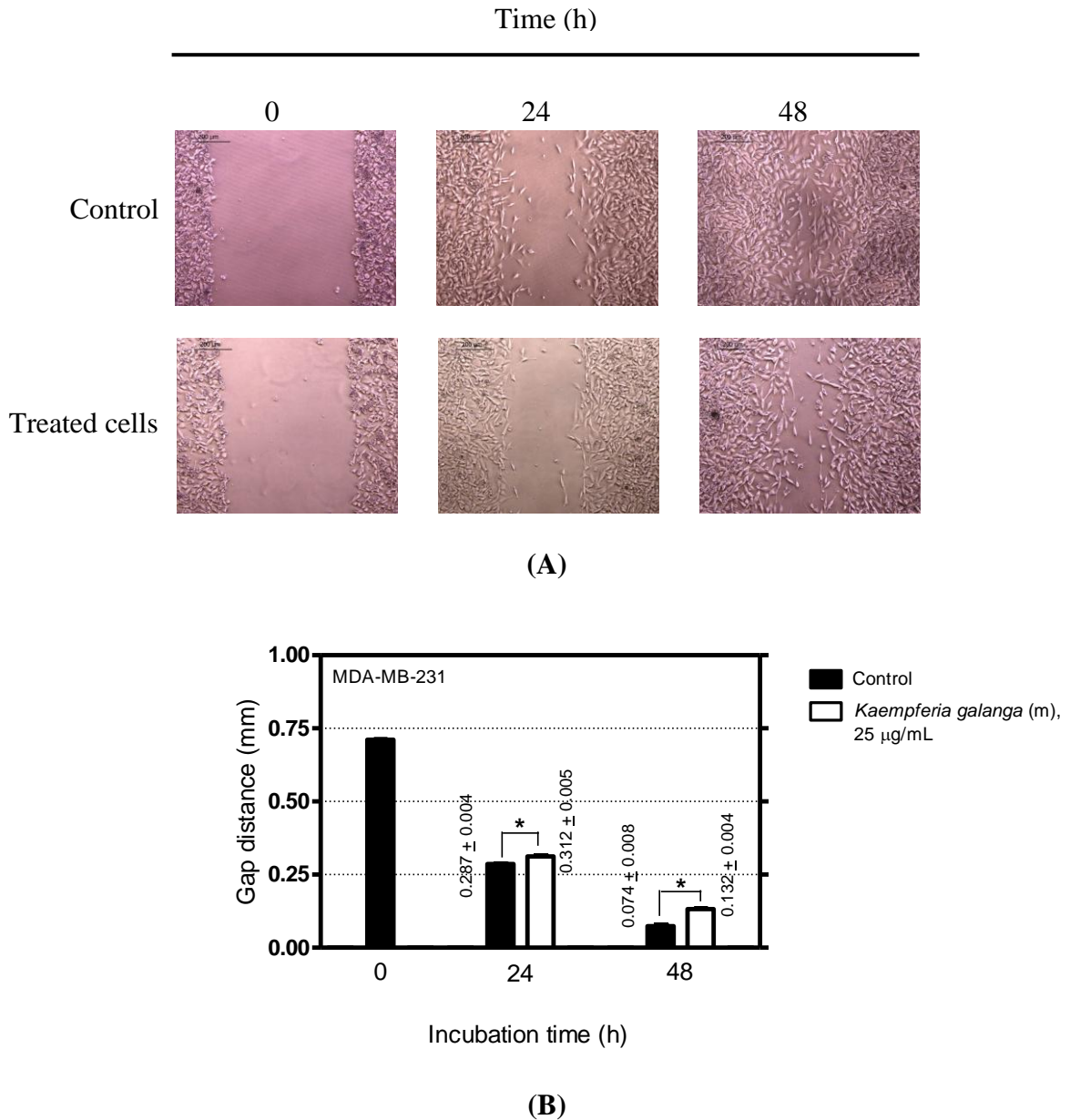
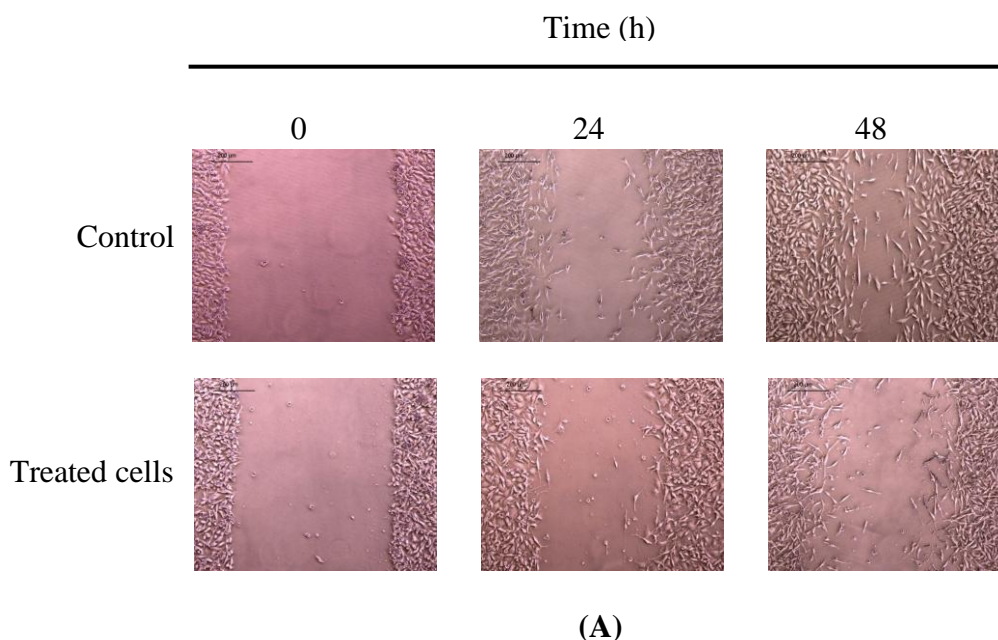
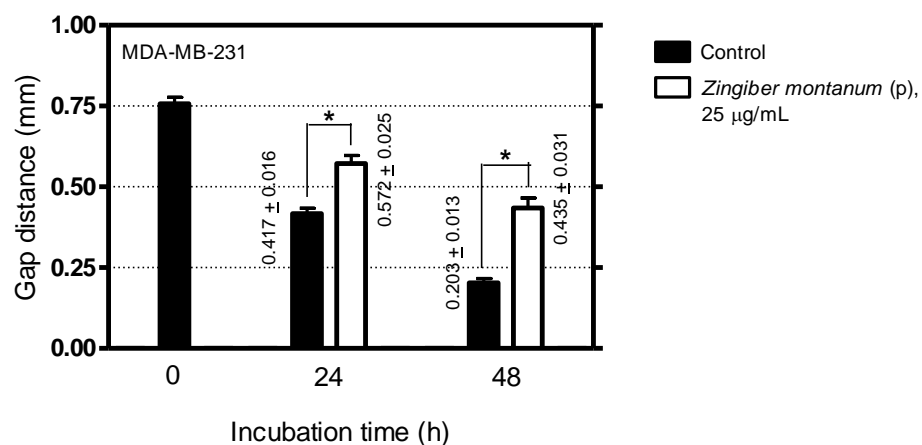


Figure 4.55: Effects of crude methanol extract of *Kaempferia galanga* at 25 µg/mL on migration in MDA-MB-231 cells. After wounding, the cells treated with vehicle alone (Control) and methanol extract of *Kaempferia galanga* at 25 µg/mL were (A) photographed under a phase-contrast microscope (magnification, 50×) and (B) the migrating distances were measured and plotted at 0 h, 24 h, and 48 h. The sample was assayed in triplicates (N = 3), and statistically significant difference ($p < 0.05$) according to paired-sample t -test was indicated as * above each bar.

Effects of crude petroleum ether extract of *Z. montanum* (tested at 25 µg/mL) on the migration of MDA-MB-231 cells are shown in Figure 4.56. The untreated MDA-MB-231 cells (negative control) spread along the wound edges at 24 h (gap distance, 0.417 mm) and became highly colonised at 48 h (gap distance, 0.203 mm). In contrast, for MDA-MB-231 cells treated with the extracts spread along the wound edges were seen to be slower than that of the untreated cells [Figure 4.56 (A)], with gap distances 0.572 mm and 0.435 mm at 24 h and 48 h, respectively [Figure 4.56 (B)]. Statistical analysis using paired-sample *t*-test ($p < 0.05$) indicate significance differences between the gap distances of control and treated cells (at 24 h and 48 h) [Figure 4.56 (B)]. This showed that petroleum ether extract of *Z. montanum* exhibited significant inhibitory effect on migration of MDA-MB-231 cells. It delayed the cell migration of MDA-MB-231 cells compared to that of the control cells in a time-dependent manner.





(B)

Figure 4.56: Effects of crude petroleum ether extract of *Zingiber montanum* at 25 µg/mL on migration in MDA-MB-231 cells. After wounding, the cells treated with vehicle alone (Control) and petroleum ether extract of *Zingiber montanum* at 25 µg/mL were (A) photographed under a phase-contrast microscope (magnification, 50×) and (B) the migrating distances were measured and plotted at 0 h, 24 h, and 48 h. The sample was assayed in triplicates (N = 3), and statistically significant difference ($p < 0.05$) according to paired-sample *t*-test was indicated as * above each bar.

Effects of crude chloroform extract of *Z. montanum* (tested at 25 µg/mL) on the migration of MDA-MB-231 cells are shown in Figure 4.57. The untreated MDA-MB-231 cells (negative control) spread along the wound edges at 24 h (gap distance, 0.417 mm) and became highly colonised at 48 h (gap distance, 0.203 mm). In contrast, for MDA-MB-231 cells treated with the extracts spread along the wound edges were seen to be slower than that of the untreated cells [Figure 4.57 (A)], with gap distances 0.524 mm and 0.366 mm at 24 h and 48 h, respectively [Figure 4.57 (B)]. Statistical analysis using paired-sample *t*-test ($p < 0.05$) indicate significance differences between the gap distances of control and treated cells (at 24 h and 48 h) [Figure 4.57 (B)]. This showed that chloroform extract of *Z. montanum* exhibited significant inhibitory effect on migration of MDA-MB-231 cells. It

delayed the cell migration of MDA-MB-231 cells compared to that of the control cells in a time-dependent manner.

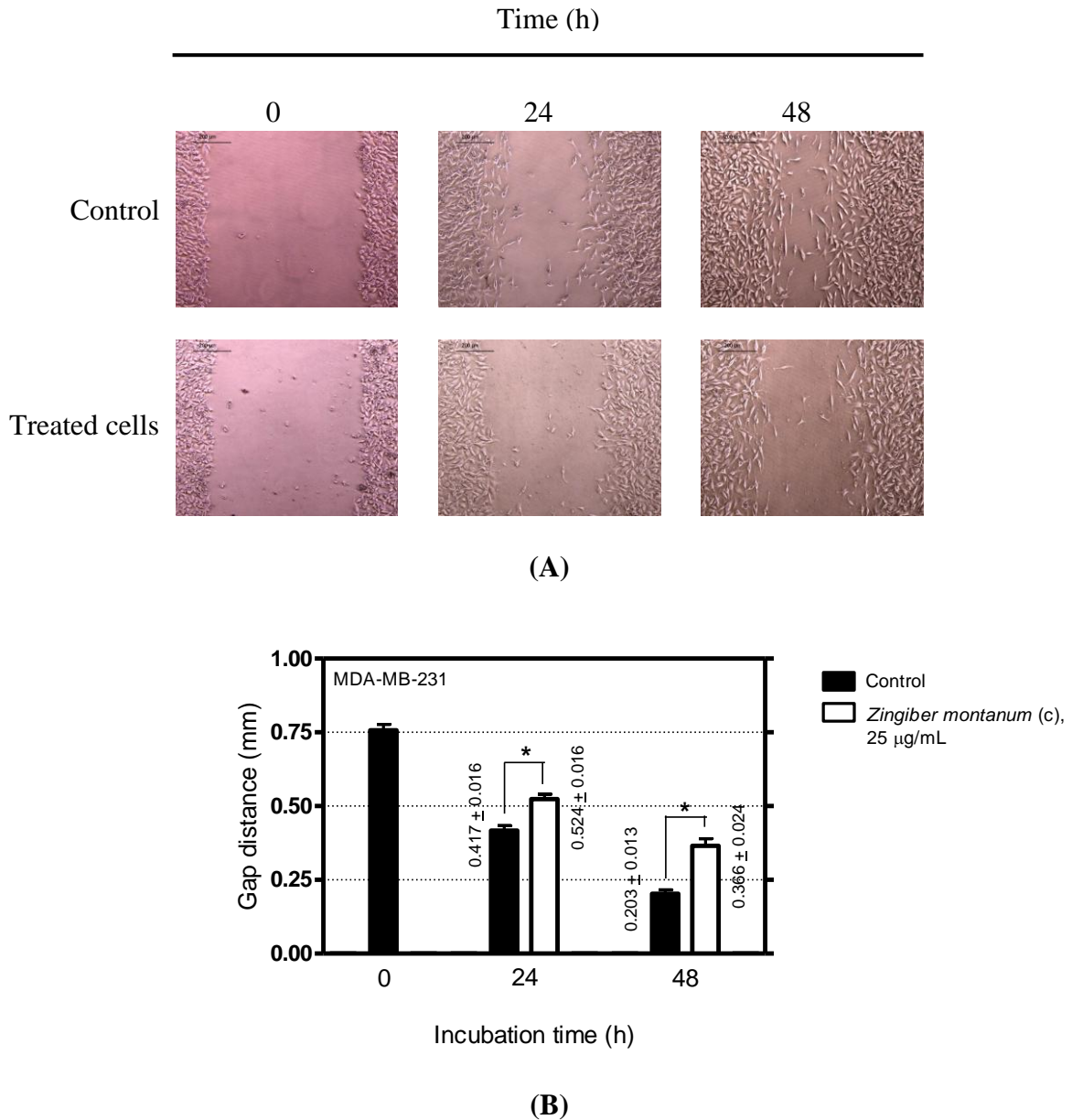
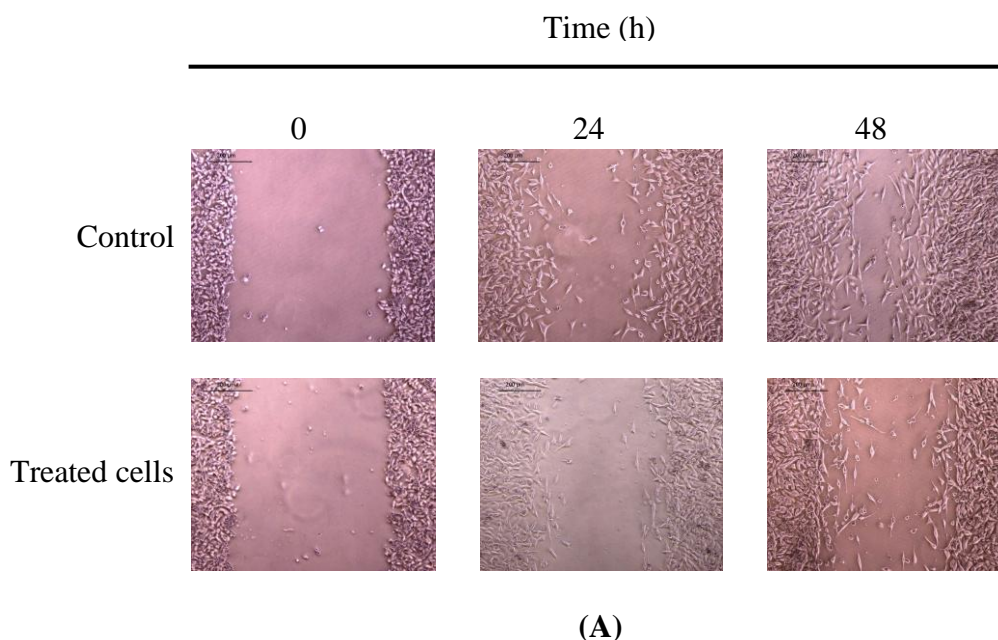
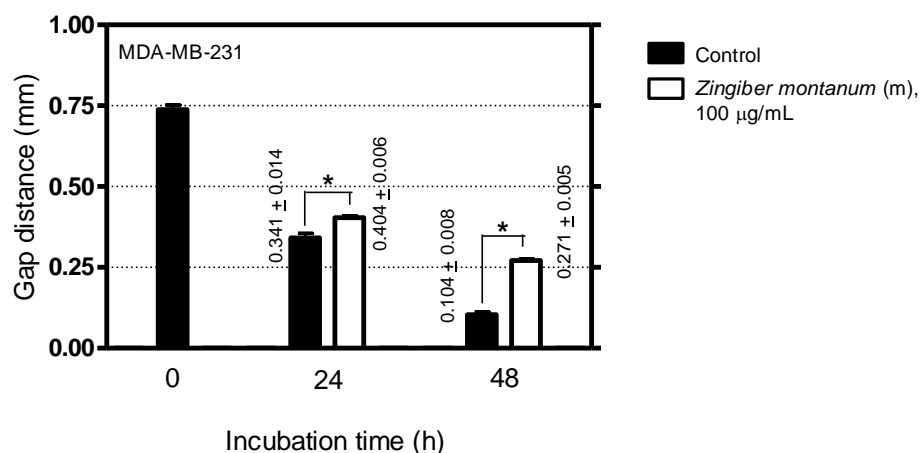


Figure 4.57: Effects of crude chloroform extract of *Zingiber montanum* at 25 µg/mL on migration in MDA-MB-231 cells. After wounding, the cells treated with vehicle alone (Control) and chloroform extract of *Zingiber montanum* at 25 µg/mL were (A) photographed under a phase-contrast microscope (magnification, 50×) and (B) the migrating distances were measured and plotted at 0 h, 24 h, and 48 h. The sample was assayed in triplicates (N = 3), and statistically significant difference ($p < 0.05$) according to paired-sample t -test was indicated as * above each bar.

Effects of crude methanol extract of *Z. montanum* (tested at 100 $\mu\text{g}/\text{mL}$) on the migration of MDA-MB-231 cells are shown in Figure 4.58. The untreated MDA-MB-231 cells (negative control) spread along the wound edges at 24 h (gap distance, 0.341 mm) and became highly colonised at 48 h (gap distance, 0.104 mm). In contrast, for MDA-MB-231 cells treated with the extracts spread along the wound edges were seen to be slower than that of the untreated cells [Figure 4.58 (A)], with gap distances 0.404 mm and 0.271 mm at 24 h and 48 h, respectively [Figure 4.58 (B)]. Statistical analysis using paired-sample *t*-test ($p < 0.05$) indicate significance differences between the gap distances of control and treated cells (at 24 h and 48 h) [Figure 4.58 (B)]. This showed that methanol extract of *Z. montanum* exhibited significant inhibitory effect on migration of MDA-MB-231 cells. It delayed the cell migration of MDA-MB-231 cells compared to that of the control cells in a time-dependent manner.





(B)

Figure 4.58: Effects of crude methanol extract of *Zingiber montanum* at 100 µg/mL on migration in MDA-MB-231 cells. After wounding, the cells treated with vehicle alone (Control) and methanol extract of *Zingiber montanum* at 100 µg/mL were (A) photographed under a phase-contrast microscope (magnification, 50×) and (B) the migrating distances were measured and plotted at 0 h, 24 h, and 48 h. The sample was assayed in triplicates (N = 3), and statistically significant difference ($p < 0.05$) according to paired-sample *t*-test was indicated as * above each bar.

Effects of crude petroleum ether extract of *Z. officinale* (tested at 25 µg/mL) on the migration of MDA-MB-231 cells are shown in Figure 4.59. The untreated MDA-MB-231 cells (negative control) spread along the wound edges at 24 h (gap distance, 0.351 mm) and became highly colonised at 48 h (gap distance, 0.132 mm). In contrast, for MDA-MB-231 cells treated with the extracts spread along the wound edges were seen to be slower than that of the untreated cells [Figure 4.59 (A)], with gap distances 0.550 mm and 0.457 mm at 24 h and 48 h, respectively [Figure 4.59 (B)]. Statistical analysis using paired-sample *t*-test ($p < 0.05$) indicate significance differences between the gap distances of control and treated cells (at 24 h and 48 h) [Figure 4.59 (B)]. This showed that petroleum ether extract of *Z. officinale* exhibited significant inhibitory effect on migration of MDA-MB-231 cells. It

delayed the cell migration of MDA-MB-231 cells compared to that of the control cells in a time-dependent manner.

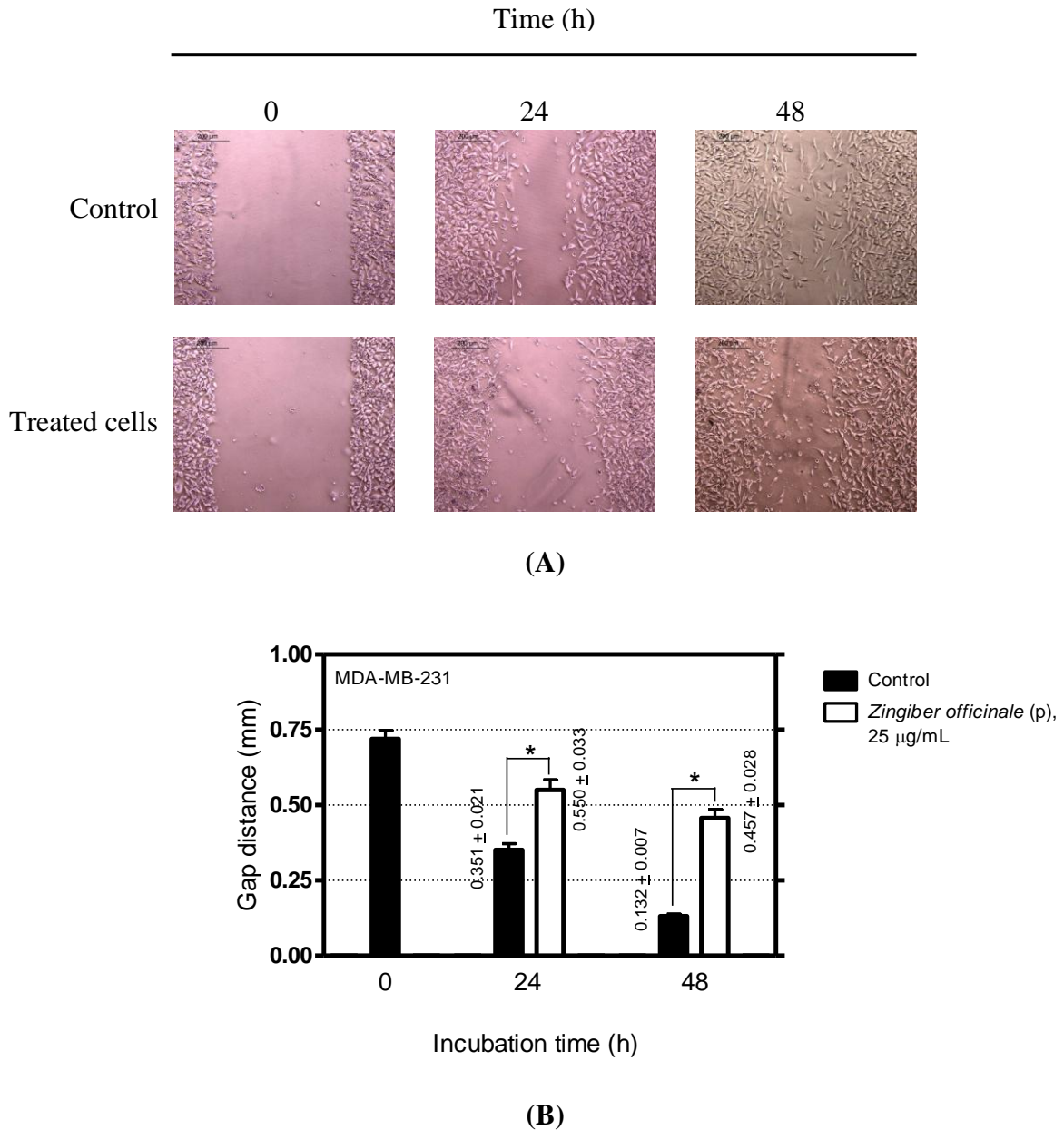
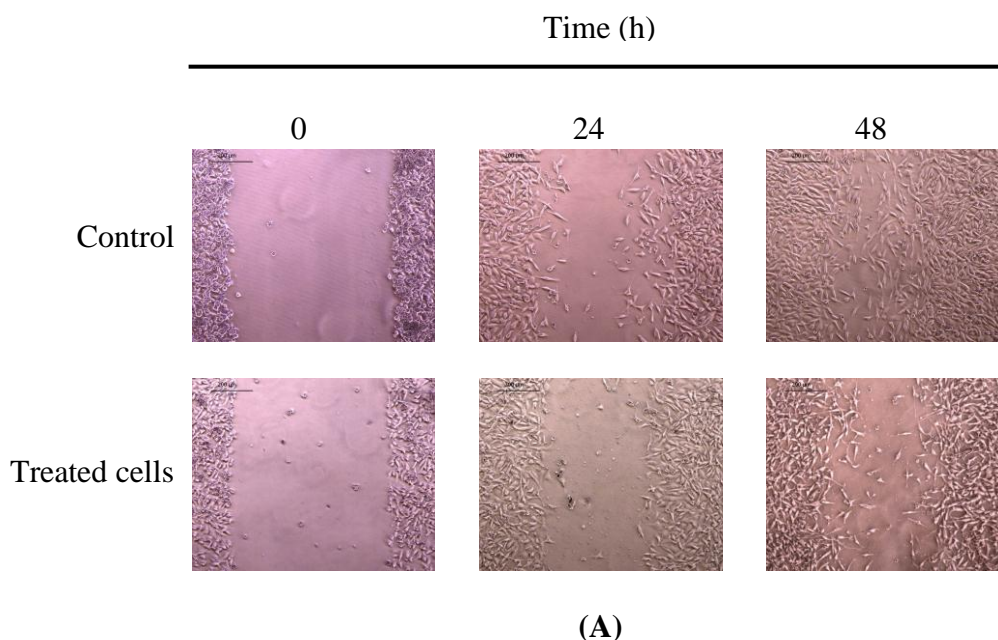
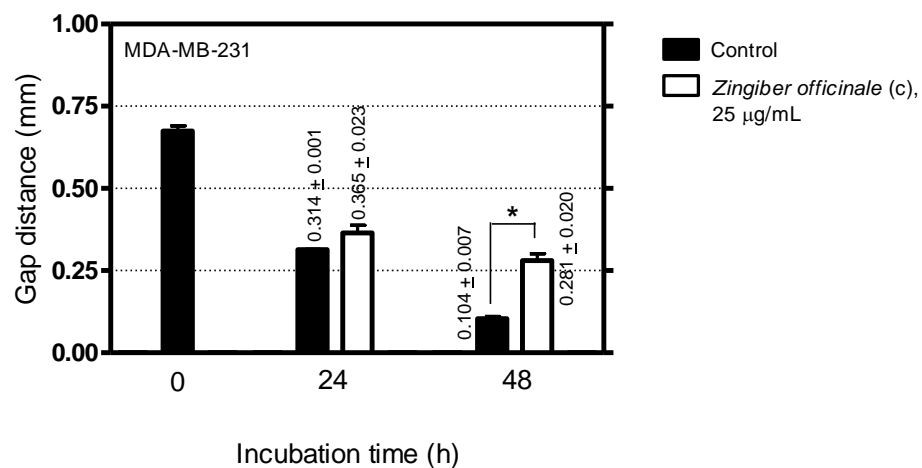


Figure 4.59: Effects of crude petroleum ether extract of *Zingiber officinale* at 25 µg/mL on migration in MDA-MB-231 cells. After wounding, the cells treated with vehicle alone (Control) and petroleum ether extract of *Zingiber officinale* at 25 µg/mL were (A) photographed under a phase-contrast microscope (magnification, 50×) and (B) the migrating distances were measured and plotted at 0 h, 24 h, and 48 h. The sample was assayed in triplicates (N = 3), and statistically significant difference ($p < 0.05$) according to paired-sample t -test was indicated as * above each bar.

Effects of crude chloroform extract of *Z. officinale* (tested at 25 $\mu\text{g}/\text{mL}$) on the migration of MDA-MB-231 cells are shown in Figure 4.60. The untreated MDA-MB-231 cells (negative control) spread along the wound edges at 24 h (gap distance, 0.314 mm) and became highly colonised at 48 h (gap distance, 0.104 mm). In contrast, for MDA-MB-231 cells treated with the extracts spread along the wound edges were seen to be slower than that of the untreated cells [Figure 4.60 (A)], with gap distances 0.365 mm and 0.281 mm at 24 h and 48 h, respectively [Figure 4.60 (B)]. Statistical analysis using paired-sample *t*-test ($p < 0.05$) indicate significance differences between the gap distances of control and treated cells at 48 h [Figure 4.60 (B)]. This showed that chloroform extract of *Z. officinale* exhibited significant inhibitory effect on migration of MDA-MB-231 cells. It delayed the cell migration of MDA-MB-231 cells compared to that of the control cells in a time-dependent manner.





(B)

Figure 4.60: Effects of crude chloroform extract of *Zingiber officinale* at 25 µg/mL on migration in MDA-MB-231 cells. After wounding, the cells treated with vehicle alone (Control) and chloroform extract of *Zingiber officinale* at 25 µg/mL were (A) photographed under a phase-contrast microscope (magnification, 50×) and (B) the migrating distances were measured and plotted at 0 h, 24 h, and 48 h. The sample was assayed in triplicates (N = 3), and statistically significant difference ($p < 0.05$) according to paired-sample *t*-test was indicated as * above each bar.

Effects of crude methanol extract of *Z. officinale* (tested at 100 µg/mL) on the migration of MDA-MB-231 cells are shown in Figure 4.61. The untreated MDA-MB-231 cells (negative control) spread along the wound edges at 24 h (gap distance, 0.401 mm) and became highly colonised at 48 h (gap distance, 0.147 mm). In contrast, for MDA-MB-231 cells treated with the extracts spread along the wound edges were seen to be slower than that of the untreated cells [Figure 4.61 (A)], with gap distances 0.421 mm and 0.250 mm at 24 h and 48 h, respectively [Figure 4.61 (B)]. Statistical analysis using paired-sample *t*-test ($p < 0.05$) indicate significance differences between the gap distances of control and treated cells at 48 h [Figure 4.61 (B)]. This showed that methanol extract of *Z. officinale* exhibited significant inhibitory effect on migration of MDA-MB-231 cells. It delayed the cell

migration of MDA-MB-231 cells compared to that of the control cells in a time-dependent manner.

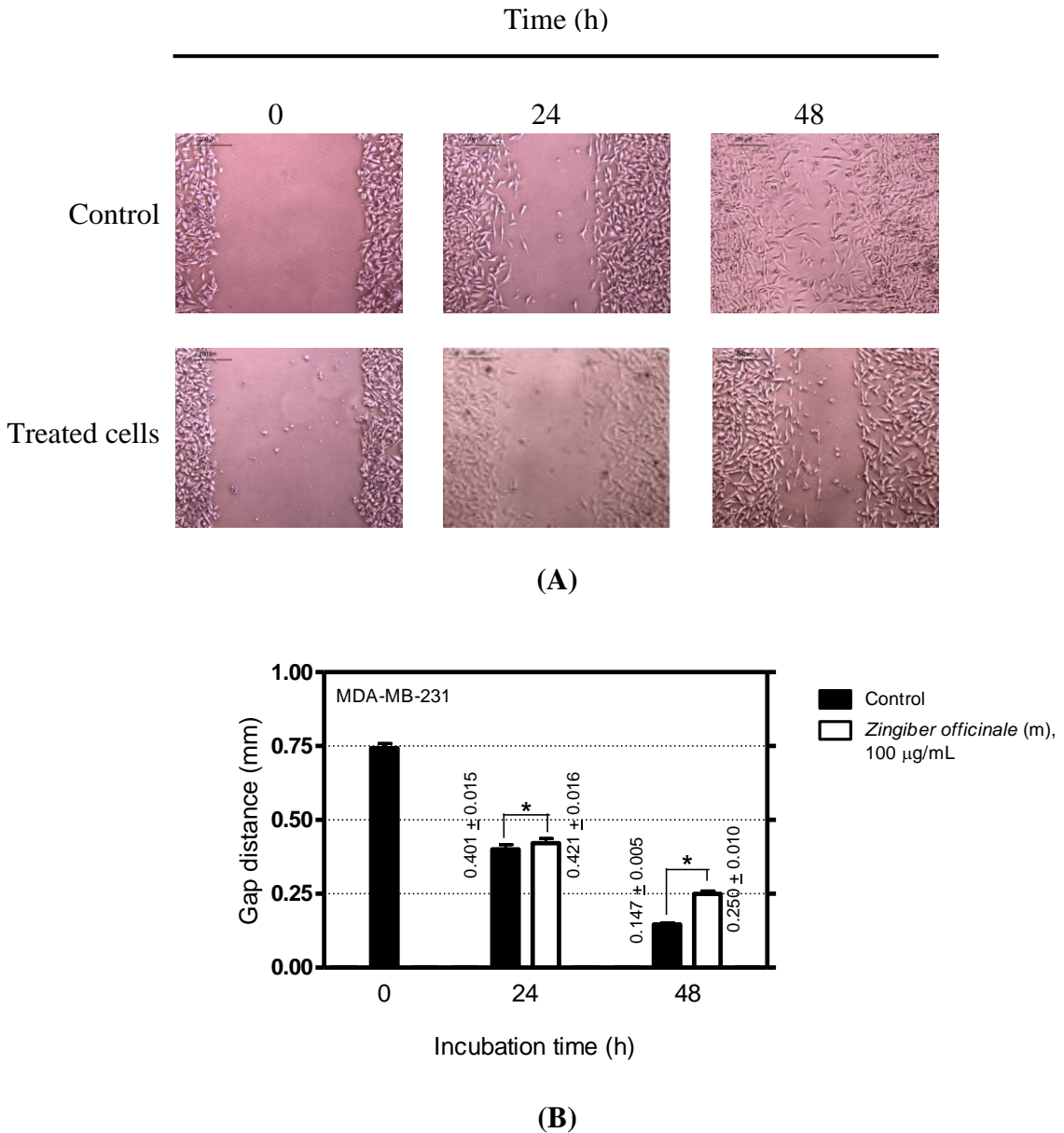
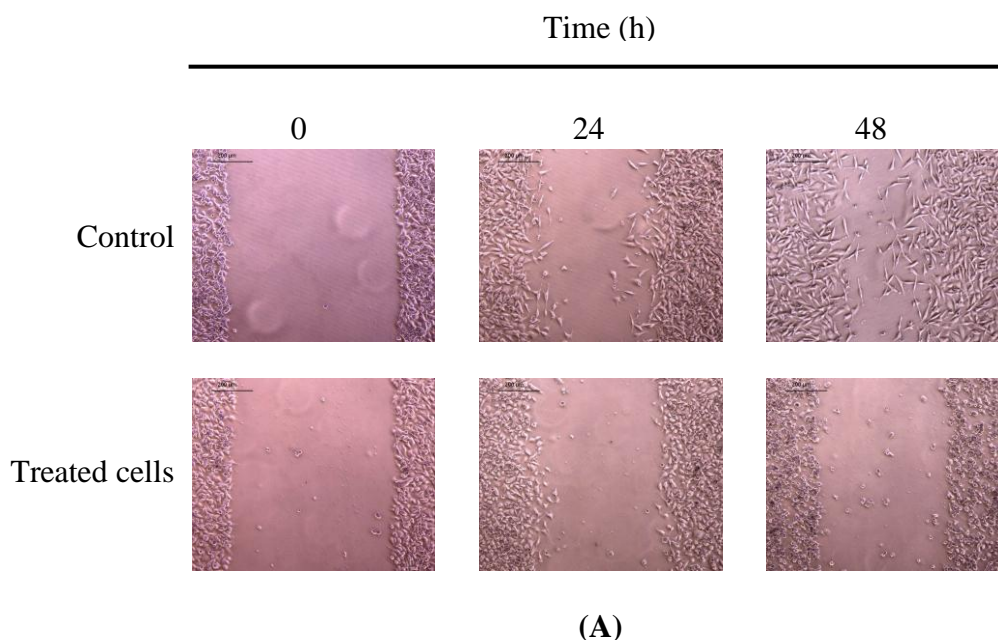
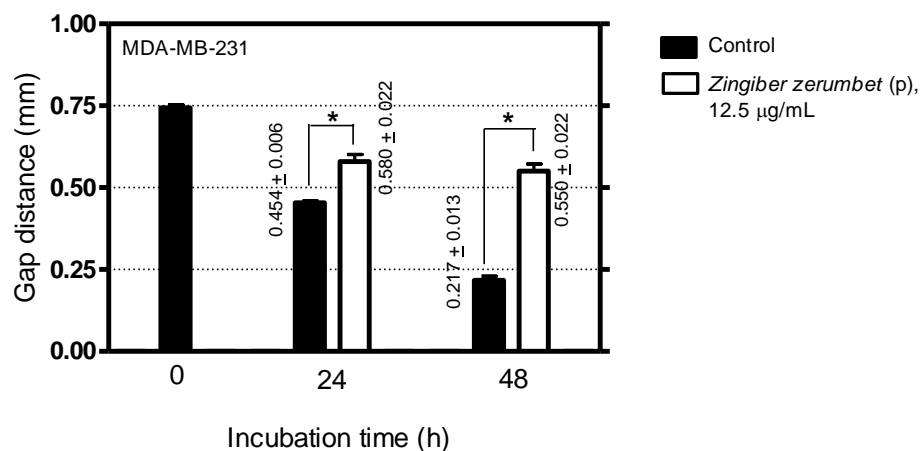


Figure 4.61: Effects of crude methanol extract of *Zingiber officinale* at 100 µg/mL on migration in MDA-MB-231 cells. After wounding, the cells treated with vehicle alone (Control) and methanol extract of *Zingiber officinale* at 100 µg/mL were (A) photographed under a phase-contrast microscope (magnification, 50×) and (B) the migrating distances were measured and plotted at 0 h, 24 h, and 48 h. The sample was assayed in triplicates (N = 3), and statistically significant difference ($p < 0.05$) according to paired-sample *t*-test was indicated as * above each bar.

Effects of crude petroleum ether extract of *Z. zerumbet* (tested at 12.5 µg/mL) on the migration of MDA-MB-231 cells are shown in Figure 4.62. The untreated MDA-MB-231 cells (negative control) spread along the wound edges at 24 h (gap distance, 0.454 mm) and became highly colonised at 48 h (gap distance, 0.217 mm). In contrast, for MDA-MB-231 cells treated with the extracts spread along the wound edges were seen to be slower than that of the untreated cells [Figure 4.62 (A)], with gap distances 0.580 mm and 0.550 mm at 24 h and 48 h, respectively [Figure 4.62 (B)]. Statistical analysis using paired-sample *t*-test ($p < 0.05$) indicate significance differences between the gap distances of control and treated cells at 48 h [Figure 4.62 (B)]. This showed that petroleum ether extract of *Z. zerumbet* exhibited significant inhibitory effect on migration of MDA-MB-231 cells. It delayed the cell migration of MDA-MB-231 cells compared to that of the control cells in a time-dependent manner.





(B)

Figure 4.62: Effects of crude petroleum ether extract of *Zingiber zerumbet* at 12.5 µg/mL on migration in MDA-MB-231 cells. After wounding, the cells treated with vehicle alone (Control) and petroleum ether extract of *Zingiber zerumbet* at 12.5 µg/mL were (A) photographed under a phase-contrast microscope (magnification, 50×) and (B) the migrating distances were measured and plotted at 0 h, 24 h, and 48 h. The sample was assayed in triplicates (N = 3), and statistically significant difference ($p < 0.05$) according to paired-sample *t*-test was indicated as * above each bar.

Effects of crude chloroform extract of *Z. zerumbet* (tested at 25 µg/mL) on the migration of MDA-MB-231 cells are shown in Figure 4.63. The untreated MDA-MB-231 cells (negative control) spread along the wound edges at 24 h (gap distance, 0.314 mm) and became highly colonised at 48 h (gap distance, 0.104 mm). In contrast, for MDA-MB-231 cells treated with the extracts spread along the wound edges were seen to be slower than that of the untreated cells [Figure 4.63 (A)], with gap distances 0.470 mm and 0.412 mm at 24 h and 48 h, respectively [Figure 4.63 (B)]. Statistical analysis using paired-sample *t*-test ($p < 0.05$) indicate significance differences between the gap distances of control and treated cells at 48 h [Figure 4.63 (B)]. This showed that chloroform extract of *Z. zerumbet* exhibited significant inhibitory effect on migration of MDA-MB-231 cells. It delayed the

cell migration of MDA-MB-231 cells compared to that of the control cells in a time-dependent manner.

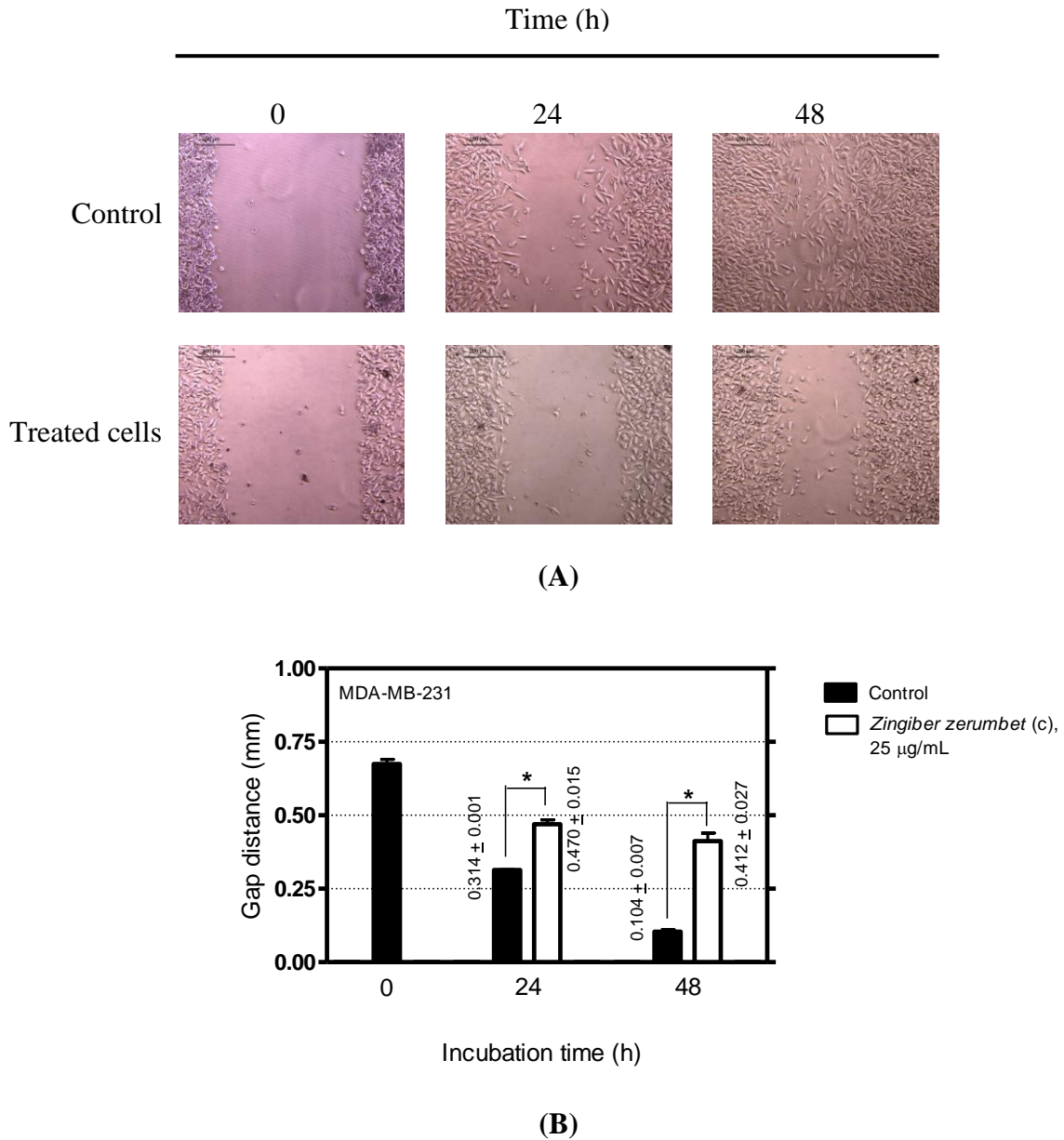
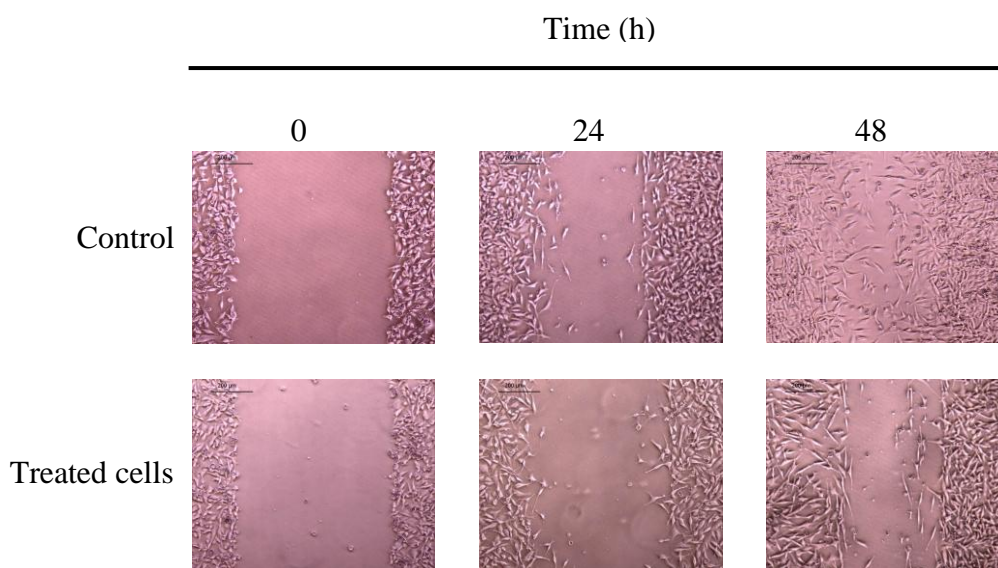
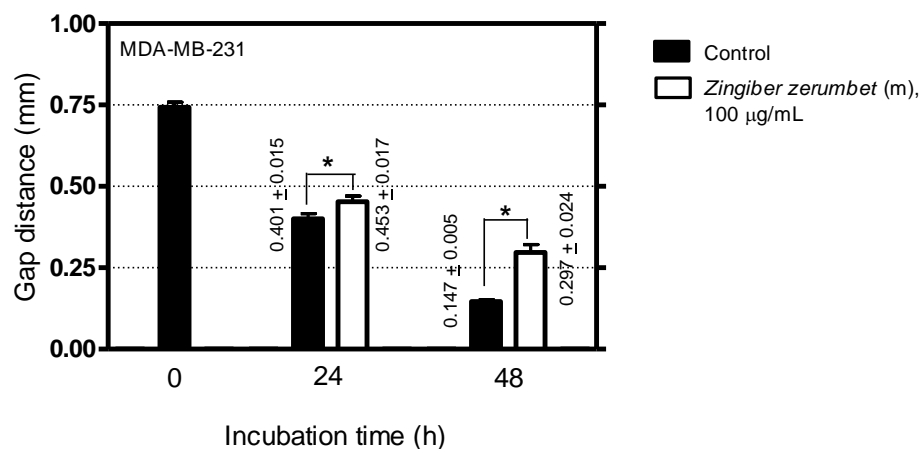


Figure 4.63: Effects of crude chloroform extract of *Zingiber zerumbet* at 25 µg/mL on migration in MDA-MB-231 cells. After wounding, the cells treated with vehicle alone (Control) and chloroform extract of *Zingiber zerumbet* at 25 µg/mL were (A) photographed under a phase-contrast microscope (magnification, 50×) and (B) the migrating distances were measured and plotted at 0 h, 24 h, and 48 h. The sample was assayed in triplicates (N = 3), and statistically significant difference ($p < 0.05$) according to paired-sample t -test was indicated as * above each bar.

Effects of crude methanol extract of *Z. zerumbet* (tested at 100 µg/mL) on the migration of MDA-MB-231 cells are shown in Figure 4.64. The untreated MDA-MB-231 cells (negative control) spread along the wound edges at 24 h (gap distance, 0.401 mm) and became highly colonised at 48 h (gap distance, 0.147 mm). In contrast, for MDA-MB-231 cells treated with the extracts spread along the wound edges were seen to be slower than that of the untreated cells [Figure 4.64 (A)], with gap distances 0.453 mm and 0.297 mm at 24 h and 48 h, respectively [Figure 4.64 (B)]. Statistical analysis using paired-sample *t*-test ($p < 0.05$) indicate significance differences between the gap distances of control and treated cells at 48 h [Figure 4.64 (B)]. This showed that methanol extract of *Z. zerumbet* exhibited significant inhibitory effect on migration of MDA-MB-231 cells. It delayed the cell migration of MDA-MB-231 cells compared to that of the control cells in a time-dependent manner.



(A)



(B)

Figure 4.64: Effects of crude methanol extract of *Zingiber zerumbet* at 100 µg/mL on migration in MDA-MB-231 cells. After wounding, the cells treated with vehicle alone (Control) and methanol extract of *Zingiber zerumbet* at 100 µg/mL were (A) photographed under a phase-contrast microscope (magnification, 50×) and (B) the migrating distances were measured and plotted at 0 h, 24 h, and 48 h. The sample was assayed in triplicates (N = 3), and statistically significant difference ($p < 0.05$) according to paired-sample *t*-test was indicated as * above each bar.

[6]-Gingerol (1,[4'-hydroxy-3'-methoxyphenyl]-5-hydroxy]-3-decanone) is one of the major pungent elements of ginger (*Z. officinale*), has been found to exhibit anti-metastatic activity of MDA-MB-231 human breast cancer cells (Lee, Seo, Kang, & Kim, 2008). Therefore, it was used as the positive control in this assay. The results in Figure 4.65 demonstrated that 12.5 µg/mL of [6]-Gingerol exhibited significant inhibitory effect on migration of MDA-MB-231 cells at 48 h [Figure 4.65 (B)]. It delayed the cell migration of MDA-MB-231 cells compared to that of the control cells in a time-dependent manner [Figure 4.65 (A)].

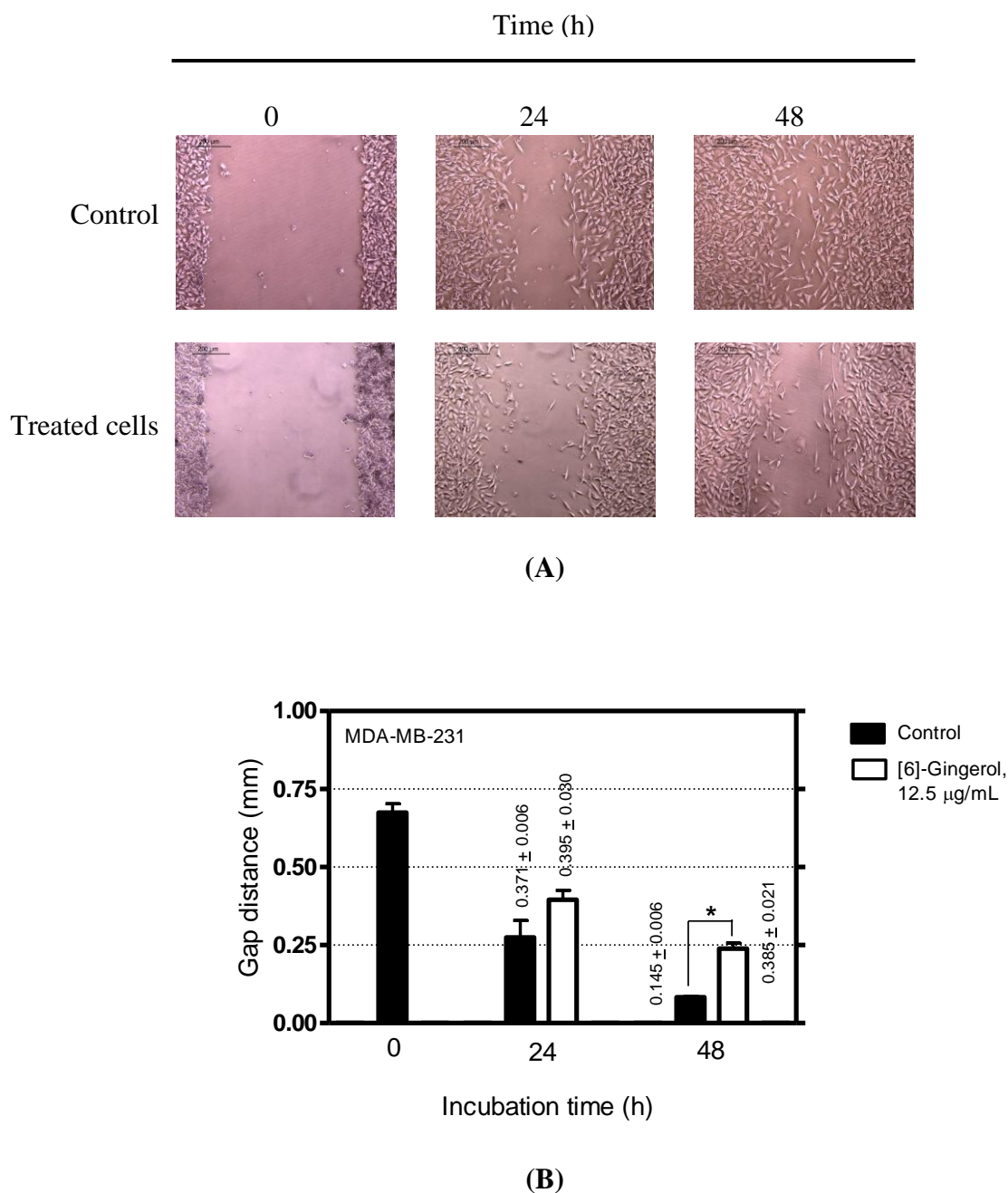


Figure 4.65: Effects of [6]-Gingerol at 12.5 µg/mL on migration in MDA-MB-231 cells. After wounding, the cells treated with vehicle alone (Control) and [6]-Gingerol at 100 µg/mL were (A) photographed under a phase-contrast microscope (magnification, 50×) and (B) the migrating distances were measured and plotted at 0 h, 24 h, and 48 h. The sample was assayed in triplicates (N = 3), and statistically significant difference ($p < 0.05$) according to paired-sample t -test was indicated as * above each bar.

4.4.1 Comparisons of the Zingiberaceae extracts on inhibitory effects of cell migration activity of MDA-MB-231 cells

Absolute migration capability (MC_A) was used as the parameter for evaluating migration capability of breast cancer cell line (MDA-MB-231) after treated with crude *Zingiberaceae* extracts *in vitro*. MC_A value for untreated cells (negative control) was 6.03×10^{-3} mm/h at 48 h of incubation time, which represented the migration capability of MDA-MB-231 cells in normal conditions. Untreated cells were able to invade the scratched area that is fully re-colonised at 48 h later.

In the Scratch wound assay, the largest gaps observed after treated with the extracts reveal the most effective agent in anti-migration. The MDA-MB-231 cells treated with *Zingiberaceae* extracts spreading along the wound edges would have become slower than that of cells with vehicle alone. In comparison with the MC_A values (Table 4.6), all of the tested *Zingiberaceae* extracts except crude methanol extract of *C. aeruginosa* (tested at 100 $\mu\text{g/mL}$) did inhibit or slow down the migration activity of MDA-MB-231 cells. However, the overall results revealed that Zingiberaceae plants are good candidate for anti-migration activities.

Based on the results in Table 4.6, petroleum ether and chloroform extracts of *A. galanga* (tested at 12.5 $\mu\text{g/mL}$) inhibited migration of MDA-MB-231 cells effectively, with MC_A values -5.73×10^{-3} mm/h and -8.02×10^{-3} mm/h at 48 h of incubation time, respectively. The smaller the value of MC_A manifests the lower migration capability. Negative MC_A values represented no migration activity could be observed. Besides these extracts, several extracts showed effective anti-migration activities as well, which were chloroform extract of *C. domestica* (tested at 12.5 $\mu\text{g/mL}$), and petroleum ether extract of *Z.*

zerumbet (tested at 12.5 µg/mL), with MC_A values 1.35×10^{-4} mm/h and 1.63×10^{-3} mm/h at 48 h of incubation time.

It was interesting that most of methanol extracts of *Zingiberaceae* which did not inhibit cell proliferations of MDA-MB-231 at 100 µg/mL, did slow down the cell migration at 48 h time point. These extracts are methanol extracts of *A. galanga* (MC_A , 5.78×10^{-3} mm/h), *C. mangga* (MC_A , 5.72×10^{-3} mm/h), *Z. montanum* MC_A , 4.43×10^{-3} mm/h), *Z. officinale* (MC_A , 4.81×10^{-3} mm/h) , and *Z. zerumbet* (MC_A , 4.45×10^{-3} mm/h). The only inactive extract in anti-migration activity was methanol extract of *C. aeruginosa* at 100 µg/mL. The MC_A values for the cells treated with it was 8.13×10^{-3} mm/h at 24 h and 7.04×10^{-3} mm/h at 48 h, which were obviously greater than the MC_A values of untreated cells (MC_A , 7.35×10^{-3} mm/h at 24 h; MC_A 6.03×10^{-3} mm/h at 48 h).

In the comparisons of MC_A values between 24 h and 48 h of incubation time, several extracts showed anti-migration activity only at 48 h of incubation time. These extracts were methanol extract of *A. galanga* (tested at 100 µg/mL), petroleum ether extract of *C. xanthorrhiza* (tested at 25 µg/mL), and methanol extract of *K. galanga* (tested at 25 µg/mL). MC_A values for methanol extract of *A. galanga* at 24 h incubation time was 7.63×10^{-3} mm/h, but decreased to 5.78×10^{-3} mm/h at 48 h later. MC_A values for petroleum ether extract of *C. xanthorrhiza* at 24 h incubation time was 7.65×10^{-3} mm/h, but decreased to 5.83×10^{-3} mm/h at 48 h later. MC_A values for methanol extract of *K. galanga* at 24 h incubation time was 7.60×10^{-3} mm/h, but decreased to 5.68×10^{-3} mm/h at 48 h later. Based on the scenarios, Scratch wound assay is much better to be performed at 48 h time point rather than just 24 h, which could better elaborate the anti-migration activities of each crude *Zingiberaceae* extracts.

Table 4.6: Absolute migration capability of *Zingiberaceae* extracts determined by Scratch wound assay using MDA-MB-231 cells

Zingiberaceae species	Solvent ¹	Concentration (µg/mL)	Absolute migration capability, MC _A (mm/h)	
			MDA-MB-231 cell line, incubation status	
			24 h	48 h
Control	-	0	7.35×10^{-3}	6.03×10^{-3}
<i>Alpinia galanga</i>	p	12.5	-8.75×10^{-4}	-5.73×10^{-4}
	c	12.5	-8.75×10^{-4}	-8.02×10^{-4}
	m	100	7.63×10^{-3}	5.78×10^{-3}
<i>Boesenbergia rotunda</i>	p	12.5	5.21×10^{-3}	2.98×10^{-3}
	c	12.5	4.29×10^{-3}	2.53×10^{-3}
	m	25	5.90×10^{-3}	4.54×10^{-3}
<i>Curcuma aeruginosa</i>	p	25	3.21×10^{-3}	1.93×10^{-3}
	c	50	1.31×10^{-3}	1.06×10^{-3}
	m	100	8.13×10^{-3}	7.04×10^{-3}
<i>Curcuma domestica</i>	p	12.5	4.96×10^{-3}	4.45×10^{-3}
	c	12.5	5.63×10^{-4}	1.35×10^{-4}
	m	12.5	3.27×10^{-3}	2.85×10^{-3}
<i>Curcuma mangga</i>	p	100	1.38×10^{-3}	1.17×10^{-3}
	c	25	1.90×10^{-3}	1.34×10^{-3}
	m	100	7.33×10^{-3}	5.72×10^{-3}
<i>Curcuma xanthorrhiza</i>	p	25	7.65×10^{-3}	5.83×10^{-3}
	c	12.5	4.94×10^{-3}	4.34×10^{-3}
	m	50	6.58×10^{-3}	5.42×10^{-3}
<i>Kaempferia galanga</i>	p	100	4.38×10^{-3}	2.71×10^{-3}
	c	25	4.73×10^{-3}	3.80×10^{-3}
	m	25	7.60×10^{-3}	5.68×10^{-3}
<i>Zingiber montanum</i>	p	25	3.65×10^{-3}	3.25×10^{-3}
	c	25	4.50×10^{-3}	3.90×10^{-3}
	m	100	6.08×10^{-3}	4.43×10^{-3}
<i>Zingiber officinale</i>	p	25	3.44×10^{-3}	2.69×10^{-3}
	c	25	5.96×10^{-3}	3.85×10^{-3}
	m	100	6.06×10^{-3}	4.81×10^{-3}
<i>Zingiber zerumbet</i>	p	12.5	2.63×10^{-3}	1.63×10^{-3}
	c	25	3.88×10^{-3}	2.54×10^{-3}
	m	100	5.65×10^{-3}	4.45×10^{-3}
[6]-Gingerol	-	12.5	5.38×10^{-3}	4.32×10^{-3}

¹ Solvents used in extraction: p: petroleum ether, c: chloroform, m: methanol; (-) not tested.

4.5 Qualitative Analysis Using Thin-layer Chromatography

Three most potential *Zingiberaceae* tested based on the screening tests were crude chloroform extract of *A. galanga*, crude chloroform extract of *C. domestica*, and crude petroleum ether extract of *Z. zerumbet*. Petroleum ether extract of *Z. zerumbet* showed the strongest NO inhibitory activity in activated macrophages, RAW 264.7, whereas chloroform extracts of *A. galanga* and *C. domestica* showed the potent effects in anti-proliferation and anti-migration activities against human breast cancer cells, MDA-MB-231. More importantly, these extracts possess SX values distinctly greater than 100 (Table 4.4), which indicated their promising properties for further studies in the development of anti-cancer drugs.

The extracts were subjected for qualitative analysis using TLC to determine a large extent of nature substances or chemical groups present in the crude extracts. Types of compounds detected from the TLC tests for crude chloroform extract of *A. galanga*, crude chloroform extract of *C. domestica*, and crude petroleum ether extract of *Z. zerumbet* were presented in Table 4.7, Table 4.8 and Table 4.9, respectively. These are known as the results of preliminary chemical tests.

Based on Table 4.7, 15 compounds were detected in the crude chloroform extract of *A. galanga*. Nine (60%) of the compounds containing conjugated double bonds, or double bond. Twelve compounds were detected in the crude chloroform extract of *C. domestica* (Table 4.8). It was interesting to observed that C₆ (R_f = 0.66) showed positive results for all of the detection methods applied. Eleven (92%) of the compounds containing conjugated double bonds and eight (67%) were organic compounds. For crude petroleum ether extract of *Z. zerumbet*, 15 compounds were detected (Table 4.9). Seven (47%) of the compounds were from the group of secondary compound, terpenoids.

Table 4.7: Qualitative analysis of crude chloroform extract of *Alpinia galanga* using thin-layer chromatography

Labeled compound ¹	R _f ²	Daylight	UV light at 254 nm	UV light at 365 nm	Iodine vapour	50% H ₂ SO ₄	Dragendorff's reagent	Vanillin/H ₂ SO ₄ reagent	Types of compounds detected
A ₁	0.05	-	-	-	brown	-	-	-	Compounds with double bonds
A ₂	0.15	-	red	green	brown	-	-	purple	Compounds containing conjugated double bonds; fluorescent compounds; and terpenoids
A ₃	0.18	-	-	-	brown	-	-	-	Compounds with double bonds
A ₄	0.26	-	red	-	brown	-	-	-	Compounds with conjugated double bonds; and compounds with double bonds
A ₅	0.35	-	red	-	-	-	-	-	Compounds containing conjugated double bonds
A ₆	0.56	-	-	yellow	-	-	-	-	Fluorescent compounds
A ₇	0.63	-	-	-	-	black	-	purple	Organic compounds; and terpenoids
A ₈	0.65	-	red	green	brown	-	-	-	Compounds containing conjugated double bonds; fluorescent compounds; and compounds with double bonds.
A ₉	0.71	-	red	-	-	-	-	-	Compounds containing conjugated double bonds
A ₁₀	0.75	-	-	-	-	-	-	yellow	Phenols
A ₁₁	0.79	-	red	-	brown	yellow	-	-	Compounds containing conjugated double bonds; compounds with double bonds; and organic compounds
A ₁₂	0.83	-	red	-	brown	black	-	-	Compounds containing conjugated double bonds; compounds with double bonds; and organic compounds
A ₁₃	0.85	red	-	blue	brown	-	-	-	Coloured substances; fluorescent compounds; and compounds with double bonds
A ₁₄	0.89	yellow	red	-	-	-	-	-	Coloured substances; compounds with conjugated double bonds
A ₁₅	0.96	-	blue	-	brown	-	-	-	Compounds with conjugated double bonds; and compounds with double bond

¹Resolved compounds of crude chloroform extract of *Alpinia galanga* observed as bands on the stationary phase using several detection methods/spray reagents.

²R_f: Retardation factor calculated by Eq. (6).

Table 4.8: Qualitative analysis of crude chloroform extract of *Curcuma domestica* using thin-layer chromatography

Labeled compound ¹	R _f ²	Daylight	UV light at 254 nm	UV light at 365 nm	Iodine vapour	50% H ₂ SO ₄	Dragendorff's reagent	Vanillin/H ₂ SO ₄ reagent	Types of compounds detected
C ₁	0.09	-	red	-	-	brown	orange	-	Compounds containing conjugated double bonds; organic compounds; and alkaloids
C ₂	0.15	-	red	-	-	brown	-	-	Compounds containing conjugated double bonds; and organic compounds
C ₃	0.25	-	red	-	-	brown	-	-	Compounds containing conjugated double bonds; and organic compounds
C ₄	0.33	-	red	-	-	brown	-	yellow	Compounds containing conjugated double bonds; organic compounds; and phenols
C ₅	0.49	-	red	-	-	black	-	purple	Compounds containing conjugated double bonds; organic compounds; and terpenoids
C ₆	0.66	yellow	yellow	yellow	brown	black	orange	red	Coloured substances; compounds containing conjugated double bonds; fluorescent compounds; compounds with double bonds; organic compounds; alkaloids; and phenols
C ₇	0.74	-	red	-	-	brown	-	-	Compounds containing conjugated double bonds; and organic compounds
C ₈	0.80	-	red	-	-	brown	-	-	Compounds containing conjugated double bonds; and organic compounds
C ₉	0.84	-	red	-	-	-	-	purple	Compounds containing conjugated double bonds; and terpenoids
C ₁₀	0.88	-	red	-	-	-	-	-	Compounds containing conjugated double bonds
C ₁₁	0.90	-	-	blue	-	-	-	-	Fluorescent compounds
C ₁₂	0.95	-	red	-	brown	-	-	red	Compounds containing conjugated double bonds; compounds with double bonds; and phenols

¹Resolved compounds of crude chloroform extract of *Curcuma domestica* observed as bands on the stationary phase using several detection methods/spray reagents.

²R_f: Retardation factor calculated by Eq. (6).

Table 4.9: Qualitative analysis of crude petroleum ether extract of *Zingiber zerumbet* using thin-layer chromatography

Labeled compound ¹	R _f ²	Daylight	UV light at 254 nm	UV light at 365 nm	Iodine vapour	50% H ₂ SO ₄	Dragendorff's reagent	Vanillin/H ₂ SO ₄ reagent	Types of compounds detected
Z ₁	0.08	-	red	yellow	-	-	-	-	Compounds containing conjugated double bonds; and fluorescent compounds
Z ₂	0.13	-	-	-	brown	brown	-	purple	Compounds with double bonds; oorganic compounds; and terpenoids
Z ₃	0.16	yellow	-	-	-	-	-	purple	Coloured substances; and terpenoids
Z ₄	0.20	-	red	yellow	-	-	-	-	Compounds containing conjugated double bonds; and fluorescent compounds
Z ₅	0.23	-	-	blue	-	-	-	-	Fluorescent compounds
Z ₆	0.38	-	-	-	brown	-	-	purple	Compounds with double bonds; and terpenoids
Z ₇	0.59	-	-	-	-	brown	-	purple	Organic compounds; and terpenoids
Z ₈	0.61	-	-	-	brown	brown	-	purple	Compounds with double bonds; organic compounds; and terpenoids
Z ₉	0.63	-	red	-	-	-	-	-	Compounds containing conjugated double bonds
Z ₁₀	0.64	yellow	-	-	brown	-	-	-	Coloured substances; and compounds with double bonds
Z ₁₁	0.68	-	red	-	-	-	-	purple	Compounds containing conjugated double bonds; and terpenoids
Z ₁₂	0.71	-	red	-	-	-	-	-	Compounds containing conjugated double bonds
Z ₁₃	0.75	-	-	yellow	brown	-	-	-	Fluorescent compounds; and compounds with double bond
Z ₁₄	0.90	-	-	blue	brown	-	-	purple	Fluorescent compounds; compound with double bonds; and terpenoids
Z ₁₅	0.98	-	-	yellow	-	-	-	-	Fluorescent compounds

¹Resolved compounds of crude petroleum ether extract of *Zingiber zerumbet* observed as bands on the stationary phase using several detection methods/spray reagents.

²R_f: Retardation factor calculated by Eq. (6).

CHAPTER 5

5.0 Discussion

5.1 Extraction of the Selected Zingiberaceae Species

Solvent extraction is the most popular method of extract preparation from natural products. The solvents have the potential in extracting different classes of chemical compounds based on their polarity properties. Since there was no preconception about the chemical nature of the active compounds that were being sought, Soxhlet extraction was carried out in order to extract the *Zingiberaceae* rhizomes of *A. galanga*, *B. rotunda*, *C. aeruginosa*, *C. domestica*, *C. mangga*, *C. xanthorrhiza*, *K. galanga*, *Z. montanum*, *Z. officinale*, and *Z. zerumbet* exhaustively with a range of solvent of increasing polarity, namely petroleum ether, chloroform and methanol.

Petroleum ether is a solvent with low polarity, commonly used in extracting chemical classes of compounds, such as waxes, fats, fixed oils or volatile oils. Chloroform is commonly used to extract chemical classes of alkaloids, aglycones and volatile oils. Higher polarity solvent, such as methanol is specifically used to extract sugar, amino acids and glycosides (Houghton & Raman, 1998). Three crude extracts were generated from each *Zingiberaceae* species, and a total of 30 extracts from ten selected *Zingiberaceae* species were obtained for the screening programmes.

Conventional soxhlet extraction is a very simple methodology that is easily applicable and requires only little training. It was used in preparing crude extracts of ten selected *Zingiberaceae* rhizomes in this research. The petroleum ether, chloroform and methanol solvents in the distillation flask were heated at their boiling temperature at 45°C, 62°C and 65°C, respectively. The vapour formed passed through the side-arm and up into the sample compartment, where the vapour liquefied due to the cooling effect from the

reflux condenser. The liquid dripped into the thimble and the extracts collected in the sample compartment unloaded back to the distillation flask once it reached the top of the siphon. The process was repeated and the extracts collected in the distillation flask, gradually became more and more concentrated. The extraction for each sample with a particular solvent took an average of three days to complete. A relatively small volume of fresh solvent was needed since the solvent was being recycled, but the volume used should effectively be proportional to the time for which the process was allowed to continue (Houghton & Raman, 1998).

Conventional Soxhlet extraction has several advantages that result in it being one of the most efficient leaching techniques to date (Luque de Castro & Priego-Capote, 2009). One of its most outstanding advantages is that the sample is repeatedly being exposed to the recyclable fresh portion of the extracting solvent which facilitates the displacement of the transfer equilibrium (Luque de Castro & García-Ayuso, 1998; Luque de Castro & Priego-Capote, 2009). Based on its continuous-discrete characteristic of operation, it is useful for achieving exhaustive extraction of plant material with a particular solvent, where 100% yield of particular component is desired. It is also an efficient way of performing exhaustive extraction when using a series of solvents with increasing polarity, such as petroleum ether, hexane, chloroform, methanol, and water (Houghton & Raman, 1998).

Besides that, a relatively high temperature is maintained in this Soxhlet extractor system where heat is applied directly to the distillation flask and reaches the extraction cavity to some extent (Luque de Castro & García-Ayuso, 1998; Luque de Castro & Priego-Capote, 2009). In addition, extract collected in the bulk liquid form can be subjected directly to rotary evaporation without filtration after the leaching step. Moreover, it can extract more sample mass compared to the latest alternatives, such as microwave-assisted

extraction and supercritical fluid extraction (Luque de Castro & Priego-Capote, 2009). A relatively small volume of fresh solvent is required as the solvent is being recycled throughout the operation. Since the basic apparatus of Soxhlet extractor is inexpensive, the sample throughput can be increased by simultaneous extraction in parallel (Luque de Castro & García-Ayuso, 1998).

Although conventional Soxhlet extraction is a simple technique, several precautionary steps were carried out in order to obtain optimize yield. Separate items of glassware for the Soxhlet extractor were cleaned and dried before operating the extraction in order to discard any unnecessary volatile substances which would probably pollute the purity of the solvent. Besides that, it was necessary to dry the thimble with plant sample properly in between the changes of solvent to prevent carry-over of traces of the previous solvent into the next one. Large scale operation is not suitable to be carried out if using solvents with high boiling points, such as methanol and water, since the whole apparatus below the reflux condenser need to be at this high temperature for effective movement of the solvent vapour (Houghton & Raman, 1998). This may further increase the risk of thermal decomposition. Thus, small scale conventional Soxhlet extraction was carried out in this research as it was more efficient even though it was comparably more time-consuming than the large scale operation.

5.2 Effects of the Zingiberaceae Extracts on Nitric Oxide Inhibitory Activity

Enhancement of macrophage responses without stimulating inflammatory activity could be beneficial not only in normal tissue homeostasis, such as clearing dead cells or cell debris, but also in aiding in recovery from certain inflammatory diseases (Savill & Fadok, 2000). Petroleum ether, chloroform, and methanol extracts from ten selected *Zingiberaceae*

species such as *A. galanga*, *B. rotunda*, *C. aeruginosa*, *C. domestica*, *C. mangga*, *C. xanthorrhiza*, *K. galanga*, *Z. montanum*, *Z. officinale*, and *Z. zerumbet* were evaluated for their *in vitro* NO inhibitory activities in LPS-stimulated murine macrophage cells, RAW 2647.

The data presented in this study indicated that 29 out of 30 tested crude *Zingiberaceae* extracts (except methanol extract of *Z. zerumbet*) were shown to have exerted negative a significant immunomodulatory effects on various LPS-mediated immune responses. Among them, is crude petroleum ether extract of *Z. zerumbet* which exerted the strongest NO inhibitory activity (IR > 75% at 1.56 µg/mL) in LPS-activated RAW 264.7 cells.

These extracts showed significant inhibition of NO production in LPS-stimulated macrophage cells. This phenomenon is quite similar to the exposure of macrophages to apoptotic cells. Based on the previous reports, the presence of apoptosis cells induce phagocytosis but suppress inflammatory responses (Fadok *et al.*, 1998; Voll *et al.*, 1997), in order to reduce the tissues damage due to inappropriate inflammation or autoimmune responses during the clearance of the apoptotic cells (Savill & Fadok, 2000).

Nitric oxide is a cytotoxic and inflammatory molecule which can interact with oxygen and superoxide to form RNS can result in DNA damages, mutations and eventually leading to carcinogenesis (Ippoushi *et al.*, 2003). Excessive NO production by cells is known to be regulated by a number of cytokines. Cytokine, such as interferon- γ (IFN- γ) can exert direct NO-stimulatory function on it own (Liew *et al.*, 1991; Sakurai *et al.*, 1996; Stuehr & Marletta, 1987; Werner-Felmayer *et al.*, 1990), while other cytokines usually provide an additional signal for the activation of NO by IFN- γ (Kmoníčková *et al.*, 2007). The levels of NO and cytokines are interdependent, as high level of NO inhibits the

secretion of IFN- γ , while low NO concentrations stimulates its secretion (Niedbala, Wei, Piedrafita, Xu, & Liew, 1999).

iNOS plays crucial roles in the sustainable production of NO in macrophage cells (Min *et al.*, 2009). High amount of NO generation due to up-regulation of iNOS is associated with enhanced secretion of cytokines, such as TNF- α , IL-10 and IL-1. Nuclear factor (NF)- κ B is known to be the major transcription factor to regulate iNOS gene expression (Konkimalla *et al.*, 2010). In un-stimulated cells, NF- κ B subunits (p65 and/or p50) form a complex with inhibitory factor I κ B- α which remained inactive in the cytosol. Upon stimulation of pro-inflammatory signals such as LPS, I κ B- α is phosphorylated by I κ B- β kinase (IKK) and become inactive through ubiquitin-mediated degradation. Then, the released NF- κ B subunits are translocated into the nucleus and acts as transcription factor in the LPS-induced iNOS expression in macrophage cells (Guha & Mackman, 2001).

Two prominent pathways of iNOS inhibitory activity include suppression of iNOS gene expression, and direct inhibition of iNOS enzyme activity (Kim *et al.*, 1998). Several phytochemicals with NO inhibitory activity have been shown to suppress the induction and translocation of NF- κ B from the cytoplasm to nucleus (Ko *et al.*, 2005). Since iNOS-induced NO generation is implicated with the conversion of L-arginine to L-citrulline, several L-arginine analogs have been reported to be iNOS inhibitors, i.e. N^G-nitro-L-arginine methyl ester (L-NAME), N-iminoethyl-L-ornithine (L-NIO), and N^G-nitro-L-arginine (L-NNA) (Kim *et al.*, 1998). In this study, L-NAME was used as the positive control, which inhibit NO generation in activated murine macrophages as a results of iNOS inhibition. The inhibitory effects of NO in LPS-stimulated RAW 264.7 cells were believed to accompany blockage of certain cytokine secretions, particularly TNF- α , as well as the suppression of

NF- κ B and iNOS activities. However, the NO-related signaling pathway should further investigated in order to get a better view of the mechanisms.

Regulations of NO production and/or iNOS activity are therefore, important avenues for cancer therapy and prevention. It is clear that the *in vitro* screening on NO inhibition activity by the selected crude *Zingiberaceae* extracts may effectively modulate the function of activated-macrophage by inhibiting NO production. NO acts as a marker of cytokine-stimulatory effects of agents and behave the bidirectional character of NO and cytokines interdependency (Kmoníčková *et al.*, 2007). Nonetheless, NO inhibitory effects on the functional activation of macrophages, by inflammatory stimuli, have demonstrated that the selected *Zingiberaceae* species as promising anti-inflammatory medicinal plant, which are capable of treating macrophage-mediated acute or chronic diseases, such as septic shock and rheumatoid arthritis.

Reports on NO inhibition in LPS-activated macrophage cells have been reported on *Hibiscus cannabinus*. *H. cannabinus* or commonly known as Kenaf from the Malvaceae family has been long used as folk medicine in India and Africa for the treatment of blood and throat disorders, bilious condition, fever and puerperium. Studies showed that ethanol extract of *H. cannabinus* fresh leaves dose-dependently inhibited NO generation and strongly suppress PGE₂ production and COX-II expression in LPS-activated macrophages, RAW 264.7 (Lee *et al.*, 2007). The suppression effects of *H. cannabinus* on pro-inflammatory mediators (NO and PGE₂) in LPS-activated macrophage cells resembled the effects of *Zingiberaceae* extracts in this study.

Various local vegetables in Malaysia (locally called 'ulam') such as *Melicope ptelefolia*, *Partulaca oleracea*, and *Persicaria tenella* have been reported to exhibit potent NO inhibitory activities on LPS-activated macrophage cells, RAW 264.7. Crude methanol

extracts of the leaves from *M. ptelefolia*, *P. oleracea*, and *P. tenella* exerted NO inhibitory activities in a concentrations-dependent manner (Abas, Lajis, Israf, Khozirah, & Kalsom, 2006). The suppression effects of these traditional vegetables on NO production in activated RAW 264.7 cells resembled the effects of *Zingiberaceae* extracts in this study.

Free radicals liberated from macrophage cells are important in inflammatory processes because they are implicated in the activation of NF- κ B, which induces the transcription of inflammatory cytokines and COX-2. Antioxidants have been shown to be able to block the activation of NF- κ B effectively through the stabilization of NF- κ B/I κ B- α complex (Abas *et al.*, 2006). *Zingiberaceae* species, *H. cannabinus*, *M. ptelefolia*, *P. oleracea*, and *P. tenella* contain constituents that can inhibit NO production in activated macrophages. All of these plants also exhibited radical-scavenging activities (Abas *et al.*, 2006; Gosslau & Chen, 2004; Lee *et al.*, 2007; Manson, 2003; Surh & Ferguson, 2003; Wei *et al.*, 2005). This study further suggests that local herbs might have beneficial chemopreventive effects in addition to providing potential new sources of natural antioxidants and NO production inhibitors.

Nitric oxide assay is regarded as an efficient, economical, and relatively reliable method in primary screening for intrinsic immunostimulatory activity of compounds through the point of view in cytokine secretion in human cell system. The presented study demonstrated that various crude extracts of local *Zingiberaceae* species exhibited NO inhibition activities on LPS-stimulated NO generation in RAW 264.7 cells. Overproduction of NO are carcinogenic and therefore, reduction of excessive NO generation using phytochemicals are a promising avenue for cancer prevention. The undisputable advantage of this screening platform is its sensitivity, general feasibility, low cost, and possibility of large scale performance.

5.3 Effects of the Zingiberaceae Extracts on MDA-MB-231 Cell Proliferation or Viability

Breast cancer is the second leading cause of cancer mortality affecting women in both developed and developing countries (Jemal *et al.*, 2007). Current treatments for the pathology include excision surgery, chemotherapy, radiotherapy, as well as frequently supported by adjuvant chemo- or hormone-therapies (Lin *et al.*, 2009; Tsai *et al.*, 2007). Majority of the cases that result in metastasis still relied on conventional therapeutic agents, however, the problem of drug resistance in breast cancer has been the major obstacle in chemotherapeutic treatment (Tannin-Spritz, Grossman, Dovrat, Gottfried, & Bergman, 2007). High incidence of mortality is also associated with poor prognosis for the metastatic disease, especially in hormone-independent cancer (Bange, Zwick, & Ullrich, 2001; Cuzick, Warwick, Pinney, Warren, & Duffy, 2004; Houssami, Cuzick, & Dixon, 2006; Roy, Baliga, & Katoyar, 2005). Based on this scenario, a highly metastatic oestrogen-independent human breast cancer cells, MDA-MB-231 was opted for this study. Uncontrollable proliferations are critical stage in both carcinogenesis and metastasis.

In carcinogenesis, there are several stages in the formation of cancer cells, which involves initiation, promotion, and progression stages. Uncontrollable cell proliferations occurred in the promotion stage that cancer cells proliferate massively and transformed into malignant cells. Then, malignant cells proliferate and transformed into malignant tumours, entering the progression stage. Once the formation of malignant tumours, metastasis occurs. Metastasis can be defined as the capability of malignant tumours to detach from the primary tumour mass, entering the blood stream or lymphatic channels, followed by localization and growth (cell proliferations) of secondary tumour at the new sites. Thus, inhibition of cancer cell proliferations is vital prior to the inhibition of metastasis.

Thirty crude *Zingiberaceae* extracts were tested against oestrogen-independent human breast cancer cells, MDA-MB-231 for 48 h using conventional MTT assay. A significant dose-dependent anti-proliferative effect ($IC_{50} < 30 \mu\text{g/mL}$) has been exhibited by 12 (40%) of the extracts, whereas eight (27%) other extracts were inactive ($IC_{50} > 100 \mu\text{g/mL}$) in inhibiting the proliferation or viability of MDA-MB-231 cells. Moreover, 6 (20%) of the extracts possess IC_{50} values lower or equal to $10 \mu\text{g/mL}$. These extracts were petroleum ether and chloroform extracts of *A. galanga*, petroleum ether and chloroform extracts of *B. rotunda*, chloroform extract of *C. domestica*, and petroleum ether extract of *Z. zerumbet*. Based on Table 4.3, most of the active ones were petroleum ether and chloroform extracts, while methanol extracts were mostly showed no appreciation loss of the cell growth. The only methanol extract with $IC_{50} < 30 \mu\text{g/mL}$ was methanol extract of *C. domestica*. These *Zingiberaceae* extracts possess chemopreventive properties as demonstrated by their ability to inhibit proliferations of MDA-MB-231 cells.

Petroleum ether and chloroform extracts of *A. galanga* exhibited the strongest growth inhibition against MDA-MB-231 breast cancer cells, with IC_{50} values, $2.87 \mu\text{g/mL}$ and $6.19 \mu\text{g/mL}$, respectively. Previous phytochemical studies on *A. galanga* rhizome revealed various biological activities among which are antifungal, antibacterial, antimycobacterial, antiviral, anticancer, antitrypanosomal (Chappuis *et al.*, 2007). The cytotoxicity of *A. galanga* against highly metastatic breast cancer cells, MDA-MB-231 is reported for the first time in this study.

Rhizomes of *B. rotunda* was used for treatments such as aphthous ulcer, dry mouth, stomach discomfort, leucorrhoea, dysentery, applied in lotions for rheumatism and muscular pains (Burkill, 1935). The biological properties of *B. rotunda* includes antimutagenic, antitumor, antibacterial, antifungal, analgesic, antipyretic, antispasmodic, anti-

inflammatory and insecticidal activities (Cheenpracha *et al.*, 2005). In this study, petroleum ether and chloroform extracts of *B. rotunda* showed strong anti-proliferative activities ($IC_{50} \leq 10 \mu\text{g/mL}$) on MDA-MB0231 cells. The cytotoxicity of *B. rotunda* against highly metastatic breast cancer cells, MDA-MB-231 is also reported for the first time in this study.

Previous phytochemical studies of *C. domestica* extracts from the rhizome revealed the presence of turmerin (a water-soluble peptide), essential oils (e.g. turmerones, atlantones and zingiberene), and curcuminoids (e.g. curcumin). Curcumin has been reported as the most active constituents with numerous biological activities such as antioxidant, anti-inflammatory and cancer chemotherapeutic properties. Curcumin has been shown to exhibit growth inhibitory effects *in vitro* in cancer cell lines derived from human prostate, large intestine, bone, leukaemia, and breast. It also been reported to induced apoptotic cell death by cell cycle arrest in the S and G2/M phases in the MCF-7 human breast tumour cell line (Sharma *et al.*, 2005). In the present study, petroleum ether, chloroform and methanol extracts of *C. domestica* showed pronounce inhibitory effects ($IC_{50} < 20 \mu\text{g/mL}$) on MDA-MB-231 breast cancer cells. These results are in good agreement with those previously reported studies concerning the anticancer activities *in vitro* against breast cell lines derived from malignant tumours (Aggarwal, Kumar, & Bharti, 2003; Sharma *et al.*, 2005).

Zerumbone was identified as the main component in the volatile oils extracted from the rhizome of *Z. zerumbet* (Kitayama *et al.*, 1999). Zerumbone had been reported to possess various biological properties such as anti-inflammation, anti-carcinogenesis, anti-proliferative, and anti-HIV activities (Dai *et al.*, 1997). In this study, petroleum ether extract of *Z. zerumbet* exerted pronounce anti-proliferative effects (IC_{50} , 7.46 $\mu\text{g/mL}$) against MDA-MB-231 breast cancer cells. The anti-proliferative effects on MDA-MB-231

cells could be due to the presence of zerumbone, the major compound in the volatile oils extracted using petroleum ether solvent.

All of these data suggested that extracts from the selected *Zingiberaceae* species, especially *A. galanga*, *B. rotunda*, *C. domestica*, and *Z. zerumbet* deserved further investigations in order to determine secondary metabolites with cytotoxic properties. The selected extracts obtained from these species were subjected for *in vitro* toxicity study on human lung fibroblast cells, MRC-5 (Section 5.4) in order to determine their promising values to be recommended for future studies such as isolation, *in vivo*, preclinical and clinical investigations.

5.4 Cytotoxicity of the Zingiberaceae Extracts on MRC-5 Cells

Cytotoxicity tests against cancer cell lines are the most common screening methods employed in the search for new anticancer drugs. Cytotoxicity assays currently applied in the developmental stages of anticancer drug are able to reveal compounds with the highest cytotoxic activity, but are not predictive of their potential toxicity (Popiolkiewicz *et al.*, 2005). Based on the scenarios, appropriate selection of the preliminary screening tests are substantially in order to obtain the desired active substance for preclinical and clinical studies.

In the drug discovery process, toxicity studies are usually conducted on animals before clinical trials. The disadvantages of performing toxicity study right before clinical examination are time-consuming, expensive and require a large number of animals for the experiment (Popiolkiewicz *et al.*, 2005). In addition, there is always high possibility that the active substance is highly toxic *in vivo*. Thus, it is better to select the least toxic compounds among the active ones using *in vitro* toxicity assay at the primary screening

stage. Besides that, cell lines can be obtained easily obtained from ATCC, which is another advantage of performing *in vitro* toxicity studies.

In the present study, conventional MTT assay was utilized as the *in vitro* toxicity assay using human lung fibroblast cell line (MRC-5). Assessment of the extracts' cytotoxic activity against cancer cell line must be conducted prior to the toxicity test. Based on the results obtained from cell proliferation and viability assay (a cytotoxicity assay) using MDA-MB-231 cells, six most active extracts with IC_{50} 10 μ g/mL or less were selected for toxicity testing. This was especially important that the cytotoxic activity of the tested extracts between MDA-MB-231 human breast cancer cells and normal, non-tumourigenic MRC-5 human lung fibroblast cells were compared.

A special parameter, known as selectivity index (SX) was applied in order to assess the selectivity of tested compounds towards tumour cells (Popiolkiewicz *et al.*, 2005). In this context, SX is defined as IC_{50} value obtained for MDA-MB-231 cells expressed as a percent of that of IC_{50} value from the test using MRC-5 cells. It acts as an objective indicator which enables evaluation of selectivity of the tested extracts between cancerous and non-cancerous cell lines. The SX value above 100 indicates that the cytotoxic effect of tested substance is greater towards cancer cells. The SX value of 100 or below would suggest that the tested concentration of the substance for achieving therapeutic effect is similar to or lower than the concentration causing toxic effects to normal cells. Therefore, the most promising substances for development of anti-cancer drug would have SX values distinctly higher than 100 (Popiolkiewicz *et al.*, 2005). Thus, extract with SX value more than 100 were no doubt to hold a great promise for further studies.

Conventional MTT assay is a simple, robust and relatively inexpensive test. It is a very efficient and applicable method for selection of the most appropriate substance for

further studies. The testing of the extracts in seven concentrations and incubating cells with tested extracts were carried out for 48 h rather than 24 h because prolonged incubation time (48 h) was recommended to provide comparable experimental conditions to the standard cytotoxicity test (Monks *et al.*, 1991). This was especially important as to compare tested extracts between human breast cancer cells, MDA-MB-231 and normal, non-tumorigenic human lung fibroblast cells, MRC-5, because cytotoxicity test on the latter was conducted for 48 h.

Assessment of the toxicity revealed that the most active extract against proliferation and viability of human breast cancer cells, MDA-MB-231 cells – crude petroleum ether extract of *Alpinia galanga* was equally cytotoxic against normal human lung fibroblast cells, MRC-5 (SX = 100), and that such extract can be excluded for further testing. Five other tested Zingiberaceae extracts with SX values distinctly higher than 100, have raised their possibility to serve as a new, active, but less toxic group of potential anticancer agents. This approach will facilitate appropriate estimation of the effective dose for toxicity tests on animals in the subsequent stage of drug development process. Obviously, this method can definitely reduce the number of animals required for *in vivo* testing and reducing the costs.

5.5 Effects of the Zingiberaceae Extracts on Migration of MDA-MB-231 Cells

Breast cancer accounts for approximately 20% mortality in the world, and 76% of all breast tumours have been categorized as invasive breast cancers. Breast tumours are capable of metastasis to local lymph nodes as well as to organs such as bone, lung and liver (Shanmugaraj *et al.*, 2010). Metastasis is a complex and multi-steps process which involves cell adhesion, invasion and motility (Chu *et al.*, 2007; Lee *et al.*, 2008). Therefore,

interruption at one or more of these points is an important approach for anti-metastatic therapy.

In the present study, anti-migration activities of 30 crude *Zingiberaceae* extracts were examined on MDA-MB-231 cells, a highly metastatic human breast carcinoma cells using scratch wound assay. Cells were seeded into six-well plate and cultured to confluence. A wound was scratch along the diameter of each well using 200 μ L-pipette tip. The wounded cell monolayer was incubated with and without (negative control) *Zingiberaceae* extract in 1%-serum media for 48 h at 37°C, with 5% CO₂. The assay was used because the ability of tumour cells to migrate is closely associated to their metastatic potentiality.

In vitro methods for cell migration study usually use system with 2D surfaces. *In vitro* 2D cell migration assays are prominently utilized because it is easy to be handled for screening tests that usually involve a large number of samples, which leads to the high statistical reliability of the results obtained (Entschladen *et al.*, 2005). However, 2D model is inadequate since cell migration in organism or *in vivo* is a 3D system, which is more complicated. Nevertheless, 2D assays as applied in the present study are already very useful and appropriate for fundamental understanding of cell migration processes.

Scratch wound assay involves both cell migration and proliferation (Hayot *et al.*, 2006; Peng *et al.*, 2006), which means that anti-migration activity observed may accompanied by anti-proliferative activity. In this assay, 1% FBS DMEM was used as to reduce the possibilities to the minimum that the observed wound closure was due to cell proliferation. All of the *Zingiberaceae* extracts tested except methanol extract of *Curcuma aeruginosa* significantly inhibited migration of MDA-MB-231 human breast cancer cells. Several *Zingiberaceae* extracts exhibited anti-migration activities despite being in inhibiting proliferation of MDA-MB-231 cells. These extracts were methanol extracts of A.

galanga, *C. mangga*, *Z. montanum*, *Z. officinale*, and *Z. zerumbet*; as well as petroleum ether extract of *C. mangga*, and *K. galanga*.

The pathological migration of tumour cells is a crucial event in tumour progression for tumour spreading, invasiveness and metastasis (Entschladen *et al.*, 2004; Feldner & Brandt, 2002). Invasion of tumour cells occurs initially by interacting with extracellular matrix (ECM), through the process of cell matrix adhesion. When the tumour transform to malignant tumour and detach from the primary tumour mass, they attack the surrounding basement membranes (BMs) in order to adhere to its meshwork of connective tissues, eg., Type IV collagen, laminin, and fibronectin (Pignatelli & Stamp, 1995).

The BM is the largest barrier between malignant cells and the bloodstream. The connectives tissues associated with vascular BMs must be degraded before the malignant tumours can penetrate it into the blood circulating system (Stetler-Stevenson, Aznavoorian, & Liotta, 1993; Yu, Hewitt, Kleiner, & Stetler-Stevenson, 1996). Once the malignant cell traversed the BMs to enter the bloodstream, dispersion of malignant tumours starts to occur extensively within the body (Liotta *et al.*, 1980). Obviously, invasion of malignant tumours through BM is a critical step for the occurrence of metastasis (Chen & Thompson, 2003).

Cell motility is another crucial characteristic of cancer cells in which migration of the cells from primary sites to secondary organ occurs. Sequence of events occur in cell migration process include membrane protrusion (lamellipodia or filopodia), adhesion to ECM, cell body translocation, and tail retraction. Hundreds of proteins inside and outside the cell are controlling these processes which imply actin dynamics. Therefore, proteins involves in cell motility are important targets for the development of anti-cancer drugs (Fenteany & Zhu, 2003; Giganti & Friederich, 2003; Rao & Li, 2004). The results revealed

that crude *Zingiberaceae* extracts (except methanol extract of *Curcuma aeruginosa*) could reduce the migration of MDA-MB-231 cells.

The mechanism by which *Zingiberaceae* inhibits cell migration is not yet clear. However, it has been well documented that breast cancer cells secrete matrix metalloproteinases (MMPs), which promote cancer progression by boosting cancer cell growth, invasion, and migration (Kohn & Liotta, 1995; Lee *et al.*, 2008). MMPs are a family of zinc-dependent enzymes which consists of propeptide, catalytic, hinge and COOH-terminal domains. In order to function, MMPs require catalytic removal of the propeptide domain (Kohn & Liotta, 1995).

Involvement of multigene family of zinc-dependent endopeptidases of MMPs, particularly MMP-2 and MMP-9 in the aspect of cell-migration have been studied prominently. MMP-2 and MMP-9 are unique because of the inclusion of three fibronectin Type II repeats within their catalytic domain (Kohn & Liotta, 1995). MMP-2 and MMP-9 play a crucial role in proteolytic degradation of ECM for regulating cancer cell migration process (Chena, Hsieh, Chiou, & Chub, 2005). In addition, overexpression of MMP-2 and MMP-9 stimulates angiogenesis, which speeds up cancer metastasis. Thus, new drug development by targeting this pathway is also an important approach to control cancer metastasis.

Anti-migration and anti-proliferation activities against MDA-MB-231 breast cancer cells have also been observed in other plants such as *Plumbago zeylanica* from the Family of Plumbaginaceae. *P. zeylanica* is a common household plant remedy for diarrhea in India. (Shanmugaraj *et al.*, 2010). The major constituents in *P. zeylanica* include naphthoquinones, steroids, sugars, naphthalenones, alkanes, triterpenes and amino acids (Veluri & Diwan, 1999). The study showed that *P. zeylanica* methanolic extract (PME) and its pure

compound, 3 β -hydroxylup-20(29)-ene-27,28-dioic acid (PZP) were observed to effectively inhibit cell migration and proliferation of MDA-MB-231 breast cancer cells by regulating the expression of MMPs by inhibiting MMP-2 and MMP-9 secretion (Shanmugaraj *et al.*, 2010). In this light, investigation on the mechanism of active *Zingiberaceae* extracts against the migration of MDA-MB-231 cells can be conducted by targeting the expression of MMP-2 and MMP-9 using gelatin zymogen and immunoblot analysis.

Some studies on anti-migration activity against MDA-MB-231 breast cancer cells using natural products have been reported. One of them is *Citrullus colocynthis* L. from the Family of Cucurbitaceae. *C. colocynthis* is commonly known as Sherry or Handal, is used in folk people in rural areas as purgative, anti-rheumatic and used as the remedy for skin infections. Based on the studies, cucurbitacin glucosides isolated from *C. colocynthis* showed anti-migration and anti-proliferative activities against MDA-MB-231 breast cancer cells (Tannin-Spitz *et al.*, 2007). Besides that, Sanguinarine, a benzophenanthridine alkaloid derived from the root of *Sanguinaria canadensis* was reported to inhibit metastasis and invasion of MDA-MB-231 breast cancer cells (Choi *et al.*, 2009). Anti-migration effects of *P. zeylanica*, *C. colocynthis* and *S. canadensis* resemble the anti-migration effects of *Zingiberaceae* extracts in this study using scratch wound assay. This again reveals the potentiality of local herbs for anti-cancer researches especially for combating highly metastatic breast cancer.

Cell migration is a multifactorial process, providing multiple targets for new drug development in order to control the metastasis activity (Sabe, 2003). To date, the present study is the first to demonstrate that varieties of local *Zingiberaceae* species can significantly inhibit metastatic process of MDA-MB-231 human breast cancer cells. Cancer metastasis is a complex process and therefore multi-assay strategies are needed to obtain

maximum benefit from the screening of anti-migration drugs in order to identify the potential compounds.

5.6 Qualitative Analysis Using Thin-layer Chromatography

Thin-layer chromatography is a useful form of chromatography which is widely used to identify chemical groups present in a crude extract. In this experiment, the crude extract was applied as a narrow, horizontal line on the TLC plate rather than a circular spot in order to enable the eyes to more easily distinguish substances that run very close together on the chromatogram. Although some components of the extracts may be coloured and can be observed at daylight, most of them have little or no colour and thus, use of UV lights and chromogenic or fluorogenic spray reagents were applied to make them visible.

The constituents of natural products are either fluorescent (i.e. emit visible light when expose to UV light) or absorb UV light (i.e. observed as a dark area when exposed to UV light). Layer fluorescing at 254 nm and 365 nm (Houghton & Raman, 1998) were used in this experiment. Besides exposure to UV lights and iodine vapour, a few spray reagents (i.e. sulphuric acid reagent, Dragendorff's reagent, and vanillin/sulphuric acid reagent) were applied to make the colourless substance appeared to be coloured. Since the constituents present in the crude extracts were unknown, the used of reagents containing sulphuric acid is recommended (Houghton & Raman, 1998) as it oxidizes many compounds to give coloured derivatives on heating.

Three crude *Zingiberaceae* extracts subjected for TLC tests were petroleum ether extract of *Z. zerumbet*, chloroform extracts of *A. galanga* and *C. domestica*. Crude petroleum ether extract of *Z. zerumbet* was found to be the most promising extract in modulating activated macrophages, RAW 264.7 by suppressing NO generation. Based on

the previous studies, volatile oils of the rhizomes contain zerumbone, humulene, and camphene (Nhareetsomchit & Nurshukriyah, 2003). The major component of the rhizomes is zerumbone (2,6,10-cycloundecatrien-1-one, 2,6,9,9-tetramethyl-, (E,E,E)-), which is a monocyclic sesquiterpene containing cross-conjugated dienone system (Kitayama et al., 1999; Kitayama et al., 2002). Qualitative analysis of this extract using TLC indicated that 47% of the compounds detected were terpenoids.

In the correlation of the current TLC results and the previous studies, the resolved compound of crude petroleum ether extract of *Z. zerumbet*, (Z_{11} , $R_f = 0.68$) (Table 4.9) contains conjugated double bonds and belongs to terpenoids group, which apparently compatible with the characteristic of zerumbone. Sesquiterpene zerumbone has been studied for various biological activities including anti-carcinogenesis (Takada, Murakami, & Aggarwal, 2005) and anti-inflammation (Elliott & Brimacombe, 1987; Murakami *et al.*, 2003). Crude petroleum ether extract of *Z. zerumbet* exerted prominent effects in NO inhibitory activity in activated macrophages RAW 364.7 cells, anti-proliferative ($IC_{50} = 7.46$) and anti-migration ($MC_A = 1.63 \times 10^{-3}$ mm/h tested at 12.5 $\mu\text{g/mL}$ for 48 h) activities against oestrogen-independent human breast cancer cells, MDA-MB-231. Most of the biological activities may probably due to the presence of major component, zerumbone (Takada *et al.*, 2005).

On the other hand, crude chloroform extract of *A. galanga* was selected as one of the potent extract for further studies because of its prominent effects in anti-proliferative ($IC_{50} = 6.19$ $\mu\text{g/mL}$) and anti-migration ($MC_A = -8.02 \times 10^{-4}$ mm/h tested at 12.5 $\mu\text{g/mL}$ for 48 h) activities against MDA-MB-231 cells. Results of the TLC test (Table 4.7) showed that two compounds (A_2 , $R_f = 0.15$ and A_7 , $R_f = 0.63$) belonging to the terpenoids group and one compound (A_{10} , $R_f = 0.75$) belonging to the phenol group were detected. Most of

the compounds detected contain conjugated double bonds and/or double bonds. Some works on isolating compounds from the rhizome of *A. galanga* have been carried out and published. The main compounds found in the rhizome are phenylpropanoids, and most abundantly of which are 1'S-1'-acetoxychavicol acetate (Chappuis *et al.*, 2007), 1'S-1'-acetoxyeugenol acetate (Laguna, 2003), and p-coumaryl diacetate (Desjeux, 2001) etc. Most of the biological activities such as antifungal, antibacterial, antimycobacterial, antiviral, anticancer, antitrypanosomal etc are due to the presence of phenylpropanoids (Kaur *et al.*, 2010).

Crude chloroform extract of *C. domestica* was found to be the second best extract in anti-migration activity ($MC_A = 1.35 \times 10^{-4}$ mm/h tested at 12.5 μ g/mL for 48 h) against MDA-MB-231 cells. Even though it does not rank as the best extract for any of the screening tests, it exerted potent effects in all of the screening tests carried out in this study. Based on the TLC test results (Table 4.8), the compounds detected were mainly organic compounds with conjugated double bonds. One of the resolved compounds (C_6 , $R_f = 0.66$) detected interestingly showed positive results for all of the detection systems used in the TLC.

The rhizome of *C. domestica* consists of turmerin (a water-soluble peptide), essential oils (e.g. turmerones, atlantones and zingiberene) and curcuminoids including curcumin [1,7-bis-(4-hydroxy-3-methoxyphenyl)-1,6-heptadiene-3,5-dione] (Sharma *et al.*, 2005). Curcuminoids are phenolic compounds derived from turmeric, and curcumin commonly called diferuloylmethane is a hydrophobic polyphenol, which is generally regarded as the most active constituents of the rhizome of *C. domestica* (Anand *et al.*, 2008). Curcumin has been widely studied over the past three decades. It possesses antioxidant, anti-inflammatory, cancer chemopreventive and potentially chemotherapeutic

properties (Anand *et al.*, 2008; Sharma *et al.*, 2005). The effects of crude chloroform extract of *C. domestica* in NO inhibition, anti-proliferative, and anti-migration activities in this study are strongly thought to be due to presence of the active constituents.

CHAPTER 6

6.0 Conclusion

Scientific knowledge in immunomodulatory and anti-metastatic aspects of 30 crude *Zingiberaceae* extracts obtained from ten local *Zingiberaceae* species have been studied using *in vitro* screening tests. In the immunomodulatory aspect, NO assay was applied as to evaluate their potentials as an immunomodulator in suppressing NO generation in activated macrophage cells, RAW 264.7. In the anti-metastatic aspect, their anti-proliferative and anti-migration potentials against highly metastatic hormone-independent human breast cancer cells, MDA-MB-231 were evaluated using conventional MTT assays and Scratch wound assay.

Based on the results obtained in NO assay, 29 of the *Zingiberaceae* extracts showed NO inhibitory activity of various intensities at 1.56–100 µg/mL. Among these extracts, 19 exerted strong NO inhibitory activity (IR > 70%) at various concentrations. Potential candidates were crude petroleum ether extract of *A. galanga* and *Z. zerumbet*, both exerting more than 75% of NO inhibitory activities at a low concentration. Overproduction of NO causes DNA mutation, protein modification, and thereby cellular damages which result in carcinogenesis. Besides that, carcinogenesis related to chronic inflammation caused by bacterial or viral infection in certain organs might be due to excessive and prolonged oxidative insults of macrophages. Based on this scenario, the tested *Zingiberaceae* extracts were good candidate as an immunomodulator which can effectively modulate macrophage functions by suppressing the overproduction of NO.

In the anti-metastatic aspects, substance which possesses anti-proliferative activity is important to inhibit cancer metastasis. The screening test on anti-proliferative potentials by the *Zingiberaceae* extracts showed that 12 of them (IC₅₀ < 30 µg/mL) could be

considered for further purifications based on the criteria adopted from the American National Cancer institute. Six of them ($IC_{50} \leq 10 \mu\text{g/mL}$) exhibited pronounce anti-proliferative effects against MDA-MB-231 cells. These six most potential extracts were crude petroleum ether and chloroform extracts of *A. galanga*, crude petroleum ether and chloroform extracts of *B. rotunda*, crude chloroform extract of *C. domestica*, and crude petroleum ether extract of *Z. zerumbet*. The strongest cytotoxicity activity was detected for the petroleum ether extract of *A. galanga*.

In the process of searching anti-cancer drug from natural products, assessment of their potential toxicity is vital in order to select the least toxic extracts among the active ones. In vitro toxicity test with the application of selectivity index (SX) enabled the selection of the most desirable extracts for further optimization. Five other extracts were showed to be more prone to kill cancerous cells than non-cancerous cells ($SX > 100$), and are therefore potential for further testing.

Then, anti-migration effects of the *Zingiberaceae* extracts against MDA-MB-231 cells were evaluated. The most effective extracts screened were crude petroleum ether and chloroform extracts of *A. galanga*, crude chloroform extract of *C. domestica*, and crude petroleum ether extract of *Z. zerumbet*. Crude chloroform extracts of *A. galanga* and *C. domestica*; as well as petroleum ether extract of *Z. zerumbet* which effectively inhibited or slowed down the migration of MDA-MB-231 cells, were previously showed to be the promising candidates in NO inhibition and anti-proliferative activities as well.

As a conclusion, this was the first report demonstrating that varieties of local *Zingiberaceae* species were potent inhibitor of NO generation in activated macrophages, and also act as potent agents in anti-proliferative and anti-migration of highly metastatic human breast cancer cells, MDA-MB-231. It is needless to say that extended researches on

isolation and identification of the active compound, as well as the evaluation of their chemopreventive potential *in vivo* are necessary in order further affirm their biological activities.

REFERENCES

- Abas, F., Lajis, N. H., Israf, D. A., Khozirah, S., & Kalsom, Y. U. (2006). Antioxidant and nitric oxide inhibition activities of selected Malay traditional vegetables. *Food Chemistry*, *95*, 566–573.
- Aggarwal, B. B., & Kumar, A., Bharti, A. C. (2003). Anticancer potential of curcumin: Preclinical and clinical studies. *Anticancer Research*, *23*, 363–398.
- Aggarwal, B. B., & Shishodia, S. (2004). Suppression of the nuclear factor-kappaB activation pathway by spice-derived phytochemicals: Reasoning for seasoning. *Annals of New York Academy of Sciences*, *1030*, 434–441.
- Aggarwal, B. B., & Shishodia, S. (2006). Molecular target of dietary agents for prevention and therapy of cancer. *Biochemical Pharmacology* *71*, 1397–1421.
- Agarwal, S. S., & Singh, V. K. (1999). Immunomodulators: A Review of Studies on Indian Medicinal Plants and Synthetic Peptides. *PINSA B65 3 & 4*, 179–204.
- Ahmad, S., Ahmad, A., Schneider, K. B., & White, C. W. (2006). Cholesterol interferes with the MTT assay in human epithelial-like (A549) and endothelial (HLMVE and HCAE) cells. *International Journal of Toxicology*, *25*, 17–23.
- Ali, B. H., Blunden, G., Tanira, M. O., & Nemmar, A. (2008). Some phytochemical, pharmacological and toxicological properties of ginger (*Zingiber officinale* Roscoe): A review of recent research. *Food and Chemical Toxicology*, *46*, 409–420.
- Altman, R. D., & Marcussen, K. C. (2001). Effects of ginger extract on knee pain in patients with osteoarthritis. *Arthritis and Rheumatism*, *44*, 2531–538.
- Anand, P., Thomas, S. G., Kunnumakkara, A. B., Sundaram, C., Harikumar, K. B., Sung, B., ... Aggarwal, B. B. (2008). Biological activities of curcumin and its analogues (Congeners) made by man and Mother Nature. *Biochemical Pharmacology*, *76*, 1590–1611.
- Andreesen, R., Scheibenbogen, C., Brugger, W., Krause, S., Meerpohl, H. G., Leser, H. G., ... Lohr, G. W. (1990). Adoptive transfer of tumor cytotoxic macrophages generated in vitro from circulating monocytes: A new approach to cancer immunotherapy. *Cancer Research*, *50*, 7450–7456.
- Awang, D. V. C. (1992). Ginger. *Canadian Pharmaceutical Journal*, *125*, 309–311.
- Balakrishnan, N. P., & Bhargava, N. (1984). The genus *Curcuma* L. (Zingiberaceae) on Andaman and Nicobar Islands. *The Journal of the Bombay Natural History Society*, *81*, 510–514.
- Bange, J., Zwick, E., & Ullrich, A. (2001). Molecular targets for breast cancer therapy and prevention. *Nature Medicine*, *7*, 548–552.

- Barbour, S. E., Wong, C., Rabah, D., Kapur, A., & Carter, A. D. (1998). Mature macrophage cell lines exhibit variable responses to LPS. *Molecular Immunology*, *35*, 977–987.
- Barlozzari, T., Leonhardt, J., Wiltrout, R. H., Heberman, R. B., & Reynolds, C. W. (1985). Direct evidence for the role of LGL in the reduction of experimental metastasis. *Journal of Immunology*, *134*, 2783–2789.
- Bartsch, J. E., Staren, E. D., & Appert, H. E. (2003). Matrix metalloproteinase expression in breast cancer. *Journal of Surgical Research*, *110*, 383–932.
- Beutler, B. (2004). Innate immunity: An overview. *Molecular Immunology*, *40*, 845–859.
- Bode, A. M., Ma, W. Y., Surh, Y. J., & Dong, Z. (2001). Inhibition of epidermal growth factor-induced cell transformation and activator protein 1 activation by [6]-gingerol. *Cancer Research*, *61*, 850–853.
- Bogdan, C. (2001). Nitric oxide and the immune response. *Nature Immunology*, *2*, 907–916.
- Bordia, A., Verma, S. K., & Srivastava, K. C. (1997). Effect of ginger (*Zingiber officinale* Rosc.) and fenugreek (*Trigonella foenum graecum* L.) on blood lipids, blood sugar and platelet aggregation in patients with coronary artery disease. *Prostaglandin Leukotrienes and Essential Fatty Acids*, *56*, 379–384.
- Bresnihan, B. (1999). Pathogenesis of joint damage in rheumatoid arthritis. *Journal of Rheumatology*, *26*, 717–719.
- Brouk, B. (1975). *Plants consumed by man*. Academic Press, London. pp. 429.
- Bua-in, S., & Paisooksantivatana, Y. (2009). Essential oil and antioxidant activity of Cassumnar Ginger (*Zingiberaceae*: *Zingiber montanum* (Koenig) Link ex Dietr.) collected from various parts of Thailand. *Kasetsart Jurnal (Natural Science)*, *43*, 467–475.
- Burkill, I. H., 1935. *A Dictionary of the Economic Products of the Malay Peninsula Volume I*, pp 1078-1079. London: Government of the Straits Settlements & Federated Malay State by the Crown agents for the colonies.
- Burmester, G. R., Stuhlmuller, B., Keyszer, G., & Kinne, R. W. (1997). Mononuclear phagocytes and rheumatoid synovitis. Mastermind or workhorse in arthritis? *Arthritis and Rheumatology*, *40*, 5–18.
- Campbell N. A., & Reece, J. B. (2005). *Biology* (7th ed.). San Francisco, CA: Benjamin Cummings. pp. 92–120.

- Canning, M. T., Postovit, L. M., Clarke, S. H., & Graham, C. H. (2001). Oxygen-mediated regulation of gelatinase and tissue inhibitor of metalloproteinases-1 expression by invasive cells. *Experimental Cell Research*, 267, 88–94.
- Carmeliet, P. (2000). Mechanisms of angiogenesis and arteriogenesis. *Nature Medicine*, 6, 389–395.
- Cecchini, M. G., Wettewald, A., van der Pluijm, G., & Thalmann, G. N. (2005). Molecular and biological mechanisms of bone metastasis. *EAU Update Series*, 3, 214–226.
- Chambers, A. F., Naumov, G. N., Varghese, H. J., Nadkarni, K. V., MacDonald, I. C., & Groom, A. C. (2001). Critical steps in hematogenous metastasis: An overview. *Surgical Oncology Clinics of North America*, 10 (2), 243 – 255 vii.
- Chappuis, F., Sundar, S., Hailu, A., Ghalib, H., Rijal, S., Peeling, R. W., ... Boelaert, M. (2007). Visceral leishmaniasis: What are the needs for diagnosis treatment and control. *Nature Reviews Microbiology*, 5, 873.
- Cheenpracha, S., Karalai, C., Ponglimanont, C., Subhadhirasakul, S., & Tewtrakul, S. (2005). Anti-HIV-1 protease activity of compounds from *Boesenbergia pandurata*. *Bioorganic and Medicinal Chemistry*, 16, 1710-1714.
- Chen, J., & Thompson, L. U. (2003). Lignans and tamoxifen, alone or in combination, reduce human breast cancer adhesion, invasion and migration in vitro. *Breast Cancer Research and Treatment*, 80, 163–170.
- Chena, P. N., Hsieh, Y. S., Chiou, H. L., & Chub, S. C. (2005). Silibinin inhibits cell invasion through inactivation of both P13K-Akt and MAPK signaling pathways. *Chemical-Biological Interactions*, 156, 141–150.
- Chi, Y. S., Cheon, B. S., & Kim, H. P. (2001). Effect of wogonin, a plant flavone from *Scutellaria radix*, on the expression of cyclooxygenase-2 and the induction of inducible nitric oxide synthase in lipopolysaccharide-treated RAW 264.7 cell. *Biochemical Pharmacology*, 61, 1195–1203.
- Chien, T. Y., Chen, L. G., Lee, C. J., Lee, F. Y., & Wang, C. C. (2008). Anti-inflammatory constituents of *Zingiber zerumbet*. *Food Chemistry*, 110, 584–589.
- Chithra, M., Martin, K. P., Sunandakumari, C., & Madhusoodanan, P. V. (2005). Protocol for rapid propagation, and to overcome delayed rhizome formation in field established in vitro derived plantlets of *Kaempferia galangal* L. *Scientia Horticulturae*, 104, 113 – 120.
- Cho, C. S., & Leung, K. N. (2007). In vitro and in vivo immunomodulating and immunorestorative effects of *Astragalus membranaceus*. *Journal of Ethnopharmacology*, 113, 132–141.

- Choi, Y. H., Choi, W. Y., Hong, S. H., Kim, S. O., Kim, G. Y., Lee, W. H., ... Yoo, Y. H. (2009). Anti-invasive activity of sanguinarine through modulation of tight junctions and matrix metalloproteinase activities in MDA-MB-231 human breast carcinoma cells. *Chemico-Biological Interactions*, *179*, 185–191.
- Chu, D. M., Miles, H. Toney, D., Ngyuen, C., & Marciano-Cabral, F. (1998). Amebicidal activity of plant extracts from Southeast Asia on *Acanthamoeba* spp. *Parasitology Research*, *84*, 746–752.
- Chu, S. C., Yang, S. F., Liu, S. J., Kuo, W. H., Chang, Y. Z., & Hsieh, Y. S. (2007). In vitro and in vivo antimetastatic effects of *Terminalia catappa* L. leaves on lung cancer cells. *Food Chemistry Toxicology*, *7*, 1194–1201.
- Claassen, E., de Leeuw, W., de Greeve, P., Hendriksen, C., & Boersma, W. (1992). Freund's complete adjuvant: An effective but disagreeable formula. *Research in Immunology*, *143*, 478–483.
- Coleman, J. W. (2001). Nitric oxide in immunity and inflammation. *International Immunopharmacology*, *1*, 1397–406.
- Clerici, M., & Shearer, G. M. (1992). A Th1 and Th2 switch is a critical step in the etiology of HIV infection. *Immunology Today*, *14*, 107–111.
- Cragg, G. M., & Newman, D. J. (2000). Antineoplastic agents from natural sources: Achievements and future directions. *Expert Opinion on Investigational Drugs*, *9*, 1–15.
- Cuzick, J., Warwick, J., Pinney, E., Warren, R. M., & Duffy, S. W. (2004). Tamoxifen and breast density in woman at increased risk of breast cancer. *Journal of the National Cancer Institute*, *96*, 621–628.
- Dai, J. R., Cardellina, J. H., McMahon, J. B., & Boyd, M. R. (1997). Zerumbone, an HIV-inhibitory and cytotoxic sesquiterpene of *Zingiber aromaticum* and *Zingiber zerumbet*. *Natural Product Letters*, *10*, 115–118.
- Davis, G. E., & Senger, D. R. (2005). Endothelial extracellular matrix: biosynthesis, remodeling, and functions during vascular morphogenesis and neovessel stabilization. *Circulation Research*, *97*, 1093–1107.
- Davis, L., & Kuttan, G. (2000). Immunomodulatory activity of *Withania somnifera*. *Journal of Ethnopharmacology*, *71*, 193–202.
- Deharo, E., Baelmans, R., Gimenez, A., Quenevo, C., & Bourdy, G. (2004). In vitro immunomodulatory activity of plants used by the Tecana ethnic group in Bolivia. *Phytomedicine*, *11*, 516–522.

- Denizot, F., & Lang, R. (1986). Rapid colorimetric assay for cell growth and survival. Modifications to the tetrazolium dye procedure giving improved sensitivity and reliability. *Journal of Immunological Methods*, 89, 271–277.
- Desjeux, P. (2001). The increase in the risk factors for leishmaniasis worldwide. *Transactions of the Royal Society of Tropical Medicine and Hygiene*, 95, 239.
- Devasagayam, T. P. A., & Sainis, K. B. (2002). Immune system and antioxidants, especially those derived from Indian medicinal plants. *Indian Journal of Experimental Biology*, 40, 639–655.
- Dorai, T., & Aggarwal, B. B. (2004). Role of chemopreventive agents in cancer therapy. *Cancer Letters*, 215, 129–140.
- Eccles, S. A. (2004). Parallels in invasion and angiogenesis provide pivotal points for therapeutic intervention. *International Journal of Developmental Biology*, 48, 583–598.
- Egeblad, M., & Werb, Z. (2002). New functions for the matrix metalloproteinases in cancer progression. *Nature Reviews Cancer*, 2, 161–174.
- Eigner, D., & Sholz, D. (1999). *Ferula asa-foetida* and *curcuma longa* in traditional medical treatment and diet in Nepal. *Journal of Ethnopharmacology*, 67, 1–6.
- Elliot, S., & Brimacombe, J. (1987). The medicinal plants of Gunung Leuser National Park, Indonesia. *Journal of Ethnopharmacology*, 19, 285–317.
- Entschladen, F., Drell IV, T. L., Lang, K., Mansur, K., Palm, D., Bastian, P., ... Zaenker, K. S. (2005). Analysis methods of human cell migration. *Experimental Cell Research*, 307, 418 – 426.
- Entschladen, F., Drell, T. L., Lang, K., Joseph, J., & Zaenker, K. S. (2004). Tumour cell migration, invasion, and metastasis: Navigation by neurotransmitters. *The Lancet Oncology*, 5, 254–258.
- Evans, R., Kamdar, S. J., & Duffy, T. M. (1991). Tumor-derived products induce Il-1 a, Il-1 b, Tnf a, and Il-6 gene expression in murine macrophages: Distinctions between tumor- and bacterial endotoxin-induced gene expression. *Journal of Leukocyte. Biology*, 49, 474–482.
- Fadok, V. A., Bratton, D. L., Konowal, A., Freed, P. W., Westcott, J. Y., & Henson, P. M. (1998). Macrophages that have investigated apoptotic cells in vitro inhibit proinflammatory cytokine production through autocrine/paracrine mechanisms involving TGF-beta, PGE₂, and PAF. *The Journal of Clinical Investigation*, 101, 890–898.
- Feldner, J. C., & Brandt, B. H. (2002). Cancer cell motility – On the road from c-erbB-2 receptor steered signaling to actin recognition. *Experimental Cell Research*, 272, 93–108.

Felley-Bosco, E. (1998). Role of nitric oxide in genotoxicity: Implication for carcinogenesis. *Cancer Metastasis Rev.*, 17, 25–37.

Fenteany, G., & Zhu, S. (2003). Small-molecule inhibitors of actin dynamics and cell motility. *Current Topics in Medicinal Chemistry*, 3, 593–616.

Fidler, I. J. (1970). Metastasis: Quantitative analysis of distribution and fate of tumor emboli labelled with ¹²⁵I-5-iodo-2'-deoxyuridine. *Journal of the National Cancer Institute*, 45 (4), 773–782.

Fidler, I. J. (1991). Cancer metastasis. *British Medical Bulletin*, 47, 157–177.

Fidler, I. J. (1999). Critical determinants of cancer metastasis: Rationale for therapy. *Cancer Chemotherapy and Pharmacology*, 43, S3–S10.

Folkman, J. (2006). Angiogenesis. *Annual Review of Medicine*, 57, 1–18.

Freshney, R. I. (2005). *Culture of animal cells: A manual of basic techniques*. Hoboken, New Jersey: John Wiley & Sons Inc.

George, M., & Pandalai, K. M. (1949). Investigations on plant antibiotics. Part IV. Further search for antibiotic substances in Indian medicinal plants. *Indian Journal of Medical Research*, 37, 169–181.

Giganti, A., & Friederich, E. (2003). The actin cytoskeleton as a therapeutic target: State of the art and future directions. *Progress in Cell Cycle Research*, 5, 511–525.

Glukhova, M., Koteliansky, V., Sastre, X., & Thiery, J. P. (1995). Adhesion systems in normal breast and in invasive breast carcinoma. *American Journal of Pathology*, 146, 706–716.

Goodwin, A. M. (2007). In vitro assays of angiogenesis for assessment of angiogenic and anti-angiogenic agents. *Microvascular Research*, 74, 172–183.

Gorelik, L., Prokhorova, A., & Mokyr, M. B. (1994). Low-dose melpharan-induced shift in the production of a Th2-type cytokine to a Th1-type cytokine in mice bearing a large MOPC-315 tumor. *Cancer Immunology Immunotherapy*, 39, 117–126.

Gossiau, A., & Chen, K. Y. (2004). Nutraceuticals, apoptosis and disease prevention. *Nutrition*, 20, 95–102.

Gracie, J. A., Forsey, R. J., Chan, W. L., Gilmour, A., Leung, B. P., Greer, M. R., ... McInnes, I. B. (1999). A proinflammatory role for IL-18 in rheumatoid arthritis. *Journal of Clinical Investigation*, 104, 1393–1401.

Grant, K. L., & Lutz, R. B. (2000). Alternatives therapies: ginger. *American Journal of Health-System Pharmacy*, 57, 945–947.

- Green, L. C., Wagner, D. A., Glogowski, J., Skipper, P. L., Wishnok, J. S., & Tannenbaum, S. R. (1982). Analysis of nitrate, nitrite, and [15N]nitrate in biological fluids. *Analytical Biochemistry*, *126*, 131–138.
- Grewal, I. S., & Flavell, R. A. (1996). The role of CD40 ligand in costimulation and T-cell activation. *Immunological Reviews*, *153*, 85–106.
- Guha, M., & Mackman, N. (2001). LPS induction of gene expression in human monocytes. *Cell Signal*, *13*, 85–94.
- Gupta, S. K., & Banerjee, A. B. (1976). Isolation of ethyl p-methoxycinnamate, the major antifungal principle of *Curcuma zedoaria*. *Loidia*, *39*, 218–222.
- Hackett, C. J. (2003). Innate immune activation as a broad-spectrum biodefense strategy: Prospects and research challenges. *Journal of Allergy and Clinical Immunology*, *112*, 686–694.
- Hathcock, K. S., Laszlo, G., Pucillo, C., Linsley, P., & Hodes, R. J. (1994). Comparative analysis of B7-1 and B7-2 costimulatory ligands: Expression and function. *The Journal of Experimental Medicine*, *180*, 631–640.
- Hayot, C., Debeir, O., Van Ham, P., Van Damme, M., Kiss, R., & Decaestecker, C. (2006). Characterization of activities of actin-affecting drugs on tumor cell migration. *Toxicology and Applied Pharmacology*, *211*, 30–40.
- Hirst, D. G., & Robson, T. (2007). Nitrosative stress in cancer therapy. *Frontiers in Bioscience*, *12*, 3406–3418.
- Holtum, R. E. (1950). *The Zingiberaceae of the Malay Peninsula, Volume XIII*, pp 106-117. Garden's Bulletin, Singapore.
- Hoover, K. B., Liao, S. Y., & Bryant, P. J. (1998). Loss of the tight junction MAGUK ZO-1 in breast cancer: Relationship to glandular differentiation and loss of heterozygosity. *American Journal of Pathology*, *153*, 1767–1773.
- Houghton, P. J., & Raman, A. (1998). *Laboratory handbook for the fractionation of natural extracts* (pp. 29–41). London: Chapman & Hall.
- Houssami, N., Cuzick, J., & Dixon, J. M. (2006). The prevention, detection, and management of breast cancer. *Medical Journal of Australia*, *184*, 230–234.
- Huang, G. C., Chien, T. Y., & Wang, C. C. (2005). Antitumor effects of zerumbone from *Zingiber zerumbet* in P-388D cells in vitro and in vivo. *Planta Medica*, *71*, 219–224.

- Huang, L., Yagura, T., & Chen, S. (2008). Sedative activity of hexane extract of *Kaempferia galangal* L. and its active compounds. *Journal of Ethnopharmacology*, *120*, 123–125.
- Hwang, J. K., Shim, J. S., & Pyun, Y. R. (2000). Antibacterial activity of xanthorrhizol from *Curcuma xanthorrhiza* against oral pathogens. *Fitoterapia*, *71*, 321–323.
- Ikawati, Z., Wahyuono, S., & Maeyama, K. (2001). Screening of several Indonesian medicinal plants for their inhibitory effect on histamine release from RBL-2H3 cells. *Journal of Ethnopharmacology*, *75*, 249–256.
- Ippoushi, K., Azuma, K., Ito, H., Horie, H., & Higashio, H. (2003). [6]-Gingerol inhibits nitric oxide synthesis in activated J774.1 mouse macrophages and prevents peroxynitrite-induced oxidation and nitration reactions. *Life Sciences*, *73*, 3427–3437.
- Ippoushi, K., Takeuchi, A., Ito, H., Horie, H., & Azuma, K. (2007). Antioxidative effects of daikon (*Raphanus sativus* L.) and ginger (*Zingiber officinale* Roscoe) in rats. *Food Chemistry*, *102*, 237–242.
- Ischiropoulos, H., Zhu, L., & Beckman, J. S. (1992). Peroxynitrite formation from macrophage-derived nitric oxide. *Archives of Biochemistry and Biophysics*, *298* (2), 446–451.
- Jang, T. J., & Kim, D. K. (2002). Inducible nitric oxide synthase expression of tumor and stromal cells is associated with the progression of 7,12-dimethylbenz[a]anthracene-induced rat mammary tumors. *Cancer Letters*, *182*, 121–126.
- Jantan, I., Rafi, I. A. A., & Jalil, J. (2005). Platelet-activating factor (PAF) receptor-binding antagonist activity of Malaysian medicinal plants. *Phytomedicine*, *12*, 88–92.
- Jemal, A., Siegel, R., Ward, E., Murray, T., Xu, J., & Thun, M. J. (2007). Cancer statistics 2007. *CA: A Cancer Journal for Clinicians*, *57*, 43–66.
- Jiang, D. J., Jiang, J. L., Tan, G. S., Huang, Z. Z., Deng, H. W., & Li, Y. J. (2003). Demethylbellidifolin inhibits adhesion of monocytes to endothelial cells via reduction of tumor necrosis factor alpha and endogenous nitric oxide synthase inhibitor level. *Planta Medica*, *69*, 1150–1152.
- Kala, C. P. (2006). Preserving Ayurvedic Herbal Formulations by Vaidyas: The traditional healers of the Uttaranchal Himalaya region in India. *American Botanical Council*, *70*, 42–50.
- Kanjanapothi, D., Panthong, A., Lertprasertsuke, N., Taesotikul, T., Rujjanawate, C., Kaewpinit, D., ... Pitasawat, B. (2004). Toxicity of crude rhizome extract of *Kaempferia galangal* L. (Proh Hom). *Journal of Ethnopharmacology*, *90*, 359–365.

- Karp, G. (2008). Cell and molecular biology (5th ed.), *The cell and molecular biology of the immune system* (pp. 693–718) Hoboken, New Jersey: John Wiley & Sons Inc.
- Katiyar, S. K., Agarwal, R., & Mukhtar, H. (1996). Inhibition of tumor promotion in SENCAR mouse skin by ethanol extract of *Zingiber officinale* rhizome. *Cancer Research*, *56*, 1023–1030.
- Kaur, A., Singh, R., Dey, C. S., Sharma, S. S., Bhutani, K. K., & Singh, I. P. (2010). Antileishmanial phenylpropanoids from *Alpinia galanga* (Linn.) Willd.. *Indian Journal of Experimental Biology*, *48*, 314–317.
- Kerwin, J. F., & Heller, M. (1994). The arginine–nitric oxide pathway: A target for new drugs. *Medical Research Reviews*, *14* (1), 23–74.
- Kim, J. H., Lee, B. J., Kim, J. H., Yu, Y. S., & Kim, K. W. (2009). Anti-angiogenic effect of caffeic acid on retinal neovascularization. *Vascular Pharmacology*, *51*, 262–267.
- Kim, J. K., Oh, S. M., Kwon, H. S., Oh, Y. S., Lim, S. S., & Shin, H. K. (2006). Anti-inflammatory effect of roasted licorice extracts on lipopolysaccharide-induced inflammatory responses in murine macrophages. *Biochemical and Biophysical Research Communications*, *345*, 1215–1223.
- Kim, O. K., Murakami, A., Nakamura, Y., & Ohigashi, H. (1998). Screening of edible Japanese plants for nitric oxide generation inhibitory activities in RAW 264.7 cells. *Cancer Letters*, *125*, 199–207.
- Kim, S. O., Chun, K. S., Kundu, J. K., & Surh, Y. J. (2004). Inhibitory effects of [6]-gingerol on PMA-induced COX-2 expression and activation of NF- κ B and p38 MAPKin mouse skin. *Biofactors*, *21*, 27–31.
- Kimoto, T., Arai, S., Kohguchi, M., Aga, M., Nomura, Y., Micallef, M.J., ... Mito, K. (1998). Apoptosis and suppression of tumor growth by artemisinin C extracted from Brazilian propolis. *Cancer Detection and Prevention*, *22*, 506 – 515.
- Kinne, R.W., Brauer, R., Stuhlmuller, B., Palombo-Kinne, E., & Burmester, G. R. (2000). Macrophages in rheumatoid arthritis. *Arthritis Research*, *2*, 189–202.
- Kitayama, T., Nagao, R., Masuda, T., Hill, R. K., Morita, M., Takatani, M., ... Okamoto, T. (2002). The chemistry of zerumbone IV: Asymmetric synthesis of zerumbol. *Journal of Molecular Catalysis B: Enzymatic*, *17*, 75–79.
- Kitayama, T., Okamoto, T., Hill, R. K., Kawai, Y., Takahashi, S., Yonemori, S., ... Sawada, S. (1999). Chemistry of zerumbone. Simplified isolation, conjugate addition reactions, and a unique ring contracting transannular reaction of its dibromide. *Journal of Organic Chemistry*, *64*, 2667–2672.

Kiuchi, F., Nakamura, N., Tsuda, Y., Kondo, K., & Yoshimura, H. (1988). Studies on crude drugs effective on visceral larva migrans. II. Larvisidal principles in *Kaempferia Rhizoma*. *Chemical and Pharmaceutical Bulletin*, 36 (1), 412–415.

Klein, S. A., Dobmeyer, J. M., Dobmeyer, T. S., Pape, M., Ottmann, O. G., Helm, E. B., ... Rossol, R. (1997). Demonstration of the Th1 and Th2 cytokine shift during the course of HIV-1 infection using cytoplasmic cytokine detection on single cell level by flow cytometry. *AIDS*, 11, 1111–1118.

Klimoto, T., Arai, S., Kohguchi, M., Aga, M., Nomura, Y., Micallef, M. J., ... Mito, K. (1998). Apoptosis and suppression of tumor growth by artemillin C extracted from Brazilian propolis. *Cancer Detection and Prevention*, 22, 506–515.

Klimp, A. H., de Vries, E. G., Scherphof, G. L., & Daemen, T. (2002). A potential role of macrophage activation in the treatment of cancer. *Critical Reviews in Oncology/Hematology*, 44, 143–161.

Kmoníčková, E., Melkusová, P., Farghali, H., Holý, A., & Zídek, Z. (2007). Nitric oxide production in mouse and rat macrophages: A rapid and efficient assay for screening of drugs immunostimulatory effects in human cells. *Nitric Oxide*, 17, 160–169.

Ko, H. C., Kuo, Y. H., Wei, B. L., & Chiou, W. F. (2005). Laxifolone A suppresses LPS/IFN-gamma-induced NO synthesis by attenuating NF-kappaB translocation: Role of NF-kappaB p105 level. *Planta Medica*, 71, 514–519.

Kohn, E. C., & Liotta, L. A. (1995). Molecular insights into cancer invasion: Strategies for prevention and intervention. *Cancer Research*, 52, 1856–1862.

Kominsky, S. L. (2006). Claudins: Emerging targets for cancer therapy. *Expert Reviews in Molecular Medicine*, 8, 1–11.

Konkimalla, V. B., Blunder, M., Bauer, R., & Efferth, T. (2010). Inhibition of inducible nitric oxide synthase by bis(helenalinyl)glutarate in RAW 264.7 macrophages. *Biochemical Pharmacology*, 79 (11), 1573–1580.

Kosuge, T., Yokota, M., Sugiyama, K., Saito, M., Iwata, Y., Nakura, M., ... Yamamoto, T. (1985). Studies of anticancer principles in Chinese medicines. II. Cytotoxic principles in *Biota orientalis* (L.) ENDL. and *Kaempferia galangal* L.. *Chemical and Pharmaceutical Bulletin*, 33, 5565–5567.

Laguna, F. (2003). Treatment of leishmaniasis in HIV-positive patients. *Annals of Tropical Medicine and Parasitology*, 97, S135.

Landino, L. M., Crews, B. C., Timmons, M. D., Morrow, J. D., & Marnett, L. J. (1996). Peroxynitrite, the coupling product of nitric oxide and superoxide, activates prostaglandin biosynthesis. *Proceedings of the National Academy of Sciences of the United States of America*, 93, 15069–15074.

- Langner, E., Greifenberg, S., & Gruenwald, J. (1998). Ginger: history and use. *Advances in Therapy*, *15*, 25–44.
- Lantz, R. C., Chen, G. J., Solyom, A. M., Jolad, S. D., & Timmermann, B. N. (2005). The effect of turmeric extracts on inflammatory mediator production. *Phytomedicine*, *12*, 445–452.
- Laundry de Mesquita, M., Elias de Paula, J., Pessoa, C., Odorico de Moraes, M., Costa-Lotuf, L. V., Grougnet, R., ... Espindola, L. S. (2009). Cytotoxic activity of Brazilian Cerrado plant used in traditional medicine against cancer cell lines. *Journal of Ethnopharmacology*, *123*, 439–445.
- Lechner, M., Lirk, P., & Rieder, J. (2005). Inducible nitric oxide synthase (iNOS) in tumor biology: The two sides of same coin. *Seminars in Cancer Biology*, *15*, 277–289.
- Lee, E., & Surh, Y. J. (1998). Induction of apoptosis in HL-60 cells by pungent vanilloids, [6]-gingerol and [6]-paradol. *Cancer Letters*, *134*, 163–168.
- Lee, H. S., Seo, E. Y., Kang, N. E., & Kim, W. K. (2008). [6]-Gingerol inhibits metastasis of MDA-MB-231 human breast cancer cells. *Journal of Nutritional Biochemistry*, *19*, 313–319.
- Lee, Y. G., Byeon, S. E., Kim, J. Y., Lee, J. Y., Rhee, M. H., Hong, S., ... Cho, J. Y. (2007). Immunomodulatory effect of Hibiscus cannabinus extract on macrophage functions. *Journal of Ethnopharmacology*, *113*, 62 – 71.
- Liekens, S., De Clercq, E., & Neyts, J. (2001). Angiogenesis: regulators and clinical applications. *Biochemical Pharmacology*, *61*, 253–270.
- Liew, F. Y., Li, Y., Severn, A., Milliot, S., Schmidt, J., Salter, M., & Moncada, S. (1991). A possible novel pathway of regulation by murine T helper type-2 (T_h2) cells of a T_h1 cell activity via the modulation of the induction of nitric oxide synthase in macrophages. *European Journal of Immunology*, *21*, 2489–2494.
- Lin, K. L., Su, J. C., Chien, C. M., Tseng, C. H., Chen, Y. L., ... Lin, S. R. (2009). Naphthol[1,2-*b*]furan-4,5-dione induces apoptosis and S-phase arrest of MDA-MB-231 cells through JNK and ERK signaling activation. *Toxicology in Vitro*, *17* (19), 7021–7030.
- Lingen, M. W. (2001). Role of leukocytes and endothelial cells in the development of angiogenesis in inflammation and wound healing. *Archives of Pathology and Laboratory Medicine*, *125*, 67–71.
- Liotta, L. A., Steeg, P. S., & Stetler-Stevenson, W. G. (1991). Cancer metastasis and angiogenesis: An imbalance of positive and negative regulation. *Cell*, *64*, 327–336.

- Liotta, L. A., Tryggvason, K., Garbisa, S., Hart, I., Foltz, C. M., & Shafie, S. (1980). Metastatic potential correlates with enzymatic degradation of basement membrane collagen. *Nature*, *284*, 67–68.
- Liu, J., Zhang, X., Yang, F., Li, T., Wei, D., & Ren, Y. (2005). Antimetastatic effect of a lipophilic ascorbic acid derivative with antioxidation through inhibition of tumor invasion. *Cancer Chemotherapy and Pharmacology*, *2*, 1–7.
- Lock, J. M. (1985). *Zingiberaceae*. East African Governments: Balkema. pp. 40.
- Lolis, E., & Bucala, R. (2003). Therapeutic approaches to innate immunity: Severe sepsis and septic shock. *Nature Reviews Drug Discovery*, *2*, 635–645.
- Luque de Castro, M. D., & García-Ayuso, L. E. (1998). Soxhlet extraction of solid materials: An outdated technique with a promising innovative future. *Analytica Chimica Acta*, *369*, 1–10.
- Luque de Castro, M. D., & Priego-Capote, F. (2009). Soxhlet extraction: Past and Present panacea. *Journal of Chromatography A*, *1217* (16), 2383–2389.
- Mannello, F., Tonti, G., & Papa, S. (2005). Matrix metalloproteinase inhibitors as anticancer therapeutics. *Current Cancer Drug Targets*, *5*, 285–298.
- Manson, M. M. (2003). Cancer prevention: The potential for diet to modulate molecular signaling. *Trends in Molecular Medicine*, *9*, 11–18.
- Mascolo, N., Jain, R., Jain, S. C., & Capasso, F. (1989). Ethnopharmacologic investigation of ginger (*Zingiber officinale*). *Journal of Ethnopharmacology*, *27*, 129–140.
- Masuda, Y., Kikuzaki, H., Hisamoto, M., & Nakatani, N. (2004). Antioxidant properties of gingerol related compounds from ginger. *Biofactors*, *21*, 293–296.
- Michaelsson, E., Holmdahl, M., Engstrom, A., Burkhardt, H., Scheynius, A., & Holmdahl, R. (1995). Macrophages, but not dendritic cells, present collagen to T cells. *European Journal of Immunology*, *25*, 2234–2241.
- Migliorini, P., Corradin, G., & Corradin, S. B. (1991). Macrophage NO₂⁻ production as a sensitive and rapid assay for the quantitation of murine IFN- γ . *Journal of Immunological Methods*, *139*, 107–114.
- Min, H. Y., Kim, M. S., Jang, D. S., Park, E. J., Seo, E. K., & Lee, S. K. (2009). Suppression of lipopolysaccharide-stimulated inducible nitric oxide synthase (iNOS) expression by a novel humulene derivative in macrophage cells. *International Immunopharmacology*, *9*, 844–849.

- Miyoshi, N., Nakamura, Y., Ueda, Y., Abe, M., Ozawa, Y., Uchida, K., & Osawa, T. (2003). Dietary ginger constituents, galanals A and B, are potent apoptosis inducers in human T lymphoma Jurkat cells. *Cancer Letters*, *199*, 113–119.
- Monks, A., Scudiero, D., Skehen, P., Shoemaker, R., Paull, K., Vistica, D., ... Vaigroff, A. (1991). Feasibility of a high-flux anticancer drug screen using a diverse panel of cultured human tumor cell lines. *Journal of the National Cancer Institute*, *83* (11), 757–766.
- Mook, O. R., Frederiks, W. M., & Van Noorden, C. J. (2004). The role of gelatinases in colorectal cancer progression and metastasis. *Biochimica et Biophysica Acta*, *1750*, 69–89.
- Mosmann, T. R., & Coffman, R. L. (1989). Th1 and Th2 cells: Different patterns of lymphokine secretion lead to different functional properties. *Annual Review of Immunology*, *7*, 145–174.
- Mossman, T. (1983). Rapid colorimetric assay for cellular growth and survival: Application to proliferation and cytotoxicity assays. *Journal of Immunological Methods*, *16*, 55–63.
- Murakami, A., Hayashi, R., Takana, T., Kwon, K. H., Ohigashi, H., & Safitri, R. (2003). Suppression of dextran sodium sulfate-induced colitis in mice by zerumbone, a subtropical ginger sesquiterpene, and nimesulide: separately and in combination. *Biochemical Pharmacology*, *66* (7), 1253–1261.
- Murakami, A., & Ohigashi, H. (2007). Targeting NOX, iNOS and COX-2 in inflammatory cells: Chemoprevention using food phytochemicals. *International Journal of Cancer*, *121*, 2357–63.
- Murakami, A., Takahashi, D., Kinoshita, T., Koshimizu, K., Kim, H. W., Yoshihiro, A., ... Ohigashi, H. (2002). Zerumbone, a Southeast Asian ginger sesquiterpene, markedly suppresses free radical generation, proinflammatory protein production, and cancer cell proliferation accompanied by apoptosis: The α,β -unsaturated carbonyl group is a prerequisite. *Carcinogenesis*, *23* (5), 795–802.
- Murakami, A., Tanaka, T., Lee, J. Y., Surh, Y. J., Kim, H. W., Kawabata, K., ... Ohigashi, H. (2004). Zerumbone, a sesquiterpene in subtropical ginger, suppresses skin tumor initiation and promotion stages in ICR mice. *International Journal of Cancer*, *110*, 481–490.
- Nhareetsomchit, M., & Nurshukriyah, M. H. (2003). Anti-inflammatory property of ethanol and water extracts of Zingiber zerumbet. *Indian Journal of Pharmacy*, *35*, 181–182.
- Niedbala, W., Wei, X. Q., Piedrafita, D., Xu, D., & Liew, F. Y. (1999). Effects of nitric oxide on the induction and differentiation of T_H1 cells. *European Journal of Immunology*, *29*, 2498–2505.
- Oršolić, N., & Bašić, I. (2003). Immunomodulation by water-soluble derivative of propolis (WSDP) a factor of antitumor reactivity. *Journal of Ethnopharmacology*, *84*, 265–273.

- Oršolić, N., Knežević, A. H., Šver, L., Terzić, S., & Bašić, I. (2004). Immunomodulatory and antimetastatic action of propolis and related polyphenolic compounds. *Journal of Ethnopharmacology*, *94*, 307–315.
- Othman, R., Ibrahim, H., Mohd, M. A., Mustafa, M. R., & Awang, K. (2006). Bioassay-guided isolation of a vasorelaxant active compound from *Kaempferia galangal* L. (2006). *Phytomedicine*, *13*, 61–66.
- Overall, C. M., & Lopez-Otin, C. (2002). Strategies for MMP inhibition in cancer: innovations for the post-trial era. *Nature Reviews Cancer*, *2*, 657–672.
- Park, E. J., & Pizzuto, J. M. (2002). Botanicals in cancer chemoprevention. *Cancer Metastasis Review*, *21*, 231–255.
- Peng, C. C., Chen, K. C., Peng, R. Y., Chyau, C. C., Su, C. H., & Hsieh-Li, H. M. (2007). Antrodia camphorate extract induces replicative senescence in superficial TCC, and inhibits the absolute migration capability in invasive bladder carcinoma cells. *Journal of Ethnopharmacology*, *109*, 93–103.
- Peng, C. C., Chen, K. C., Peng, R. Y., Su, C. H., & Hsieh-Li, H. M. (2006). Human urinary bladder cancer T24 cells are susceptible to the *Antrodia camphorata* extracts. *Cancer Letters*, *243*, 109–119.
- Penna, S. C., Medeiros, M. V., Aimbire, F. S., Faria-Neto, H. C., Sertie, J. A., & Lopes-Martins, R. A. (2003). Anti-inflammatory effect of the hydralcoholic extract of *Zingiber officinale* rhizomes on rat paw and skin edema. *Phytomedicine*, *10*, 381–385.
- Pepper, M. S. (2001). Role of the matrix metalloproteinase and plasminogen activator-plasmin systems in angiogenesis. *Arteriosclerosis, Thrombosis, and Vascular Biology*, *21*, 1104–1117.
- Perry L. M. (1980). *Medicinal plants of East and Southeast Asia: Attributed properties and uses*. The MIT Press, Cambridge, MA, p. 442.
- Perwez Hussain, S., & Harris, C. C. (2007). Inflammation and cancer: An ancient link with novel potentials. *International Journal of Cancer*, *121*, 2373–2380.
- Pignatelli, M. & Stamp, G. (1995). Integrins in tumour development and spread. *Cancer Surv.*, *24*, 113 – 127.
- Pongbunrod, S. (1979). *Mai-Tet-Murng-Thai: Medicinal characteristic of foreign and Thai traditional medicines*, 1st ed., Khrungthon Press, Bangkok, Thailand, p. 493.
- Popiolkiewicz, J., Polkowski, K., Skierski, J. S., & Mazurek, A. P. (2005). In vitro toxicity evaluation in the development of new anti-cancer drugs—genistein glycosides. *Cancer Letters*, *229*, 67–75.

- Radtke, O. A., Kiderlen, A. F., Kayser, O., & Kolodziej, H. (2004). Gene expression profiles of inducible nitric oxide synthase and cytokines in *Leishmania major*-infected macrophage-like RAW 264.7 cells treated with gallic acid. *Planta Medica*, *70*, 924–928.
- Rao, J., & Li, N. (2004). Microfilament actin remodeling as a potential target for cancer drug development. *Current Cancer Drug Targets*, *4*, 345–354.
- Ribatti, D., Vacca, A., Nico, B., Roncali, L., & Dammacco, F. (2001). Postnatal vasculogenesis. *Mechanisms of Development*, *100*, 157–163.
- Rogers, A. E., Zeisel, S. H., & Groopman, J. (1993). Diet and carcinogenesis. *Carcinogenesis*, *14*, 2205–2217.
- Rose, P., Huang, Q., Ong, C. N., & Whiteman, M. (2005). Broccoli and watercress suppress matrix metalloproteinase-9 activity and invasiveness of human MDA-MB-231 breast cancer cells. *Toxicology and Applied Pharmacology*, *209*, 105–113.
- Rosmagnani, S. (1994). Lymphokine production by human T cells in disease states. *Annual Review of Immunology*, *12*, 227–257.
- Roy, A. M., Baliga, M. S., & Katiyar, S. K. (2005). Epigallocatechin-3-gallate induces apoptosis in estrogen receptor-negative human breast carcinoma cells via modulation in protein expression of p53 and Bax and caspase-3 activation. *Molecular Cancer Therapeutics*, *4*, 81–90.
- Rundhaug, J. E. (2005). Matrix metalloproteinases and angiogenesis. *Journal of Cellular and Molecular Medicine*, *9*, 267–285.
- Ruslay, S., Abas, F., Shaari, K., Zainal, Z., Maulidiani, Sirat, H., ... Lajis, N. H. (2007). Characterization of the components present in the active fractions of health gingers (*Curcuma xanthorrhiza* and *Zingiber zerumbet*) by HPLC-DAD-ESIMS. *Food Chemistry*, *104*, 1183–1191.
- Sabe, H. (2003). Requirement for Arf6 in cell adhesion, migration, and cancer cell invasion. *Journal of Biochemistry*, *134*, 485–489.
- Sakurai, S., Kamachi, K., Konda, T., Miyajima, N., Kohase, M., & Yamamoto, S. (1996). Nitric oxide induction by pertussis toxin in mouse spleen cells via gamma interferon. *Infection and Immunity*, *64*, 1309–1313.
- Salvemini, D., Misko, T. P., Masferrer, J. L., Seibert, K., Currie, M. G., & Needleman, P. (1993). Nitric oxide activates cyclooxygenase enzymes. *Proceedings of the National Academy Sciences of the United States of America*, *90*, 7240–7244.
- Savill, J., & Fadok, V. (2000). Corpse clearance defines the meaning of cell death. *Nature*, *407*, 784–788.

- Sawa, T., & Ohshima, H. (2006). Nitritative DNA damage in inflammation and its possible role in carcinogenesis. *Nitric Oxide*, *14*, 91–100.
- Schantz, S. P., Brown, B. W., Lira, E., Taylor, S. L., & Beddingfield, N. (1987). Evidence for the role of natural immunity in the control of metastatic spread of head and neck cancer. *Cancer Immunology Immunotherapy*, *25*, 141–148.
- Schepetkin, I. A., & Quinn, M. T. (2006). Botanical polysaccharides: Macrophage immunomodulation and therapeutic potential. *International Immunopharmacology*, *6*, 317–333.
- Sekine, Y., Yumioka, T., Yamamoto, T., Muromoto, R., Imoto, S., Sugiyama, K., ... Matsuda, T. (2006). Modulation of TLR4 signaling by a novel adaptor protein signal-transducing adaptor protein-2 in macrophages. *Journal of Immunology*, *176*, 380–389.
- Shanmugaraj, S., Selvaraj, S., Murugan, V. P., Rajaganapathy, B. R., Shanmuganathan, M, V., Devaraj S. N., ... Subhadra, L. B. (2010). 3 β -Hydroxylup-20(29)-ene-27,28-dioic acid dimethyl ester, a novel natural product from *Plumbago zeylanica* inhibits the proliferation and migration of MDA-MB-231 cells. *Chemico-Biological Interactions*, *188*, 412–420.
- Sharma, R. A., Gescher, A. J., & Steward, W. P. (2005). Curcumin: The story so far. *European Journal of Cancer*, *41*, 1955–1968.
- Sharma, S. S., & Gupta, Y. K. (1998). Reversal of cisplatin induced delay in gastric emptying in rats by ginger (*Zingiber officinale*). *Journal of Ethnopharmacology*, *62*, 49–55.
- Shukla, Y., & Singh, M. (2007). Cancer preventive of ginger: a brief review. *Food and Chemical Toxicology*, *45*, 683–690.
- Sirirugsa, P. (1992). A revision of the genus *Boesenbergia* Kuntz (Zingiberaceae) in Thailand. *Natural History Bulletin of the Siam Society*, *40*, 67–90.
- Soler, A. P., Miller, R. D., Laughlin, K. V., Carp, N. Z., Klurfeld, D. M., & Mullin, J. M. (1999). Increased tight junctional permeability is associated with the development of colon cancer. *Carcinogenesis*, *20*, 1425–1431.
- Sonel, M., & Kuttan, G. (1999). Immunomodulatory and anti-tumour activities of *Tinospora cordifolia*. *Fitoterapia*, *70*, 35–43.
- Songsiang, U., Pitchuanom, S., Boonyarat, C., Hahnvajanawong, C., & Yenjai, C. (2010). Cytotoxicity against cholangiocarcinoma cell lines of zerumbone derivatives. *European Journal of Medicinal Chemistry*, *45* (9), 1–9.
- Soxhlet, F. (1879). Die gewichtsanalytische Bestimmung des Milchfettes. *Dinglers' Polytechnisches Journal*, *232*, 461.
- Sporn, M. B. (1996). The war on cancer. *Lancet*. *347*, 1377–1381.

- Srivastava, K., & Mustafa, T. (1992). Ginger (*Zingiber officinale*) in rheumatism and musculoskeleton disorders. *Medical Hypotheses*, 39, 342–348.
- Srivastava, S., Chitranshi, N., Srivastava, S., Dan, M., Rawat, A., & Pushpangadan, P. (2006). Pharmacognostic evaluation of *Curcuma aeruginosa* Roxb. *Natural Product Science*, 12, 162–165.
- Stetler-Stevenson, W. G., Aznavoorian, S., & Liotta, L. (1993). Tumor cell interactions with the extracellular matrix during invasion and metastasis. *Annual Reviews of Cell and Developmental Biology*, 9, 541–573.
- Stuehr, D. J., & Marletta, M. A. (1987). Induction of nitrite/nitrate synthesis in murine macrophages by BCG infection, lymphokines or interferon- γ . *Journal of Immunology*, 139, 518–525.
- Stuehr, D. J., & Nathan, C. (1989). A macrophage product responsible for cytostasis and respiratory inhibition in tumor target cells. *Journal of Experimental Medicine*, 169, 1543–1555.
- Stuhlmuller, B., Ungethum, U., Scholze, S., Martinez, L., Backhaus, M., Kraetsch, H. G., ... Burmester, G. R. (2000). Identification of known and novel genes in activated monocytes from patients with rheumatoid arthritis. *Arthritis and Rheumatology*, 43, 775–790.
- Suffness, M., & Pezzuto, J. M. (1990). Assays related to cancer drug discovery. In K. Hostettmann (Ed.), *Methods in plant biochemistry: Assays for Bioactivity*, 6 (71–133). London: Academic Press.
- Suhaila, M., Suzana, S., Saleh, H. E., Ali, A. M., & Sepiah, M. (1996). Antimycotic screening of 58 Malaysian plants against plant pathogens. *Pesticide Science*, 47, 259 – 264.
- Sunila, E. S., & Kuttan, G. (2004). Immunomodulatory and antitumour activity of *Piper longum* Linn. and Piperine. *Journal of Ethnopharmacology*, 90, 339–346.
- Surh, Y. (1999). Molecular mechanisms of chemopreventive effects of selected dietary and medicinal phenolic substances. *Mutation Research*, 428, 305–327.
- Surh, Y. J. (2002). Anti-tumor promoting potential of selected spice ingredients with antioxidative and anti-inflammatory activities: a short review. *Food and Chemistry Toxicology*, 40, 1091–1097.
- Surh, Y. J. (2003). Cancer chemoprevention with dietary phytochemicals. *Nature Reviews Cancer*, 3, 768–780.

- Surh, Y. J., & Ferguson, L. R. (2003). Dietary and medicinal antimutagens and anticarcinogens: Molecular mechanisms and chemopreventive potential – highlights of a symposium. *Mutation Research*, 523, 1–8.
- Surh, Y. J., Lee, E., & Lee, J. M. (1998). Chemopreventive properties of some pungent ingredients present in red pepper and ginger. *Mutation Research*, 402, 259–267.
- Surh, Y. J., Park, K. K., Chun, K. S., Lee, L. J., Lee, E., & Lee, S. S. (1999). Anti-tumor-promoting activities of selected pungent phenolic substances present in ginger. *Journal of Environmental Pathology, Toxicology and Oncology*, 18, 131–139.
- Szabó, C., Mitchell, A., Thiernemann, C., & Vane, J. R. (1993). Nitric oxide-mediated hyporeactivity to noradrenaline precedes the induction of nitric oxide synthase in endotoxin shock. *British Journal of Pharmacology*, 108, 786–792.
- Szabó, C., Thiernemann, C., & Vane, J. R. (1993). Dihydropyridine antagonists and agonists of calcium channels inhibit the induction of nitric oxide synthase by endotoxin in cultured macrophages. *Biochemical and Biophysical Research Communications*, 196 (2), 825–830.
- Takada, Y., Murakami, A., & Aggarwal, B. B. (2005). Zerumbone abolishes NF- κ B and I κ B α kinase activation leading to suppression of anti-apoptotic and metastatic gene expression, upregulation of apoptosis, and downregulation of invasion. *Oncogene*, 24 (46), 6957–6969.
- Takeuchi, T., Ueki, T., Sasaki, Y., Kajiwara, T., Li, B., Moriyama, L., & Kawabe, K. (1997). Th2-like response and antitumor effect of anti-interleukin-4mAb in mice bearing renal cell carcinoma. *Cancer Immunology Immunotherapy*, 43, 375–381.
- Tannin-Spitz, T., Grossman, S., Dovrat, S., Gottlieb, H. E., & Bergman, M. (2007). Growth inhibitory activity of cucurbitacin glucosides isolated from *Citrullus colocynthis* on human breast cancer cells. *Biochemical Pharmacology*, 73, 56–67.
- Tewtrakul, S., & Subhadhirasakul, S. (2007). Anti-allergic activity of some selected plants in the Zingiberaceae family. *Journal of Ethnopharmacology*, 109, 535–538.
- Thaina, P., Tungcharoen, P., Wongnawa, M., Reanmongkol, W., & Subhadhirasakul, S. (2009). Uterine relaxant effects of *Curcuma aeruginosa* Roxb. Rhizome extracts. *Journal of Ethnopharmacology*, 121, 433–443.
- Thejass, P., & Kuttan, G. (2007). Immunomodulatory activity of Sulforaphane, a naturally occurring isothiocyanate from broccoli (*Brassica oleraceae*). *Phytomedicine*, 14, 538–545.
- Thompson, A. (1998). *The cytokine handbook* (3rd ed.). New York: Academic Press. pp. 491-516.

- Trevisi, L., Pighin, I., Bazzan, S., & Luciani, S. (2006). Inhibition of 3-(4,5-dimethylthiazol-2-yl)-2,5-diphenyltetrazolium bromide (MTT) endocytosis by ouabain in human endothelial cells. *FEBS Letters*, *580*, 2769–2773.
- Tsai, S. L., Suk, F. M., Wang, C. I., Liu, D. Z., Hou, W. C., Lin, P. J., ... Liang, Y. C. (2007). Anti-tumor potential of 15,16-dihydrotanshinone I against breast adenocarcinoma through inducing G1 arrest and apoptosis. *Biochemical Pharmacology*, *74*, 1575–1586.
- Tsikas, D. (2007). Analysis of nitrite and nitrate in biological fluids by assays based on Griess reaction: Appraisal of the Griess reaction in the L-arginine/nitric oxide area of research. *Journal of Chromatography B*, *851*, 51–70.
- Tu, J., Sun, H. S., & Ye, Y. P. (2008). Immunomodulatory and antitumor activity of triterpenoid fractions from the rhizomes of *Astilbe chinensis*. *Journal of Ethnopharmacology*, *119*, 266–271.
- Van Hinsbergh, V. W., Engelse, M. A., & Quax, P. H. (2006). Pericellular proteases in angiogenesis and vasculogenesis. *Arteriosclerosis, Thrombosis, and Vascular Biology*, *26*, 716–728.
- Vani, G., Vanisree, A. J., & Shyamaladevi, C. S. (2006). Histone H1 inhibits the proliferation of MCF 7 and MDA MB 231 human breast cancer cells. *Cell Biology International*, *30*, 326–331.
- Veluri, V., & Diwan, V. D. (1999). Phytochemical and pharmacological aspects of *Plumbago zeylanica*. *Indian Drugs*, *36* (12), 724–730.
- Verma, S. P., & Goldin, B. R. (2003). Copper modulates activities of genistein, nitric oxide, and curcumin in breast tumor cells. *Biochemical and Biophysical Research Communications*, *310*, 104–108.
- Vimala, S., Norhanom, A. W., & Yadav, M. (1999). Anti-tumor promoter activity in Malaysian ginger rhizobia used in traditional medicine. *British Journal of Cancer*, *80*, 110–116.
- Voll, R. E., Hermann, M., Roth, E. A., Stach, C., Kalden, J. R., & Girkontaite, I. (1997). Immunosuppressive effects of apoptotic cells. *Nature*, *390*, 350–351.
- Wang, W. H., & Wang, Z. M. (2005). Studies of commonly used traditional medicine-ginger. *Zhongguo Zhong Yao Za Zhi*, *30*, 1569–1573.
- Wei, Q. Y., Ma, J. P., Cai, Y. J., Yang, L., & Liu, Z. L. (2005). Cytotoxic and apoptotic activities of diarylheptanoids and gingerol-related compounds from the rhizome of Chinese ginger. *Journal of Ethnopharmacology*, *102*, 177–184.
- Weiss, L. (1990). Metastatic inefficiency. *Advances in Cancer Research*, *54*, 159–211.

- Werner-Felmayer, G., Werner, E. R., Fuchs, D., Hausen, A., Reibnegger, G., & Wachter, H. (1990). Tetrahydrobiopterin-dependent formation of nitrite and nitrate in murine fibroblasts. *J. Exp. Med.*, *172*, 1599–1607.
- Wu, D., & Kai, L. (2000). Zingiberaceae. *Flora of China*, *24*, 322–377.
- Xia, Y., & Zweier, J. L. (1997). Superoxide and peroxynitrite generation from inducible nitric oxide synthase in macrophages. *Proceedings of National Academy Sciences of the United States of America*, *94*, 6954–6958.
- Xing, Z., & Wang, J. (2000). Consideration of cytokines as therapeutics agents and targets, *Current Pharmaceutical Design*, *6*, 599–611.
- Yap, L. C., Tang, S. W., Mohd Aspollah Sukari, Ee. C. L., Marwadi Rahmani, & Khaida Khalid. (2007). Characterization of flavonoid derivatives from *Boesenbergia rotunda* (L.). *The Malaysian Journal of Analytical Sciences*, *11*, 154–159.
- Yoon, S. O., Kim, M. M., & Chung, A. S. (2001). Inhibitory effect of selenite on invasion of HT1080 tumor cells. *The Journal of Biological Chemistry*, *276*, 20085–20092.
- Yoon, T. J., Yoo, Y. C., Lee, S. W., Shin, K. S., Choi, W. H., Hwang, S. H., ... Park, W. M. (2004). Anti-metastatic activity of *Acanthopanax senticosus* extract and its possible immunological mechanism of action. *Journal of Ethnopharmacology*, *93*, 247–253.
- Young, H. Y., Luo, Y. L., Cheng, H. Y., Hsieh, W. C., Liao, J. C., & Peng, W. H. (2005). Analgesic and anti-inflammatory activities of [6]-gingerol. *Journal of Ethnopharmacology*, *96*, 207–210.
- Yu, A. E., Hewitt, R. E., Kleiner, D. E., & Stetler-Stevenson, W. G. (1996). Molecular regulation of cellular invasion – Role of gelatinase A and TIMP-2. *Biochemistry and Cell Biology*, *74*, 823–831.
- Zhou, H. L., Deng, Y. M., & Xie, Q. M. (2006). The modulatory effects of the volatile oil of ginger on the cellular immune response in vitro and in vivo mice. *Journal of Ethnopharmacology*, *105*, 301–305.
- Zucker, S., Cao, J., & Chen, W. T. (2000). Critical appraisal of the use of matrix metalloproteinase inhibitors in cancer treatment. *Oncogene*, *19*, 6642–6650.

APPENDIX I: PREPARATION OF DILUENTS AND REAGENTS

1.0 Preparation of Diluents and Reagents

Preparation of diluents and reagents for NO assay, Cell Proliferation and Viability assay, Cytotoxicity assay and Scratch Wound assay are shown in Section 1.1.1 – 1.1.4.

1.1.1 Diluents and Reagents for Nitric Oxide Assay

(a) Trypan Blue

Trypan Blue is the stain most commonly used in distinguishing viable and nonviable cells. Viable cell excludes the dye, while nonviable cell absorbs the dye and appear blue under the haemocytometer. Trypan Blue solution (0.4%) needed for cell count was prepared by adding 0.2 g of Trypan Blue (Sigma, USA) powder to 50 mL of distilled water (dH₂O). It was kept at room temperature.

(b) Lipopolysaccharide

Lipopolysaccharide (LPS) was used as the inducer of NO generation in RAW 264.7 cell. LPS from *Escherichia coli* strain Serotype 055:B5 (Sigma, USA) was reconstituted with basic Dulbecco's Modified Eagle's Medium (DMEM) with phenol red (Sigma, USA), containing high glucose of 4500 mg/mL, L-glutamine, HEPES (Bio Basic, Canada) and sodium bicarbonate (NaHCO₃) (AnalaR, England) at 12.5 mg/mL. It was frozen at -80°C in aliquots of 20 µL.

(c) Diluents

Three types of diluents, namely diluent A, diluent B and diluent C were prepared. The diluents were tissue culture media with or without dimethyl sulfoxide (DMSO) (Sigma, USA). Diluent A was prepared by adding DMEM without phenol red (Kimberly, USA), with HEPES and L-glutamine with 5% heat-inactivated fetal bovine serum (FBS) (PAA Laboratories GmbH, Australia), and 0.2% DMSO. Diluent B was prepared by adding DMEM without phenol red, with HEPES and L-glutamine with 5% heat-inactivated FBS. Diluent C was prepared by mixing 4980 µL of diluent B with 20 µL of LPS which gave the final concentration of LPS, 10 µg/mL. Diluent A and diluent B were stored at 4°C in the refrigerator, whereas diluent C was prepared fresh immediately before used.

(d) N-nitro-L-arginine methyl ester hydrochloric

N-nitro-L-arginine methyl ester hydrochloric (L-NAME) is an NOS inhibitor. In order to obtain L-NAME of final concentration, 250 µM in 0.2% DMSO, 1 mg of L-NAME (Sigma, USA) was mixed with 7.4 mL of diluent A. The prepared reagent was kept in a 15 mL centrifuge tube (Orange Scientific, Belgium) wrapped with aluminum foil as it was light sensitive. It was kept at 4°C in the refrigerator.

(e) Griess reagent

Griess reagent (100 mL) was prepared by mixing 2.5% phosphoric acid (H₂PO₄) (Sigma, USA) (3 mL of 85% H₂PO₄ was dissolved in 97 mL deionized water), 1% sulphanilamide (Sigma, USA) (0.1 g of sulphanilamide was dissolved to 10 mL of 2.5% H₂PO₄), and 0.1% naphthyl ethylene diamine dihydrochloride (Sigma, USA) (0.01 g of naphthyl ethylene diamine dihydrochloride was dissolved in 10 mL of 2.5% H₂PO₄). Griess reagent was prepared fresh immediately before use.

1.1.2 Diluents and Reagents for Cell Proliferation and Viability Assay

Two types of diluents, namely diluent A, diluent B were prepared. The diluents were tissue culture media with or without DMSO. Diluent A was prepared by adding

DMEM with phenol red, containing high glucose of 4500 mg/mL, L-glutamine, HEPES, and sodium bicarbonate, supplemented with 10% heat-inactivated FBS, 2% penicillin-streptomycin, 1% amphotericin B, and 0.2% DMSO. Diluent B was prepared by adding DMEM with phenol red, containing high glucose of 4500 mg/mL, L-glutamine, HEPES, and sodium bicarbonate, supplemented with 10% heat-inactivated FBS with 2% penicillin-streptomycin and 1% amphotericin B. Diluent A and diluent B were stored at 4°C.

1.1.3 Diluents and Reagents for Cytotoxicity Assay

Two types of diluents, namely diluent A, diluent B were prepared. The diluents are tissue culture media with or without DMSO. Diluent A was prepared by adding Minimum Essential Medium Eagle (MEM) with phenol red (Sigma, USA), containing L-glutamine, HEPES, sodium bicarbonate, and sodium pyruvate supplemented with 10% heat-inactivated FBS, 2% penicillin-streptomycin, 1% amphotericin B, and 0.2% DMSO. Diluent B was prepared by adding MEM with phenol red, containing L-glutamine, HEPES, sodium bicarbonate, and sodium pyruvate supplemented with 10% heat-inactivated FBS with 2% penicillin-streptomycin and 1% amphotericin B. Diluent A and diluent B were stored at 4°C.

1.1.4 Diluents and Reagents for Scratch Wound Assay

Two types of diluents, namely diluent A, diluent B were prepared. The diluents were tissue culture media with or without DMSO. Diluent A was prepared by adding DMEM with phenol red, containing high glucose of 4500 mg/mL, L-glutamine, HEPES, and sodium bicarbonate, supplemented with 1% heat-inactivated FBS, 2% penicillin/streptomycin, 1% amphotericin B, and 0.2% DMSO. Diluent B was prepared by adding DMEM with phenol red, containing high glucose of 4500 mg/mL, L-glutamine, HEPES, and NaHCO₃, supplemented with 1% heat-inactivated FBS, 2% penicillin-streptomycin and 1% amphotericin B. Diluent A and diluent B were stored at 4°C.

APPENDIX II: CELL CULTURE PROTOCOL

1.0 Preparation and Sterilization

1.1 Preparation and Sterilization of Apparatus and Liquids

All stocks of chemicals and glassware used in cell culture works were labeled and reserved for that purpose alone. All apparatus, liquids and reagents must be sterilized in order to come in contact with cultures. Methods of sterilization include dry heat, moist heat or autoclaving, irradiation, chemical, and filtration. The choice of sterilization methods depend mainly on the stability of the items at high temperature. Sterilization methods that were applied during the research was on-going were stated in Table 1.1.

Table 2.1: Methods of sterilization and the limitations (Freshney, 2005)

Methods	Conditions	Materials	Limitations
Dry heat	180°C, 2 h	Heat stable: metals and glass.	Some carrying may occur, e.g., of indicating tape and cotton plugs.
Moist heat	121°C, 20 min	Heat-stable liquids: water, salt solutions, autoclaveable media. Moderately heat-stable plastics: silicones, polycarbonate, nylon, polypropylene.	Steam penetration requires steam-permeable packaging. Large fluid loads need time to heat up.
Irradiation: Short wave UV	254 nM, 50–100, 30 min	Flat surfaces, circulating air.	Will not reach shadow areas. Spore resistant.
Filtration	0.1- to 0.2µm porosity	All aqueous solutions; particularly suitable for heat-labile reagents and media.	Not suitable for some solvents, e.g., DMSO. Slow with viscous solutions.

1.1.1 Apparatus

Non-sterile apparatus such as glassware and recyclable plastic were rinsed with tap water and soaked in cell culture 7X detergent (Culture Lab, Australia) overnight. After soaking for one day, the apparatus were brushed with bottle brush to scrub out the residues. Then, they were rinsed thoroughly with four changes of tap water followed by three changes of dH₂O. After rinsing thoroughly, the apparatus were dried in drying oven (Memmert) at 45–50°C. After drying, bottles were loosely capped with screw caps (loosened one complete turn); the mouth of open mouthed glassware such as beakers were wrapped with aluminum foil; whereas recyclables plastic such as syringe without needle, centrifuge tubes and microtubes were packed in plastic bag for autoclaving. The apparatus were sterilized using the appropriate methods as stated in Table 1.2.

Both glass and plastic pipettes were used in cell culture work. Plastic pipettes (Orange Scientific, Belgium) were bought sterile and could be only used once. Glass pipettes were reusable, therefore must be washed carefully in order to remove all retained residues. Glass pipettes were rinsed immediately with tap water and soaked in cell culture 7X detergent overnight after usage. Then, they were rinsed in tap water a few times followed by three changes of dH₂O. After that, the pipettes were transferred to drying oven and dried with tips uppermost. Dried pipettes were sorted by size and stored dust free for sterilization. The pipettes were placed in appropriate pipette canisters according to their size and dry heat at 180°C for 2 h.

Table 2.2: Sterilization of equipment and apparatus (Freshney, 2005)

Item	Sterilization
Ampoules for freezer, glass	Dry heat ¹
Ampoules for freezer, plastic	Autoclave ² , but usually bought sterile
Apparatus containing glass and silicone tubing	Autoclave
Disposable tips for micropipettes	Autoclave in autoclavable dispensers
Filter, reusable	Autoclave
Glassware	Dry heat
Glass bottles with screw caps	Autoclave with cap slack
Instruments	Dry heat
Magnetic stirrer bars	Autoclave
Pasteur pipettes, glass	Dry heat
Pipettes, glass	Dry heat
Screw caps	Autoclave
Silicone tubing	Autoclave
Stoppers, rubber and silicone	Autoclave

¹Dry heat, 180°C for 2 h

²Autoclave, 121°C for 20 min



Figure 2.1: *Sterilizing Oven.* Dry heat sterilization of pipettes is carried out at 180°C for 2 hours.



Figure 2.2: Pipette canisters were placed with spaces between to allow circulation of hot air in the sterilizing oven.

1.1.2 Liquids

Sterile liquids could be obtained through moist heat sterilization and filtration depend the characteristics. Heat-stable liquids such as water or dH_2O , salt solutions or PBS, and some specially formulated media can be sterilized using moist heat sterilization or autoclaving. On the other hand, heat-labile liquids such as cell culture media can be sterilized by micropore filtration, which may be by positive pressure, through different ranges of filter sizes, or by negative pressure using a vacuum flask with filter attached. The sterilization methods for various reagents and media were showed in Table 1.3. On the whole, most reagents were sterilized through filtration if they are heat labile, and by autoclaving if they were heat-stable.



Figure 2.3: Autoclave. Heat-stable liquids such as distilled water and phosphate buffer saline used for cell culture works are sterilized by autoclaving.



Figure 2.4: Reusable filter. Polypropylene, in line, Luer fitting or known as swinnex.



Figure 2.5: Disposable Sterilizing Filter. Sartorius 25-mm sterile syringe filter with 0.2 μ M pore size.

Table 2.3: Sterilization of liquids and the storage conditions (Freshney, 2005)

Solution	Sterilization	Storage
Agar	Autoclave ¹ or boil	Room temperature
Amino acids	Filter ²	4°C
Antibiotics	Filter	- 20°C
Bacto-peptone	Autoclave	Room temperature
Bovine serum albumin	Filter (used stacked filters)	4°C
Carboxymethyl cellulose	Steam, 30 min	4°C
Collagenase	Filter	- 20°C
DMSO	Self-sterilizing, dispense into aliquots in sterile centrifuge tubes	Room temperature; keep dark, avoid contact with rubber or plastics (except polypropylene)
EDTA	Autoclave	Room temperature
Glucose, 20%	Autoclave	Room temperature
Glucose, 1-2%	Filter (low concentrations; caramelizes if autoclaved)	Room temperature
Glutamine	Filter	- 20°C
Glycerol	Autoclave	Room temperature
Growth factors	Filter (low protein binding)	- 20°C
HEPES	Autoclave	Room temperature
HCL, 1 M	Filter	Room temperature
Lactalbumin hydrolysate	Autoclave	Room temperature
Methocel	Autoclave	4°C
MTT	Filter	4°C
NaHCO ₃	Filter	Room temperature
NaOH, 1 M	Filter	Room temperature
Phenol red	Autoclave	Room temperature
Salt solutions (without glucose)	Autoclave	Room temperature
Serum	Filter; use stacked filters	- 20°C
Sodium pyruvate, 100 mM	Filter	- 20°C
Transferrin	Filter	- 20°C
Tryptose	Autoclave	Room temperature
Trypsin	Filter	- 20°C
Vitamines	Filter	- 20°C
Water	Autoclave	Room temperature

¹Autoclave, 121°C for 20 min

²Filter, 0.2-µm pore size

1.2 Preparation and Sterilization of Media

1.2.1 Basic DMEM medium

One bottle of DMEM powder with phenol red, high glucose of 4500 mg/mL, L-glutamine, without sodium bicarbonate (10.4 g/L) (Sigma, USA) was used to make 1L of basic media. DMEM powder must be stored between 4-6°C. Sterile distilled water (1L) was added to a sterile Graduated Erlenmeyer flask with capacity and head space, 1L. The

flask was placed on a magnetic stirrer (Thermolyne) which was set to 200 rpm, and a magnetic stirrer bar was added to the medium and started stirring.

One bottle of DMEM powder was opened and the contents were added slowly to the flask while mixing. Next, 2 g of sodium bicarbonate (NaHCO_3) (AnalaR, England) and 0.5206 g of HEPES (Bio Basic, Canada) were added to the medium while mixing as well. The powder form was stirred until completely dissolved. The pH of the medium was adjusted with hydrochloric acid (HCl) solution to pH 7.4 using the pH Meter (Thermo). When all of the constituents were completely dissolved, the magnetic stirrer bar was removed and the flask was brought to the biohazard hood (Escco Class II Biohazard Safety Cabinet) immediately for sterilization. The medium was filtered through autoclaved swinnex (Figure 1.4) into a sterile laboratory bottle. Sterile medium in the bottle was stored at 4°C in the refrigerator (Whirlpool).



Figure 2.6: Escco Class II Biohazard Cabinet. A Class II biohazard cabinet is used to provide aseptic conditions for cell culture works in the laboratory.

1.2.2 Supplemented DMEM 10% medium

Basic DMEM, heat-inactivated FBS (Sigma, USA), Penicillin/Streptomycin (Sigma, USA) and Amphotericin B (Sigma, USA) were thawed in the water bath at 37°C. In the biohazard hood, 90 mL of basic DMEM was pipetted into a sterile beaker. Then, 10 mL of heat-inactivated FBS, 2 mL of Penicillin/Streptomycin and 1 mL of Amphotericin B were added to the solution. The solution was mixed a few times using 20 mL disposable syringe without needle (Terumo, Japan), and the solution was filtered through a 0.2- μm disposable syringe driven filter (Sartorius, Germany) (Figure 5) into a sterile laboratory bottle. The supplemented DMEM 10% medium was kept at 4°C in the refrigerator and thawed in the water bath at 37°C before used.

1.2.3 Supplemented DMEM 20% medium

Supplemented DMEM 10% medium and heat-inactivated FBS were thawed in water bath at 37°C. In the biohazard hood, 50 mL of supplemented 10% DMEM was transferred into a sterile beaker and 5ml of FBS was added to the solution. The solution was mixed a few times using a 20 mL disposable syringe without needle. Then, the solution was filtered through 0.2- μm disposable syringe driven filter into a laboratory bottle. The

supplemented DMEM 20% medium was kept at 4°C in the refrigerator and thawed in the water bath at 37°C before used.

1.2.4 Freezing DMEM medium

Basic DMEM and heat-inactivated FBS were thawed in a water bath at 37°C. In the biohazard hood, 8ml of basic DMEM, 10 mL of heat-inactivated FBS, and 2 mL of DMSO were transferred into a sterile beaker and mixed well using syringe without needle. After that, the solution was filtered through 0.2-µm disposable syringe driven filter into a sterile laboratory bottle. The medium was kept at 4°C in a refrigerator and thawed in room temperature before used.

1.2.5 Phosphate buffer saline (PBS) pH 7.2

Distilled water (1L) was added to a sterile Graduated Erlenmeyer flask with capacity and head space, 1L. The flask was placed on a magnetic stirrer which was set to 200 rpm, and a magnetic stirrer bar was added to the medium and started stirring. Then, 1.52 g of sodium hydrogen phosphate (Na_2HPO_4) (AnalaR, England), 0.58 g of potassium dihydrogen phosphate (KH_2PO_4) (Merck, Germany), and 8.5 g of sodium chloride (NaCl) (Sigma, USA) were weighed and added to the solution while stirring. After that, pH of the medium was adjusted with sodium hydroxide (NaOH) solution to pH 7.2 using the pH Meter. When all of the constituents were completely dissolved, the magnetic stirrer bar was removed from the flask and filtered through Whatman filter paper into the laboratory bottle. Bottle with filtered PBS pH 7.2, with cap loosened was sterilized immediately by autoclaving at 121°C for 20 min. When the bottle was cooled down after sterilization, the cap was tightened and stored at room temperature.

1.3 Quality Control, Sterility Testing, and Storage of Media

1.3.1 Quality control

A medium used for culture work needed to be tested before used. Sterile medium that was purchased readily made was possibly relied on the quality control carried by the supplier, except for any special requirements needed for the medium. However, the culture media used were prepared from powder and sterilized in the laboratory. Therefore, quality control involving both sterility check and culture testing were required to confirm the sterility.

1.3.2 Sterility testing

All of the culture media prepared were subjected for sterility check before used. Freshly prepared supplemented DMEM (10 mL) and freezing media (10 mL) were pipetted to a tissue culture flask (Fisher Scientific, Nunc) and incubated at 37°C, 5% CO_2 and 95% air in the humidified incubator for at least three days. If any of the samples become cloudy, or any sign of contamination is detected, the whole batch the source prepared should be discarded. Preparation and sterilization steps would be done prior to get a completely sterile media for cell culture work.

Moist heat sterilization or autoclaving is a highly effective method for heat stable solution such as H_2O and PBS pH 7.2. Sterility check for autoclaved solutions were much less essential, provided that improper monitoring of the temperature and time spent for autoclaving was carried out.

1.3.3 Storage

Briefly, media made up without glutamine should last for 6–9 months at 4°C. Media with glutamine, serum, or antibiotics could be stored for 2–3 weeks only. Thus, media with labile constituents should be prepared freshly and used within 3 weeks of preparation at 4°C or stored at –20°C. Bottles of medium should be avoided to expose for a few hours under the fluorescent light. A dark freezer is recommended for a long-term storage.



Figure 2.7: Refrigerator. Refrigerator with door open showing bottles of cell culture media stored at 4°C.

2.0 Cell Culture

2.1 Reviving cells

Cells were kept in the liquid nitrogen (LN₂) tank (MVE, USA) and stored at –196°C. Supplemented 20% medium was thawed in water bath at 37°C. In the biohazard hood, 1 mL of supplemented DMEM 20% medium was pipetted into a 15 mL of centrifuge tube (Orange Scientific, Belgium). After that, cryovial (Simport, Canada) from the respective canisters was retrieved from the LN₂ tank, and the cryovial was placed in a plastic beaker filled with ice. The code of the cells and the date of cryopreservation were recorded in the cell culture record book.

The cryovial was swirled in the water bath at 37°C. When the cells in the cryovial were melted, the cryovial was brought to the biohazard hood immediately. The cells were transferred into the 15 mL centrifuge tube containing 1ml of supplemented DMEM 20% medium, followed by centrifuged (Kubota) at 1000 rpm for 5 min. After centrifugation, the supernatant was discarded, and 1 mL of supplemented DMEM 20% medium was added to the cell pellet which was then mixed well using a pipettor (1000 µL) (Eppendorf, Germany).

Supplemented DMEM 20% (9 mL) was pipetted into a tissue culture flask. Then, the cells in the 15 mL centrifuge tube were transferred into the tissue culture flask using the pipettor. Finally, the cells were observed under microscope and maintained in the humidified incubator at 37°C, with 5% CO₂ and 95% air. Growth of cell culture was observed every two days and the old media was replaced with fresh supplemented DMEM 20% media. When the cells were fully confluent, the cells were subcultivated.

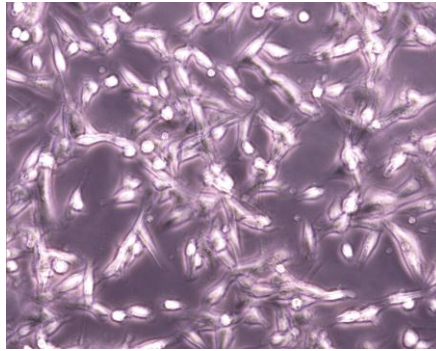


Figure 2.8: Example of Cell Morphology in Culture. Subconfluent human breast cancer cell line, MDA-MB-231 (oestrogen-receptor negative, ER-) was observed under phase-contrast microscope with magnification 100 \times .

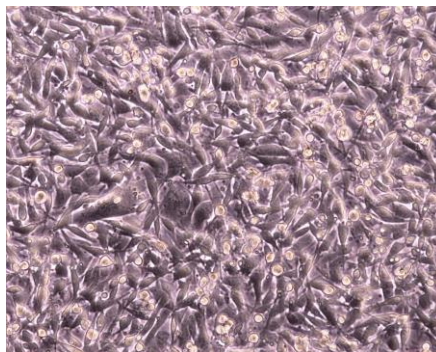


Figure 2.9: Example of Cell Morphology in Culture. Confluent human breast cancer cell line, MDA-MB-231 (oestrogen-receptor negative, ER-) was observed under phase-contrast microscope with magnification 100 \times .

2.2 Subculture of cells

Supplemented DMEM 10% medium was thawed in the water bath at 37°C. Accutase (1 mL) (Innovative Cell Technologies, San Diego, CA), the cell detachment solution was thawed at room temperature. In the biohazard hood, old media in the tissue culture flask was discarded and the cells were washed with 10 mL of sterile PBS, pH 7.2. Then, 3 mL of PBS was pipetted into the tissue culture flask and subsequently added with 1 mL of accutase. After that, the tissue culture flask was incubated in the humidified incubator at 37°C, with 5% CO₂ and 95% air for 5–10 min.

After 5 min incubation time, the tissue culture flask was tapped gently in order to make sure all of the cells were detached. The detached cells were transferred into a 15 mL centrifuge tube, and centrifuged at 1000 rpm for 5 min. While waiting centrifugation to complete, 9ml of supplemented DMEM 10% media was pipetted into each of three new tissue culture flasks. After centrifugation, the supernatant was discarded and the cell pellet was mixed with 3ml of supplemented DMEM 10% media using a pipettor (1000 μ L). Then, the cells suspension (1 mL) was distributed into each flask and maintained in the humidified incubator at 37°C, with 5% CO₂ and 95% air.



Figure 2.10: CO_2 incubator. CO_2 incubator (Shel Lab) with door open showing cell culture flasks and multi-well plates.

2.3 Cryopreservation of cells

The cells were maintained in fresh supplemented 10% DMEM media for 24–48 h before cryopreservation was done. Freezing medium was thawed at room temperature. In the biohazard hood, old media in the tissue culture flask was discarded and the cells were washed with 10 mL of sterile PBS, pH 7.2. Then, 3 mL of PBS was pipetted into the tissue culture flask and subsequently added with 1 mL of accutase. After that, the tissue culture flask was incubated in the humidified incubator at 37°C, with 5% CO_2 and 95% air for 5–10 min.

After 5 min incubation time, the tissue culture flask was tapped gently in order to make sure all of the cells were detached. The detached cells were transferred into the 15 mL centrifuge tube, and centrifuge at 1000 rpm for 5 min. After centrifugation, supernatant was discarded and the cell pellet was mixed well with 3 mL of freezing media in the centrifuge tube using a pipettor (1000 μ L). Next, 1 mL of cell suspension was distributed into three cryovials each. The cryovials were labeled and placed in a styrofoam cup and suspended in LN_2 vapour (–120°C) in the dewar for 4 h. Eventually, the cryovials were placed into cryocane and the cane was kept in the dewar canister. The canister was plunged into LN_2 (–196°C).



Figure 2.11: *Liquid Nitrogen Freezer (MVE).* Narrow-necked freezer with storage on canes in canisters at -196°C .



Figure 2.12: *Interior of Liquid Nitrogen Freezer.* Six canisters were positioned under shoulder of the freezer.



Figure 2.13: *Canes in Canister.* Cryovials are clipped onto aluminum cane, placed in the canister, and stored in the liquid nitrogen tank at -196°C .

APPENDIX III: SODIUM NITRITE STANDARD CURVE

1.0 Generation of Sodium Nitrite Standard Curve

Protocol for generation of Sodium Nitrite (NaNO_2) Standard Curve had been discussed in Chapter 3 (sections 3.3.5 and 3.3.6). A two-fold serial dilution of NaNO_2 was performed, starting at 100 μM to 1.56 μM (Chapter 3, Figure 3.4). The optical density at 540 nm (OD_{540}) obtained using the Emax precision microplate reader (Molecular Devices) was presented in Table 2.1.

Table 3.1: Absorbance readings at 540 nm for a two-fold serial dilution of sodium nitrite conducted using a flat-bottom 96-well plate

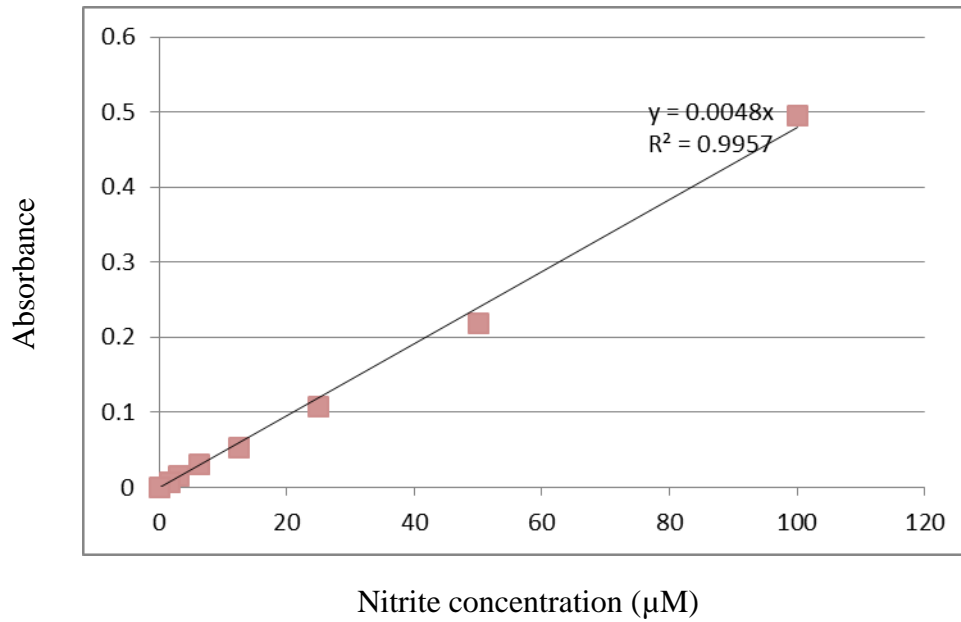
	Absorbance (n = 3)		
A	0.539	0.521	0.534
B	0.276	0.227	0.262
C	0.140	0.146	0.145
D	0.086	0.092	0.087
E	0.069	0.066	0.064
F	0.048	0.054	0.050
G	0.041	0.043	0.043
H	0.036	0.036	0.035

Three absorbance readings for each row (A–H) in Table 2.1 were averaged and transform to be more presentable as in Table 2.2.

Table 3.2: Transformed data for plotting Sodium Nitrite Standard Curve

	Concentration (μM)	Average of Absorbance (ABS)	ABS – Blank (Blank, H = 0.036)
A	100	0.531	0.495
B	50	0.255	0.219
C	25	0.144	0.108
D	12.5	0.088	0.052
E	6.25	0.066	0.03
F	3.13	0.051	0.015
G	1.56	0.042	0.006
H	0	0	0

Absorbance (ABS – Blank) versus NaNO_2 concentration was plotted in a linear least square regression format (Figure 2.1) using Microsoft Exel 2010.



y = absorbance

x = nitrite concentration

y = mx + c

m = coefficient

c = constant = 0

R² must be 0.95 and above

Figure 3.1: Sodium Nitrite Standard Curve. Nitrite concentrations were determined from a least squares linear regression analysis of NaNO₂ standard curve.

APPENDIX IV: THIN-LAYER CHROMATOGRAPHY PROTOCOL

1.0 Optimization Method for Development of Mobile Phase

The PRISMA system introduced by Nyiredy in 1985 (Houghton & Raman, 1998) was applied in the optimization of mobile phase development for TLC in this study. There are nine groups of solvents which are classified based on their 'solvent strength' (related to its polarity) as listed in Table 3.1.

The selected crude extract was run in one example of each group of the solvents. Three solvents giving the best resolution of the components of the crude extract were identified. A PRISMA construction (Figure 3.1) was drawn from these three solvents. Height of each vertical side corresponds to calculated solvent strength for each solvent.

The solvent strengths of the two highest sides are then reduced by proportionate adding of hexane to bring them both to the same solvent strength as the lowest of the three. A 1:1:1 combination of the three adjusted solvents was then used as the mobile phase for TLC testing of the extract. If the zones run too high, hexane was added until satisfactory retardation factor (or R_f value) was obtained.

Table 4.1: Solvent groups for PRISMA TLC optimization (Houghton & Raman, 1998)

Group	Solvents	Solvent strength
1	Hexane	0
2	<i>n</i> -Butylether	2.1
	<i>i</i> -Propylether	2.4
	Methyl- <i>t</i> -butylether	2.7
	Diethylether	2.8
	<i>n</i> Butanol	3.9
3	<i>i</i> -Propanol	3.9
	<i>n</i> -Propanol	4.0
	Ethanol	4.3
	Methanol	5.1
	Tetrahydrofuran	4.0
4	Pyridine	5.3
	Methoxyethanol	5.5
	Dimethylformamide	6.4
	Acetic acid	6.0
5	Formamide	9.6
	Dichloromethane	3.1
6	Dichloroethane	3.5
	Ethyl acetate	4.4
7	Butanone	4.7
	Dioxan	4.8
	Acetone	5.1
	Acetonitrile	5.8
	Toluene	2.4
8	Benzene	2.7
	Nitrobenzene	4.4
	Chloroform	4.1
9	Nitromethane	6.0
	Water	10.2

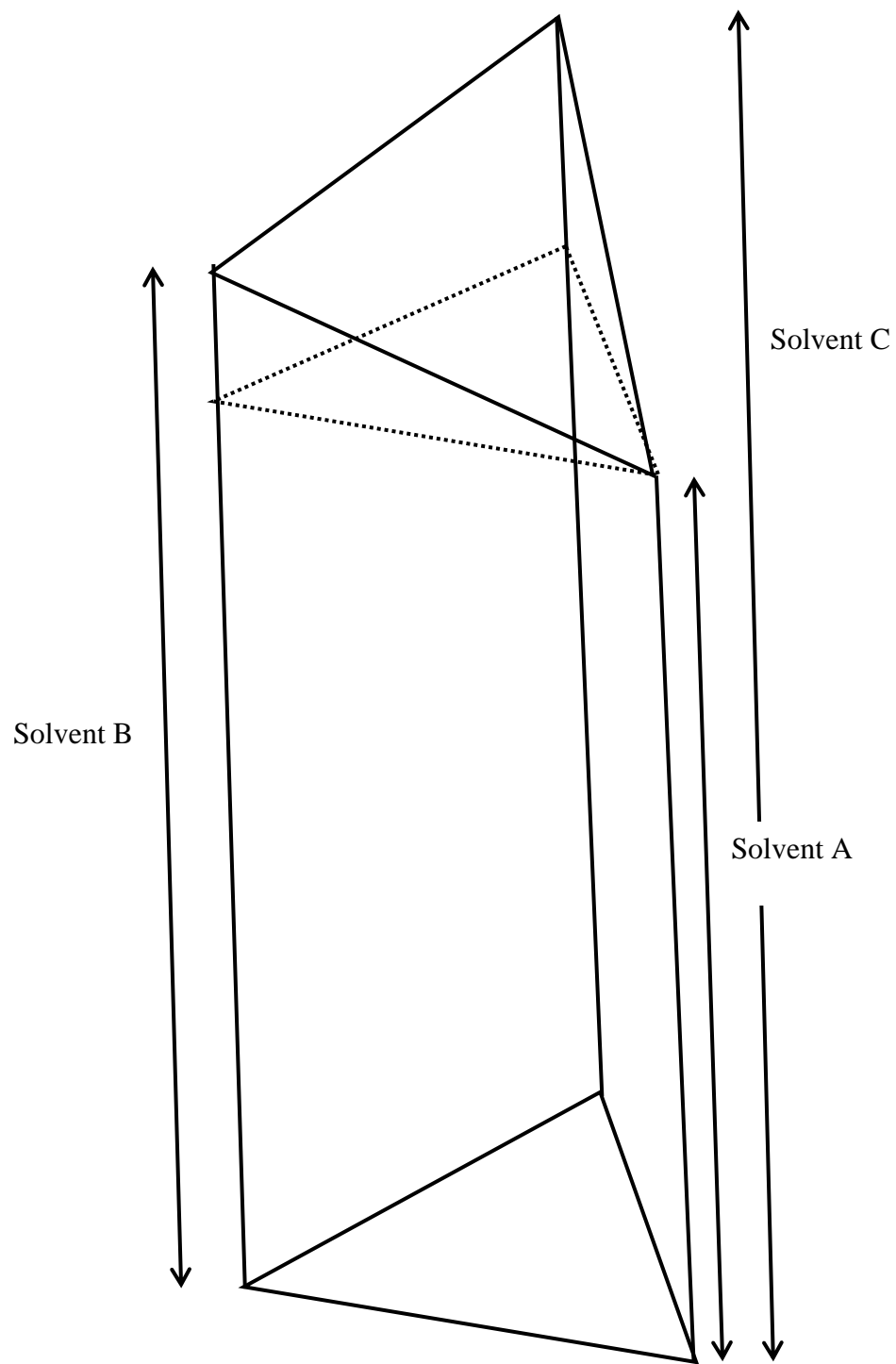


Figure 4.1: PRISMA construction from three mobile phases giving best separation.
Height of each vertical side corresponds to calculated solvent strength for each solvent.

2.0 Preparation of Chromogenic Sprays

2.1 50% Sulphuric Acid

Spray reagent, 50% sulphuric acid (H_2SO_4) was prepared manually in the laboratory by mixing 50 mL sulphuric acid with 50 mL dH_2O .

2.2 Dragendorff's Reagent

Dragendorff's reagent is available commercially or can be prepared manually in the laboratory. Firstly, 1.7 g basic bismuth nitrate was dissolved in 100 mL mixture of water-acetic acid (dH_2O -HOAc) (80:20). Next, 40 g potassium iodide (KI) was dissolved in 100 mL dH_2O . Then, a 1:1 mixture of the two solutions was made. This was the stock solution. Finally, 5 mL of each of the solutions were mixed and added to 20 g acetic acid in 70 mL dH_2O for the spraying solution.

2.3 Vanillin/Sulphuric Acid Reagent

Vanillin/sulphuric acid reagent can be prepared manually in the laboratory. Two types of spraying solutions were prepared. Solution A was prepared by mixing 5 mL sulphuric acid with 95 mL ethanol. Solution B was prepared by adding 1 g vanillin in 100 mL ethanol. TLC plate was sprayed with Solution A and followed by Solution B, and subjected to be heated at 110°C .